New techniques for the characterisation of single reeds in playing conditions

Alberto Muñoz Arancón

UNIVERSITE BRETAGNE LOIRE

Le Mans Université

Thèse de Doctorat

Alberto MUÑOZ ARANCÓN

Mémoire présenté en vue de l'obtention du
grade de Docteur de l'Université du Maine
sous le label de L'Université Nantes Angers Le Mans

École doctorale : SPIGA

Discipline : 60
Spécialité : Acoustique
Unité de recherche : Laboratoire d'Acoustique de l'Université du Maine — UMR CNRS 6613

Soutenue le 28 septembre
Thèse N° : 2017LEMA1031

New techniques for the characterisation of single reeds in playing conditions

Nouvelles techniques pour la caractérisation des anches simples en situation de jeu

JURY

Rapporteurs :	**David SHARP**, Professeur des Universités, Open University, Milton Keynes **Christophe VERGEZ**, Directeur de Recherche, LMA, Marseille
Examinateurs :	**Vasileios CHATZIIOANNOU**, Maître de Conférences, MDW, Vienne **Pauline EVENO**, Docteure, Chef d'Entreprisse, SYOS, Paris **François GAUTIER**, Professeur des Universités, LAUM, Le Mans
Directeur de Thèse :	**Bruno GAZENGEL**, Professeur des Universités, LAUM, Le Mans
Co-directeur de Thèse :	**Jean-Pierre DALMONT**, Professeur des Universités, LAUM, Le Mans
Co-encadrant de Thèse :	**Jean-François PETIOT**, Professeur des Universités, IRCCyN, Nantes

"L'homme n'est qu'un roseau le plus faible de la nature; mais c'est un roseau pensant"
"Man is but a reed, the most feeble thing in nature; but he is a thinking reed"

Pensées, Blaise Pascal

Remerciements

Je souhaite tout d'abord remercier très sincèrement mes directeurs de thèse, Bruno Gazengel, Jean-Pierre Dalmont et Jean-François Petiot. Je leur suis profondément reconnaissant de m'avoir accordé leur confiance dès le début et de m'avoir guidé dans ce chemin d'apprentissage pour mener à bien ce travail.

Je remercie Bruno Gazengel pour tout ce que j'ai pu apprendre à ses côtés, pour son enthousiasme, son investissement et son active participation à ces travaux. Je remercie également Jean-Pierre Dalmont pour apporter le regard éclairé du physicien à cette recherche. Finalement, ce travail n'aurait pas été possible sans la contribution de Jean-François Petiot dans l'analyse statistique des données et tests subjectifs.

Ce travail n'aurait pas été réalisable sans le soutien de l'Université du Maine et le Ministère de l'Enseignement Supérieur et de la Recherche, qui a financé cette thèse.

Je tiens à souligner également les grandes qualités humaines et scientifiques de Joël Gilbert et je le remercie pour son accueil au sein du Laboratoire d'Acoustique de l'Université du Maine. Merci également à Anne-Marie Brulé et Valérie Hermann pour leur aide et leur disponibilité concernant les aspects administratifs. Je veux aussi exprimer ma gratitude envers les collègues avec lesquels j'ai eu la chance de travailler lors de ma mission complémentaire d'enseignement (Christophe Ayrault, Cédric Faure, Frédéric Ablitzer...) et dans le groupe de recherche Physique des Instruments de Musique (Pierric Lotton, Marthe Curtit de l'Institut Technologique Européen des Métiers de la Musique...).

La réalisation d'expériences n'aurait pas été possible sans l'aide du pôle technique et mécanique du LAUM, c'est à dire, d'Emmanuel Brasseur, James Blondeau, Stéphane Lebon, Hervé Mezière, Patrick Collas, éric Egon, Jacky Maroudaye et Lionel Guilmeau. Je les remercie vivement pour leur contribution dans la mise en place des montages expérimentaux, leurs conseils techniques et leur disponibilité, ainsi que d'avoir toléré mes constantes appropriations, licites ou pas, de matériel.

Je remercie les membres du Centre de Transfert de Technologie du Mans, notemment Cécile Le Roux, pour leur aide précieuse dans le développement des Compositions Assistées par Ordinateur des dispositifs expérimentaux développés pour cette thèse.

Je remercie les étudiants avec qui j'ai eu le plaisir de collaborer, en particulier Ewen Conan, Anne Bouvet, Laurianne Delcor et Vincent Dangla, et qui ont contribué à ce projet.

Les musiciens, à qui est dédiée la thématique de cette thèse, ont eu un rôle participatif dans ce projet. Je remercie Jean-Marc Dormeau, Stéphane Charlot, Martin Naturel, Samuel Diabaté, Isabelle Cauchas, Maria Falcó Frigols et Charlotte Saverna pour leur disponibilité et leur riche contribution au projet en participant aux tests et mesures.

Toujours dans l'Université du Maine, grand merci aux amis du Service Culture et de l'Espace de la Vie étudiante, qui m'ont nourri avec leurs cours et activités culturelles.

J'exprime également ma gratitude envers les membres du jury qui m'ont fait l'honneur d'accepter d'évaluer mon travail. Je suis reconnaissant envers les rapporteurs, pour l'intérêt et le temps qu'ils ont consacré à la lecture critique de ce document. J'adresse également ma gratitude aux autres membres du jury pour leur disponibilité et pour l'intérêt qu'ils ont manifesté à l'égard de cette recherche en s'engageant à être examinateurs.

Je veux remercier très chaleureusement les amis de la fanfare Takasouffler, qui m'ont donné un nouveau souffle dans chaque répétition et concert. J'exprime ma gratitude à Jean-Marc Dormeau pour apporter sa bonne humeur et grande qualité humaine, et à Jean-Baptiste Doc pour les discussions scientifiques et sympathiques autour d'un café ou une petite mousse. A Vivien Denis, pluri-instrumentiste, compositeur, danseur et ami, dont j'ai été témoin de grands succès.

Et finalement, un grand merci à ma famille, qui a vécu ce projet depuis la distance, pour me donner tout son soutien, et en spécial à mon frère Miguel, qui à participé dans la correction du manuscrit.

Contents

List of Figures

List of Tables

Avant-propos

Certains instruments à vent utilisent des anches pour produire du son à partir d'une pression constante créée par le musicien. En particulier, la clarinette et le saxophone utilisent une anche simple qui est installée sur le bec. Les facteurs d'anches classifient les anches par rapport à leur coupe et leur force. Néanmoins, des anches de la même marque, coupe et force peuvent être considérées comme subjectivement différentes par les musiciens [2] et ne pas satisfaire complètement leurs exigences en terme de qualité. En conséquence, il y a un besoin de mieux caractériser les anches à l'aide d'indicateurs objectifs qui répondent aux attentes des musiciens.

Une quantité importante de descripteurs des propriétés physiques de l'anche a été proposée dans la littérature, mais il n'émerge pas de candidats clairs pour décrire la qualité des anches. Une grande variété de techniques de mesure pour caractériser les anches a été documentée. La plupart de ces techniques sont statiques ou vibroacoustiques, du fait de la difficulté d'observer l'anche en situation de jeu. Néanmoins, réaliser les mesures en situation de jeu s'approche de la situation dans laquelle les musiciens perçoivent les différences de qualité des anches.

Cette thèse propose de nouveaux outils de mesure qui peuvent être appliqués à la caractérisation des anches. En particulier, l'objectif est de rendre possible la mesure en situation de jeu. Ces outils sont un bec instrumenté, qui permet la mesure du déplacement de l'anche et de la différence de pression de part et d'autre de l'anche, et une bouche artificielle, qui cherche à imiter le jeu d'un musicien de façon contrôlable et répétable en même temps que permettant une installation facile et rapide de l'anche.

Le document se structure autour de deux articles. Le premier, "*Estimation of saxophone reed parameters during playing*", est le sujet du Chapitre 2 et il est publié dans le journal *Journal of the Acoustical Society of America* [3]. Le deuxième, "*Comparison of real and artificial playing of a single-reed instrument using an artificial mouth*", est soumis au journal *Acta Acustica united with Acustica* et il est presenté au Chapitre 4.

Le manuscrit est organisé de la façon suivante : le Chapitre 1 contient l'état de l'art concernant la thématique de cette recherche, le Chapitre 2 présente le développement du bec instrumenté et d'une méthode pour estimer les paramètres équivalents de l'anche en situation de jeu, le Chapitre 3 explique une campagne de mesures sur les anches qui utilise des approches subjectives et objectives, le Chapitre 4 décrit le développement de la bouche artificielle et sa comparaison avec le jeu d'un musicien. Enfin, le Chapitre 5 détaille les conclusions et perspectives de ce travail.

Introduction

The history of the reed instruments is closely related to the use of the giant cane. In the origins of these instruments, the entire instrument was made of cane [4], and it is during their evolution that the mouthpiece separates from the body and that they are made of other materials. The most commonly used reeds come from the plant *Arundo donax L.* [5].

The *Arundo donax L.* grows in many regions across the globe and favours Mediterranean climates. It is common in France, India, China, South Africa, England, Spain, Australia and the south of the United States. The Var region, in France, is the main area of commercial exploitation for the production of reeds for musical instruments.

Among the elements that constitute the musical instrument, the reed presents the most variability due to its biological origins. Each reed exhibits individual properties that may or may not satisfy player's expectations [6, 7]. In addition, the reed is subject to changes produced by external factors during its life time [8], and it deteriorates with use. In particular, reeds are sensitive to moisture and temperature conditions. As an alternative, some manufacturers offer synthetic reeds, which try to imitate cane reeds while ensuring stability. Different reed materials exist today such as plastic or composites, but the use of synthetic reeds is still in development.

After a process of growing, selection and curing, the cane is cut to produce the reeds [4]. Reed makers cut the cane and profile it to a particular shape. All reeds from the same template have identical thickness, and are sorted according to their strength using a mechanical stiffness measurement. Clarinet and saxophone players can choose among different reed brands, shapes and strengths. Usually the musician adapts the reed strength to the mouthpiece tip opening. Different reed shapes produce distinct timbres [9]. The conundrum is that reeds of the same brand, cut and strength may be considered subjectively as different by musicians [2]. The commercial classification of reeds does not entirely satisfy the musicians' demand of quality. In consequence, there is a need to better characterise reeds with objective indicators that respond to musicians' expectations.

The manufacturing and quality control of the reeds relies on semi-empirical principles derived from the historical evolution of the craftsmanship and lutherie. Musical Acoustics provides a new and complementary approach to these methods, helping manufacturers and musicians to better understand the functioning of the musical instruments and proposing new criteria and methods for quality control.

In the scientific literature, many descriptors of the reed properties have been proposed, but no clear candidates to describe reed quality have emerged. A wide variety of measurement techniques to characterise reeds has been documented. Most of these techniques are static or vibro-acoustic, because of the difficulty to observe the reed behaviour while playing. However, performing measurements in playing conditions comes closer to the situation in which musicians perceive the differences in quality between reeds. Unlike other methods, this approach considers the interaction of the reed with the lip and the mouthpiece.

This thesis proposes new measuring tools that can be applied to reed characterisation. More specifically, the aim is to enable measurements in playing conditions. These tools are an instrumented mouthpiece, which allows for the measurement of reed displacement and pressure difference across the reed, and an aspirating artificial mouth, which searches to imitate in a controllable and reproducible manner a musician's playing. This artificial mouth can be applied to the characterisation of reeds, aiming to predict reed quality and to explain the differences perceived by musicians.

The document is structured around two articles. The first one, "Estimation of saxophone reed parameters during playing", is the issue of Chapter 2 and it is published in the Journal of the Acoustical Society of America [3]. The second one, "Comparison of real and artificial playing of a single-reed instrument using an artificial mouth", is submitted to Acta Acustica united with Acustica and is presented in Chapter 4.

The manuscript is organised as follows: Chapter 1 contains the state of the art concerning the topic of this research, Chapter 2 presents the development of the instrumented mouthpiece and a method for the estimation of equivalent reed parameters in playing conditions, Chapter 3 explains a measurement campaign for reed characterisation using subjective and objective approaches, Chapter 4 describes the development of the artificial mouth and its comparison with a musician's playing, and Chapter 5 details the conclusions and perspectives of the work.

Chapter 1

State of the art

This chapter presents the previous research related to the topic of this thesis. Firstly, an overview of the physics of the reed and the musical instrument is presented. The diverse measurement techniques for the characterisation of the reeds described in the literature are summarized next, together with some attempts to relate these objective measurements with subjective classifications of reeds. Finally, different artificial mouths existing in the literature are described.

1.1 Physics of the woodwinds

This section introduces a simple model of the woodwind instruments, composed by three equations, which permits inscribing the reed in its physical context. In addition, physical models of the reed of different complexity are explained.

1.1.1 The three-equations model

Woodwinds are auto-oscillating systems. The steady energy that the musician communicates into the instrument is transformed into self-sustained oscillations (sound) in the resonator (passive resonator) through the action of a source of strong non linearity (non-linear element) [10]. This process is schematized in Fig. 1.1.

The instrument is usually divided into exciter and resonator. The reed-mouthpiece-lip system forms the exciter, and the body of the instrument (the bore) the resonator. The reed, coupled to the musician's lip and the mouthpiece, acts as a pressure-controlled valve [11, 12]. The pressure excess produced by the musician tends to close the reed. This kind of valve was classified by Helmholtz as an inward-striking reed. It participates

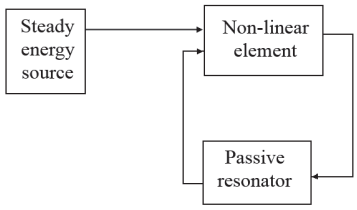

FIGURE 1.1: Block diagram of a woodwind seen as an auto-oscillating system.

in the non-linear relation between the air pressure generated by the musician and the air flow in the entry of the resonator. The resonator is usually characterized by its input impedance at low-level acoustic pressures, assuming linear behaviour. The impedance Z is the transfer function relating the flow U entering the instrument to the pressure P_{mp} at the entry of the bore, that is, in the mouthpiece (see Eq. 1.1). It expresses the reaction of the system to an excitation as a function of the frequency (angular frequency ω in Eq. 1.1). When the exciter is coupled to the air column, the resonances of the air column are excited, generating waves inside the resonator.

$$Z(\omega) = \frac{P_{mp}(\omega)}{U(\omega)}. \tag{1.1}$$

The player interacts with both the exciter and the resonator in order to control the sound [13, 14]. The musician controls the blowing pressure and the embouchure, which involves the placement and muscular action of the lip on the reed. These parameters, blowing pressure and lip position, are the main control parameters of the exciter of the instrument. The musician's lip and the mouthpiece are intrinsic parts of the exciter. The player also has an active control of the resonator through the fingering, which adapts the impedance of the instrument and varies the oscillation frequencies of the air column from note to note. The musician can affect the tuning of the instrument to some extent with the blowing pressure, the embouchure and also with the interaction of the vocal tract with the instrument, although this last is not considered in this model. In the oscillation loop, part of the energy is lost (heat) and part is radiated (sound), giving a feedback of the produced sound to the player, who may vary the control parameters to obtain the desired sound.

The reed dynamics are usually modelled as a damped mass-spring oscillator. The model of the one-degree-of-freedom oscillator is given in Eq. 1.2.

$$M\ddot{y}(t) + R\dot{y}(t) + Ky(t) = -\Delta P(t). \tag{1.2}$$

In Eq. 1.2, the variable y is the reed displacement (note that it is negative), and $\Delta P(t)$ is the pressure difference across the reed as a function of time. It is given by the difference of the pressure in the musician's mouth P_m and the pressure inside the mouthpiece P_{mp} (see Fig. 1.2). The parameters K, R and M are respectively the equivalent stiffness, damping and mass of the reed per unit of area. The reed displacement in rest position is 0 and the closed position is $-H$. The lip imposes the rest position of the reed (see Fig. 1.2).

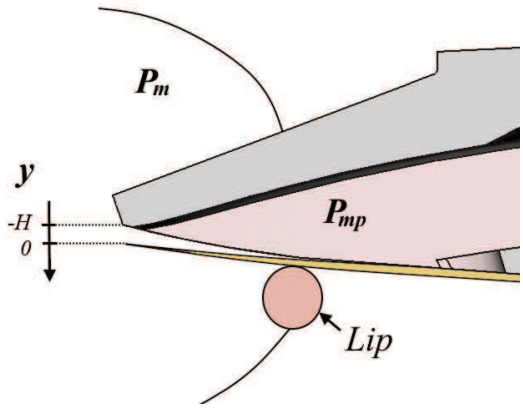

FIGURE 1.2: Schema of the variables of the physical model of the reed.

The pressure difference across the reed ΔP is related to the particle velocity u in the reed channel as derived from the Bernoulli equation in Eq. 1.3, where ρ is the air density [15].

$$\frac{\rho u^2}{2} = \Delta P. \tag{1.3}$$

The volume velocity U_{in} is obtained from the particle velocity multiplied by the cross section of the channel, of width w and varying with the reed position y. This considers that the particle velocity is uniform in the cross section of the channel and that the cross section is rectangular [16]. The Eq. 1.4 supposes $P_m \geq P_{mp}$ and $y \geq -H$.

$$U_{in} = w(H + y) \cdot u = w(H + y)\sqrt{\frac{2\Delta P}{\rho}}. \tag{1.4}$$

The volume velocity as a function of the pressure difference can be easily approximated neglecting the reed dynamics and substituting $y = \frac{-\Delta P}{K}$ in Eq. 1.4, as shown in Eq. 1.5. This function is represented in Fig. 1.3.

$$U_{in} = w(H + \frac{-\Delta P}{K})\sqrt{\frac{2\Delta P}{\rho}}. \tag{1.5}$$

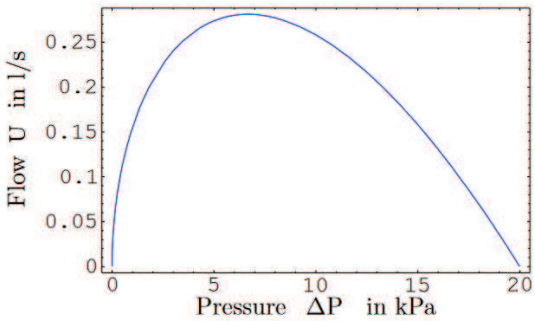

FIGURE 1.3: Volume flow as a function of the pressure difference across the reed. Figure taken from [1].

In this figure, it can be seen that at the beginning, the flow rises from zero to a maximum with increasing blowing pressure. After this maximum, the flow decreases until zero. At this point, the reed channel closes completely. This point is characterised by the closing pressure $P_c = KH$. In the increasing part of the curve, the conductance of the system (obtained as the first derivative) is positive, meaning that the reed acts as a resistance to the air flow. However, in the decreasing part of the curve, the conductance is negative and the reed acts as an acoustic generator. In this part of the curve, the generation of self-sustained oscillations is possible [11]. As a result, the threshold pressure for the beginning of the auto-oscillations is the maximum of the characteristic $U(\Delta P)$, which is at $\frac{1}{3}P_c$, ignoring losses [17].

The role of the resonator in the flow entering the instrument is included through the impulse response function h, obtained as the inverse Fourier transform of the input admittance ($1/Z$, with Z the input impedance in Eq. 1.1). The volume velocity U_{in} as a function of time is expressed in terms of the impulse response h and the pressure in the mouthpiece P_{mp} as given in Eq. 1.6.

$$U_{in} = [h * P_{mp}](t). \tag{1.6}$$

The reed also produces an air flow U_r, impulsed by its vibrating equivalent surface S_r.

$$U_r = S_r \dot{y} \tag{1.7}$$

The total incoming volume flow in the instrument is given by

$$U = U_{in} + U_r = [h * P_{mp}](t) + S_r \dot{y}. \tag{1.8}$$

The model composed by Eq. 1.2, 1.4, and 1.8 [18] is known as the three-equations lumped model of the single reed instruments. A simpler version is the two-equations model composed by Eq. 1.5 and 1.8. The reed is in some way considered in each equation of the model, hence its importance in the physics of the sound of the woodwinds.

1.1.2 Physical models of the reed

The diverse physical models of the reed used in different works are discussed here. The models are ordered from those with lower dimensions and fewer variables to those of increasing complexity. Note that all the models are presented in the reference frame presented above (and the most extensively used in the literature), so some of them do not appear as written in the given citation. The context and relevance of these models are discussed further in this text, in §2.2.

1.1.2.1 Lumped models

The simplest reed model is the low-frequency model where the reed is considered a spring. A pressure difference ΔP excites the reed, which is characterized by an effective stiffness by unit of area K, and results in the reed tip displacement y (Eq. 1.9).

$$Ky = -\Delta P, \tag{1.9}$$

As explained in §1.1.1, this simple model permits to obtain auto-oscillations of the air column of the instrument [19].

A more complete model is the damped mass-spring oscillator [10], where the terms corresponding to the equivalent mass M and equivalent damping R are added.

$$M\ddot{y} + R\dot{y} + Ky = -\Delta P. \tag{1.10}$$

Some modifications of this model can be done in order to include the lip-reed-mouthpiece interactions.

The effect of bending of the reed on the lay of the mouthpiece was modelled by Chatzioannou et al. [20] as a conditional contact force, written in form of a power law. This

non-linear part is added to the linear stiffness K as shown in Eq. 1.11 to write a non-linear spring model.

$$Ky - K_c(\lfloor y - y_c \rfloor)^\alpha = -\Delta P, \tag{1.11}$$

where K_c and α are power-law constants and the non-linear part is written

$$\lfloor y - y_c \rfloor = \begin{cases} y - y_c & \text{if} \quad y < y_c, \\ 0 & \text{if} \quad y \geq y_c. \end{cases} \tag{1.12}$$

In Eq. 1.12, y_c is the displacement value below which the power law becomes active. They used this non-linear stiffness in the damped mass-spring oscillator of Eq. 1.10.

The action of the player can also be included in the reed model of Eq. 1.10. Ducasse [21] proposed to consider the reed parameters as functions of the reed position (see Eq. 1.13). In this model, the parameters $K(y)$ and $M(y)$ are primarily related to the reed density and longitudinal flexibility and they also depend on the geometry of both the reed and the mouthpiece, taking into account the bending of the reed on the lay of the mouthpiece (with varying parameters, differently to Chatziioannou [20]). The damping $R(y)$ is considered to be mainly produced by the lip, so that the reed is considered a highly-damped reed. The reed by itself is lightly damped and it tends to oscillate at its resonance frequency (producing a squeak) but the damping introduced by the lip allows the player-instrument system to oscillate at the resonance frequency of the resonator [22]. Ducasse proposed to include the action of the musician's tongue (in attacks) by adding a damped mass-spring term. This translates into a variable mass in Eq. 1.13. All the parameters are considered to be dependent of the reed position y, in order to take into account the curling of the reed on the mouthpiece.

$$M(y)\ddot{y} + \frac{dM}{dy}\dot{y}^2 + R(y)\dot{y} + K(y)y = -\Delta P. \tag{1.13}$$

On the other hand, Chatziioannou et al. [23] included the action of the tongue by varying the parameters $M(y)$, $R(y)$ and H in the attacks. They used this description to compare tongue-separated tones and pressure-separated tones.

1.1.2.2 Beam models

The reed can also be modelled as a beam. The differential equation of the transverse vibrations of an isotropic and homogeneous beam clamped at one end and driven by an

external longitudinal force was given by Kinsler et al. [24]. It is presented in Eq. 1.14.

$$\rho A \frac{\partial^2 y}{\partial t^2} = -Y A \kappa^2 \frac{\partial^4 y}{\partial x^4} + F, \tag{1.14}$$

where ρ is the mass density of the beam, A is the cross-sectional area (assuming rectangular cross section then $A = b \cdot w$, with b the beam thickness and w the beam width), Y is the Young modulus and κ is the radius of gyration. For a beam with rectangular cross section, $\kappa = b/\sqrt{12}$.

Damping can be included in Eq. 1.14 by adding the term in the first part of the equation (see Eq. 1.15).

$$\rho A \frac{\partial^2 y}{\partial t^2} + R \frac{\partial y}{\partial t} = -Y A \kappa^2 \frac{\partial^4 y}{\partial x^4} + F, \tag{1.15}$$

where R is the damping per unit length.

The reed is thinner in the tip than in its shoulder. This variation of the beam thickness can also be considered in the model. The differential equation of a non-uniform clamped beam is given in Eq. 1.16

$$\rho A(x) \frac{\partial^2 y}{\partial t^2} + R \frac{\partial y}{\partial t} = -\frac{\partial^2}{\partial x^2} \left(Y A(x) \kappa^2 \frac{\partial^2 y}{\partial x^2} \right) + F, \tag{1.16}$$

where the cross section $A(x)$ is variable thus the thickness $b(x)$ is a local variable. Then, the radius of gyration $\kappa(x)$ is also a local variable. This description of the reed was used by Stewart et al. [25] and Sommerfeld et al. [26].

In order to take into account the interaction of the reed with the mouthpiece, Stewart et al. [25] proposed to use varying functions for the reed mass and damping. Sommerfeld et al. [26] used a varying function for the damping to take into account the role of the musician's lip as a damper.

The internal viscoelastic losses can be included as proposed by da Silva et al. [27]. Completing this model with the damping, Avanzini et al. [28] proposed the model given in Eq.1.17.

$$\rho A(x) \left(\frac{\partial^2 y}{\partial t^2} + \gamma_R \frac{\partial y}{\partial t} \right) = -\frac{\partial^2}{\partial x^2} \left[Y A(x) \kappa^2 \left(1 + \eta \frac{\partial}{\partial t} \right) \frac{\partial^2 y}{\partial x^2} \right] + F, \tag{1.17}$$

where the coefficient η represents the magnitude of the internal viscoelastic losses and γ_R accounts for damping of the surrounding fluid.

The interaction of the lip was modelled by Avanzini et al. [28] as a linear spring exerting an elastic force in the region of application of the lip and by an increase of the damping γ_R in this region. The reed-lay interaction was defined as a contact force that acts in the profile of the lay of the mouthpiece $y_{lay}(x)$. The resulting force relating the pressure difference across the reed and the reed tip displacement is linear for low-level displacements and non-linear for large displacements. This was represented with a power law by Chatziioannou et al. [20] in the previous lumped model (Eq. 1.11). Another result of this numerical experiment was that the reed does not smoothly curl up onto the lay of the mouthpiece, but a discontinuity appears. They defined the variable "separation point" as the point of contact between lay and reed that is closest to the tip. The separation point evolves with the amplitude of the reed displacement (so that the free-moving surface of the reed changes) and presents an abrupt change, implying that some reed-lay collisions may occur before the reed tip reaches the lay of the mouthpiece.

In the beam-type models, the torsional modes of the reed and the effect of the ridge in the vamp of the reed can also be taken into account [29–31].

1.1.2.3 Plate models

Some models take into account geometry of the reed vamp, i.e., the fact that the reed is thinner in its borders than in its heart.

Guimezanes [32] used a finite-element thick-plate model of the reed to perform a modal analysis of the vibration of the reed alone. He considered different vamp profiles and different mechanical parameters in order to observe their role in small vibrations of the reed.

Casadonte [33] used a Midlin thick-plate equation describing the reed and including the lip and the teeth, and performed a modal analysis of the system. He simulated the scraping of the reed in different points by varying the reed thickness in the simulation.

Ducasse [29] performed a modal simulation of the reed installed on a mouthpiece and observed the ten first modes of the reed, stating that the torsional models may be affected by the contact with the lay of the mouthpiece and limiting the validity of the model.

1.2 Reed characterisation methods

Multiple methods have been applied to the experimental characterisation of reeds. This section summarizes different measurement techniques for reeds in laboratory or playing

conditions. Some research has been also done in the subjective characterisation of reeds by musicians. The studies concerning subjective characterisation of reeds and its relation with objective measurements are also described here.

1.2.1 Objective measurements of reed properties

Reed makers use calibration techniques that measure the static stiffness of the reed or the hardness of the material. A comparison of these methods with the ease of play experienced by a musician has been performed by Gangl et al. [34]. They used a reed hardness (compliance) tester, measuring the compression of the material when pressing with a spring, and a customized stiffness tester, measuring reed displacement (produced with a weight-beam) and restoring force of the reed (measured with a strain gauge). A classification of a set of reeds by an expert musician in playing conditions was compared with the objective classifications of the reeds using the previous methods, showing that the stiffness measurement is a better indicator than the hardness for the ease of playing.

Optical methods have been applied to the study of the reeds' behaviour and quality. Pinard et al. [35] related the vibrational modes of the reed, installed on a mouthpiece and excited with a loudspeaker, to the quality of the reed as assessed by two professional musicians. They suggested that the presence of symmetry in the first torsional mode could be an indicator of musical quality, as well as the proximity between the second torsional mode and the second flexural mode. They repeated the experiments for dry and wet reeds, obtaining lower frequencies for the wet reeds but the same trends. Taillard et al. [36] compared holographic measurements with numerical simulations to provide a statistical model describing the mechanical properties of the reed. Stetson [37] used digital holography to compare the vibrational modes of cane reeds and synthetic reeds of different brands. He showed that the fundamental modes of cane reeds lie above the range of playing frequencies of the instrument, whereas those of synthetic reeds do not. He showed that the synthetic reeds had fundamental frequencies lower than the cane reeds, both wet and dry. This is an important assessment of the difference between cane and synthetic reeds. He also measured the reed profiles in dynamic conditions under a static flow by real-time fringe interferometry. He showed that the reed exhibits some plastic behaviour and that asymmetry in the displacement may be related to poor musical quality. Picart et al. [38], [39] used digital Fresnel holography to study the reed behaviour under forced excitation, using a loudspeaker, and under auto-oscillations, using an artificial mouth. They showed that the reed, in auto-oscillating regime in a clarinet, exhibits a square-like displacement and that strong impacts are seen in the closing of the reed. These works by Stetson and Picart et al. provide measurement

methods for the reed displacement profile in dynamic excitation, suitable for artificial mouths but not for real playing conditions.

Mukhopadhyay et al. [40] measured electromagnetic impedance of the reed in magnitude and phase using planar electromagnetic sensors and provided a preliminary classification of reeds. The method is a non-intrusive one, but the relation of the provided classification of reeds with standard classifications of reeds is not studied and the usefulness of the measurements is undetermined.

Anatomical indicators of the reeds quality have also been searched using methods in Biology. Casadonte [33] detailed that the cane reed tissue has a thin outer part (epidermis), a middle part (fibre band) and a thick inner part (inner cortex). The epidermis and the fibre band are separated by small vascular bundles. The inner cortex contains stem tissue (composed by parenchyma cells) and larger vascular bundles. The vascular bundles comprise three tissues: xylem, pholem and sclereids (thick fibre rings). He repeated experiments done by Veselak [41], obtaining weak statistical correlations between musical quality and the size of parenchyma cells, the size of the vascular bundles and the number of broken or twisted fibre rings. Kolesik et al. [42] used confocal laser scanning microscopy to determine the relation between anatomical properties of the reed and their musical performance, showing that good musical performance was related to a high proportion of vascular bundles with continuous fibre rings, and bundles with a high proportion of fibre and low proportion of xylem and pholem. Glave et al. [43] performed nuclear microprobe analysis and scanning electron and light microscopy, finding non-concluding statistical relations with the fundamental levels of the elements Si, P, S, Cl, K and Ca with the quality of the reed material. Kawasaki et al. [44] used different microscopic biomechanical measurements to characterise two reeds of different musical quality, reasserting that it is linked to cane with continuous vascular bundles and homogeneous fibre rings. They observed also that the measured Young modulus was lower for the reed classified as higher in strength by the manufacturer, without being able to explain this inconsistency. Kemp et al. [45] performed microstructural analysis of slices of cane and also measured the internal friction using vibro-acoustic excitation in order to study their evolution under mechanical loading and moisture cycling, aiming to reproduce the musicians' use of the reeds. The internal friction was found to be dependent on frequency, moisture and cyclic loading. Microstructural cracks appeared in the fatigue cycles and in the moisture cycles due to local differences in swelling behaviour, contributing to increase the decrement values at high frequencies. They found statistically significant correlations between logarithmic decrement and vascular bundle orientation at 700 Hz (p-value= 0.0435) and logarithmic decrement and parenchyma cell diameter at 1000 Hz (p-value= 0.0259). How the measurements performed by the previous authors [33, 41–43] determine the response of the reed in playing conditions is

unstudied. It would be very interesting to relate these biological attributes to the equivalent mechanical properties of the reed while playing. With the lack of this information, the deterioration measurements done by Kemp et al. [45] seem more conclusive. Kemp et al. also measured an important difference of the vascular bundle orientation within one part of a cane stem, which is a plausible evidence of the variability of reeds.

Mechanical characterisation methods have also been applied to the study of reeds. Lord et al. [46] measured the Young modulus and the loss tangent depending on frequency for sections of dry and wet tube cane using a shaker and ultrasonic transducers, and compared the results with a theoretical model. The dynamic elastic properties of the reed have been measured using mechanical methods by Marandas et al. [47]. He proposed to measure and model viscoelastic behaviour for dry reeds and viscoplastic behavior for wet reeds, the measurement of the reeds Young modulus being insufficient for their classification. The experiments consisted in measuring the recuperation time for a displacement produced using a lever. This work showed that the elastic description of the reed seems insufficient to account for the reed mechanics. The effect of extractives and difference of humidity on cane reed were studied by Obataya et al. [48] measuring the Young modulus and the internal friction using a vibrational method. They showed that the extractives enhanced the stiffness of the dry part of the reed and increased the internal friction at high frequencies under relatively high humidity. The effect of humidity on cane reed tubes has been studied by Akahoshi et al. [49] measuring the Young modulus, loss tangent and resonance frequency from an impact on the cane and using a laser. They observed that the Young modulus and the loss tangent decreased and the resonance frequency increased along wet-dry cycles. These evidences of the different properties of the dry and wet reed were extrapolated to conclude that the reed in playing situation, moist by the musician's saliva, is mechanically different to the dry reed. These results are in the same line that those obtained by Pinard et al. [35] and Kemp et al. [45]. Pinard et al. [35] measured the impact of the wetting of the reeds on their modal response using wet reeds directly measured after a musician uses them. Kemp et al. [45] used artificial wetting conditions, highly controllable, but with no reference of the real wetting in playing conditions.

Guimezanes [32] measured the thickness profile of some reeds, observing strong differences between them and also asymmetries for each reed. He compared vibro-acoustic measurements of these reeds under small oscillations to adjust manually the parameters issued from numerical modal analysis. He showed that the Young modulus and the shear modulus are functions of the thickness of the reed, instead of global variables. Gazengel et al. [50] used a vibro-acoustic bench containing a loudspeaker and a microphone to measure compliance, resonance frequency and Q factor of the reed through modal analysis. Their results showed that the differences in compliance in a set of 50 reeds

identical in cut, brand and strength were correlated to subjective differences in "ease of play". They concluded that small vibrations do not allow for the measurement of the reed properties that are relevant for the musician because playing conditions are characterised by large vibrations, in which the effect of the mouthpiece is not negligible.

1.2.2 Objective measurements in real playing conditions

As discussed in §1.1.2, the mechanical parameters of the reed by itself differ from the equivalent parameters of the lip-reed-mouthpiece system in playing conditions. Furthermore, the way to include the musician's gesture in the model is an unsolved question. Some researchers have developed experimental methods in order to measure the reed dynamics in playing conditions for the estimation of the equivalent reed parameters or the monitoring of the musical gesture. Some of these works provided insight in the physical modelling of the musical gesture and in role of the vocal tract or the tonguing.

Boutillon and Gibiat [51] obtained the linear stiffness of the reed by measuring the pressure inside the mouthpiece while playing, and knowing the impedance of the instrument from a previous measurement. Chatziioannou and Walstijn [20] used a mouthpiece instrumented with three microphones to measure the pressure and the flow in the mouthpiece. From these measurements it was possible to estimate the parameters of the non-linear harmonic oscillator with damping and inertia. Wang et al. [52] proposed a convex optimisation method to estimate the fingering of the played note and the reed stiffness from measured impulse responses of the saxophone and a radiated pressure measurement, though they did not focus in the stiffness measurement. These studies considered a physical model of the entire instrument and not only the reed, requiring some approximations.

Concerning the attack and the tonguing, Chatziioannou et al. [23] used a strain gauge installed on the reed to measure the deformation of the reed during articulations. Li et al. performed measurements of different types of attack using an instrumented mouthpiece [53]. Their measurements showed that tonguing prevented or stopped the reed vibration and allowed to increase or maintain the blowing pressure above the oscillation threshold, managing faster attacks or *staccatos*. Their results agreed with the musical intuition of the musicians participating in the study (the notion of oscillation threshold may be intuitively known by musicians). Also, the measured decay time of tongue-ended notes were similar to those calculated from the bandwidths of the bore resonances. In this study they measured the reed deformation but not displacement. Instead, measuring the reed displacement would allow relating the physical model and the musical gesture.

It would be interesting to calibrate the strain gauge with respect to a displacement measurement. Li et al. [54] reproduced different attacks in an artificial mouth to investigate how blowing pressure, lip force, and tonguing parameters affect transients. Their results showed that large tongue force and acceleration produce more rapid changes in flow, starting notes sooner after the tongue release and also increasing the third harmonic during the transient. They showed a hysteresis region on the pressure-lip force diagram, where regenerative oscillations were not produced spontaneously by increasing blowing pressure only, and where tongue action initiated sustained notes at low pressure.

Concerning the estimation of playing parameters, Petiot et al. [2] used two microphones to measure the pressure in the saxophone bell and inside the musician's mouth. They studied the relation of the estimated playing parameters with the subjective characterization of a set of reeds. Two musicians played a set of 20 reeds, carrying out two sessions with five repetitions of a pattern of notes. The obtained objective parameters were related to the results of subjective tests with a panel of 10 musicians, producing a predictive model. The advantage of the measurements in playing conditions is that the authors were able to measure in realistic conditions with respect to the assessing of reeds' quality naturally performed by musicians, but the method has the disadvantage of introducing variability due to the musicians' gesture.

The role of the vocal tract on the played notes has also been studied. Measurements by Chen et al. [55] and Scavone et al. [56] showed that for low pitch the oscillations are controlled by the impedance of the instrument whereas for high pitches, specially in the *altissimo* register, the oscillations are controlled by the impedance of the vocal tract. Adjustments of the vocal tract also allow the musician to produce throat *glissandi*, as shown by Fritz [57] and Chen et al. [58]. Different measurement techniques to measure the vocal tract resonances have been summarized by Wolfe et al. [59].

1.2.3 Correlation between subjective and objective characterisation of reeds

The assessment of the musical quality or the search for descriptors of timbre are typical issues in Musical Acoustics. In particular, some research concerns the description of the woodwinds timbre or the reeds' quality. There have been attempts to relate some of the objective measurements presented in the previous sections to subjective classifications of reeds according to their quality. In this section, an overview of the subjective classification of reeds and the correlations with objective measurements in static or dynamic conditions is presented.

Some studies deal with the quality and timbre descriptors of musical instruments [60–65]. Some other works are focused in the perception of the sound of the musical instrument [14, 66, 67] and some concern simulated musical sounds [68]. Regarding woodwinds, Gridley [69] studied the description of the saxophone sound using different adjectives, Kendall et al. [70] studied the verbal attributes of simultaneous wind instruments, and Nykänen [71] used verbal attribute magnitude estimation and principal component analysis to identify the perceptual dimensions of verbal attributes describing the saxophone sound. Barthet et al. [72] studied the correlation between timbre, timing and dynamic descriptors and the dissimilarities between simulated clarinet tones with different control parameters or recorded expressive performances [73].

In the reed characterisations performed by Pinard et al. [35] or Stetson [37], one or two expert musicians classified the reeds as good or bad. In the work by Pinard et al., a set of 24 reeds was classified in four categories of musical quality (from "very poor" to "very good") by two expert musicians. Both testers mostly agreed on the classification of the reeds. There seemed to be a relation between the quality of the reeds and the holographic observation of a strong first torsional mode and a minor difference between the second flexural and torsional modes. In this work, they did not perform a statistical analysis of the observed relationships to quantify these correlations. The generalization of the results needed further tests with a greater number of reeds. Stetson [37] compared the displacement of a good and a mediocre reed under a static flow, showing that the displacement presented stronger asymmetries for the mediocre reed than for the good one. However, he only used two reeds and this statement requires a systematic study. In the works by Pinard et al. and Stetson, the relation between the modal response of the reed installed on a mouthpiece and the reed behaviour in playing conditions is not fully developed. In the case of the work by Mukhopadhyay et al. [40], one musician rated in a ten-points scale a set of 25 reeds according to the parameters "ease of attack", "ease of sustenance", and "tone quality" in the low, middle and high registers of a saxophone, and then obtained an average parameter. This processing of the data is questionable. Only the ratings of 8 among the 25 reeds are given for comparison with the objective measurements. The authors stated that the average quality factor is related to the ratio between the reed impedance and the air impedance, but the correlation is not quantified. In these works, the musicians were skilled, but the repeatability of the musicians' assessments of the reeds were not studied to evaluate their performance as reed testers.

Casadonte [33] used the descriptors "overall quality" (bad vs. good), 'timbre' (dark vs. bright), "strength" (soft vs. hard), "noise" (buzzy vs. fluid), "stability" (squeaky vs. stable) and "acoustic strength" (weak-bodied vs. full-bodied). The reeds were rated for these descriptors on a one to seven scale by several highly skilled clarinet students. He

used 80 reeds of different brands and similar force. No repetitions of the tests were performed. The Pearson correlation matrix of the descriptors revealed stronger correlations of the "acoustic strength" and the "noise" with the "quality" (0.731 and 0.623 respectively), weaker correlations between the "stability" and the "timbre" with the "quality" (0.455 and -0.399 respectively), and no significant correlation between "strength" and "quality" (-0.131). On that basis, he studied the relation of these subjective descriptors with objective mesoscopic measurements of the same set of reeds. No significant correlation appeared between the measured "mass" and the subjective descriptors, though a positive correlation was found between the "number of vascular bundles" and the "quality" (0.631).

When testing the reeds, musicians verify the performance of the reed with respect to some musical requirements (as done in [42]). Kolesik et al. asked two experienced clarinetists to classify a set of 150 reeds in three categories ("good", "fair" or "bad") according to their performance in different tasks: ability to produce a clear tone over the range of the instrument, ability to produce clear and rapid articulations over the range of the instrument, ability to produce smooth slurs between high and low notes, ability to play the note F_4 (clarinet pitch) with the conventional fingering in tune, ability to play the note A_6 easily in tune, and ability to play without great effort upward to C_7. For the rest of the work, they retained the 60 reeds classified in the same categories for all the indicators and for both musicians. They found separable groups of reeds corresponding to anatomical features of the vascular bundles in the inner cortex matching the subjective classification of the reeds (vascular bundles with large, continuous fibre rings related to the category of good reeds).

Obataya et al. [48] used the descriptors "sonority", "richness", "softness", "ease of vibration" and "response" in scales from 1 (poor) to 5 (excellent). Their panel of musicians was constituted of 32 professional clarinetists and the reeds were ten commercial reeds. The tests were performed before and after changing the water content or the extractives content of the reeds in three subsets. The descriptors "sonority", "richness" and "softness" decreased under water extraction, and the glucose impregnation seemed to recover the original values of these descriptors and decrease the "ease of vibration" and "response". Their results suggested that the tone quality of the reed was degraded with the removal of extractives. It seems that they averaged the evaluations of the 32 musicians in order to obtain these results. The large amount of musicians participating in the study is an added value of this research, though it would be interesting to analyse the performance of the panel of musicians.

Gazengel et al. [50] used the descriptors "ease of playing", "brightness", "roundness",

"projection" and "global quality". The subjective classification of the reeds was performed by a single expert musician and professional tester. The evaluation of the reeds was repeated three times, concluding a high repeatability in the musician's evaluations. They used a set of 50 reeds with identical cut, brand and strength, and a set containing 150 reeds with 3 different cuts but identical in brand, strength and static compliance. Their results showed that the perceptual space was almost bidimensional for the first set of reeds, and composed by the "ease of playing" (highly correlated to "brightness") and "roundness", and unidimensional for the second set, this dimension being created by all the descriptors (which were correlated). The study of the correlation coefficients between subjective descriptors and mechanical parameters measured on a vibro-acoustic bench showed that the static and dynamic compliance were correlated with the descriptor "ease of playing" for the first set of reeds, while the correlations are too low to make a link between the perceptual space and the objective parameters for the second set of reeds. The use of the subjective descriptors "ease of playing", "brightness" and "global quality" was inspired by the work by Petiot et al. [2].

Petiot et al. [2] used the descriptors "softness", "brightness" and "global quality" for saxophone reeds. The panel of musicians was constituted of 10 musicians and the set of reeds had 20 individuals. The subjective tests included a training phase and an evaluation phase on a continuous scale. The tests were repeated twice. A consonance analysis using Principal Component Analysis showed more agreement in the "softness" (54.6% of variance on the first component) than in the "brightness" (29.3% of variance on the first component) and in the "global quality" (29.2% of variance on the first component). While the musicians were concordant for "softness" and "brightness", subgroups appeared for the descriptor "global quality", which is the descriptor expressing the preferences of the saxophonist. Objective playing parameters (threshold pressure, Spectral Centroid, etc) obtained by two musicians were related to the subjective characterisation of the reeds through data modelling to establish a predictive model of the reed quality. They concluded that objective measurements of less variability, obtained for example with an artificial mouth, may improve the reed classification through a predictive model.

The quality indicators used in the previous works were chosen according to musical practice and intuition. Though the subjective characterisation of the reeds in these studies agrees with these criteria, no scientific support is provided for any of the particular choices. Works specifically concerning the study of the verbal attributes and the selection of the subjective descriptors of the quality of the reed have not been found.

1.3 Artificial mouths

The study of reed mechanics in playing conditions is a common issue in Musical Acoustics. Measurements in real playing conditions are difficult to perform: the accessibility for the instrumentation is limited, and the measurements are barely repeatable due to the musician's musical gesture. In order to deal with this complication, different devices recreating artificially the instrument play have been developed. These devices are commonly known as artificial mouths.

The most extensively used artificial mouths are blowing systems in which the reed, installed on the mouthpiece, is enclosed in a volume that searches to imitate the musician's mouth. A pressure is created in this cavity to produce auto-oscillations. An artificial lip made of some specific material is held against the reed to recreate the musician's embouchure.

In 1940, McGinnis et al. [74] used this kind of device to perform stroboscopic observations of a reed, mounted on a mouthpiece and connected to a clarinet. In this device, the lip consisted in a rubber pad tightened by a screw simulating the teeth. They observed the motion of the reed during a complete cycle: the reed remains closed for half of the complete cycle, and it remains approximately motionless at the position of maximal aperture for roughly a quarter of cycle. They also observed squeaks, associated to transverse modes of oscillation.

In 1961, Backus [75] used an artificial mouth in which the acoustic pressure inside the mouthpiece was measured with a microphone and the displacement of the tip of the reed was observed by means of a photoelectric method. In this case, the teeth and lip were reproduced using a brass wedge with a piece of neoprene foam. The acoustic pressure and reed tip displacement signals were obtained, though they were not calibrated. Backus measured the sound level inside the mouthpiece for soft tones (around 160 dB) and loud tones (around 166 dB), and inside the blowing chamber (around 30 dB lower than the pressure inside the mouthpiece). The reed tip displacement measurements obtained by a photoelectric method confirm the stroboscopic observations by McGinnis et al. Backus observed the reed behaviour for different lip configurations, notes and dynamic levels. For soft tones, the pressure inside the mouthpiece is sine-shaped, while for louder tones it is more squared-shaped.

Wilson et al. [22] investigated the possible modes of operation of a reed-resonant-tube system as a function of the reed damping. They used an artificial mouth with a simplified cylindrical mouthpiece. The reeds of the study were metal reeds of different lengths. Damping variations of the reeds were achieved by attaching non-hardening Perma-gum to the reeds. They showed that the system resonates at the tube mode

for heavily-damped reeds, and at the reed mode (producing squeaks in a clarinet) for lightly-damped reeds.

Thompson [12] used an artificial mouth to measure the playing frequency and a different device to measure the resonance of the reed alone. Comparing both measurements, he studied the role of the reed resonance on the tone production of the clarinet. He found that the reed frequency contributes to the amplitude of harmonics when the frequencies match. He also performed measurements in playing conditions, showing that the musician can adjust the reed resonance frequency from 2 to 3 kHz.

Bak et al. [76] measured the relation between blowing pressure and playing frequency in an artificial mouth. A system enabling the control of the lip force on the reed, the application point of the force and the damping of the lip was used, and the blowing pressure and the acoustic pressure in the mouthpiece were measured. They observed that the playing frequency increases with the blowing pressure for a given lip force.

Van Zon [77] and Gilbert [78] used a prototype of artificial mouth developed by Meynial [79]. A hot wire measured the flow velocity at the entry of the reed channel and an optical system measured the reed tip opening. The distance of the artificial lip to the reed tip and the force of the lip on the reed were controlled, but neither of these variables could be measured. Later, this prototype of artificial mouth was used by Gazengel [80] and Ollivier [81]. In the work by Ollivier, the artificial lip consisted of a cylindrical latex balloon of small diameter (1 cm) in which a piece of foam saturated with water was inserted. The pressure difference between the inside and the outside of the mouthpiece was measured with a differential pressure sensor, and the reed slit opening was measured with a laser beam and a photoelectric diode. In order to detect the contact of the reed with the lay of the mouthpiece, he used a mouthpiece with electric contacts on the lay and a digital-to-analog converter. The measurement showed that, for low blowing pressures, the reed oscillates freely, for higher pressures, it leans on the mouthpiece and the tip oscillates freely, and for even higher pressures, the reed tip rebounds against the mouthpiece before the middle part of the reed makes contact with the mouthpiece. These kinds of reed behaviours have been also discussed by Ducasse [29], Gazengel [80] and Walstijn [82].

Idogawa [83] and Kobata [84] used an artificial mouth for clarinet equipped with a semiconductor pressure gauge measuring the mean blowing pressure, a microphone measuring the mouthpiece pressure, an optoelectronic system measuring the reed tip displacement, and a hot wire anemometer measuring the flow velocity at the entry of the reed channel. They studied the different vibrational states of the clarinet for different blowing pressures, reed openings at the equilibrium (imposed by the lip) and lengths of the reed inserted into the blowing chamber (and respectively lip distance to the reed tip, as the

lip was fixed on the mouth cavity). The artificial lip was made of silicon rubber and the reed was a Bari plastic reed. They found four main regimes of behaviour: a rest regime at low blowing pressures (0-2 kPa), a regime of high pitches or reed squeaks (2-5 kPa), a resonator vibrational state (where continuous frequency shifts are observed, together with jumps to relative harmonics), and a closed reed state for high pressures (above 12 kPa). Transitions between the vibrational states showed hysteresis and, in these boundaries, aperiodic or quasi-periodic states appeared. Regarding the vibrational states classification, they observed a linear relation between the reed aperture imposed by the lip and the distance of the lip to the reed tip. Studying the relation between acoustic pressure in the mouthpiece and reed displacement, they observed that the reed movement is restricted by the lip and the mouthpiece, but they did not find a model for this phenomenon.

Some authors have performed measurements in artificial mouths in quasi-static conditions. In these conditions, the reed does not oscillate, and the characteristic of the reed can be statically observed from the opening to the closing position. Benade [85] attained the quasi-static conditions by increasing the losses of the instrument filling the resonator with fiber glass. Ollivier [81] and Dalmont et al. [16] achieved the same goal by using a diaphragm upstream in the resonator to increase the losses and attaching an additional mass to the reed. Two pressure sensors on each side of the diaphragm allowed them to measure the air flow. For this experience, they used a Plasticover synthetic reed. This same artificial mouth could also work in dynamic conditions by removing the mass on the reed and the diaphragm at the entry of the resonator. Later, Dalmont et al. [86] used the artificial mouth in quasi-static and dynamic conditions to investigate the oscillation and extinction thresholds of the clarinet. Muñoz Arancón et al. [87] used an artificial mouth with a longer or a shorter resonator to control the losses and achieve either quasi-static or dynamic excitation of the reed.

Mayer [88] developed an artificial mouth and tested the response of two synthetic reeds (Plasticover and Fibracell) and a cane reed. He compared the responses of the synthetic reeds and the response of the natural reed in wet and dry conditions. He showed that the dry reed needs slightly higher pressure and twice as much lip contact pressure to oscillate.

Bergeot et al. [89] used a pressure-controlled artificial mouth [90], equipped with a servo-valve, to study the dynamic oscillation thresholds of the clarinet and the appearance of bifurcations. The closed-loop pressure control allowed them to regulate the blowing pressure time profile with high precision. This same principle was used in the artificial mouth employed by Doc et al. [91] to study the influence of the control parameters and the bore inharmonicity in the oscillation regimes of the alto saxophone. In this

artificial mouth, the artificial lip was made with a latex tube filled with water through a syringe, which controlled the bearing force of the lip on the reed and consequently the reed opening. A model [16] of the non-linear characteristic of the exciter relating the maximal flow and the maximal pressure in the entry of the reed channel allowed them to estimate the control parameter 'maximal aperture of the reed' from the direct measurements of input flow and blowing pressure in the artificial mouth. The parameters maximal aperture of the reed and blowing pressure were used as control parameters. They showed that quasi-periodic oscillations appear when inharmonicity exists, and that the change of the control parameters can strongly modify the modulation frequency, even if the inharmonicity is constant. Ferrand et al. [92] showed that the dynamic pressure obtained in the artificial mouth as a function of the blowing pressure strongly depends on the embouchure configuration, in coherence with the results obtained by Dalmont et al. [86].

Artificial mouths can also be used for the testing of musical instruments, as did Noreland et al. [93]. They optimized numerically the tone hole geometry of a clarinet, built a prototype, and tested it with a mouthpiece and a Plasticover reed in an artificial mouth.

Another use of artificial mouths is their application the development of mechanical musicians, also including fingering systems and eventually an artificial tongue. Solis et al. [94] have gathered some references. In that work, the principle of the Waseda saxophonist, with anthropomorphic design, is explained. The artificial lip of the Waseda robot [95] is made of a thermoplastic rubber, and a T-shaped metallic pin is used to mimic the teeth. Almeida et al.[96] developed a mechanical clarinetist with robotic fingers and an artificial mouth to perform an automatic cartography of the produced sound as a function of the blowing pressure, the lip force on the reed and the position of application of the lip on the reed. In this artificial mouth, a leak valve in the air-tight chamber and a servo-tongue are included to precisely control different musical attacks. The artificial lip is a layer of flexible plastic pushed against the reed by a rigid, curved plate controlled by two servo-motors forcing the plate onto the reed from its extremities and controlling its force and position by their relative action. The authors plot the constant-frequency lines and constant-intensity lines in the characteristic lip force vs. blowing pressure for the measured playing range. Their repeatability tests showed that the calibration of the control parameters is very sensitive to small changes in the reed, the mouthpiece and the initial position of the lip.

In a later model [97] of this artificial mouth, the artificial lip was replaced by a rectangular prism of polyurethane foam with three engraved lines enabling the installation of a steel bar hanging a mass and applying a constant force on the reed. The system was used to explore how the artificial-mouth control parameters (blowing pressure, lip

force and lip position), in combination with the reed stiffness, affect pitch, sound level and spectrum. Three different kinds of synthetic reeds of two different strengths were used in the experiment. Regarding the influence of the lip position, they found that the long-bite embouchure requires much higher lip forces to play than the middle position, and a wide region produces squeaks (probably because of reduced damping [22]), and the short-bite embouchure requires lower forces, produces weaker higher harmonics and less stable frequency. With respect to the influence of the reed stiffness, they found that a stiffer reed restricts the range of frequencies that may be played with a given fingering, and that squeaks are produced for moderate values of lip force while they are not produced for softer reeds. They obtained also experimental confirmation of the reed fatigue: the reeds become softer with their use. Using this same artificial mouth with an artificial tongue controlled by a lever with a mass, Li et al. [98] showed that the use of the tongue allows accessing the lower threshold pressures obtained in decreasing sense when hysteresis exists even in increasing pressures.

Artificial mouths have also been developed for the study of brass instruments [99], human voice [100, 101] or double reed instruments [1, 102].

Almeida et al. [1] used the same principle than Dalmont et al. [16] to measure the quasi-static characteristic of double-reed instruments in an adapted artificial mouth. Grothe [102] investigated the influence of the control parameters (blowing pressure and lip force on the reed) on the produced frequency, and characterized these embouchures through the reed parameters estimation obtained from the non-linear characteristic of the instrument. The lip is mounted on a load cell such that the integral force exerted to the lip can be measured. This artificial mouth operates both in quasi-static and in dynamic conditions.

In the majority of the aforementioned works, the artificial mouth is set in a given configuration for the all measurements, generally one characterised by a satisfying sound. This criterion is subjective and should be substituted by objective foundations. Only some authors [83, 97] characterised the complete working range of the artificial mouths leading to oscillations. The repeatability of the measurements using artificial mouths is not quantified in the previous works. Furthermore, the comparison of the measurements produced with an artificial mouth with the real playing of a musician has never been done.

The use of artificial mouths makes it possible to measure the reed displacement in playing conditions using optical methods (laser, vibrometer, etc) that cannot be used in real playing conditions. Concerning the control parameters of the artificial mouths, it is clear that one of the parameters is the blowing pressure, but the parameters describing the embouchure are less consensual and harder to measure. Some authors use reed tip

opening and others lip force or equivalent. Different kinds of artificial lips are used, and their realism is unstudied. Only a work by Guimezanes [32] compares the response of a musician's lip with the response of artificial lips.

In these artificial mouths, the reed remains enclosed in a cavity and is hardly accessible. Most of the works used synthetic reeds, which are more resistant and stable in time. In some cases, authors used wet cane reeds. However, the humidity of the reed is difficult to control and measure, and they vary with the ambient conditions (this was done, for example, in [1]).

1.4 Summary

The behaviour of the reed in playing conditions has been described in the literature using many physical models. However, the experimental observation of the reed behaviour remains challenging. Measurement techniques of different nature have been applied to objectively characterise the reed, but most of them cannot be used in playing conditions or require physical approximations. Although many descriptors have been proposed, no clear candidates to describe reed quality have emerged. The use of artificial mouths facilitates the observation of the reed in playing conditions. However, the similarity of the artificial excitation of the reed with the real playing is not assessed in the literature.

Chapter 2

Estimation of saxophone reed parameters during playing

This chapter contains the article "Estimation of saxophone reed parameters during playing", published in the Journal of the Acoustical Society of America [3], and two complements. The motivation of this study is the need to characterise the behaviour of reeds in playing conditions, in order to better understand their perceived differences in quality.

The article presents an instrumented mouthpiece that measures the reed displacement and the pressure difference across the reed in playing conditions, and a method for the estimation of equivalent reed parameters. The system is applied to a cylindrical resonator and one reed. The displacement measurement uncertainties are studied and their repercussion on the estimated parameters is assessed using a Monte-Carlo method. Reed models of different complexity are implemented, and their accuracy is compared for different dynamic levels.

The first complement to this article (§2.9) presents the application of the method, validated for one reed and a cylindrical resonator, to measurements using a saxophone and a set of 20 reeds in order to study the accuracy of the physical models of the reed behaviour in this instrument.

The second complement (§2.10) is a qualitative comparison of measurements using the instrumented mouthpiece for different musical gestures of a semiprofessional saxophonist and a beginner, with pedagogic interest. This work was presented in the symposium "Learning and Teaching Music in the Twenty-First Century: The Contribution of Science and Technology" [103].

The Computer-Aided Design drawings of the instrumented mouthpiece are given in Appendix A of this document. The principle and conditioning of the displacement sensors

and the study of the uncertainties in the reed displacement measurements are detailed in Appendix B. The explicit implementation of the reed models for the parameter estimation is explained in Appendix C.

It is important to note that the reference frame used in the physical model in the article is not the one used in Chapter 1. In this case, the reed displacement is positive and it varies from 0 (closed reed position) to H (maximal opening). The reason of this change is that it allows taking into account the fact that the maximal aperture of the reed is a slowly varying function depending on the musician's embouchure. The reed position $y = 0$ must not be mistaken with the rest position of the reed.

Estimation of saxophone reed parameters during playing

Alberto Muñoz Arancón, Bruno Gazengel, Jean-Pierre Dalmont, Ewen Conan.
Laboratoire d'Acoustique de l'Université du Maine
UMR CNRS 6613, Avenue Olivier Messiaen,
72085 Le Mans cedex 9, France

Abstract

An approach for the estimation of single reed parameters during playing, using an instrumented mouthpiece and an iterative method, is presented. Different physical models describing the reed tip movement are tested in the estimation method. The uncertainties of the sensors installed on the mouthpiece and the limits of the estimation method are studied. A tenor saxophone reed is mounted on this mouthpiece connected to a cylinder, played by a musician, and characterized at different dynamic levels. Results show that the method can be used to estimate the reed parameters with a small error for low and medium sound levels (*piano* and *mezzoforte* dynamic levels). The analysis reveals that the complexity of the physical model describing the reed behavior must increase with dynamic levels. For medium level dynamics, the most relevant physical model assumes that the reed is an oscillator with non-linear stiffness and damping, the effect of mass (inertia) being very small.

2.1 Introduction

In reed instruments, the physics of the sound production is closely related to the reed response. However, the variability of the reed properties and their role in the instrument behavior and musical quality perception are to date not well understood.

In order to minimize the variability of cane reeds, reed makers measure the strength of the reed using a static measurement bench giving an estimation of the reed's mechanical stiffness. However, reeds from the same manufacturer, with the same cut and the same strength can lead to large differences in the musician's subjective perception of the reed's quality. Indeed, the reed has an effect on the ease of playing, timbre [2] and also intonation. This variance is usually considered as a major drawback by players and also manufacturers, who would like to minimize it.

Different approaches have been pursued to understand or minimize these variances, but today this remains a big issue. Reed makers have developed different experimental systems to characterize the static stiffness of reeds [104, 105]. Some manufacturers offer musicians special packaging in order to keep the reed at a constant hydrometry rate.

Researchers have explored different ways to understand the link between the physics of reeds and the musicians' perception of their quality. It seems that no system measuring the static stiffness of the reed has been presented in the scientific literature. Different researchers have developed measuring devices in order to observe the reed movement while excited by an artificial mouth. Dalmont et al. [16] developed a measuring device to characterize the quasi-static stiffness of a reed mounted on a mouthpiece and excited in an aeraulic manner. Other researchers have characterized the vibroacoustic behavior of reeds using acoustic excitation. Obataya [48] characterized cane reed plates cut from cane tubes using an acoustic excitation and estimated the Young modulus and loss factor. Pinard et al. [35], Facchinetti et al. [31] and Taillard [36] studied the vibration modes of reeds using optical holography. They showed that the reed alone exhibits many vibration modes without any lip acting on it. The analysis of these modes allows estimating the properties of the cane reed material. Gazengel [106] proposed measuring the vibration response of reeds mounted on a mouthpiece with and without an artificial lip using a displacement sensor, addressing the relationship between the reed, the mouthpiece and the musician's lip together to fully understand the reed behavior. This experiment enabled the observation of the first four modes of the reed but the results varied with the reed hydrometry and the estimated parameters were not repeatable. Finally, some experiments have also been conducted on reeds played using an artificial mouth. Idogawa [83] showed that it is possible to measure the displacement of the reed tip as a function of the pressure, but he did not estimate any equivalent parameters of the reed. Using

optical holography and an artificial mouth, Picart [38] showed that the reed movement at the reed tip is complicated and different phenomena occur when the reed is open or closed on the mouthpiece.

In all the works mentioned above, the reed was characterized under artificial excitation, and no direct measurement of the reed movement was done in real playing conditions. It seems that the main difficulty is in characterizing the reed equivalent parameters in playing conditions.

The aim of the work presented here is to estimate the reed parameters in playing conditions. It uses an instrumented mouthpiece based on previous developments [107, 108] and on different physical models employed in the literature. The performance of this mouthpiece and the performance of an estimation method which gives numerical values of equivalent parameters of the reed obtained during a real playing situation are assessed. Different physical models describing the reed behavior in growing complexity are implemented to obtain the reed parameters by inverse estimation. The quality of the estimation enables an assessment of the models describing the reed behavior in playing conditions.

Section 2.2 presents the state of the art of the study of single reeds behavior. Section 2.3 presents the different models that are used for explaining the reed displacement, including non-linear models describing the fact that the reed bends against the mouthpiece lay. Section 2.4 describes the instrumented mouthpiece by introducing the implemented sensors and calibration techniques. This section concludes with examples of the measurements taken in playing conditions. Section 2.5 explains how the equivalent parameters in the model can be estimated from the measured signals. The convergence and the accuracy of the estimation method are also discussed. In Section 2.6, some results obtained for different dynamic levels are given. The order of magnitude of the reed parameters is also provided and the relevancy of the physical models is discussed. Finally, Section 2.7 presents conclusions and perspectives of this work.

2.2 State of the art

In this section, the classical models describing the reed behavior by means of mechanical parameters are presented. Different experimental methods employed to obtain reed parameters are summarized afterwards.

2.2.1 Reed modelling

In 1961, J. Backus [75] observed the reed motion and the pressure inside the mouthpiece in artificial playing conditions on a blowing machine, however, no magnitudes or physical models are presented in this work. The reed is stated to be stiffness controlled, and a phase shift of the reed displacement with respect to the pressure is observed. It is hypothesized that this shift is produced by the reed mass. In 1963, Backus proposed a small-vibration theory of the clarinet [109] in which the reed is characterized by a Single Degree Of Freedom (SDOF) oscillator. Different effects of the deformation of the reed on the lay of the mouthpiece are observed by Backus, but the modelling of these effects is not considered.

Simplifications of the SDOF oscillator are extensively used in the literature. Nederveen [110] proposed to neglect the mass of this model, as the frequency of the reed is typically 10 times higher than the playing frequency in the low register. Kergomard [19] proposed to neglect mass and damping to simplify the model, studying the generation of auto-oscillations of the musical instrument. This allowed the authors to discuss the relationships between initial conditions, transients, steady-state regimes, stability, spectrum and player's control of the instrument. This same approximation was used by Boutillon and Gibiat [51] to measure the stiffness of the reed in real and artificial conditions through the reactive power balance approach. In fact, when auto-oscillations begin (beginning of the transient), the low level approximation of the harmonic oscillator is always valid, assuming the oscillations of the instrument are sine shaped [17, 85, 97].

The role of the reed damping in the operation of the clarinet (for the linear oscillator model) was studied by Wilson and Beavers [22]. They showed that for heavily damped reeds such as those of the clarinet, the instrument plays at the low register of the instrument bore and not at the natural frequency of the reed. Theory and measurements were compared by using an artificial blowing machine to excite a simplified reed-cylinder system. Silva et al. [111] systematized and improved this work to study the oscillation threshold and the emergence of instability. Idogawa [83] performed measurements of reed characteristics in a dynamic regime with a synthetic reed mounted in an artificial mouth, observing some damping.

The effects of the reed resonance on the spectrum of the instrument were studied by Thomson [12] and later by Fletcher [13], adopting the linear oscillator model with mass, damping and stiffness.

Stewart and Strong [25] proposed a functional model of a simplified clarinet in which the beating of the reed on the mouthpiece can be taken into account, describing both the small and large amplitude reed oscillations. They modeled the reed as a clamped

bar with linear mass, damping, stiffness and Young modulus. They also stated that non-linear models for mass and stiffness should be considered to describe the bending of the reed on the mouthpiece, and a more accurate study of the contribution to the damping due to the player's lip should be developed. Sommerfeldt and Strong [26] used this same model to investigate the influence of the player's vocal tract while playing. They developed a system that enables the measurement of the displacement of the reed in playing conditions.

The need for describing the curvature of the reed on the lay of the mouthpiece was argued by Hirschberg [15]. Ducasse [112] described this effect by taking into account a non-linear stiffness. Experimental evidence of this non-linear stiffness was provided by Dalmont et al. [16], showing that the reed rolls up after a mainly linear regime.

Avanzini and Walstijn [28] used a distributed model to simulate the reed, considered as a non-uniform clamped-free bar, also taking into account the role of the lip in the reed motion by adding a conditional stiffness and damping. They found a non-linear stiffness and a separation point in the reed bending on the lay of the mouthpiece, whose experimental evidence was shown by Dalmont [16] and Ollivier [81]. Avanzini and Walstijn [113] stated that the linear oscillator model can only be used for small amplitudes, where the interaction between the reed and the mouthpiece lay is not significant, and they proposed a non-linear stiffness depending on the variable free moving surface of the reed.

The non-linearity of the stiffness was proposed to be modeled by a conditional power law by Bilbao [114], inspired by hammer-string interaction. This formulation was adopted by Chatziioannou and Walstijn [20] to estimate the clarinet reed parameters by inverse modelling.

Picart et al. [38] used an artificial mouth equipped with a digital holography system to measure the reed tip displacement as a function of time. Results showed that, during the closing, the reed strikes the mouthpiece strongly, and during the opening, the reed is subjected to flexural modes combined with torsion modes. Such modes cannot be taken into account by the 1-D models cited above. Chatziioannou [30] proposed a 2-D model of the reed and the lip interaction which is not used in this work.

2.2.2 Experimental characterization of the reed

Some researchers have suggested characterizing the reeds by using static or dynamic methods. In most of these experiments, synthetic reeds were used, as they are easier to play artificially.

Some authors have aimed to obtain the reed stiffness in static regime. This kind of measurement is privileged in the commercial domain because of the accessibility of its implementation. For the musician, reeds are characterized by their strength, usually measured with a mechanical device which imposes a static deflection of the tip. Some devices have been patented [104, 105], and some other specific systems are used by craftsmen.

In contrast with the measurements presented above, some authors have used aeraulic measurements to study the reed while it is installed on a mouthpiece. One characterization of the reed consists in determining the reed non-linear stiffness. For this, Dalmont [16] and Ferrand [115] measured the different physical quantities (pressure drop ΔP, volume flow velocity U and reed displacement y) in a quasi-static manner. Their results, obtained for a Plasticover reed (reed recovered with a film of plastic) and a Fibracell reed (cells filled with resin), showed that the quasi-static characteristic of the reed obtained on a measurement bench has a linear part and a non-linear part, and exhibits some hysteresis. Observations indicated that the expected characteristic of a reed is a non-linear stiffness, *a priori* due to the bending of the reed against the lay of the mouthpiece. Almeida [1] compared these results to the equivalent ones obtained for double reeds.

Some authors [35, 36, 48] have characterized the mechanical response of the reed using different vibroacoustic benches. In all these cases, the reed was excited with an acoustic field at a low level (100 to 110 dB SPL) compared with the level measured in a clarinet or saxophone mouthpiece (140 to 160 dB), leading to very low displacements (some μm). Gazengel [106] used a measuring bench, a tenor saxophone mouthpiece and an artificial lip placed on the reed. The physical quantities considered in this study are the acoustic pressure in the mouthpiece (created by a loudspeaker) and the reed tip displacement. An algorithm based on a least mean squares method was used to estimate the different reed parameters (equivalent mass, stiffness and damping for mode 1). The reed parameters obtained at different dates with this bench did not show a good repeatability. This suggests that the mechanical properties of reeds change significantly over time due to environmental effects, as experienced by musicians. These time-evolving mechanical characteristics of reeds were also found by Marandas *el al.* [47] and Taillard [36].

However, reed behavior in static regime and low-level dynamic regime is not the normal behavior while playing. In playing conditions, the reed is installed on a mouthpiece, and the interaction of the reed with the player must also be considered. Some studies have tried to reproduce playing conditions artificially, at high excitation level (140 to 160 dB SPL). Backus [75] presented the principle of an artificial mouth approximating the playing conditions of a clarinet, allowing the observation of the pressure inside the mouthpiece and the reed displacement. In this very first work, no calibration of

the measurements was done, so no physical magnitudes could be extracted. Later, comparison of the calibrated measurements with the model of a harmonic oscillator allowed Backus [109] to provide some values for the quality factor of the reed and the resonance frequency. Thompson [12] used an artificial blowing machine to produce auto-oscillations. A microphone installed in the mouthpiece allowed for the study of the role of the reed resonance in the instrument's spectrum.

Boutillon and Gibiat [51] obtained the linear stiffness of the reed in artificial and playing conditions by measuring the pressure inside the mouthpiece while playing, and knowing the impedance of the instrument from a previous measurement. However, the approximations used in the physical model of the instrument biases this indirect measurement of the stiffness.

Chatziioannou and Walstijn [20] used a mouthpiece instrumented with three microphones, which made possible to measure the pressure and calculate the flow in the mouthpiece. From these measurements it was possible to estimate the parameters of the non-linear harmonic oscillator described by a non-linear stiffness with damping and inertia, in playing conditions.

When aiming to measure the reed parameters, two variables of the model of the musical instrument must be measured simultaneously. Such measurements were only done by Boutillon [51] and Chatziioannou [20]. In both cases, the whole instrument model had to be considered in order to obtain the indirect measurement of the reed parameters. In this work, we propose a system that provides direct measurements of both displacement and pressure difference, allowing for the study of the reed motion separately from the whole instrument model.

2.3 Implemented models

In order to perform the inverse estimation of the reed parameters, some of the physical models referenced above have been implemented. Only 1-D models have been selected for implementation. In these models, the reed behavior is written as a function of the reed displacement and the pressure difference across the reed channel. These variables are presented in Fig. 2.1.

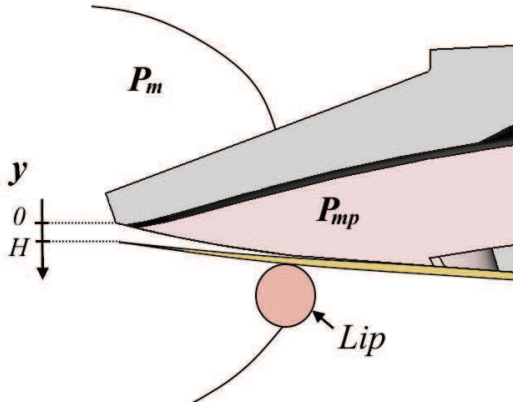

FIGURE 2.1: Schematic view of the mouthpiece-reed-lip system showing the physical variables employed in 1-D physical models to describe the reed in playing conditions.

The variables in the 1-D model are (Fig. 2.1):

- P_m, pressure in the player's mouth,
- P_{mp}, pressure inside the mouthpiece,
- y, displacement of the tip of the reed (where $y = 0$ represents the closing position and $y = H$ represents the maximal opening of the reed tip). Note that y is positive and refers to the aperture of the reed from the closed position to its maximal opening.

The reference reed model is the harmonic oscillator with inertia and damping, for which the motion of the reed in playing conditions can be described by:

$$M\ddot{y}\,(t) + R\dot{y}\,(t) + K(y(t) - H) = -\Delta P\,(t)\,, \tag{2.1}$$

where

$$\Delta P\,(t) = P_m - P_{mp}\,(t)\,, \tag{2.2}$$

and M, R, K are respectively the mass, damping and stiffness equivalent to the reed in playing conditions. Eq. 2.1 shows that the reed is beating for $\Delta P\,(t) \geq KH$, the closing pressure being $P_C = KH$.

To describe the non-linear deformation of the reed on the mouthpiece, we adopt the power-law stiffness formulation used by Bilbao [114] and Chatziioannou [20], in which the stiffness of the reed is described by Eq. 2.3, substituting the constant K in Eq. 2.1.

$$K_{nl} = \begin{cases} K - \frac{k_c(y_c - y)^\alpha}{y(t) - H} & \text{if} \quad y < y_c, \\ K & \text{if} \quad y \geq y_c. \end{cases} \tag{2.3}$$

Coefficients k_c and α describe the bending of the reed on the mouthpiece lay ($\alpha = 2$ as suggested by Chatziioannou [20]). When the reed reaches the position y_c, the power law characterized by k_c and α, describing the reed-mouthpiece interaction, becomes active.

The studied models are obtained from Eq. 2.1 considering the linear stiffness (models with subscript l hereafter) or the non-linear stiffness (models with subscript nl hereafter). Different complexity levels are considered, including the parameters shown in Table 2.1. The nomenclature of the models used in the study is also shown in Table 2.1. For example, the RK_{nl} model contains damping (R) and non-linear stiffness K_{nl}. As shown in Tab. 2.1, this model contains the parameters H, K, R, k_c and y_c.

TABLE 2.1: Summary of the equivalent reed parameters involved in the physical models implemented in this work.

		Model name					
		K_l	RK_l	MRK_l	K_{nl}	RK_{nl}	MRK_{nl}
Estimated parameters	H	X	X	X	X	X	X
	K	X	X	X	X	X	X
	R	-	X	X	-	X	X
	M	-	-	X	-	-	X
	k_c	-	-	-	X	X	X
	y_c	-	-	-	X	X	X

2.4 Experimental system

In this section, the experimental system that enables the study of the reed motion is described. Firstly, the general principle is summarized, secondly the calibration of the sensors is explained, and finally some measurements are shown.

2.4.1 Description

An adapted mouthpiece is designed allowing for the placement of different sensors. This mouthpiece is a prototype made by 3D printing from the numerical version of a commercial mouthpiece. The digitization of the original model is made by tomography. This numerical model is modified in order to install different kinds of sensors. The final model produced by CAD (computer-aided design) is shown in Fig. 2.2. The model is printed in nylon (PA12).

Three different types of sensor are installed on the instrumented mouthpiece, as shown in Fig. 2.2:

- 2 pressure sensors (Endevco 8507-C2): one measuring the pressure in the musician's mouth (P_m in the physical models), one measuring the pressure inside the mouthpiece (P_{mp} in the physical models);
- 2 photointerruptors (Kodenshi SG2BC) measuring the reed displacement y on both sides close to the tip. More details of their implementation are given in Section 2.4.2;
- 2 accelerometers (accelerometers PCB Piezotronics 352C23 associated to a PCB Piezotronics 482C Series conditioner), situated next to the lay of the mouthpiece, in order to detect the beating of the reed on the mouthpiece.

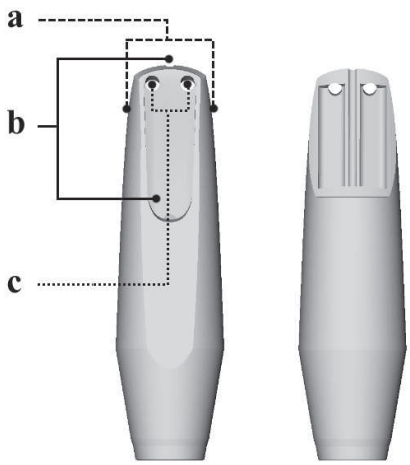

FIGURE 2.2: CAD model of the instrumented mouthpiece. The positions of the sensors are indicated in the figure as follows: a) accelerometers, b) pressure sensors, c) photointerruptors.

The measurements are taken by means of a National Instrument BNC-2110 acquisition card with a sampling frequency of 50 kHz.

2.4.2 Calibration

The static calibration of the pressure sensors is done by comparison with hydrostatic level measurements. The dynamic relative calibration of the pressure sensors is done by using a loudspeaker in a small cavity. The bandwidth of both sensors is 0-5 kHz and they show good phase matching.

The principle of the photointerruptors is presented in the Appendix (§2.8). The displacement sensors enable the measurement of the distance from the sensors to the point of the reed they face. Their position being slightly inside the mouthpiece, they measure both the displacement of the reed and the deformation of the reed inside the mouthpiece due to the transverse bending under high blowing pressure, providing some negative values for the displacement y (see criterion in Fig. 2.1). This effect complicates the detection of the reed channel closing time. The closing time estimation is improved by using accelerometers to detect when the reed strikes the mouthpiece.

A linear approximation of the sensors' sensitivity is acceptable within the reed displacement range in playing conditions as shown in the Appendix (§2.8, Fig. 2.6). Under this approximation, the calibration consists in measuring two parameters: the voltage at the closing point of the reed and the linear sensitivity of the sensors. The static calibration of the sensitivity is carried out with a controlled mechanical system pressing the reed towards the mouthpiece and whose displacement is measured by a micrometric screw. The closing voltage calibration is done while playing by using the accelerometers, which provide better accuracy than the static calibration. This technique minimizes some phenomena that bias the calibration (see Appendix in §2.8 for more details).

The detection of the closing time can be done while playing if the beating of the reed against the mouthpiece happens (*forte* dynamic levels). Two accelerometers positioned next to the lay of the mouthpiece measure the impact, and the voltage measured by the photointerruptors at this time can be associated to the closing point of the reed. For small amplitude measurements (*piano*), where impact does not happen, the closing voltage is assumed to be the same as that for *forte*, if both dynamic levels are measured successively. The quantification of the uncertainty associated to these measurements is presented in the Appendix (§2.8).

The dynamic calibration of the photointerruptors is made by comparison to a displacement sensor Philtec RC62 [116] in its linear behavior range, while exciting the reed on the measurement bench presented by Muñoz Arancón [87]. The estimated sensors' bandwidth is 0-2 kHz.

2.4.3 Measurements

Measurements are taken in playing conditions at increasing dynamic levels: *pianissimo*, *piano*, *mezzoforte* and *forte*. The *pianissimo* dynamic level is measured in artificial playing conditions and the *piano*, *mezzoforte* and *forte* dynamic levels are measured in real playing conditions.

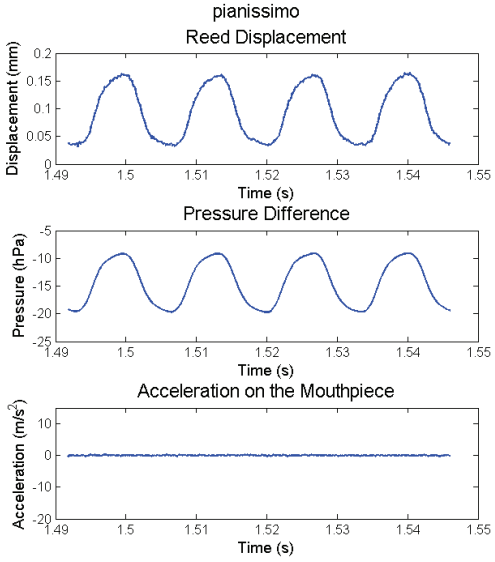

(a) *pianissimo* (artificial playing conditions)

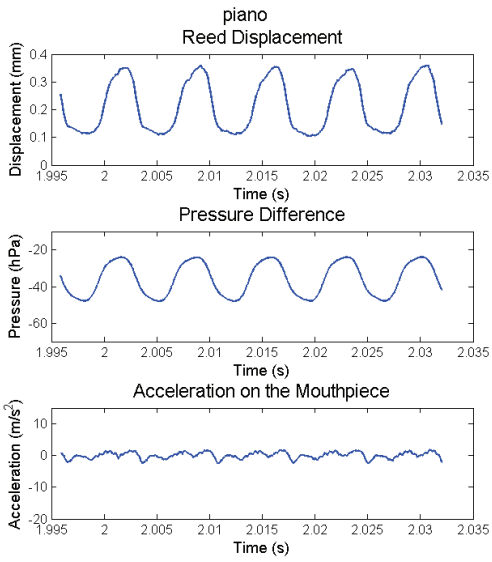

(b) *piano*

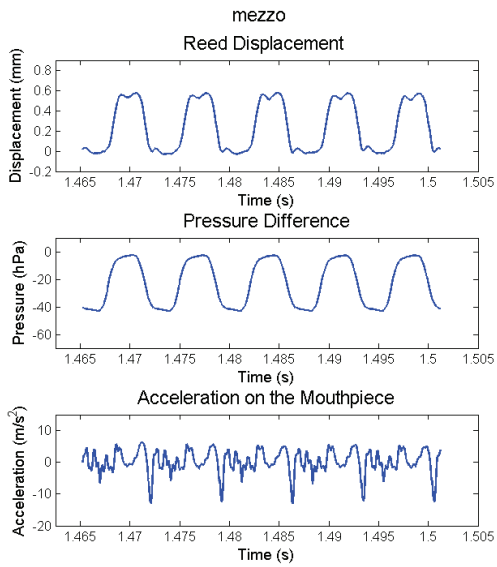

(c) *mezzoforte*

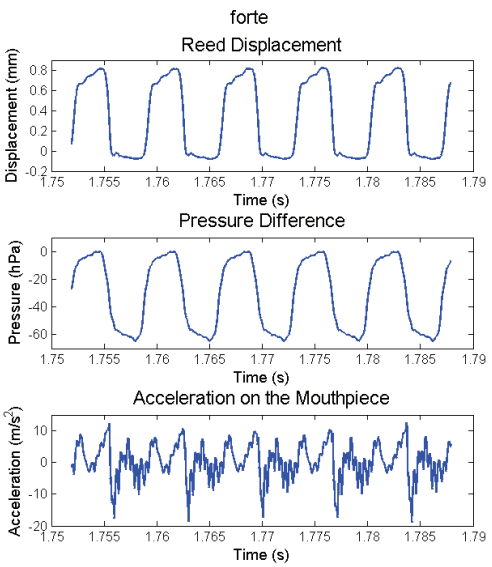

(d) *forte*

FIGURE 2.3: Measurements in playing condition for different dynamic levels. Reed displacement, pressure difference across the reed, and acceleration on the lay of the mouthpiece are presented.

The instrumented mouthpiece can be installed on an artificial mouth. For example, the mouthpiece can be installed on the artificial mouth, playing a 1 m long cylindrical pipe, whose principle is described by Muñoz Arancón [87]. The use of an artificial mouth can provide highly repeatable measurements and access to playing regimes hardly maintainable by players. In Fig. 2.3(a), a measurement obtained close to the excitation threshold (*pianissimo* dynamic level) is presented. In this figure, the measured displacement of the reed, the pressure difference between the inside and the surroundings of the mouthpiece, and the measured acceleration on the mouthpiece are shown. The sound level measured in the mouthpiece is 146 dB SPL. For the *pianissimo* dynamic level reached with this set-up, no beating of the reed on the mouthpiece is detected (Fig. 2.3(a)). The difference of pressure is approximately sinusoidal, and so is the displacement of the reed.

Three dynamic levels (*piano*, *mezzoforte* and *forte*) are measured in real playing conditions. For this purpose, the instrumented mouthpiece is installed on a resonator (a simplified clarinet consisting in a 40 cm long cylindrical pipe with 1.4 cm of inner diameter) and played by a musician. The different behavior of the reed in *piano*, *mezzoforte* and *forte* dynamic levels can be observed in Figures 2.3(b), 2.3(c) and 2.3(d) respectively. In these figures, the measured displacement of the reed, the pressure difference between the mouthpiece and the musician's mouth and the measured acceleration on the mouthpiece are shown for the different dynamic levels [1]. In order to ease the comparison of displacement and pressure difference, the plots show the pressure difference between the musician's mouth and the inside of the mouthpiece, which includes the negative sign employed in the physical model (see Eq. 2.1). Their corresponding sound levels measured inside the mouthpiece are 153 dB SPL, 158 dB SPL and 162 dB SPL.

In Fig. 2.3(b), some properties of the *piano* dynamic level can be seen, for example, the reed does not reach the closing point and the difference of pressure is centered in the static pressure produced by the musician (mouth pressure). In this dynamic level, the pressure contains only some harmonics of a square signal. The closer the auto-oscillations are to the oscillation threshold, the more sinusoidal is the difference of pressure driving the reed movement [17, 85, 97]. Fig. 2.3(b) shows some deformation of the reed on the lay of the mouthpiece. This is more easily seen in Fig. 2.5(b) (ΔP vs. y plot), which is presented further below. No impact is detected by the accelerometers.

For the *mezzoforte* dynamic level (Fig. 2.3(c)), the reed reaches the closing point. An impact is observed in the acceleration and displacement signals, and the pressure

[1] Note that the scales of the displacement and the pressure difference plots are different in each dynamic level, for readability.

becomes more squarely shaped. A free oscillation of the reed can be seen when the reed is open at around $y = 0.5$ mm.

For the *forte* dynamic level (Fig. 2.3(d)), the reed beats strongly on the mouthpiece and some negative values for the displacement are obtained, produced by the movement of the reed inside the mouthpiece due to transverse deformation. Strong impacts are detected by the accelerometers. Some free oscillations of the reed can be seen in the displacement signal for $y = 0.7$ mm (this is more easily seen in the ΔP vs. y plot of Fig. 2.5(d) further below).

2.5 Estimation method

This section presents the method implemented to estimate the reed parameters. The estimation method relates the two variables, measured displacement and measured pressure difference across the reed, of each of the implemented physical models through the optimization of the model's parameters. The parameters of the model are obtained through an iterative method. The different models presented in Section 2.3 are thus compared, assessing the relevancy of the models for different dynamic levels.

2.5.1 Principle of the parameter estimation method

The general principle of the estimation method is depicted in Fig. 2.4. A reed displacement y_{calc} is calculated from the measured pressure difference P_{meas} through a given physical model with reed equivalent parameters θ (K, R, ..., as summarized in Table 2.1). The method is initialized with a set of parameters θ_0. A loop minimizes the difference ϵ between calculated displacement and measured displacement through adjusting the reed parameters θ_{adj}. The algorithm iterates until producing the optimal set of parameters θ_{est}, and an error function $errn$ of the estimation.

More specifically, the principle of the implemented method is to minimize the performance function $P(\theta)$ shown in Eq. 2.4 for an N-points window of the signal. The N-points window of the signal contains 5 whole periods of the stationary part.

The performance function $P(\theta)$ is written as

$$P(\theta) = \frac{1}{2N} \sum_{k=1}^{N} \epsilon^2(k, \theta), \tag{2.4}$$

defined as a function of the error of the modelling ϵ,

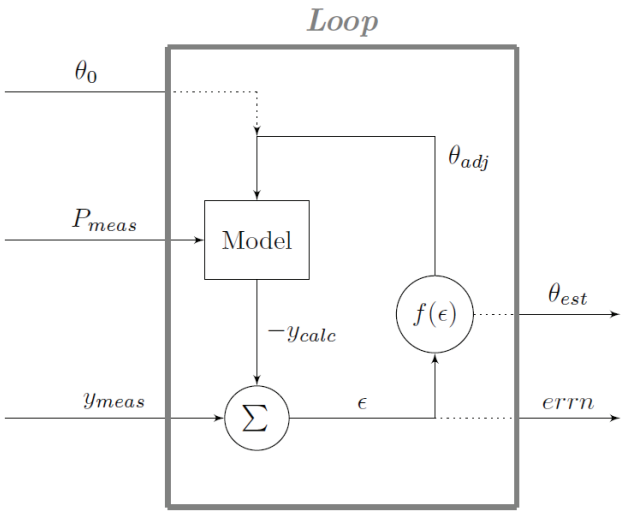

FIGURE 2.4: Principle of the estimation method.

$$\epsilon(k,\theta) = y_{meas}(k) - y_{calc}(k,\theta). \tag{2.5}$$

In this notation, $y_{meas}(k)$ is the discrete measured signal of the reed displacement, and $y_{calc}(k,\theta)$ the discrete calculated signal of reed displacement for the vector θ (which contains the parameters of the model).

The parameter updating algorithm is

$$\theta_{i+1} = \theta_i - \tilde{H}\left(\theta_i\right)^{-1} G\left(\theta_i\right), \tag{2.6}$$

where $\tilde{H}$ and G are respectively the approximated Hessian and the gradient, which are defined from the model gradient $\psi\left(k,\theta\right)$

$$\psi\left(k,\theta\right) = \frac{\partial y_{calc}\left(k,\theta\right)}{\partial\theta} \tag{2.7}$$

as

$$G(\theta) = -\frac{1}{N}\sum_{k=1}^{N}\epsilon(k,\theta)\psi(k,\theta) \tag{2.8}$$

and

$$\tilde{H}(\theta) = \frac{1}{N}\sum_{k=1}^{N}\psi(k,\theta)\psi^T(k,\theta). \tag{2.9}$$

Finally, the normal error of the estimation can be defined as

$$errn(\theta) = \sqrt{\frac{\sum_{k=1}^{N}\epsilon^2(k,\theta)}{\sum_{k=1}^{N}y_{meas}^2(k)}} \times 100[\%]. \tag{2.10}$$

2.5.2 Accuracy of the estimation method

The estimation method can either diverge or converge to a local minimum. In order to study the accuracy of the method, the estimation method is tested on simulated signals. The analysis of the accuracy of the method for the different physical models and their associated parameters is presented in this section.

Displacement signals y_{sim} are simulated from the measured pressure difference P_{meas} and one controlled set of mechanical parameters $\theta_{control}$ by means of the different implemented models. The estimation method is applied to these pairs of signals, with a set of initial parameters $\{\theta_0\}$.

Two estimations are obtained from this method: the estimation errors $errn$ (see Eq. 2.10) quantifying the accuracy of the model, and the coefficients η quantifying the bias between the estimated parameters θ_{est} and the control parameters $\theta_{control}$ (see Eq. 2.11).

$$\eta\,(\%) = 100 \cdot \left|1 - \frac{\theta_{est}}{\theta_{control}}\right|. \tag{2.11}$$

The mean bias of the parameter estimation $\langle\eta\rangle$ and the standard deviation σ_η are used as indicators of the quality of the estimations.

2.5.2.1 Convergence of the estimation method

The normal error $errn$ of the estimation is used as an indicator of the quality of the estimation. For this study, all the estimations with an error above 5% were considered divergent.

The estimation method is sensitive to the input parameters θ_0. In order to obtain convergent estimations, the input parameters must be taken from the output parameters of a simpler model estimation: a first estimation of the parameters of the lower order

model (K_l) is carried out by a least mean squares method; these parameters are then used as input parameters of the next model (RK_l or K_{nl}). This method provides convergent solutions, though it is sensitive to the initial parameters y_c and K_c [2].

The sensitivity of the estimation method to noise can be studied by taking the initial parameters of the loop θ_0 equal to the control parameters $\theta_{control}$ used to simulate the input displacement signal. For all the implemented methods, the obtained errors were far below 1%. When adding noise to the input signals (40 dB Signal to Noise Ratio), the error of the model $errn$ reached at most 2%.

2.5.2.2 Performance of the parameter estimation

The mean difference between the control and estimated parameters $\langle \eta \rangle$ is used as an indicator of the bias of the estimated parameters.

All parameters are identified with a bias far smaller than 1%. For the parameters H, K and R, the bias follows a Gaussian distribution. However, the parameters K_c, y_c and M show some inhomogeneity and their standard deviations are larger (their bias remaining under 1%).

2.5.3 Error propagation

Uncertainties in the displacement measurement are not negligible. These uncertainties have been studied when calibrating the sensors (see Appendix in §2.8). A method to quantify the sensitivity of the estimated reed parameters to these uncertainties is proposed in this section.

The explicit expressions of the uncertainties of the estimated parameters depending on the calibration errors cannot be written because of the iterative principle of the method. Therefore, a Monte-Carlo simulation has been performed to quantify this error. Two cases are studied: beating reed regime (the uncertainty of the closing point detection can be reduced by means of the impact detection) and non-beating reed regime (the uncertainty on the closing point detection is higher because the accelerometer information cannot be used).

[2] A Monte-Carlo simulation has been performed to quantify this error. A reference displacement signal is calculated from a control set of reed parameters and a measured pressure difference. The reed parameter estimation method is applied, using different input parameters for y_c and K_c simultaneously. The standard deviation of the difference between the estimated parameters and the control parameters is used as an indicator of the uncertainty of the estimated parameters. When varying y_c from 0.01 mm to 1 mm and K_c from 10^{10} Pa/m^2 to 10^{12} Pa/m^2, all the uncertainties are lower than 10^{-8} %. However, when varying K_c from 10^{10} Pa/m^2 to 10^{13} Pa/m^2, the uncertainty for y_c reaches 0.2 % and for K_c 500 %. The uncertainty due to the input parameter y_c is negligible compared to the uncertainty produced by K_c.

Simulations of the calibration of a reference displacement signal, calculated from a control set of reed parameters $\theta_{control}$ and a measured pressure difference, are carried out. For this purpose, the two calibration coefficients are randomly generated from normal distributions characterized by the means and standard deviations of these coefficients, obtained when calibrating the sensors.

The corresponding reed parameters of the models are obtained from the simulated displacement signals including uncertainty and the measured pressure difference. The standard deviation σ_η of the coefficient η (Eq. 2.11), defined from the difference of these estimated parameters and the control parameters, is used as an indicator of the uncertainty of the estimated parameters.

The comparison of the errors in the beating reed regime for the different physical models is presented in Table 2.2. The standard deviation of the calibration parameters are 3.2% for the sensitivity and 0.3% for the closing point detection. The results are given in %.

TABLE 2.2: Standard deviation of the estimated reed parameters in beating reed regime for the different physical models, in %.

		Model name					
		K_l	RK_l	MRK_l	K_{nl}	RK_{nl}	MRK_{nl}
Estimated parameters	H	3.49	3.24	3.33	3.62	3.31	3.41
	K	3.21	2.90	2.99	3.17	3.06	3.12
	R	-	2.90	2.99	-	3.06	3.13
	M	-	-	2.99	-	-	3.08
	k_c	-	-	-	6.36	6.22	6.35
	y_c	-	-	-	8.36	6.75	7.28

The uncertainties of the parameters H, K, R and M have similar values to the largest input uncertainty (that of the sensitivity), showing a good estimation for all the physical models (standard deviation around 3.2%). However, parameters k_c and y_c have uncertainties over 5%, amplified by the power law of the non-linear stiffness.

The comparison of the errors in the non-beating reed regime for the different models is presented in Table 2.3. The standard deviations of the calibration parameters are 3.2% for the sensitivity and 4.8% for the closing point detection. The results are given in %.

The results of the Monte-Carlo simulation for the non-beating reed regime show good accuracy for parameters K and R, with standard deviations around 3.2%. Parameters k_c and y_c are not well estimated because they are strongly dependent of the calibration of the closing point. This estimation problem also affects the estimation of the mass of the non-linear model MRK_{nl}, in contrast with the beating reed regime. The calculated uncertainty in the parameter H is high because in the estimations for non-beating reed regime, the maximal displacements are extrapolated. However, when taking the value of

TABLE 2.3: Standard deviation of the estimated reed parameters in non-beating reed regime for the different physical models, in %.

		Model name					
		K_l	RK_l	MRK_l	K_{nl}	RK_{nl}	MRK_{nl}
Estimated parameters	H	23.0	22.3	23.0	18.6	17.1	19.8
	K	3.18	3.13	3.12	3.06	3.23	3.23
	R	-	3.13	3.12	-	3.24	3.11
	M	-	-	3.1	-	-	49.5
	k_c	-	-	-	13.4	15.2	21.3
	y_c	-	-	-	77.7	76.1	83.7

H directly from the measurements for this regime, the total uncertainty remains around 10% (see more details in the Appendix in §2.8).

2.6 Results

The estimation method is applied to the measured signals obtained in real playing conditions. To perform the measurements, one musician played the instrumented mouthpiece on a 40 cm long cylindrical pipe. The estimation method is also applied to the measured signals obtained with an artificial mouth [87].

The results for different dynamic levels are compared: *pianissimo* in artificial playing conditions, and *piano*, *mezzoforte* and *forte* in real playing conditions.

The quality of the estimation of each model is studied in this section. The accuracy of each model to describe the reed-lip-mouthpiece mechanics in playing conditions can be discussed in view of these results. In this study, the normal error *errn* of the estimation is used as an indicator of the quality of the model. The errors obtained for each model can be seen on Table 2.4.

TABLE 2.4: Normal error *errn* for each parameter estimation for *pianissimo* (measured on artificial mouth), *piano*, *mezzoforte* and *forte* measurements.

	Model name					
	Kl	**RKl**	**MRKl**	**Knl**	**RKnl**	**MRKnl**
errn *pianissimo* (%)	4.8	3.9	3.7	3.3	1.8	1.8
errn *piano* (%)	12.2	8.0	8.0	10.5	2.6	2.6
errn *mezzoforte* (%)	22.2	15.2	14.6	19.4	6.7	4.6
errn *forte* (%)	20.4	15.2	14.3	17.2	11.4	9.2

The normal error of the estimations is larger for *forte* than for *piano* dynamic levels. In order to understand what causes these errors, the measurements and simulations are superposed on Fig. 2.5(a) for *pianissimo* signals, Fig. 2.5(b) for *piano* signals,

Fig. 2.5(c) for *mezzoforte* signals and Fig. 2.5(d) for *forte* signals. For *mezzoforte* and *forte* measurements, complex phenomena such as deformation of the reed (transverse stiffness) and collisions, which are not taken into account in the physical models, affect the parameter estimation. In *forte* measurements, a strong asymmetry between the opening and the closing of the reed is clearly noticeable, affecting suitability of the models.

In Fig. 2.5(a) (*pianissimo*), the relationship between displacement and difference of pressure is almost linear. The low-level approximation of the linear stiffness model is a good approximation to describe the behavior of the reed. The non-linear stiffness models provide some improvement. Some damping is observed. The reed movement is accurately described by the non-linear model including damping. No mass effects are observed, and considering inertia in the models does not produce any difference.

In Fig. 2.5(b) (*piano*), the existence of a non-linear stiffness is clearly visible, even in the *piano* regime. The reed never reaches the closing point $y = 0$. The surface of the curve ΔP vs. y can be explained by damping. In the *piano* regime, the inertia effect is slightly visible. The non-linear stiffness model with damping describes well the behavior of the reed.

In the *mezzoforte* regime, the same model describes rather well the behavior of the reed. The mass effects in the reed behavior can be seen near $y = 0.5$ mm and $\Delta P = 0$ hPa, and the effects of the beating of the reed on the mouthpiece can be seen for $y = 0$. The non-linear model containing mass produces a slight improvement in the estimation, though this must be taken carefully because the different behavior of the reed in its extreme displacement regimes is not considered in the physical models: in $y = 0.5$ mm and $\Delta P = 0$ hPa the resonance of the reed (the reed and the musician's lip) leads the movement, whereas in $y = 0$ mm and $\Delta P = -40$ hPa it is the rebound of the reed on the mouthpiece that dominates the movement.

In the *forte* regime, the models fail to precisely describe the behavior of the reed. The non-linearity of the stiffness is more prominent. The relation ΔP-y is mainly linear for the closing regime (bottom line of the ΔP vs. y plots in Fig. 2.5(d)), while it shows some irregularities for the opening regime (top line of the plots in Fig. 2.5(d)). The linear damping fails to explain the area in the characteristic, which may imply a non-linear damping differentiating opening and closing. This asymmetry may provide evidence that the free moving surface of the reed varies from the closing and opening conditions (similarly with the separation point), considering the different nature of the boundaries imposed by the mouthpiece and the musician's lip. The inertial effects in the reed behavior can be seen near $y = 0.8$ mm and $\Delta P = 0$ hPa for the open channel, where the MRK_{nl} model fits the reed resonance. The effects of the beating of the reed

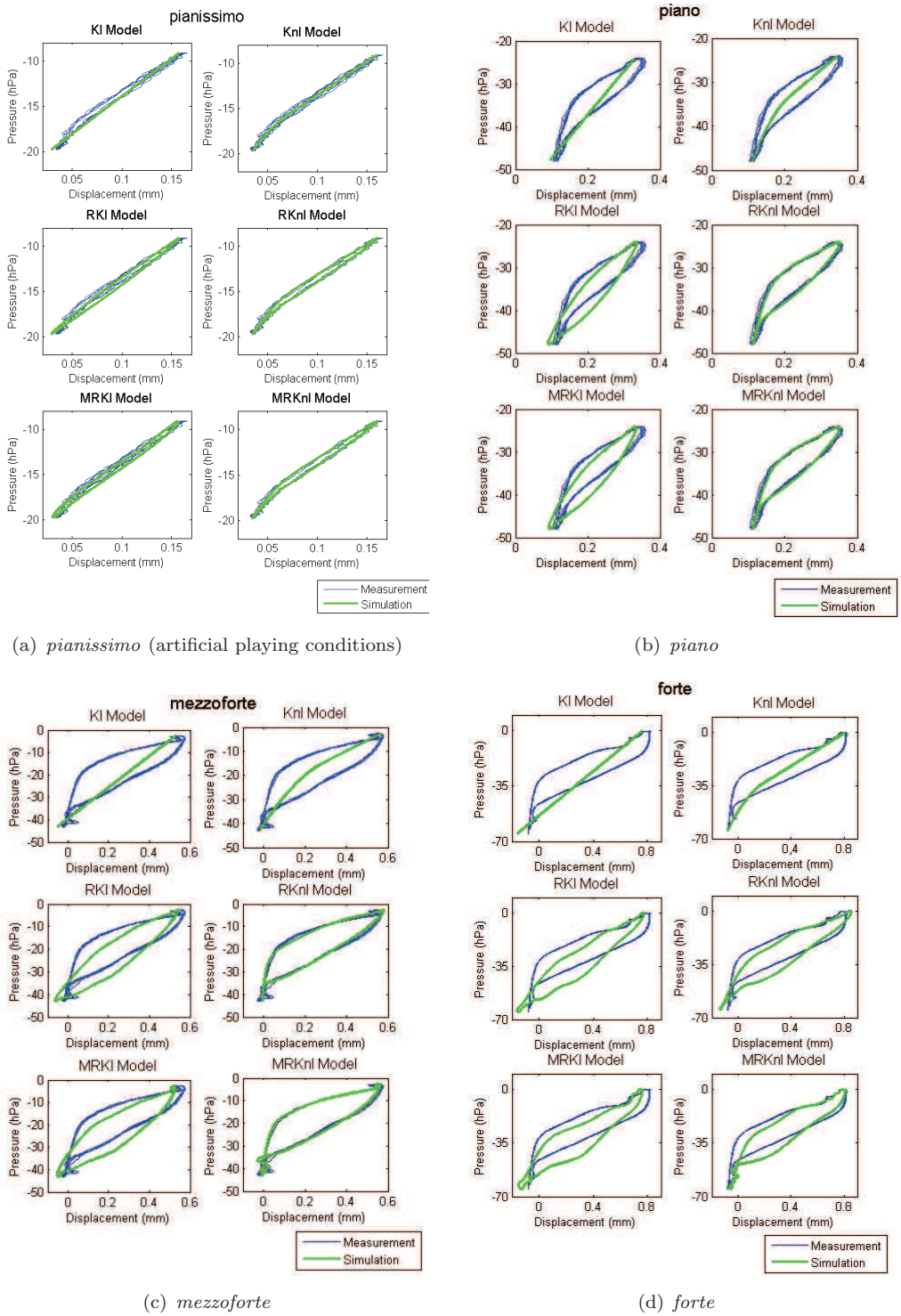

(a) *pianissimo* (artificial playing conditions)

(b) *piano*

(c) *mezzoforte*

(d) *forte*

FIGURE 2.5: Pressure difference vs. estimated and measured displacement for the different physical models.

on the mouthpiece in $y = 0$ are noticeable. However, the closed channel displacement is not well estimated. The non-linearity of the mass is more explicit for the dynamic levels with large displacement. When looking at the time evolution of the ΔP vs. y plots, the inertial components of the oscillation of the reed on the player's lip do not depend on time, while the inertial effects observed in the beating present some random behavior. More complex physical models are needed to describe the reed behavior in *forte* dynamic level.

The most relevant model is the one containing non-linear stiffness and damping. A slight effect of inertia is observed and, when it should be taken into account, a non-linear inertia is probably needed. The asymmetry of the behavior of the reed in its extreme displacement regimes produces this non-linearity: in the closing regime, the reed hits the mouthpiece, and in the opening regime, it oscillates on the musician's lip. This asymmetry is not considered in this work.

In view of these results, we can provide the values of some estimated parameters in real playing conditions, using the RK_{nl} model, for *piano* and *mezzoforte* dynamic levels, for the measured point of the reed. The estimated parameters are presented in Table 2.5. The uncertainty associated to these estimated parameters can be found in Tables 2.2 and 2.3.

TABLE 2.5: Values of the estimated parameters using the RK_{nl} model for the *piano* (p) and *mezzoforte* (mf) dynamic levels.

	K (10^6 Pa/m)	R (10^3 Pa·s/m)	k_c (10^{11} Pa/m^2)	y_c (10^{-5} m)
p	6.4	1.9	2.7	17.0
mf	4.5	1.2	14	2.4

The results of the parameter estimation using the MRK_{nl} model for the *mezzoforte* dynamic level are presented in Table 2.6. This estimation provides some improvement compared to the RK_{nl} model for the *mezzoforte* dynamic level, though the mass is not accurately estimated because a linear modelling of the inertial effects is employed. This result is presented as an insight into the value of the mass of the reed in playing conditions at this dynamic level. The uncertainty associated to these estimated parameters can be found in Table 2.2.

TABLE 2.6: Values of the estimated parameters using the MRK_{nl} model for the *mezzoforte* dynamic level.

	K (10^6 Pa/m)	R (10^3 Pa·s/m)	M (10^{-2} Pa·s/m^2)	k_c (10^{11} Pa/m^2)	y_c (10^{-4} m)
mf	4.8	1.0	26.9	7.0	0.36

2.7 Conclusion and perspectives

In this work, an instrumented mouthpiece has been developed. This device measures the pressure in the player's mouth and in the mouthpiece with a good phase matching, allowing for the measurement of the pressure drop. Two photointerruptors placed on each side of the mouthpiece at about 2 mm from the reed tip enable the measurement of the reed displacement. The main difficulty is the calibration of the reed closing position. Two accelerometers located near the reed tip on the mouthpiece enable the detection of the beating of the reed on the mouthpiece, improving the calibration of the reed closing for high playing dynamics (corresponding to beating reed regime). For low levels, the calibration of the closing position has higher uncertainty.

Assuming different physical models with growing complexity, the estimation method based on the comparison between the measured and the predicted reed displacement allows estimating the equivalent reed parameters in a convergent manner. The uncertainty in the estimated equivalent parameters is low (3 to 6%) for the beating reed regime (in which the calibration of the closing position is done using the acceleration signals). For low playing dynamics, the uncertainty is much higher for some of the parameters, but remains low (3 to 4%) for the equivalent stiffness and damping.

Results obtained using signals acquired in real playing conditions (mouthpiece connected to a cylinder and played by a musician) show that the most relevant model is the non-linear oscillator containing non-linear stiffness and damping. The smaller the reed oscillation is, the better the quality of the model because complex phenomena appear when increasing the playing dynamics: the beating of the reed on the lay of the mouthpiece, and the variation of the free-moving surface of the reed. Including the mass in the model does not significantly improve the model quality.

Future work could include improvements to the model describing the reed movement. Non-linear effects should be taken into account for the damping and the mass due to the asymmetry in the reed movement (during the opening, the reed bends and beats on the mouthpiece, and in the closing, the reed couples with the player's lip).

The experimental setup could be used for characterizing different reeds played by different musicians in order to correlate the estimated reed parameters with the musicians'

perception and to try to explain which mechanical parameters are correlated with the reed quality.

In the long term, the experimental device can be also used for gesture measurement. The time evolution of the reed parameters due to the player's musical gesture can be observed. Differences among musicians or among mouthpieces could be also studied. Finally, the device could be used for teaching clarinet or saxophone playing, with some adaptations.

2.8 Appendix

The principle of the photointerruptors is that of a transistor in which the base acts as an IR diode. The IR light emitted by the base is reflected on the surface of the reed and then measured by the receptive part of the photointerruptor. The intensity of the received light enables the measurement of the distance between the sensor and the reed.

The sensors' response is shown in Fig. 2.6. When the sensors are installed on the mouthpiece, their working range goes from the reed closing point (*CP* in the Fig. 2.6) to the reed maximal aperture in playing conditions (*MA* in the Fig. 2.6). In this range, the response of the sensors can be approximated as linear (grey box in Fig. 2.6) and the calibration is reduced to determining the slope of the response and the closing point voltage.

The reliability of the calibration system has been studied, showing good repeatability (standard deviation of 1% for the linear sensitivity and the closing voltage).

The uncertainties associated to the installation of the reed on the mouthpiece and the calibration bench can be also taken into account (standard deviation 2% for both calibration parameters).

Calibrations for different reeds show large variability depending on the different reflectivity of the cane reeds. The deviation of the calibration parameters represents a standard deviation of 10%. In consequence, a calibration must be done for each reed.

Heating of the sensors is detected for a continued use over 10 minutes, after optimization of the polarization circuit. The standard deviation of the two calibration parameters associated to this heating is 1% for 20 minutes of continuous use.

Some humidity accumulates on the reed and sensors while a musician is playing. This can vary the reflectivity of the reeds and the performance of the displacement sensors. For 1 s of play, the standard deviation of the sensitivity is estimated to be 2.4%.

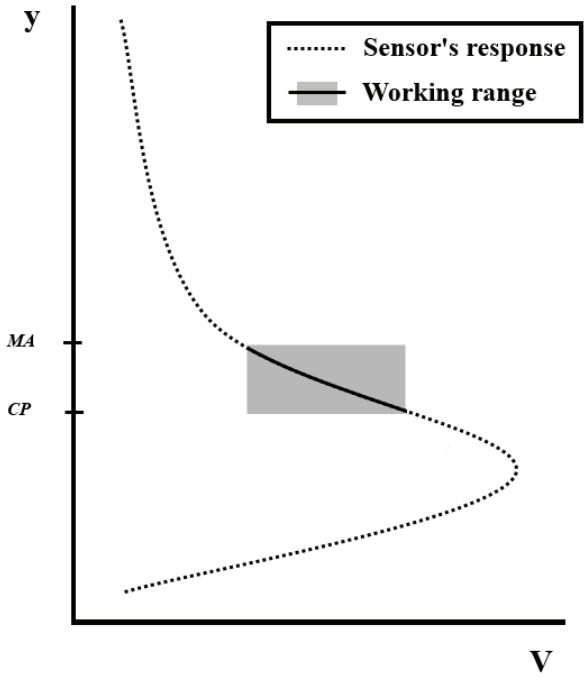

FIGURE 2.6: Sensors' response. Approximate linear response for the working range of the sensors from the reed closing point (CP) to the reed maximal aperture (MA) in playing conditions.

In beating reed regimes, the detection of the closing time is done by using accelerometers. When the acceleration signal shows a maximum, the measured voltage in the photointerruptors is associated to the closing point. The uncertainty of the detection of the closing point by using the accelerometers is 0.3% when impact happens (big oscillations). In non-beating reed regimes, a measurement in beating reed regime is taken consecutively and a mean closing point value obtained from this measurement is used to approximate the closing point. The standard deviation of this measurement is 1.8%.

This study concludes that the overall uncertainty for the sensitivity is given by a standard deviation of 3.2% (obtained from the uncertainty of the mechanical calibration and the humidification while playing). For the closing point calibrations, the standard deviation is 4.8% for the *piano* regime (obtained from the uncertainty of the mean closing point value and the humidification) and 0.3% for the *forte* regime (uncertainty due to the closing point detection).

Complements

2.9 Complement I: Application of the reed parameters estimation to saxophone

This section presents a study consisting in the application of the instrumented mouthpiece and reed parameter estimation (explained in §2) to measurements using a saxophone and 20 reeds. In a first step, a comparison is done between one measurement using one cane reed and a cylindrical resonator and one measurement using the same reed and a saxophone. Next, the performance of two physical models for the reed are compared using a saxophone and 20 cane reeds.

2.9.1 Experiment

The experiment is based on a set of measurements performed with the instrumented mouthpiece connected to a tenor saxophone. The set of measurements comprehends measurements performed with 20 reeds of different cut and brand (5 reeds D'Addario Select Jazz 3 soft, 5 reeds Rico Reserve 3.0, 5 reeds Vandoren Tradition 2 1/2, 5 reeds Vandoren ZZ 3) and by one musician. For all the measurements, the musician was asked to play at a given mean blowing pressure (31.5 hPa), provided by a multimeter that is connected to the pressure sensor in the musician's mouth. This blowing pressure ensures obtaining *mezzopiano* and *mezzoforte* playing dynamics. The duration of the acquisitions is 1 s, taking only the stationary part. The assessment of the results consists in the comparison of the normal error of the estimation *errn* (see Eq. 2.10), describing the quality of the model, when applied to the set of measurements.

Two examples of the acquired measurements using the instrumented mouthpiece and a cylindrical resonator or a saxophone are shown in Fig. 2.7. The measured displacement for the cylindrical resonator tends to a square-like signal, and it is asymmetric when comparing the open and closed phases because in the open phase the reed oscillates against the lip and in the closed phase it beats on the mouthpiece. In the case of the

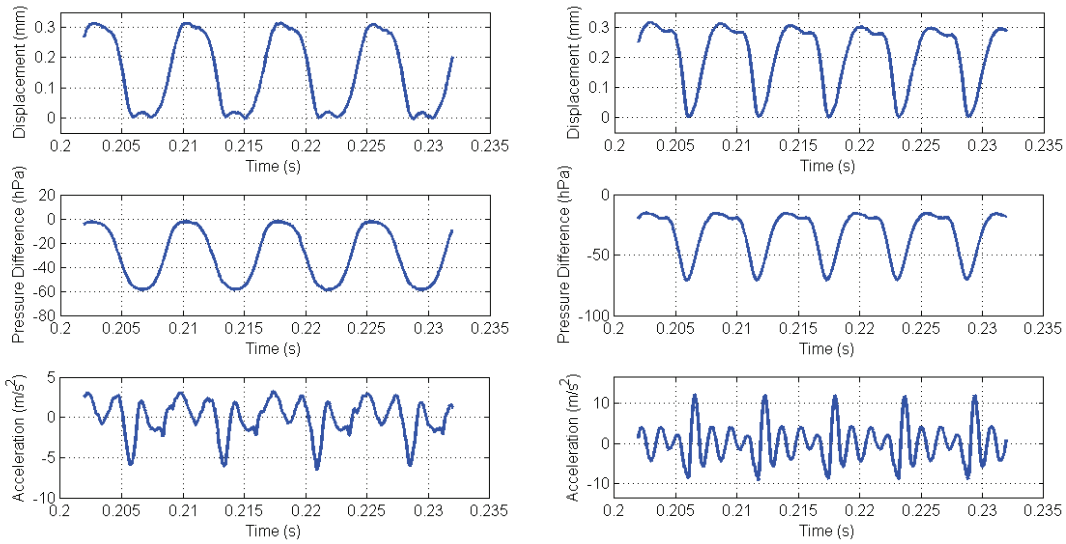

a) For a cylindrical resonator.

b) For a saxophone.

FIGURE 2.7: Measured reed displacement, pressure difference and acceleration on the mouthpiece.

saxophone, where the bore is a truncated cone, the open phase depends on the length of the conical resonator, and the closed phase depends on the truncated length of the bore. In fact, when varying the played note, the duration of the open phase varies but not the duration of the closed phase [117].

2.9.2 Performance of the models

The mean normal error of estimation *errn* for a 1s-long acquisition, for the 20 reeds, using the model with damping and non-linear stiffness (RK_{nl} model) and the model with mass, damping and non-linear stiffness (MRK_{nl} model) is shown in Fig. 2.8. The uncertainty in *errn* represented in the figure is the standard deviation from the mean normal error in the application of the estimation method to successive 5-period windows of the 1s-long measurements.

The normal errors using the MRK_{nl} model are mostly smaller than the normal errors using the RK_{nl} model (the RK_{nl} model is the case $M = 0$ of the MRK_{nl} model). The contribution of the MRK_{nl} model is the description of the inertial oscillations of the reed in the opening phase.

An example of the estimated displacement using both models for the same measurements is represented as function of time in Fig. 2.9. The difference between models in this representation is small.

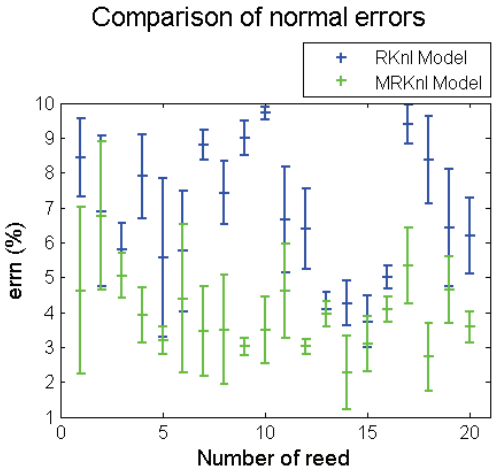

FIGURE 2.8: Average normal error and standard deviation of the estimation for 20 reeds using the RK_{nl} and the MRK_{nl} models for measurements using a saxophone.

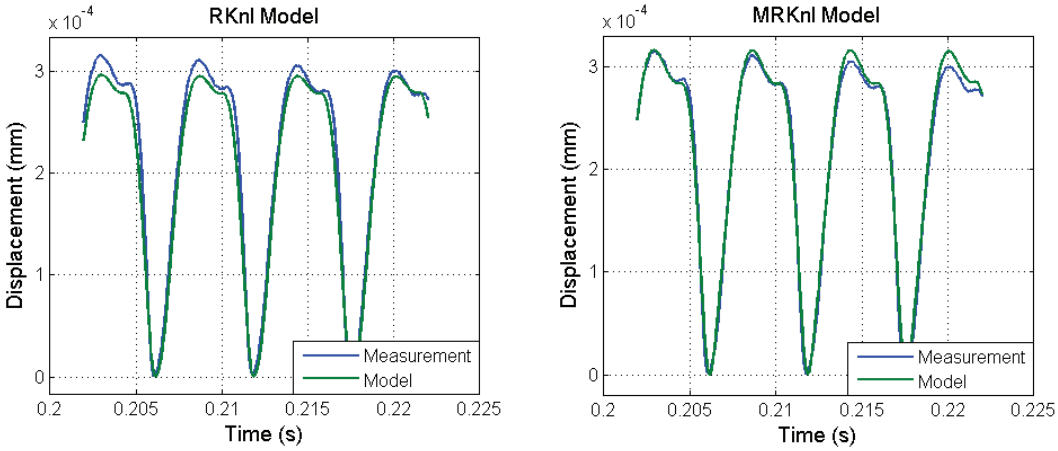

a) Using the RK_{nl} model.

b) Using the MRK_{nl} model.

FIGURE 2.9: Comparison of the measured and estimated reed displacement vs. time for measurements using a saxophone.

The estimated displacement using both models is represented as function of the pressure difference in Fig. 2.10. The MRK_{nl} model describes more accurately than the RK_{nl} model the surface in the cycle and takes into account the oscillation in the opening period ($y \approx 0.3$ mm, $\Delta P \approx -20$ hPa).

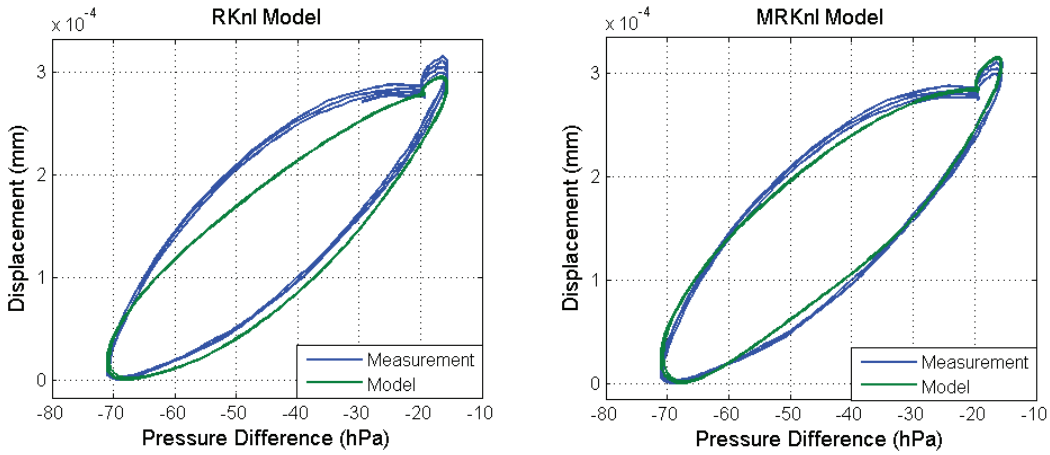

a) Using the RK_{nl} model.

b) Using the MRK_{nl} model.

FIGURE 2.10: Comparison of the measured and the estimated reed displacement vs. pressure difference for measurements using a saxophone.

The reason why the MRK_{nl} model describes more accurately the reed behaviour than the RK_{nl} model when using a saxophone may be that the closing phase in the conical resonator is a single oscillation near the mass-resonance frequency and not an oscillation of the same duration than the opening period. The difference between the opening phase and the closing phase that appeared using the cylindrical resonator (oscillations on the lip when opening or shocks on the mouthpiece when closing), visible in Fig. 2.5(c), is minimized due to the brevity of the closing period for the conical resonator.

2.10 Complement II: Application of the instrumented mouthpiece to learning and teaching music

This chapter presents a study on the application of the instrumented mouthpiece to music pedagogy. The aim is to show the kind of measurements that can be done using the instrumented mouthpiece for pedagogical purposes, and a qualitative analysis suitable for the classroom. This work was presented in the International Symposium 'Learning and Teaching Music in the Twenty-First Century: The Contribution of Science and Technology', which was held in the University of McGill (Montréal) in November 2015 [103].

2.10.1 Experiment

The purpose of the experiment is to compare musicians of different levels of expertise through the use of the instrumented mouthpiece and by using a method applicable to the classroom environment.

The experiment is performed with the collaboration of two musicians of different expertise: a beginner and a semiprofessional. The beginner is an alto saxophone player with three years of experience and without a formal education on saxophone playing, and the semiprofessional has a formal education on tenor saxophone playing and several decades of experience. Both players used the same saxophone, a Selmer Reference 54 tenor saxophone. Two families of measurements are acquired: stationary notes and attacks of different articulation. For the stationary notes, a single note G4 with a duration around 4 s was played, and for the articulated notes an ascending and descending sequence of 5 notes (G4, A4, B4, C5 and D5, in B-flat) was played. The articulations studied are *legato* attacks, *legato* with air-separated or soft-tonguing attacks ("Da" sounds) and tongue-separated *staccato* attacks ("Ta" sounds). The measurements are performed using the instrumented mouthpiece installed on a tenor saxophone. The analysis of the results consists in the visual comparison of the envelope of the pressure inside the mouth, pressure inside the mouthpiece and displacement signals.

2.10.2 Results

The results of the visual comparison of the stationary notes and the different attacks are presented below.

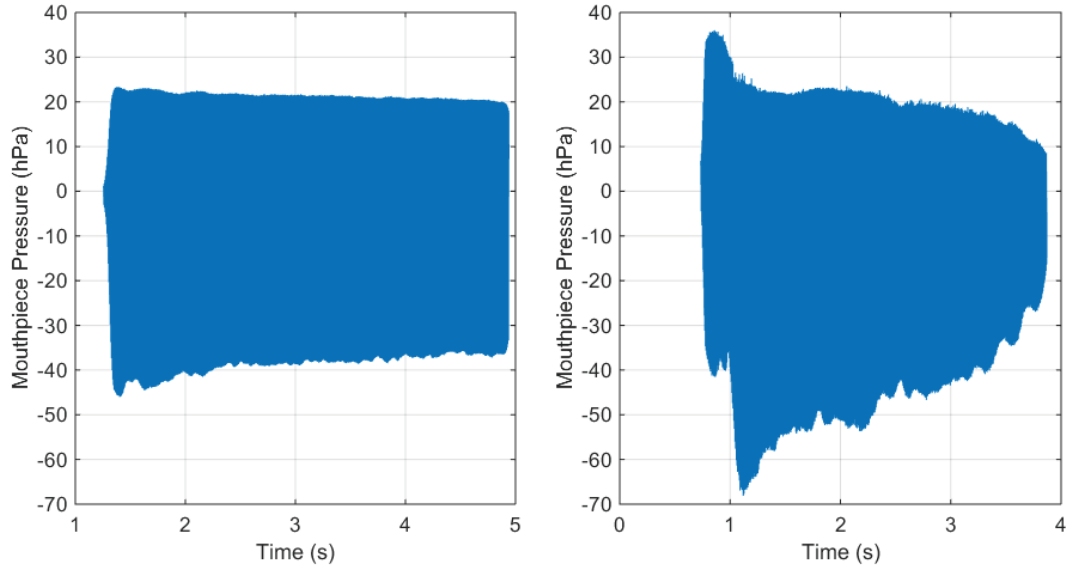

a) semiprofessional player. b) beginner.

FIGURE 2.11: Pressure inside the mouthpiece.

2.10.2.1 Single notes

The comparison of the pressure inside the mouthpiece for the beginner and the semiprofessional players is given in Fig. 2.11. The pressure inside the mouthpiece measured for the semiprofessional player has a clear attack and a constant stationary part while in the case of the beginner, the attack is less clear (the player makes a mistake controlling the pressure and restarts the note) and the stationary part is much less homogeneous.

The comparison of the reed displacement for the beginner and the semiprofessional players is given in Fig. 2.12. The stationary part of the displacement is quite homogeneous for the semiprofessional player while for the beginner the reed passes from the non-beating regime to beat and deform inside the mouthpiece.

2.10.2.2 Articulations

For the *legato* attacks, the pressure inside the musician's mouth, the reed displacement and the pressure inside the mouthpiece for the semiprofessional player and the beginner are given in Fig. 2.13. The shape of the attack is similar for both players (at 4.65 s for the semiprofessional player and at 3.47 and 3.80 for the beginner), and its duration is around 0.02 s.

For the tongue-separated notes, the signals for the semiprofessional player and the beginner are given in Fig. 2.14. When comparing the pressure inside the musicians' mouth

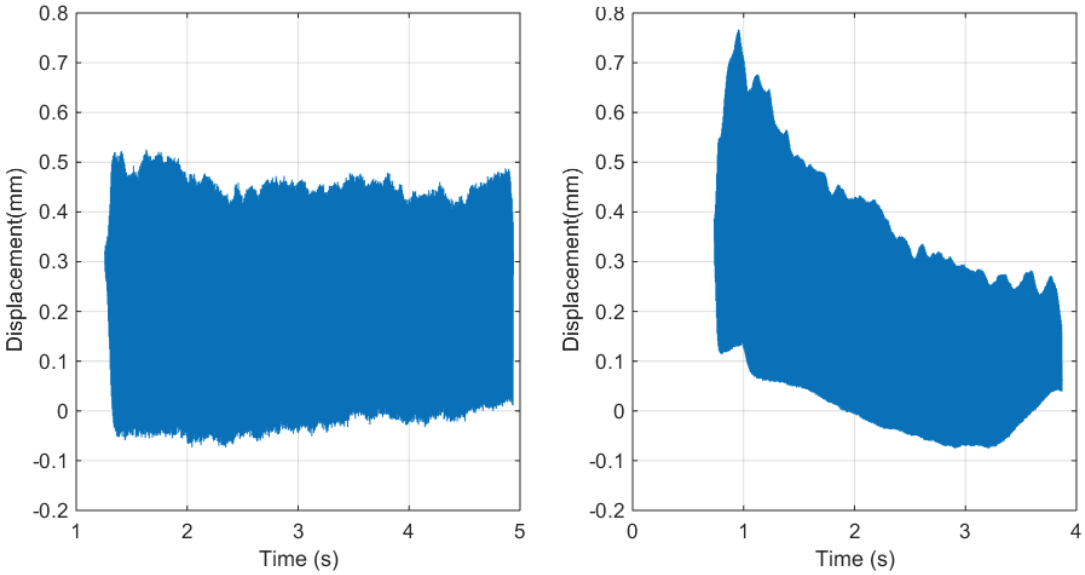

a) semiprofessional player. b) beginner.

FIGURE 2.12: Reed displacement.

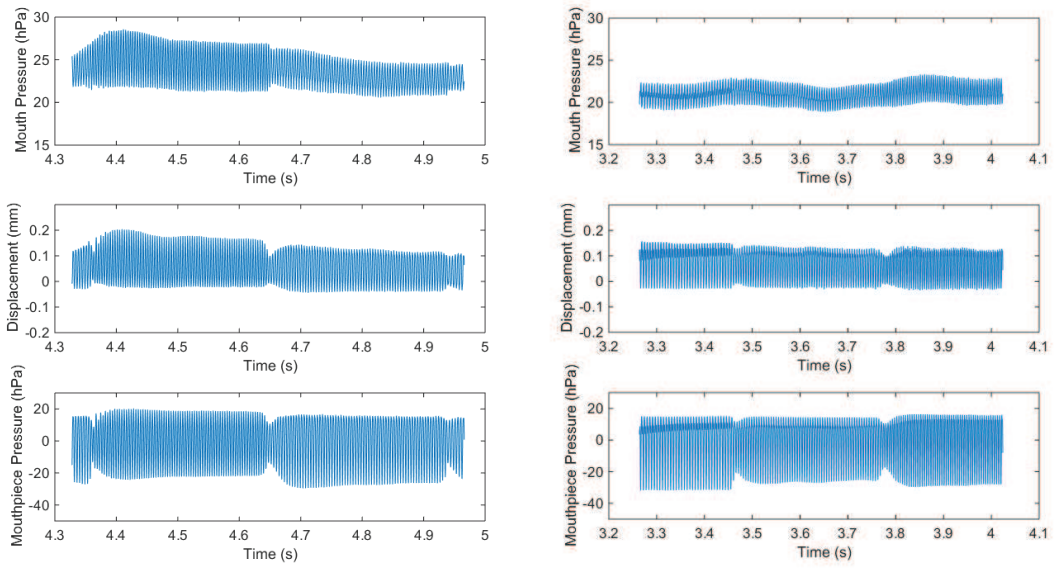

a) semiprofessional player. b) beginner.

FIGURE 2.13: Pressure in the musician's mouth, reed displacement and pressure inside the mouthpiece for *legato* attacks.

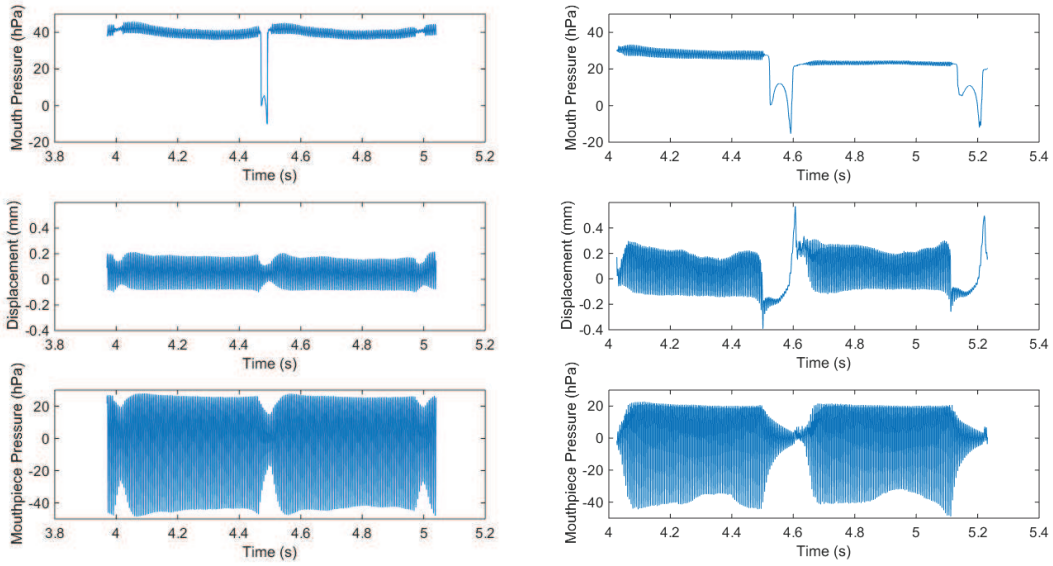

a) semiprofessional player. b) beginner.

FIGURE 2.14: Pressure in the musician's mouth, reed displacement and pressure inside the mouthpiece for tongue-separated notes.

signals, a characteristic signature reaching negative pressures can be seen for both players. This may be the effect of the tonguing. Regarding the reed displacement, a big difference between the musicians appears: the separation between the notes for the semiprofessional player is short (0.025 s) and close to the *legato* attack, whereas for the beginner a strong attack appears, in which the reed squashes into the mouthpiece, and the duration is 0.1 s. This may mean that the beginner produces a strong impact with the tongue on the reed. The resulting separation between the notes seen in the pressure inside the mouthpiece is longer for the beginner than for the semiprofessional player.

For the air-separated notes or soft-tonguing attacks, the signals for the semiprofessional player and the beginner are given in Fig. 2.15. A significant difference between both players appears for the pressure inside the mouth: pressure gaps separate the notes for the semiprofessional player (the notes are air-separated) whereas no gap appears for the beginner. Also, when comparing the reed displacement, the separation between notes is smooth for the semiprofessional player, whereas for the beginner the separations show the same signature of the tongue-separated attacks. Finally, the resulting attacks in the pressure inside the mouthpiece are slower for the beginner (0.1 s) than for the semiprofessional player (0.03 s).

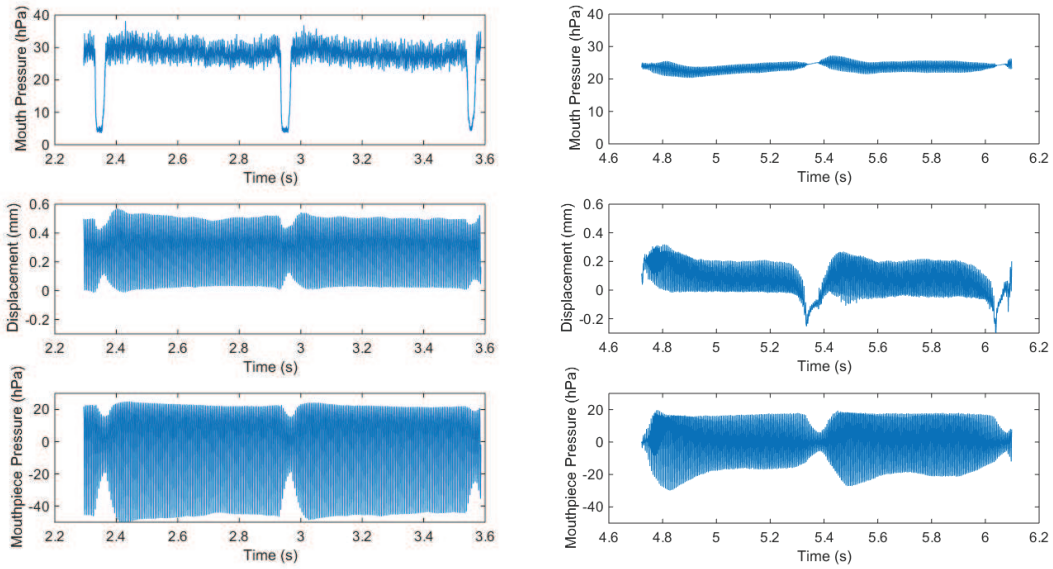

a) semiprofessional player. b) beginner.

FIGURE 2.15: Pressure in the musician's mouth, reed displacement and pressure inside the mouthpiece for soft tongue-separated notes.

2.10.3 Conclusion

The measurements presented in this complement have shown that the instrumented mouthpiece can provide a visualization of the musical gesture. The qualitative comparison of the measurements shows clear differences between musicians of different expertise, which could be used in music pedagogy. Nevertheless, the device would need to be improved in robustness and comfort for extended use.

The comparisons have shown that the stationary notes are much more constant in acoustic pressure and reed displacement for the semiprofessional player than for the beginner. Also, the signature of different kind of attacks has been observed. In the case of *legato* notes, the separations between the notes are shorter for the semiprofessional, revealing more agility and speed. For this player, the tongue-separated notes are characterised by gaps of negative pressure in the pressure inside the mouth. For the soft-tonguing attacks, these gaps are weaker and do not attend negative pressures. However, for the beginner, the gaps appear in the reed displacement. This suggests that the semiprofessional player controls the attacks by means of the air pressure and the distance between the tongue and the reed, whereas the beginner beats the reed with the tongue to produce the attacks.

Future work should be done considering more players of different standards, in order to analyse and generalise the conclusions drawn. Furthermore, quantitative analysis could

allow for the study of the link between physical variables and musical gesture, and help in the physical modelling of the gesture discussed in Chapter 1.

Chapter 3

Characterisation of reeds in playing conditions

This chapter presents a work on subjective and objective characterisation of reeds. The study links the reed quality assessment performed by musicians with parameters measured using the instrumented mouthpiece, with the aim to create a predictive model of reed quality using objective parameters.

The subjective work consists in a survey and a study based on perceptive tests. The survey is used to determine the musician's preferences about reeds and to identify the most used quality descriptors for reeds. In the perceptive tests, a set of reeds is characterised according to perceived quality by a panel of musicians. The tests are based on the results of the survey and enable the identification of the most significant descriptors of the reed quality and the evaluation of the performance of the panel. For the objective approach, physical measurements are performed in playing conditions with the same musicians and reeds using the instrumented mouthpiece. The reeds are characterised with these measurements obtaining playing parameters and equivalent reed parameters. Finally, the correlation between the subjective and objective characterisations is studied, in order to produce a predictive model of the reed quality.

3.1 Survey on reeds' quality

In order to better understand the manner in which musicians judge the quality of reeds, a survey collecting the answers of a large number of musicians is done. The representativeness of this panel is not analyzed, and the conclusions are not intended to be generalised.

Instead, the aim of this survey is to provide the guidelines of further research, quantifying the musicians' needs about reeds and identifying the subjective descriptors used by the musicians to describe the reeds' quality.

Evaluating the quality of a given reed is a current issue for single and double-reed instrument players. References to reeds quality can be found in guides for instrument practice as well as in scientific publications. For many scientific studies, the notion of good or bad reed is assumed and the subjective criteria affecting this perceived quality are intuitively chosen. In fact, there seems to be no research in quantifying the proportion of reeds of good or bad quality or in identifying the subjective criteria used by musicians to evaluate reeds' quality. In this section, we present a survey for the quantification of these issues. The survey is disseminated through the Internet, gathering around 400 answers.

3.1.1 Generalities about the survey

The survey is created using the online survey maker eSurv (`https://esurv.org/`) and translated in three languages (English, French and Spanish)[1]. The body of the survey has the format of a multiple choice questionnaire. Multiple response was not allowed and the answer was not mandatory.

The number of answers according to the language is provided in Tab. 3.1. The majority of the answers come from the English version because an important disseminator of the survey was the International Clarinet Association [118].

TABLE 3.1: Number of answers according to the language.

Language	Musicians
English	267
French	75
Spanish	33
Total	375

The questions in the survey are divided in two blocks, the first regarding the musical practice of the musicians and the second regarding the choice and evaluation of reeds.

The questions regarding the musical practice of the participants are used to characterise the population of musicians participating in the study. The questions are the following:

- Which instrument do you usually play?

[1]The link used for its dissemination is `https://esurv.org/online-survey.php?surveyID=LOIMHL_ca6f65be` for the English version

- Which musical style do you play?
- Which is your musical level?
- How much time do you practice the instrument?

Secondly, the inquiry addresses some questions regarding the choice and evaluation of the reeds. The questions are the following:

- Which reed strength do you usually use to play?
- How often do you buy new reeds?
- Choose the criteria that you consider the most representative of the reed quality. Order them according to their importance:
  - Appearance,
  - Stability in time,
  - Life time,
  - Accuracy,
  - Ease of playing,
  - Timbre,
  - Homogeneity,
  - Projection,
  - Expressivity,
  - Stiffness.

The results concerning the two blocks of questions are given in §3.1.2 and §3.1.3, respectively. Some misunderstanding of the questions are detected, so these answers are removed of the study.

3.1.2 Panel of musicians

The characteristics of the panel that answered the survey are analysed here.

The answers to the question "Which instrument do you usually play?" are given in Tab. 3.2. The most played instrument in the panel of musicians is the Soprano Clarinet in Sib (222 answers) and the Alto Saxophone (110 answers).

TABLE 3.2: Answers for "Which instrument do you usually play?".

Instrument	Musicians
Soprano Saxophone	0
Alto Saxophone	110
Tenor Saxophone	31
Baritone Saxophone	6
Soprano Clarinet in Mib	0
Soprano Clarinet in Sib	222
Bass Clarinet	6
Total	375

TABLE 3.3: Answers for the style.

Style	Musicians
Classical	234
Pop	19
Folk	6
Jazz	36
Other	80
Total	375

Concerning the musical style, the results are given in Tab. 3.3. The most practiced style in the panel of musicians is Classical Music (234 answers). Also, 80 of the musicians declared to practice other style than Classical, Pop, Folk or Jazz.

The answers for the query "Which is your musical level?" are given in Tab. 3.4. The majority of the musicians are amateurs and professionals (158 and 154 answers, respectively), and only 50 declared themselves as beginners.

TABLE 3.4: Answers for the level.

Level	Musicians
Beginner	50
Amateur	158
Professional	154
Total	362

Regarding the time of practice of the instrument, the results are given in Tab. 3.5. The majority of the musicians in the panel declared to practice the instrument several hours per day (157 answers). The second most chosen answer was a practice time of several hours per week (131 answers).

An important part of the panel are professional and amateur classical clarinetists (soprano clarinet in Sib) that regularly practice the instrument.

TABLE 3.5: Answers for the practice time.

Practice time	Musicians
one hour per week	29
several hours per week	131
one hour per day	51
several hours per day	157
Total	368

3.1.3 Reed choice and evaluation

The questions in the survey dedicated to reeds are analysed in this section. Firstly, the questions concerning the *a priori* reed choice are studied, and secondly, the study concerning the *a posteriori* classification of reeds according to their quality is presented.

3.1.3.1 Reed choice

The questions assessing the musicians' reed choice are studied here. The first question concerns the frequency of buying reeds, the second question is about the reed strength used to play and the last question concerns the amount of reeds in a box perceived as good or bad reeds to play.

The answers for the question "How often do you buy new reeds?" are given in Tab. 3.6. The number of answers decreases with the frequency of buying reeds. The most chosen answer is "less than 1 box every 3 months".

TABLE 3.6: Answers for the frequency of buying reeds.

Frequency of buying reeds	Musicians
less than 1 box every 3 months	121
1 box every 3 months	117
1 box every 2 months	57
1 box every month	47
1 box every 2 weeks	27
1 box every week	6
more than 1 box every week	0
Total	375

Reeds are classified by strength and cut for commercialization. These two parameters allow a musician to choose a reed adapted for his or her mouthpiece and playing style. The strength provides a first order measurement of the longitudinal flexibility of the reed under a static effort. The cut refers to the given shape to the vamp of the reed, which

defines a particular timbre of the reed. The choice of the reed depends on the mouthpiece employed. In order to assess the strength for reeds of different brands, a rough equivalence of cuts and strengths is provided with the survey in a comparison chart (see Fig. 3.1). This comparison chart has been produced for this survey from the comparison charts in http://www.saxplus.com/reed-strength-chart.html, http://www.mrif.gouv.qc.ca/calendrier/document/1321_comparison_anches.pdf and https://athomemusicacademy.wordpress.com/2012/02/24/. It summarises the commercial categories of reeds in groups ('A', 'B', 'C'... in columns), without identifying any particular brand.

	A	B	C	D	E	F	G	H	I	J	K	L	M	N	O	P	Q	R	S
Vandoren Juno			1,5		2	2,5		3											
Vandoren Traditional		1		1,5		2		2,5		3		3,5		4		4,5		5	
Vandoren V12							2,5		3		3,5		4			4,5		5	
Vandoren 56 Rue Lepic							2,5		3		3,5		4			4,5		5	
Vandoren V16			1,5		2		2,5		3		3,5		4			5			
Vandoren Java		1	1,5	2		2,5		3		3,5		4							
Vandoren Java Red		1	1,5		2		2,5		3	3,5		4							
Vandoren ZZ			1,5	2		2,5		3		3,5		4							
Vandoren V21							2,5		3		3,5		4			4,5		5	
Rico		1,5		2	2,5		3		3,5		4								
Rico Royal	1	1,5		2	2,5		3		3,5		4			5					
Rico Grand Concert Select								2,5		3		3,5		4		4,5		5	
Rico Grand Concert Select Evolution							2		2,5		3		3,5		4		4,5		5
Rico Select Jazz			2S		2M		2H	3S	3M		3H		4S		4M		4H		
Rico Reserve				1,5		2		2,5		3		3,5		4		4,5			
Hemke					2		2,5		3		3,5		4						
La Voz				S	MS		M		MH				H						
Plasticover	1	1,5		2			3		3,5		4		5						
Fibracell					S			MS		M		MH		H					
Rigotti Gold				2		2,5		3		3,5		4		4,5		5			

FIGURE 3.1: Comparison chart of reed forces for different brands.

At this point, the musicians were asked which strength of reed they commonly use, and they were referred to Fig. 3.1 for indicating a category (from A to S), without providing any specific information about a particular brand. Results for all instruments and musicians are given in Fig. 3.2, with a total of 157 answers. A Gaussian tendency is observed, except for the reeds classed as "J", which are comparatively less used. The mode corresponds to the reeds in the class "K" (35 players).

Regarding only the answers for clarinetists (Fig. 3.3), the mode is the class "K" (22 answers), followed by the class "I" (19 answers), and the class "J" is barely used.

In the case of the saxophonists (see Fig. 3.4), the distribution is more complex and the mode is also the class "K".

Reeds are usually sold in box of 10 items. Though the 10 reeds have same cut and strength, they are perceived as different by the musicians. Some of the reeds are judged as unsatisfactory for playing and discarded, some are playable, and some others are considered excellent. The proportion of these classes of reeds in one box may vary from one box to another.

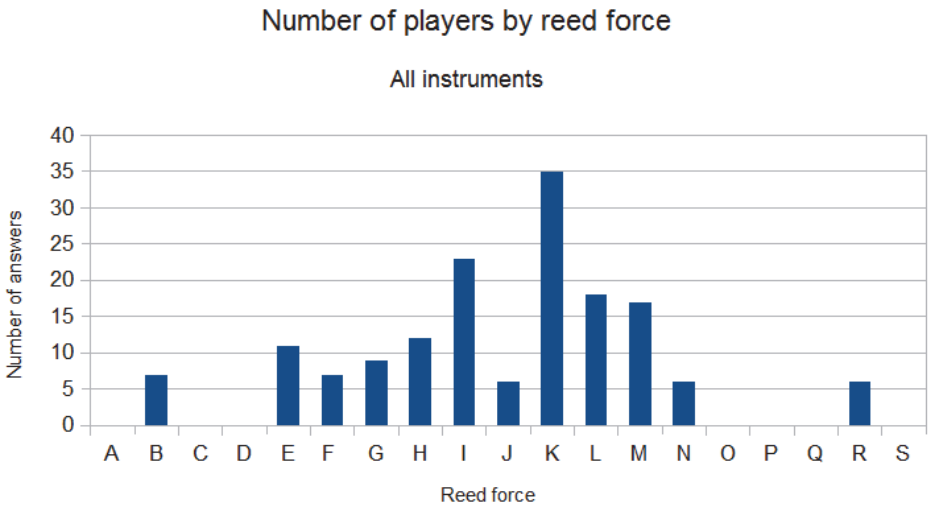

FIGURE 3.2: Number of players per reed force (see Fig. 3.1).

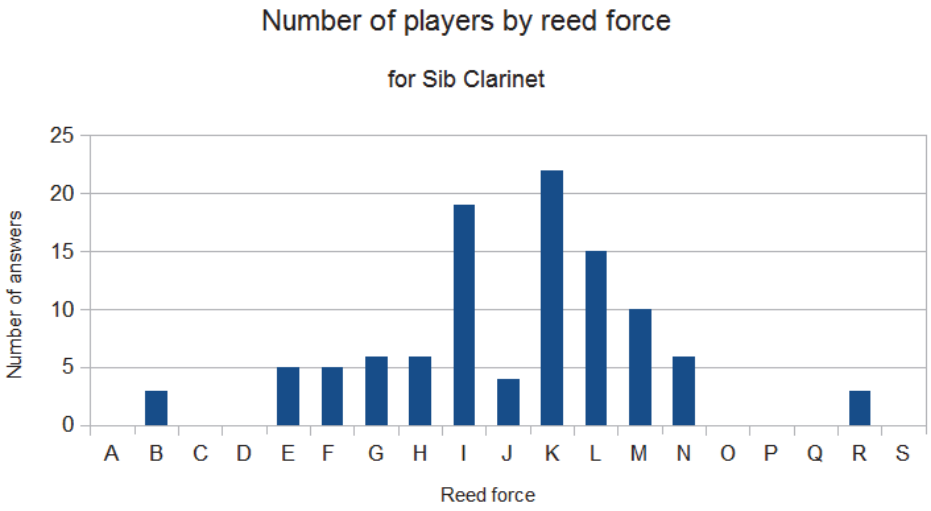

FIGURE 3.3: Number of players by reed force (see Fig. 3.1).

The question addressed at this point of the survey is how many reeds in a box of 10 are found unusable and how many are judged as good for concert (excellent quality). The results are given in Fig. 3.5. Considering the answers provided by the entire panel of musicians, in a box of 10 reeds, 3 are playable in concert and 2 are unusable (these are the modal answers, as seen in Fig. 3.5). The profiles of the histograms for playable-in-concert and unusable reeds have both a main maximum in 2 or 3 reeds and a second maximum in 7 or 8 reeds. It was verified that this second maximum does not come from subtracting the 2 or 3 playable-in-concert or unusable reeds to the total amount of 10 reeds in a box, and that the answers for the two categories of reeds are independent.

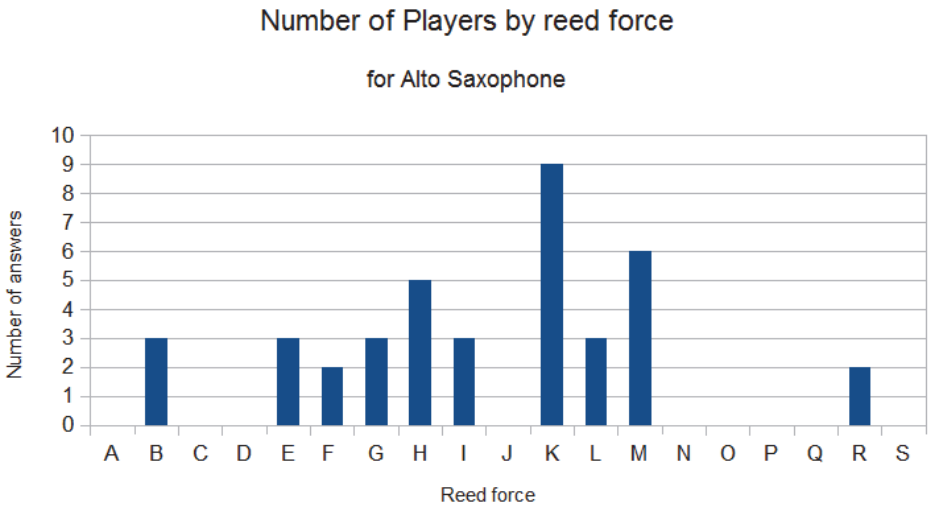

FIGURE 3.4: Number of players by reed force (see Fig. 3.1).

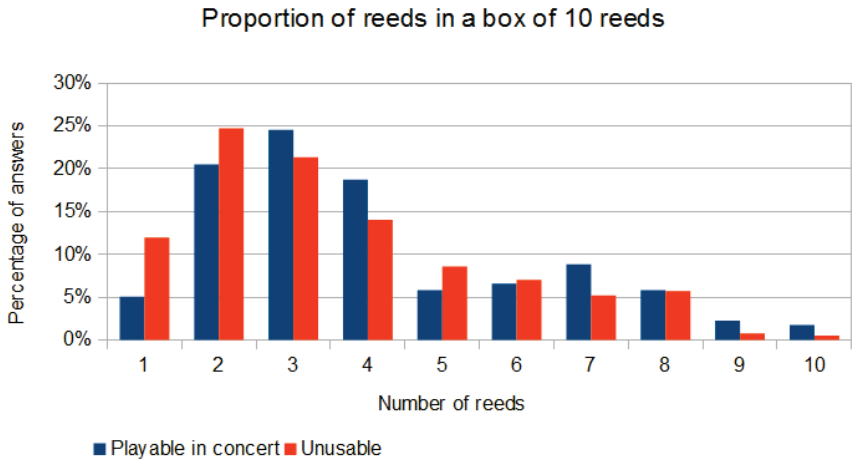

FIGURE 3.5: Results for the proportion of reeds playable in concert or unusable in a box of 10 reeds. 375 answers considered.

3.1.3.2 Criteria for classifying the reeds

The criteria used by musicians to evaluate reeds according to their quality are not clearly established and may vary from one musician to another. The aim of this part of the study is to find which criteria are reported as the most important for the quality of a reed within a given set of reed quality descriptors.

The survey provided the list of 10 quality descriptors presented below. These descriptors were chosen by a musician, based on his musical and scientific experience.

- Appearance (AP),
- Stability in time (ST),

- Life time (LT),
- Accuracy (AC),
- Ease of playing (EP),
- Timbre (T),
- Homogeneity (H),
- Projection (P),
- Expressivity (E),
- Stiffness (S).

The musicians were asked to classify these criteria from the most to the least important in their evaluation of the reed quality. The cumulated score for the rank of the 10 descriptors are given in Tab. 3.7.

TABLE 3.7: Cumulated scores for the ranks of the criteria of the reed quality.

Position	T	EP	E	AC	ST	H	LT	S	AP
1	128	111	23	28	17	14	14	26	8
2	79	79	49	40	33	38	17	22	3
3	57	62	52	46	31	54	18	19	5
4	35	40	48	51	35	32	31	20	4
5	17	24	43	30	42	38	40	32	6
6	12	20	31	37	52	23	36	22	6
7	7	8	37	26	45	30	42	25	16
8	8	4	22	19	29	34	53	50	17
9	12	9	9	15	12	22	34	45	65
10	3	4	1	5	2	6	9	18	115

In order to aggregate the answers for the whole panel of musicians, the Borda method was used [119]. The Borda method consists in assigning a weight to the position of the choice (10 for first choice, 9 for second choice, ...etc, and 1 for last choice), and to multiply the weight by the corresponding number of answers. The Borda score is the sum of the weighted answers by position.

The total scores of the criteria are given in Tab. 3.8, ordered from the largest to the smallest. These results are represented in Fig. 3.6. Three sets of descriptors can be considered. The descriptors 'timbre' and 'ease of playing' appear as the most important for the quality of the reeds. The descriptor 'Appearance' is classed as the least important descriptor of quality. The descriptors in between are closer in score and thus less distinguishable in terms of importance.

TABLE 3.8: Borda scores for the criteria of the reed quality.

T	EP	E	AC	ST	H	LT	S	AP
2933	2907	2069	1926	1765	1753	1478	1410	601

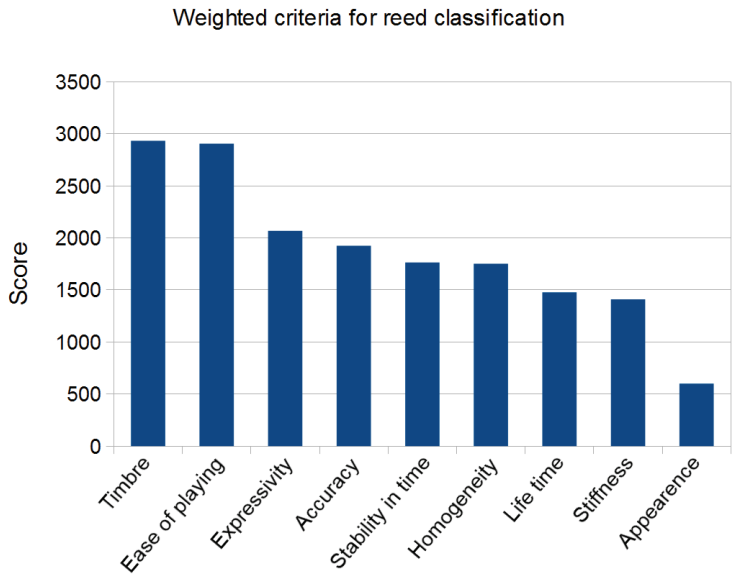

FIGURE 3.6: Scores of the reed quality criteria using the Borda criterium.

Finally, the descriptors 'timbre' and 'ease of playing' are retained for the perceptive tests as subjective descriptors for the characterisation of the reeds according to their perceived quality.

3.2 Subjective characterisation of a set of reeds by a panel of musicians

In this section, subjective tests are conducted using the quality descriptors identified with the survey (§3.1.3.2). The performance of the descriptors and the panel of musicians participating in the study are assessed.

3.2.1 Study design

The selection of the subjective quality descriptors for the reeds uses the quantitative results obtained in the survey in §3.1.3.2. The reed quality descriptors considered as the most important by the survey participants are 'ease of playing' and 'timbre'. The descriptor 'global quality' is added to the study.

Two assumptions are made for this study: the reeds properties remain constant all along the tests (reeds do not change from one evaluation to another) and the setting of the reed on the mouthpiece is accurate enough and similar for all the musicians so that it does not affect the perceived properties of the reed.

The evaluation panel, the considered set of reeds and the subjective tests procedures are detailed below.

Evaluation panel:

The panel of musicians evaluating the reeds is composed of 7 musicians, who play classical music or jazz as amateurs or professionals.

Reeds:

The set of reeds under study is composed of 20 reeds of 2 different brands and 2 different cuts (4 groups of 5 reeds) with equivalent strength (using the comparison chart in Fig. 3.1). These groups are:

- 5 reeds D'Addario Select Jazz strength 3 soft,
- 5 reeds Rico Reserve strength 3.0,
- 5 reeds Vandoren Tradition strength 2 1/2,
- 5 reeds Vandoren ZZ strength 3.

The reeds are numerated from 1 to 20 and their correspondence with the aforementioned brands is kept confidential to avoid commercial comparison.

Subjective tests:

The subjective tests are conducted using absolute evaluations on a continuous scale. The musicians put a mark on a line whose beginning and end are labelled with the extremes of a particular subjective criteria ('very ...' to 'not ... at all'). Afterwards, this is converted in a distance from 0 to 5. The criteria used to evaluate the reeds' quality are 'ease of playing' (varying from 'very easy' to 'not easy at all'), 'timbre' (varying from 'very bright' to 'not bright at all') and 'quality' (varying from 'very good' to 'not good at all'). Each musician performs the tests using her/his own saxophone and the same mouthpiece (a V16 from Vandoren). The musicians install the reed on the mouthpiece by themselves. The tests start after a free-time warm-up for the musician.

The evaluation of the reeds consists in a blind test with three repetitions (the musicians were not informed that each reed was evaluated three times). In each repetition, the reeds were given to the musicians in a random order. The musicians play freely for the evaluation of each reed.

3.2.2 Evaluation of the performance of the panel

The validity of the subjective criteria selected to describe the reed quality and the performance of the panel of musicians to evaluate the reeds are assessed using analysis of variance (ANOVA) with the linear mixed model and the Fisher's F-test [120].

In the following, the notation employed for the quantitative assessments is y_{ijk}: rating of the reed i by musician j during repetition k.

3.2.2.1 Analysis of variance for the group

The analysis of the evaluation data is done through two-way analysis of variance (ANOVA) with interaction, with the factors 'reed', 'musician', 'reed·musician', for each descriptor ('ease of playing', 'timbre' and 'quality'). The ANOVA mixed model is written as follows:

$$y_{ijk} = \mu + \alpha_i + \beta_j + \gamma_{ij} + \epsilon_{ijk}, \tag{3.1}$$

with

- μ: constant,
- α_i: effect of the reed (fixed effect). It represents the mean differences between the reeds.
- β_j: effect of the musician (random effect). It represents the mean differences between the musicians in the boundary scale position. Choosing a random effect allows for generalizing the study results to other subjects outside the evaluation panel.
- γ_{ij}: interaction 'reed·musician' (random effect). It represents the differences attributable to the pairing reed-musician.
- ϵ_{ijk}: error. It is supposed $\epsilon \approx N(0, \sigma^2)$ and independent.

The results of the Fisher's F-test of the ANOVA (p-value) are given in Tab. 3.9.

TABLE 3.9: Two-way ANOVA with interaction. Fisher's statistics and p-values of the ANOVA (mixed model) for the group, for all the descriptors, with a significance level of 5%. The non statistically significant effects are indicated in red.

		Musician	Reed	Interaction
Ease of playing	F	$F(6, 114) = 2.01$	$F(19, 114) = 3.46$	$F(114, 280) = 3.62$
	p-value	0.069	< 0.0001	< 0.0001
Timbre	F	$F(6, 114) = 4.45$	$F(19, 114) = 2.24$	$F(114, 280) = 2.68$
	p-value	< 0.0001	0.005	< 0.0001
Quality	F	$F(6, 114) = 7.32$	$F(19, 114) = 4.13$	$F(114, 280) = 1.57$
	p-value	< 0.0001	< 0.0001	0.001

The 'reed' effects are significant for all the descriptors (p-value≤ 0.05), so the panel is globally discriminant (the differences between reeds are perceived for the three descriptors). The 'musician' effect is significant for the descriptors 'timbre' and 'quality' (this shows an offset in the use of the rating scale, globally due to the fact that the musicians do not have a specific training in the evaluation task). The 'musician·reed' interaction is significant for the three descriptors. This shows either a disagreement between the musicians in the rating of the reeds or differences between musicians in the use of the scale (scaling effect).

3.2.2.2 Analysis of variance for the individuals

The analysis of the data is done through one-way analysis of variance for each musician (individual model). The ANOVA model is written as follows:

$$y_{ijk} = \mu + \alpha_i + \epsilon_{ijk}, \tag{3.2}$$

with

- μ: constant,
- α_i: effect of the reed (fixed effect). It represents the mean differences between the reeds.
- ϵ_{ijk}: error. It is supposed $\epsilon \approx N(0, \sigma^2)$ and independent.

TABLE 3.10: One-way ANOVA for each musician (m1, m2, etc). Fisher's statistics and p-value of the ANOVA for each musician and each descriptor, with a significance level of 5%. The non statistically significant effects are indicated in red.

		m1	m2	m3	m4	m5	m6	m7
Ease of playing	$F(19, 40)$	7.581	0.811	5.661	7.627	7.060	4.565	2.552
	p-value	< 0.0001	0.682	< 0.0001	< 0.0001	< 0.0001	< 0.0001	0.006
Timbre	$F(19, 40)$	5.730	1.251	5.392	4.905	4.400	1.398	0.876
	p-value	< 0.0001	0.268	< 0.0001	< 0.0001	< 0.0001	0.183	0.611
Quality	$F(19, 40)$	4.238	1.743	3.787	3.305	3.009	0.714	2.206
	p-value	< 0.0001	0.069	0.0001	0.001	0.002	0.783	0.018

The results of the ANOVA are given in Tab. 3.10.

For the musicians 1, 3, 4 and 5, the reed effect is significant with a p-value$<$ 5 % for all the descriptors (these musicians properly distinguish the reeds). The 'musician 2' is not discriminant for any of the descriptors because the differences between the reeds are too small given the repetition error (this may be because this musician usually practices alto saxophone and only recently she practices tenor saxophone). The 'musician 6' is not discriminant for the descriptors 'timbre' and 'quality', and the 'musician 7' is not discriminant for the descriptor 'timbre'.

The evaluation of the 'musician 2' for the three descriptors, the evaluations of the 'musician 6' for 'timbre' and 'quality' and the evaluations of the 'musician 7' for 'timbre' are excluded from the study, in order to define a representative evaluation of the reeds.

3.2.2.3 Analysis of the agreement between the musicians

In order to analyse the agreement between the musicians in the rating of the reeds, a Principal Components Analysis is performed [120, 121]. The PCA is a non-standardized PCA with the reeds as individuals and the musicians as variables. The analysis is done for the three descriptors. Results are given in Fig. 3.7, 3.8 and 3.9 respectively for 'ease of playing', 'timbre' and 'quality'

In all cases, two principal components (F1 and F2) explain more than the 85 % of the variance. The % of variance accounted for by the first principal component (F1) is higher for the descriptor 'ease of playing' (66%) than for 'timbre' (60%) and 'quality' (53%). The graphs also show that 'musician 1' is in opposition to the rest of the group for the

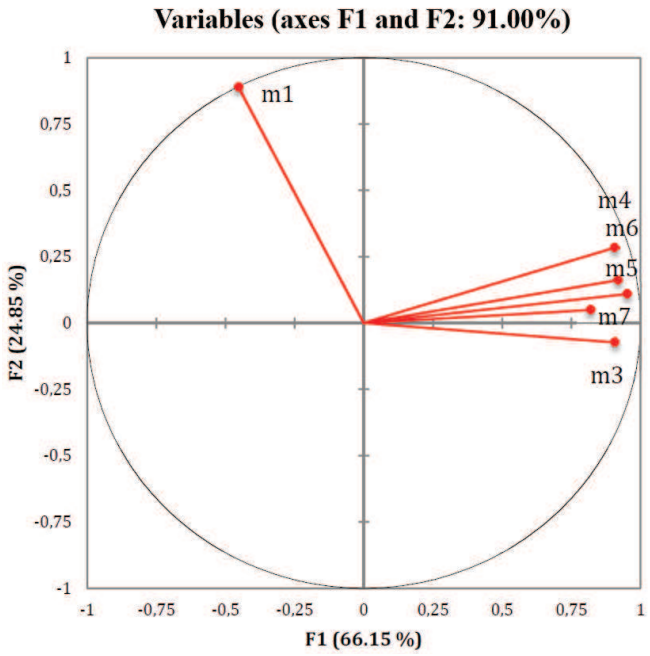

FIGURE 3.7: PCA for 'ease of playing'.

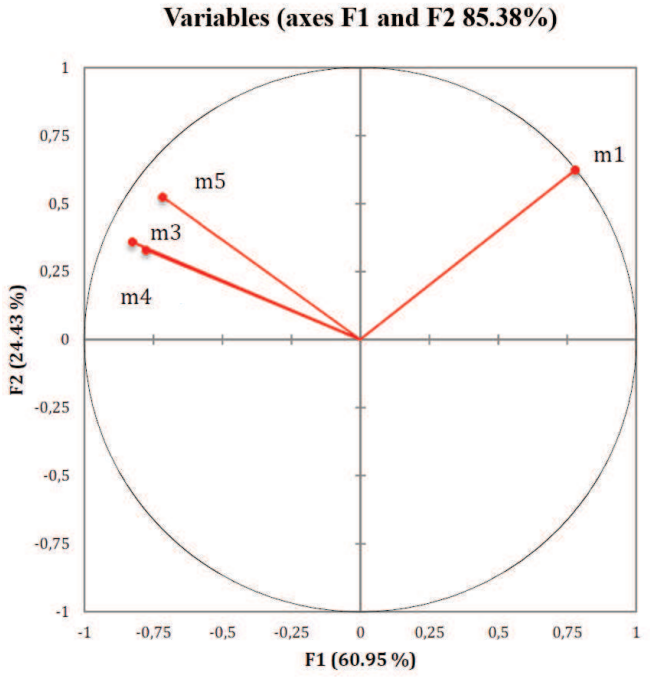

FIGURE 3.8: PCA for 'timbre'.

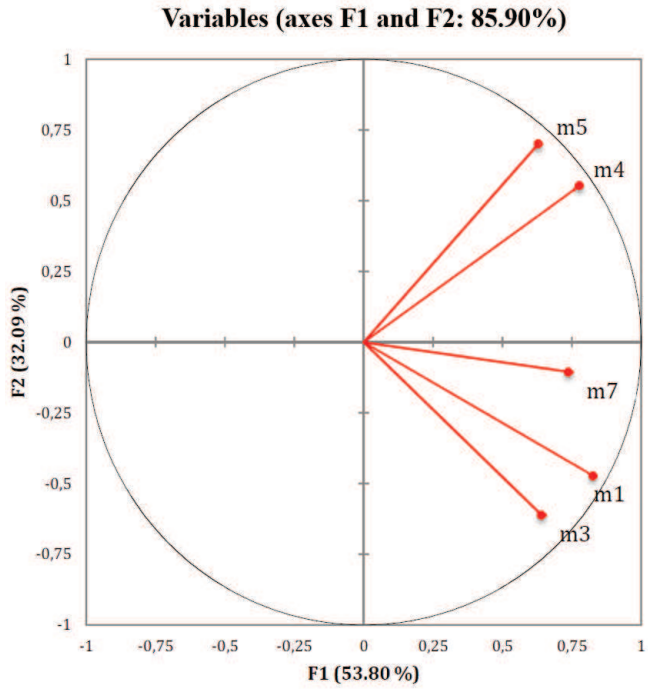

FIGURE 3.9: PCA for 'quality'.

descriptors 'ease of playing' and 'timbre'. For the descriptor 'quality', an important disagreement is observed between all the musicians, so the descriptor is removed from the study.

Given the disagreement of 'musician 1' with the rest of the group for the descriptors 'ease of playing' and 'timbre', his evaluations are excluded from the study to constitute the mean subjective evaluations.

3.2.3 Conclusion

The mean evaluation of the reeds is done considering the evaluations provided by musicians 3, 4, 5, 6 and 7 for 'ease of playing' and by musicians 3, 4 and 5 for 'timbre'. The results are shown in Fig. 3.10. The error bars represent the standard deviation of the selected evaluations of the musicians and the three repetitions (represented in the figure as $\pm\sigma$).

A strong correlation (r=0.95) is obtained between 'ease of playing' and 'timbre'. An 'easy to play' reed is judged as 'bright' and inversely. The uncertainty of the evaluations, obtained as the standard deviation from the mean for musicians and repetitions, is high (30%).

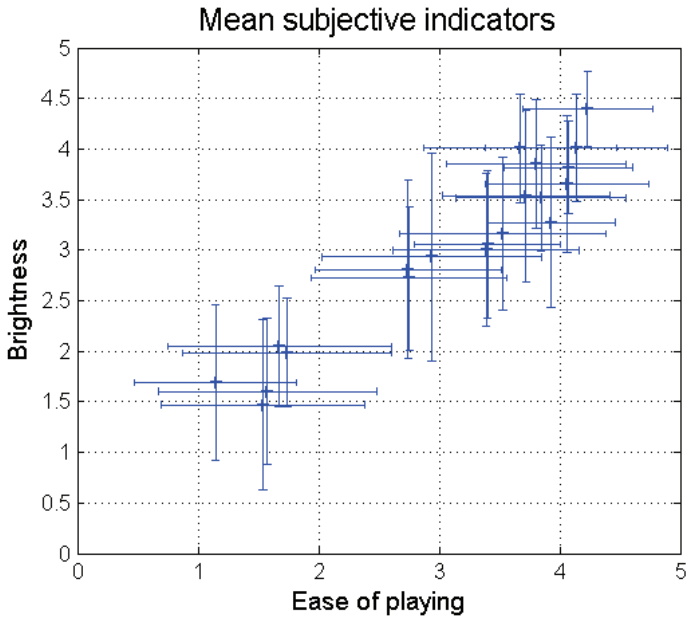

FIGURE 3.10: Mean evaluation of the 20 reeds for the descriptors 'ease of playing' and 'timbre'. The error bars correspond to the standard deviation for the repetition of the evaluations.

The results are coherent with previous research on subjective classification of reeds [2], where the descriptors 'ease of playing' and 'timbre' are the most consensual and they are strongly correlated.

3.3 Objective characterisation of a set of reeds by a panel of musicians

For this work, the musicians in the subjective study are asked to play a single note using the instrumented mouthpiece connected to a cylindrical resonator for the set of 20 reeds used in the subjective tests. The pressure inside the mouthpiece, the pressure in the musician's mouth, the reed displacement near the left part of the reed tip and the acceleration on the mouthpiece next to the right and left lays are measured. These measurements allow obtaining two sets of parameters: the playing parameters (issued from signal analysis [2]) and the reed parameters (issued from physical modelling, Chapter 2). The results for both sets of parameters are given in §3.3.2 and §3.3.3, respectively.

In order to perform the calibration of the reed displacement measurements, a calibrator specifically designed for this purpose is used. This device allows for a fast calibration of each reed and each measurement. The principle and associated uncertainty of the calibrator are explained further in this document, in §4.2.2. The Computer-Aided Design of the device is given in Appendix D.

3.3.1 Study design

The objective tests are conducted using the instrumented mouthpiece, which is based on a V16 Vandoren mouthpiece (the same model used in the subjective tests). The resonator is a 50 cm long cylinder. The musicians are given a warm-up time to get used to playing the instrumented mouthpiece and the cylindrical resonator. For the acquired tones, the attack is not considered and only the stationary part of the note is measured. The musicians are asked to play at a reference sound level (the RMS level of the pressure inside the mouthpiece is shown to the musicians by using a multimeter), in order to minimize the variability inter-musician due to the playing dynamics. The duration of the acquisitions is established in 3 s and the musicians are asked to maintain a constant playing (measurements whose deviation from the reference level is higher than 10% are discarded).

No repetitions of the measurements are performed, so no conclusions about the repeatability of the objective measurements can be assessed in this work. Only a rough estimation of the uncertainty is done by measuring 5 repetitions of the acquisition of one 1s-long tone for one reed with one musician. The standard deviation of the pressure level in the mouthpiece, used as reference for the playing level, is 11.9 %, which is lower than 1 dB. The standard deviation obtained for the estimated playing parameters is given in §3.3.2.

3.3.2 Playing parameters

The playing parameters used are listed below and their formulation is given in [2, 72]. The nomenclature and estimated uncertainty (relative standard deviation, in %, estimated from 5 repetitions of one measurement) are given in this list.

- Mean pressure in the musician's mouth $mean(P_m)$, $\sigma = 4.0\%$.
- Spectral Centroid of the pressure inside the mouthpiece $SC(P_{mp})$, $\sigma = 1.6\%$.
- Odd-harmonic Spectral Centroid of the pressure inside the mouthpiece $SCodd(P_{mp})$, $\sigma = 0.9\%$.
- Even-harmonic Spectral Centroid of the pressure inside the mouthpiece $SCeven(P_{mp})$, $\sigma = 5.6\%$.
- Odd and Even harmonic Ratio of the pressure inside the mouthpiece $OER(P_{mp})$, $\sigma = 8.7\%$.
- Tristumulus 1 of the pressure inside the mouthpiece $TR1(P_{mp})$, $\sigma = 0.1\%$.

- Tristimulus 2 of the pressure inside the mouthpiece $TR2(P_{mp})$, $\sigma = 8.0\%$.
- RMS level of the displacement at the left of the reed $RMS(y_1)$, $\sigma = 14.3\%$. The RMS level of the displacement at the right of the reed is not considered because of experimental problems.
- RMS level of the acceleration at the right of the mouthpiece $RMS(acc_1)$, $\sigma = 17.0\%$.
- RMS level of the acceleration at the left of the mouthpiece$RMS(acc_2)$, $\sigma = 12.0\%$.

It is important to note that some of the uncertainties are high, specially for the RMS levels of the displacement and the accelerations. However, these parameters are retained for the study because this uncertainty may vary from one musician to another, and the differences between the reeds may be higher than these uncertainties. In the performed measurements, it was observed that the same sound level can be produced by different embouchures (different lip positions). As the reference for the player is the sound, an important deviation in the parameters linked to the embouchure (levels of the reed displacement and the acceleration on the mouthpiece) can be expected.

In order to study the effect of the reeds on the playing parameters, a two-way analysis of variance (ANOVA) without interaction, with the factors 'reed' and 'musician', is performed for each parameter. The ANOVA model for a given playing parameter y is written as follows:

$$y_{ijk} = \mu + \alpha_i + \beta_j + \epsilon_{ijk}, \tag{3.3}$$

with

- μ: constant,
- α_i: effect of the reed (fixed effect). It represents the mean differences between the reeds.
- β_j: effect of the musician (fixed effect). It represents the mean differences between the musicians.
- ϵ_{ijk}: error. It is supposed $\epsilon \approx N(0, \sigma^2)$ and independent.

The results of the ANOVA analysis are given in Tab. 3.11. The size of the effect of each factor is assessed with η^2.

The 'reed' effect is significant for all the descriptors (differences between the reeds in the playing parameters do exist), except for '$RMS(y_1)$'. This variable is excluded from

TABLE 3.11: Fisher's statistics, p-value and η^2 for the tow-way ANOVA of the playing parameters for the factors 'musician' and 'reed'. The least significant effects (at the 5 % threshold) are indicated in red.

	Musician			Reed		
	F(6,114)	p-value	η^2 (%)	F(19,114)	p-value	η^2
$mean(P_m)$	9.82	< 0.0001	0.25	3.12	< 0.0001	0.26
$SC(P_{mp})$	46.34	< 0.0001	0.59	4.33	< 0.0001	0.17
$SCodd(P_{mp})$	46.15	< 0.0001	0.60	3.79	< 0.0001	0.16
$SCeven(P_{mp})$	24.27	< 0.0001	0.42	4.60	< 0.0001	0.25
$OER(P_{mp})$	33.20	< 0.0001	0.54	2.77	0.0004	0.14
$TR1(P_{mp})$	15.35	< 0.0001	0.36	2.52	0.001	0.19
$TR2(P_{mp})$	13.38	< 0.0001	0.33	2.39	0.002	0.19
$RMS(y_1)$	2.20	0.048	0.09	0.83	0.67	0.11
$RMS(acc_1)$	7.30	< 0.0001	0.22	2.29	0.004	0.22
$RMS(acc_2)$	16.57	< 0.0001	0.37	2.79	0.0004	0.20

the study. The 'musician' effect is significant for all the descriptors (differences between the musicians in the playing parameters are observed). The 'musician' effect is generally more important than the 'reed' effect. This means that the differences inter-musicians prevail over the differences inter-reeds.

In order to assess the consensus between the reed parameters for the different musicians, a non-standardized PCA is performed for each parameter, with the 'reeds' as individuals and the 'musicians' as variables. The percentages of inertia on the two-first principal components are given in Tab. 3.12.

An important variability between the musicians is observed for the playing parameters (the highest percentage of inertia is 64%). Four parameters are less consensual than the others: '$OER(P_{mp})$', '$TR1(P_{mp})$', '$TR2(P_{mp})$' and '$RMS(acc_2)$', so they are removed from the study. This shows that the musical gesture varies from one musician to another and that there is no global trend in the variation of these playing parameters. Each musician has a particular timbre and manner to adapt the playing strategy to each reed.

TABLE 3.12: Percentage of inertia of the first and second principal components for each playing parameter. The least consensual parameters are indicated in red.

	Principal Component 1	Principal Component 2
$mean(P_m)$	64 %	16 %
$SC(P_{mp})$	51 %	21 %
$SCodd(P_{mp})$	49 %	15 %
$SCeven(P_{mp})$	61 %	12 %
$OER(P_{mp})$	36 %	29 %
$TR1(P_{mp})$	39 %	21 %
$TR2(P_{mp})$	32 %	22 %
$RMS(acc_1)$	55 %	23 %
$RMS(acc_2)$	35 %	26 %

For the most consensual playing parameters, $mean(P_m)$, $SC(P_{mp})$, $SCodd(P_{mp})$, $SCeven(P_{mp})$ and $RMS(acc_1)$, the average playing parameters can be calculated from the playing parameters of the 7 musicians. The Pearson correlation matrix between these mean playing parameters is given in Tab. 3.13.

TABLE 3.13: Pearson correlation matrix between the average playing parameters of the seven musicians. The correlations stronger than 0.8 (or -0.8) are indicated in bold.

Variables	$mean(P_m)$	$SC(P_{mp})$	$SCodd(P_{mp})$	$SCeven(P_{mp})$	$RMS(acc_1)$
$mean(P_m)$	**1**	**-0.830**	**-0.831**	-0.709	-0.750
$SC(P_{mp})$	**-0.830**	**1**	**0.999**	**0.879**	**0.874**
$SCodd(P_{mp})$	**-0.831**	**0.999**	**1**	**0.859**	**0.868**
$SCeven(P_{mp})$	-0.709	**0.879**	**0.859**	**1**	0.754
$RMS(acc_1)$	-0.750	**0.874**	**0.868**	0.754	**1**

The correlations between the mean playing parameters are strong. The strongest correlations (above 0.8 or below -0.8) are indicated in bold in Tab.3.13. The parameter $mean(P_m)$ is negatively correlated to the other parameters, meaning that $mean(P_m)$ decreases with increasing Spectral Centroid and RMS level of the acceleration on the

right side of the mouthpiece. The correlations between $mean(P_m)$ and $SCeven(P_{mp})$ and $RMS(acc_1)$ are the weakest. The correlation between $SCeven(P_{mp})$ and $RMS(acc_1)$ is also moderate. The timbre indicators are very correlated between themselves. In particular, the $SCodd(P_{mp})$ is very strongly correlated to $SC(P_{mp})$, because the harmonics of the cylindrical resonator (odd harmonics) are the main contributors to the total Spectral Centroid.

3.3.3 Reed parameters

In addition to the playing parameters, the instrumented mouthpiece enables the estimation of reed parameters obtained by physical modelling (see Chapter 2). The reed parameters considered in this study are the reed aperture H, the linear component of the stiffness K and the damping R of the model of the oscillator containing damping and non-linear stiffness (RK_{nl}). For each reed, a set of parameters is estimated. The estimations are performed in windows of 5 periods for the 1s-long signals, to obtain the average reed parameters.

The reference sound level given to the musicians is selected in order to ensure the validity of this model according to the dynamic level (see §2.6 for more details). The results of the modelling of the measurements for each reed are accepted only when the normal error of the modelling *errn* (see §2.5.1) is inferior to 5 %. The estimated uncertainties from the 5 repetitions of one measurement and one musician are 7.5 % for K and 2.9 % for R.

Nevertheless, the presence of estimations with errors *errn* higher than 5 % complicates the statistical analysis of the descriptors. Depending on the musician, there are from 0 to 14 estimations over the 5 % error threshold, as shown in Tab.3.14. Only the 'musician 4' is considered for the reed parameters because he presents all convergent estimations.

The validity of the reed model had only been proved for one musician and one reed (see Chapter 2). Its application to different musicians and reeds shows that the accuracy of the model can vary. Different playing techniques and musical gestures may lead to different reed models. The estimation of reed parameters is only exploitable for 'musician 4'. The other musicians are discarded for this part of the study.

For the 'musician 4', the estimated beginning of the non-linear part of the stiffness y_c for the 20 reeds attains values from 0.01 mm to 0.1 mm or, referred to the maximal reed displacement, from 0.03 H to 0.25 H. This parameter has an important variability (standard deviation of 50%) and its detection seems to affect the estimation of the linear part of the stiffness K. The non-linear model of the stiffness is not completely

TABLE 3.14: Number of estimations with error $errn > 5$ % of the 20 reeds (30 estimations).

Musician	Discarded estimations
Musician 1	6
Musician 2	4
Musician 3	1
Musician 4	0
Musician 5	14
Musician 6	5
Musician 7	2

adapted to the measurements, and this introduces conditioning problems in the estimated parameters. The model does not consider the transverse deformation of the reed and it may be more suitable for the displacement of the reed at its edges. The fact that the displacement sensors are not placed at the edges of the mouthpiece may reduce the representativeness of the 1D-model employed.

In addition to that, the instrumented mouthpiece has proved to be a delicate measurement device when applying to mass measurements in real playing conditions. The sensitivity of the sensors (specially the displacement sensors) to humidity and random measurement factors may introduce high uncertainties and noise in the measurements.

3.4 Correlation between subjective and objective characterisations

The correlation between the subjective classification of reeds (§3.2) and the objective measurements (§3.3) is studied. The subjective evaluations considered are the mean of the descriptors for the selected musicians (see details in §3.2.3) and the selected objective parameters.

3.4.1 Correlation with playing parameters

The correlation between the mean subjective evaluations, for the selected musicians, and the mean playing parameters, for the selected descriptors, are given in Tab. 3.15.

TABLE 3.15: Correlation coefficient between the mean subjective evaluations and the mean playing parameters.

	Ease of playing	Timbre
$mean(P_m)$	-0.865	-0.865
$SC(P_{mp})$	0.896	0.900
$SCodd(P_{mp})$	0.816	0.810
$SCeven(P_{mp})$	0.870	0.892
$RMS(acc_1)$	0.858	0.844

Important and significant correlations between the mean subjective indicators and the mean playing parameters are observed, despite the variability among the musicians.

A standardized PCA with the reeds as individuals and mean of the selected playing parameters as variables is performed to analyse these correlations, adding the projection of the descriptors 'ease of playing' and 'timbre' as supplementary variables. The plot corresponding to the first and second principal components (F1 and F2) is given in Fig. 3.11, and the one for the first and third principal components (F1 and F3) in Fig. 3.12.

The principal dimension, explaining 86.99 % of the variance, is mainly created by $SC(P_{mp})$, $SCodd(P_{mp})$ and $RMS(acc_1)$. The subjective descriptors 'ease of playing' and 'timbre' are mainly projected on this dimension. The second dimension explains 5.91 % of the variance and is composed by $mean(P_m)$ and $SCeven(P_{mp})$. The third dimension explains 4.66 % of the variance and is composed by $RMS(acc_1)$.

Predictive models of the 'ease of playing' or the 'timbre' from the playing parameters can be proposed using multiple linear regression. There exists a strong correlation between $SC(P_{mp})$, $SCodd(P_{mp})$ and $SCeven(P_{mp})$, so only the parameter $SCeven(P_{mp})$ is considered in the modelling.

A first predictive model using two variables is calculated. The variables in the model are $mean(P_m)$ and $SCeven(P_{mp})$. The regression for a subjective descriptor y is written as given in Eq. 3.4.

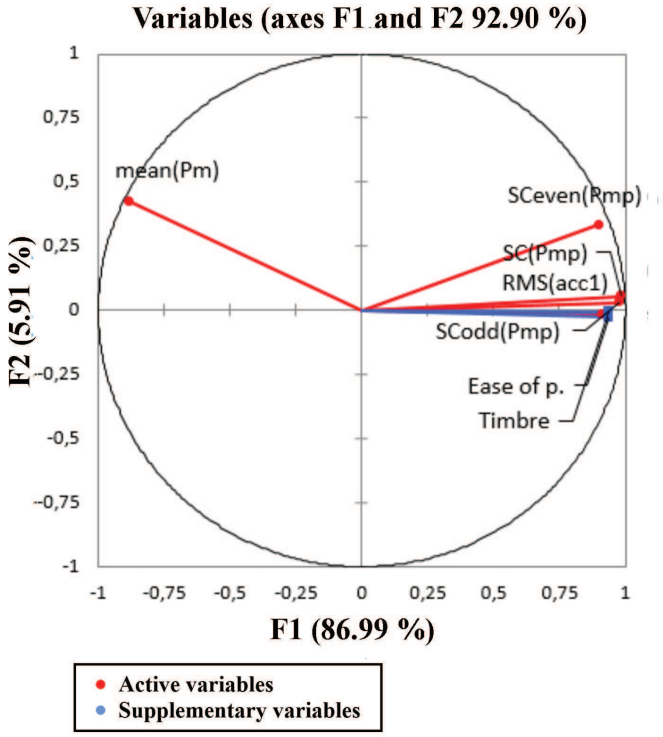

FIGURE 3.11: PCA for the playing parameters, axes F1 and F2. The subjective descriptors 'ease of playing' and 'timbre' are added as supplementary variables.

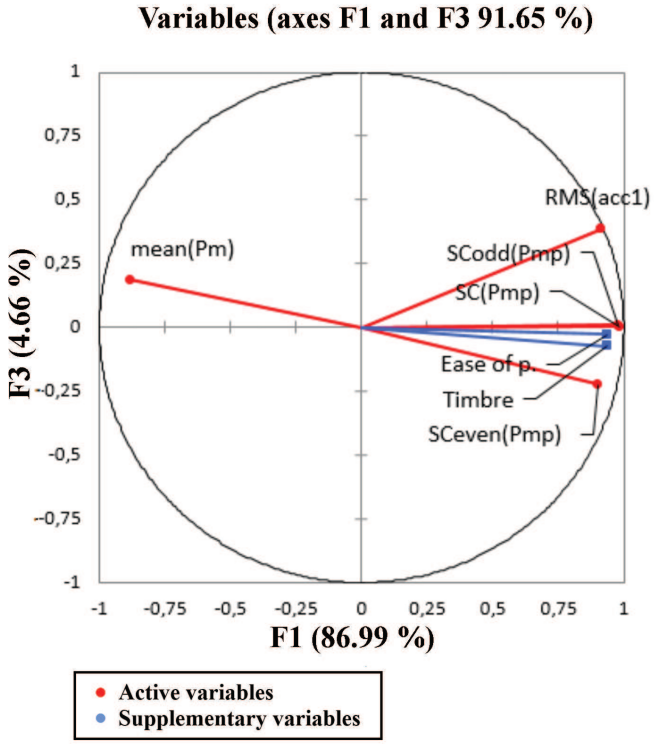

FIGURE 3.12: PCA for the playing parameters, axes F1 and F3. The subjective descriptors 'ease of playing' and 'timbre' are added as supplementary variables.

$$y_i = a \cdot mean(P_m)_i + b \cdot SCeven(P_{mp})_i + c + \epsilon_i. \tag{3.4}$$

The obtained parameters of the models for 'ease of playing' and 'timbre', as well as the goodness of fit statistics are given in Tab. 3.16. The parameters of the model significant at a 0.1 % threshold are indicated in bold.

TABLE 3.16: Coefficients of the multiple linear regression model of the mean subjective evaluations for 'ease of playing' and 'timbre' and the mean playing parameters $mean(P_m)$ and $SCeven(P_{mp})$. The significant parameters (p-value<0.001) are indicated in bold.

Descriptor y	a	b	R^2	Q^2
Ease of playing	$\mathbf{-12.954 \cdot 10^{-4}}$ $\mathbf{p < 0.001}$	$\mathbf{1.377}$ $\mathbf{p < 0.001}$	0.867	0.822
Timbre	$\mathbf{-9.098 \cdot 10^{-4}}$ $\mathbf{p < 0.001}$	$\mathbf{1.093}$ $\mathbf{p < 0.0005}$	0.893	0.852

The value of R^2, which scores the percentage of variance modelled by the regression is high for both subjective descriptors (86.7 % for the 'ease of playing' and 89.3 % for the 'timbre'). The predictive power of the model can be assessed with the value of Q^2, which measures the percentage of variance predicted by the model using cross validation. The predictive power is high both for 'ease of playing' (82.2 %) and 'timbre' (85.2 %).

All the obtained coefficients of the models are significant at 0.1 % threshold. Both subjective descriptors 'ease of playing' and 'timbre' are negatively correlated to $mean(P_m)$, meaning that 'easy to play' and 'bright' reeds need lower pressure to play that 'hard to play' and 'dull' reeds, and positively correlated to $SCeven(P_{mp})$, which is an indicator of brightness of the sound. The standardized coefficients of the models are shown in Fig. 3.13 for 'ease of playing' and in Fig. 3.14 for 'timbre'.

The played instrument is a clarinet-like resonator, which is characterised by odd resonance frequencies. The even frequencies in the spectrum can be associated to the timbre of the reed. This justifies the importance of the coefficient for $SCeven(P_{mp})$ obtained in the standardized regression.

A more accurate model using three variables can also be calculated. The chosen variables are $mean(P_m)$, $SCeven(P_{mp})$ and $RMS(acc_1)$, which are main contributors of the three independent dimensions of the PCA in Fig. 3.11 and 3.12, explaining 97.56 % of the variance. The model is optimised according to the adjusted R^2, in such a manner that the algorithm chooses among the three variables the ones that maximise this indicator. The regression is written as given in Eq. 3.5 for each subjective descriptor y. The

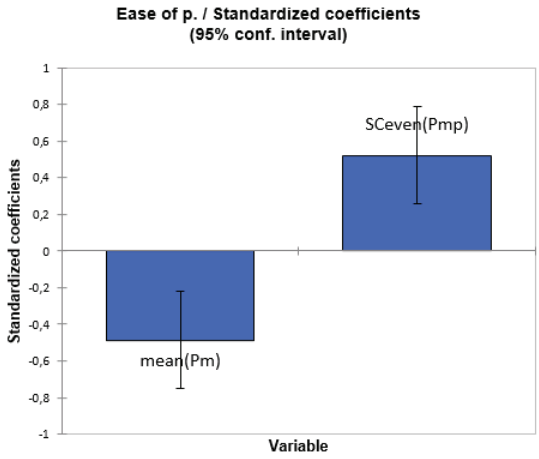

FIGURE 3.13: Standardized coefficients of the two-variable linear regression model for 'ease of playing'.

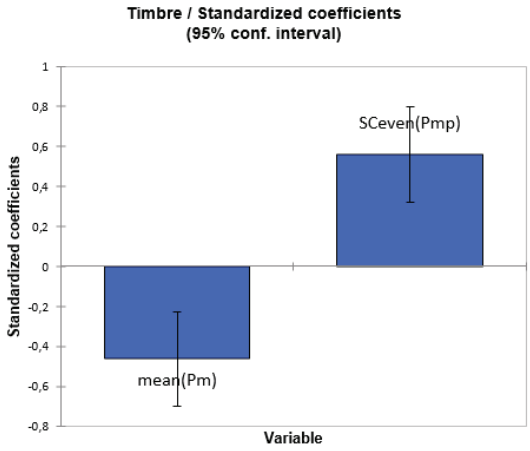

FIGURE 3.14: Standardized coefficients of the two-variable linear regression model for 'timbre'.

results of the models for 'ease of playing' and 'timbre' are given in Tab. 3.17, where the significant parameters at a 5 % threshold are indicated in bold.

$$y_i = a \cdot mean(P_m)_i + b \cdot SCeven(P_{mp})_i + c \cdot RMS(acc_1)_i + d + \epsilon_i. \tag{3.5}$$

All the coefficients are significant in the model for 'ease of playing', meaning that the three playing parameters $mean(P_m)$, $SCeven(P_{mp})$ and $RMS(acc_1)$ contribute to explain the subjective descriptor. The variable $RMS(acc_1)$ is not significant in the model for 'timbre'. The standardized coefficients of the models are shown in Fig. 3.15 for 'ease of playing' and in Fig. 3.16 for 'timbre'.

The variable $SCeven(P_{mp})$ is the most influential. The instability of the parameter

TABLE 3.17: Coefficients of the multiple linear regression model of the mean subjective evaluations for 'ease of playing' and 'timbre' and the mean playing parameters $mean(P_m)$, $SCeven(P_{mp})$ and $RMS(acc_1)$. The significant parameters (p-value<0.05) are indicated in bold.

Descriptor y	a	b	c	R^2	Q^2
Ease of playing	$\mathbf{-9.296 \cdot 10^{-4}}$ $\mathbf{p = 0.014}$	$\mathbf{1.004}$ $\mathbf{p = 0.009}$	$\mathbf{1.408 \cdot 10^{3}}$ $\mathbf{p = 0.033}$	0.901	0.852
Timbre	$\mathbf{-7.019 \cdot 10^{-4}}$ $\mathbf{p = 0.008}$	$\mathbf{0.881}$ $\mathbf{p = 0.002}$	$0.800 \cdot 10^{3}$ $p = 0.073$	0.913	0.872

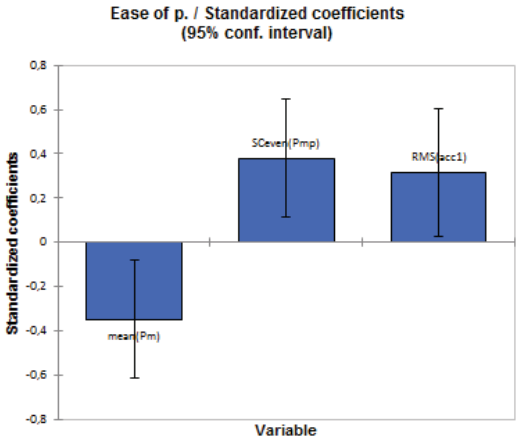

FIGURE 3.15: Standardized coefficients of the three-variable linear regression model for 'ease of playing'.

for $RMS(acc_1)$ in the model for 'timbre' can be observed in Fig. 3.16. The descriptors 'ease of playing' and 'timbre' increase with decreasing $mean(P_m)$, and increasing $SCeven(P_{mp})$ and $RMS(acc_1)$. An 'easy to play' or 'bright' reed needs lower blowing pressure to produce a given sound level, its sound is brighter (higher SC) and produces stronger impacts on the mouthpiece. The model fit is high for both descriptors (90.1 % and 91.3 % of explained variance respectively for 'ease of playing' and 'timbre'), and the predictive power of the models is high (85.2 % for 'ease of playing' and 87.2 % for 'timbre'). The models can be used to predict the descriptors from the playing parameters measurements.

These results are coherent with those obtained by Petiot et al. [2]. In that work, the predictive model was built using also variables defined in the attack transient of the played tones, and the measurements were performed with two musicians without playing level reference. Their Partial Least-Squares regression model used 13 variables and obtained an R^2 of 85 % for 'Softness' and 75 % for 'Brightness'. In this case, the model is built using a lower number of variables and a larger panel of musicians. The

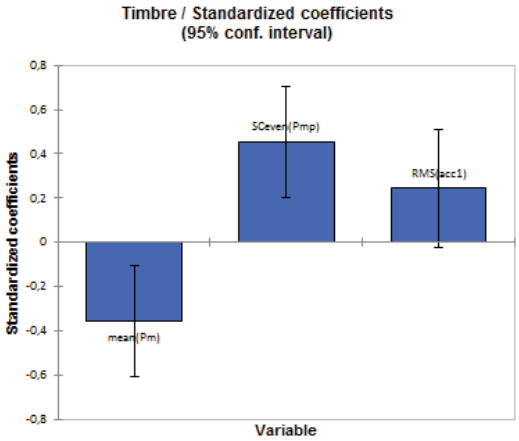

FIGURE 3.16: Standardized coefficients of the three-variable linear regression model for 'timbre'.

fact of using a reference playing level may have helped to reduce the differences between musicians and highlights the differences between reeds.

3.4.2 Correlation with reed parameters

The correlation between the reed parameters for 'musician 4' (§3.3.3) and the subjective evaluations of 'ease of playing' and 'timbre' is analysed, first for the subjective assessments of 'musician 4', and then for the average evaluations from the selected musicians. The results are given in Tab. 3.18.

In order to ascertain the validity of the subjective characterisation for the 'musician 4', it is verified that a strong correlation appears between the subjective evaluations of the 'musician 4' and the mean evaluations of the selected musicians, indicating an agreement between the musician and the rest of the panel (see Tab. 3.18).

TABLE 3.18: Correlation coefficient between the mean subjective evaluations, the subjective evaluations of 'musician 4' and the reed parameters of 'musician 4'.

	Ease of playing (Musician 4)	Timbre (Musician 4)	Ease of playing (mean)	Timbre (mean)
K	-0.6	-0.579	-0.508	-0.478
H	0.253	0.136	0.279	0.238
R	-0.527	-0.453	-0.439	-0.403

For 20 individuals, the correlations between each pair of quantitative assessments are significant for $|r| > 0.423$, at the threshold of 5 %. The highest correlations are those of the stiffness K, which are significant but moderate. The correlation is negative, meaning that the lower the 'stiffness' is, the 'easier to play' and 'brighter' the reed is. The same conclusions apply to the damping R, with the exception that the correlation with the average assessments for 'timbre' is not significant. However, the correlations with the reed aperture H are weak and not significant. The correlations between the subjective assessments of 'musician 4' and the reed parameters for the same musician are higher than those obtained for the mean subjective assessments.

In order to observe these correlations for 'musician 4', a PCA of the parameters K, H and R is performed, adding the projection of the descriptors 'ease of playing' and 'timbre' as supplementary variables. The result is given in Fig. 3.17.

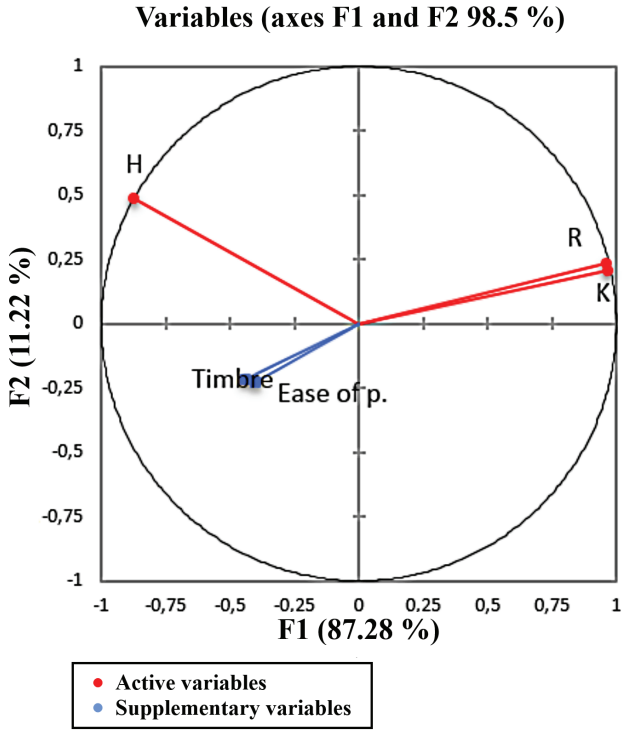

FIGURE 3.17: PCA for the reed parameters K, H and R for 'musician 4'. The subjective descriptors 'ease of playing' and 'timbre' are added as supplementary variables.

This representation confirms that stiffness and damping are correlated for the 'musician 4', as well as 'ease of playing' and 'timbre', which oppose to K and R.

A multiple linear regression model explaining 'ease of playing' or 'timbre' from K and H can be proposed (R, correlated to K, is removed from the study). The model is written as shown in Eq. 3.6. The results are given in Tab. 3.19

$$y_i = a \cdot K + b \cdot H + c + \epsilon_i. \tag{3.6}$$

TABLE 3.19: Coefficients of the multiple linear regression model of the mean subjective evaluations for 'ease of playing' and 'timbre' and the reed parameters K and H for 'musician 4'. The significant parameters (p-value<0.05) are indicated in bold.

Descriptor y	a	b	R^2	Q^2
Ease of playing	$\mathbf{-9 \cdot 10^{-8}}$ $\mathbf{p < 0.05}$	-2705 $p > 0.05$	0.28	0.015
Timbre	$\mathbf{-7 \cdot 10^{-8}}$ $\mathbf{p < 0.05}$	-2375 $p > 0.05$	0.26	0.02

Only the coefficient of K is significant for both models. The model fit is low for both descriptors (28 % for 'ease of playing' and 26 % for 'timbre'). The predictive power of the models is very low (0.015 for 'ease of playing' and 0.02 for 'timbre'), so they cannot be used to predict the reeds' subjective descriptors. Further research is needed to determine a reliable predictive model.

In fact, the comparison of the equivalent reed parameters with the perceived quality may be delicate because each musician may have a different method to adapt to the perceived quality of the reeds. In Fig. 3.18, the characteristics ΔP vs. y for a reed classified as 'easy to play' (Reed 3) and a reed classified as 'not easy to play at all' (Reed 6) by two different musicians ('musician 3' and 'musician 4') are represented. It seems that for the hard to play reed (Reed 6), 'musician 3' adapts slightly the reed aperture imposed by the lip (from 0.25 mm to 0.20 mm) whereas 'musician 4' changes radically the aperture (from 0.35 mm to 0.10 mm) and produces a greater pressure difference (from -55 hPa to -70 hPa). The variation of the stiffness from one reed to the other for both players is very different.

3.5 Conclusions

The study of the subjective classifications of a set of 20 reeds by a panel of 7 musicians has provided a robust evaluation of the reeds regarding the descriptors 'ease of playing' and 'timbre' that is coherent with previous works [2]. The quality descriptors 'ease of playing' and 'timbre', selected by means of a survey among around 400 musicians, have been shown to be correlated, so that only one dimension explains the perceived differences between reeds. The analysis of the repeatability and the consensus among the musicians has enabled the identification of the most reliable musicians, from whom average descriptors are calculated.

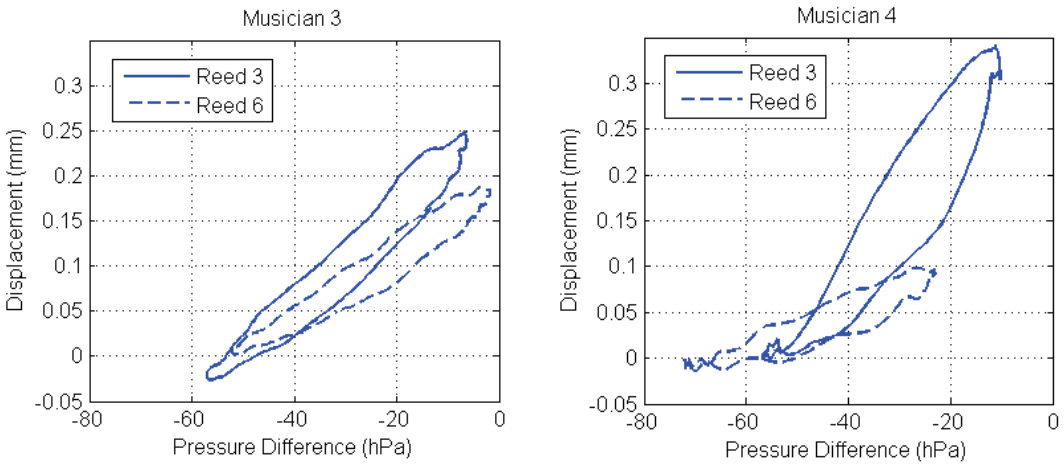

a) musician 3.

b) musician 4.

FIGURE 3.18: Reed displacement as a function of the pressure difference across the reed for an "easy to play" reed (Reed 3) and a "hard to play reed" (Reed 6).

The instrumented mouthpiece, the reed parameter estimation and the playing parameters estimation have been applied to the measurement campaign. When looking at the variance of the playing parameters, the differences inter-musician are higher than the differences inter-reed, because of the variability of the measured musical gestures. However, it is possible to identify some parameters for which there exists an agreement among musicians. Significant correlations are found between the mean values of the parameters $mean(P_m)$, $SC(P_{mp})$, $SCodd(P_{mp})$, $SCeven(P_{mp})$ and $RMS(acc_1)$, and the descriptors 'ease of playing' and 'timbre'. An accurate predictive model for 'ease of playing' and 'timbre' can be calculated by multiple linear regression, using the parameters $mean(P_m)$, $SCeven(P_{mp})$ and $RMS(acc_1)$. The predictive power of the models with three variables is 85 % for 'ease of playing' and 87 % for 'timbre'.

The use of the instrumented mouthpiece for measurement campaigns has shown its limits, specially concerning the displacement measurement. The reed parameters estimation method yields important errors depending on the musician, and the comparison of musicians is not feasible. The correlations obtained between the subjective descriptors of the reed quality and the reed parameters for one musician are weak, and the predictive model obtained cannot be used. The equivalent reed stiffness in playing conditions is negatively correlated to 'ease of playing' and 'timbre', so stiff reeds are hard to play and dull, as expected.

Several improvements to the experiment can also be proposed. The reference sound level imposed in the protocol might affect the musicians' comfort when playing or reduce the dynamics inter-reeds. Taking the mean pressure in the mouth as the pressure reference might have helped to maximize the difference between reeds because it produces different dynamics. Moreover, the resonator used in the objective measurement was a cylinder,

and not a saxophone as in the subjective tests, and the musicians were not used to playing a cylindrical resonator. Some musicians found the instrumented mouthpiece intrusive or preferred another mouthpiece model. These issues should be addressed more carefully in further campaigns.

The conclusions of this work could motivate a systematic study of the instrumental gesture aiming to explain the difference inter-musicians and the link between musical gesture and physical model of the reed. This kind of measurements could be applied to the study of the relation between reed parameters and playing parameters, as done using simulation by Barthet et al. [72].

The limitation of the instrumented mouthpiece when applied to a mass campaign in playing conditions motivates the development of a device allowing for measurements in artificial playing conditions. To this end, an artificial mouth has been developed and it is presented in Chapter 4. The purpose is to minimize the random problems affecting the sensors and to provide a control of the musical gesture ensuring the repeatability of the measurements. Besides, different sensors can be installed on the artificial mouth to study the reed dynamics because there is no size or accessibility limitation, for instance, the reed displacement or velocity can be measured by using a vibrometer.

Chapter 4

Comparison of real and artificial playing of a single-reed instrument using an artificial mouth

This chapter contains the article "Comparison of real and artificial playing of a single-reed instrument using an artificial mouth", submitted to Acta Acustica united with Acustica, and a complement.

The article presents the principle of an aspirating artificial mouth and studies its ability to reproduce a musician's playing. In order to perform the measurements, the instrumented mouthpiece presented in Chapter 2 and a specific calibrator developed for the reed displacement measurement are used. The complement provides an alternative representation of the measurements used in the article that helps in the analysis of the results.

The Computer-Aided Design of the instrumented mouthpiece and the displacement measurement calibrator used in the article is given in Appendix A. The general principle of the artificial mouth is explained in the article, and a more detailed description of the artificial lip positioning system and plate assembly of the artificial mouth are given in Appendix D.

The name of artificial mouth is chosen for coherency with the literature. Although the device does not have a closed cavity acting as the mouth, the purpose and experiments enabled are the same kind as for other artificial mouths in the literature.

Comparison of real and artificial playing of a single-reed instrument using an artificial mouth

Alberto Muñoz Arancón, Bruno Gazengel, Jean-Pierre Dalmont.
Laboratoire d'Acoustique de l'Université du Maine
UMR CNRS 6613, Avenue Olivier Messiaen,
72085 Le Mans cedex 9, France

Abstract

This work presents an aspirating artificial mouth and studies its ability to reproduce a musician's playing. The experiments are conduced using a simplified clarinet equipped with an instrumented mouthpiece. It can be played by a musician or by the artificial mouth.

The working range of the artificial mouth is studied for different artificial lip positions and blowing pressures. The playing parameters (frequency, pressure amplitude and reed displacement amplitude) obtained with the artificial mouth are compared with those obtained with a musician. This allows for the identification of the optimal working range in which the artificial mouth best reproduces the musician's playing.

The pressure difference across the reed and the displacement signals are compared for the musician and the artificial mouth. The artificial mouth reproduces accurately the closing phase, the opening phase and the closed position of the reed. In the open position, inertial effects appear in the reed displacement for the musician, but not for the artificial mouth. This reveals differences between the artificial lip and the musician's.

4.1 Introduction

Musical instruments such as clarinet or saxophone use a single cane reed that makes it possible to produce sound using a constant pressure in the musician's mouth. Reed makers classify reeds according to their cut and strength. However, for a player, different reeds of the same brand, cut and strength may be considered subjectively as different [2]. In consequence, reed makers need to better characterise reeds with objective indicators that better satisfy musician's expectations. Muñoz Arancón et al. [3] proposed a method for estimating the reed equivalent parameters in playing conditions, using an instrumented mouthpiece that measured the reed displacement and the pressure difference across the reed. In order to avoid variability due to the musician's gesture and to ensure stability and reproducibility, objective measurements of reed physical properties should be performed on a measuring bench. The measuring benches commonly used to study woodwinds in playing conditions are named artificial mouths. Most artificial mouths are composed of a closed cavity equivalent to the musician's mouth and providing an overpressure at the entry of the instrument. In such design, the reed remains enclosed in the cavity and it is not easily accessible or exchangeable [16, 83, 89, 91].

In this work, we propose a new artificial mouth that intends to accurately reproduce the musician's gesture in order to characterise reeds in realistic playing conditions, ensuring controlled and repeatable measurements. The main characteristics of this system are the following:

- it uses an aspirating source operating with a negative pressure (pressure lower than the atmospheric pressure) applied at the exit of the instrument;
- the reed remains in open air so that no cavity equivalent to the mouth is used. This property makes the reed calibration and testing easier;
- it can be played by a musician when the aspirating source is off, in order to characterise the musician's playing.

The artificial mouth is equipped with the instrumented mouthpiece described in [3]. This makes it possible to estimate the frequency, the pressure amplitude and the reed displacement amplitude. All these measurements can be obtained either when the artificial mouth is played artificially or by a musician.

This paper is organised as follows: Section 4.2 presents the artificial mouth, the instrumented mouthpiece and the measured signals. Section 4.3 studies the working range of the artificial mouth and compares the playing parameters obtained with artificial playing and with a musician. Section 4.4 presents the comparison of the pressure difference across the reed and reed displacement signals obtained with the artificial mouth and with a musician in order to assess the similarities and differences.

4.2 Artificial mouth

4.2.1 Principle

The principle of the artificial mouth is depicted in Fig. 4.1. The artificial mouth can be divided into two parts: the musical instrument and the aeraulic-control system.

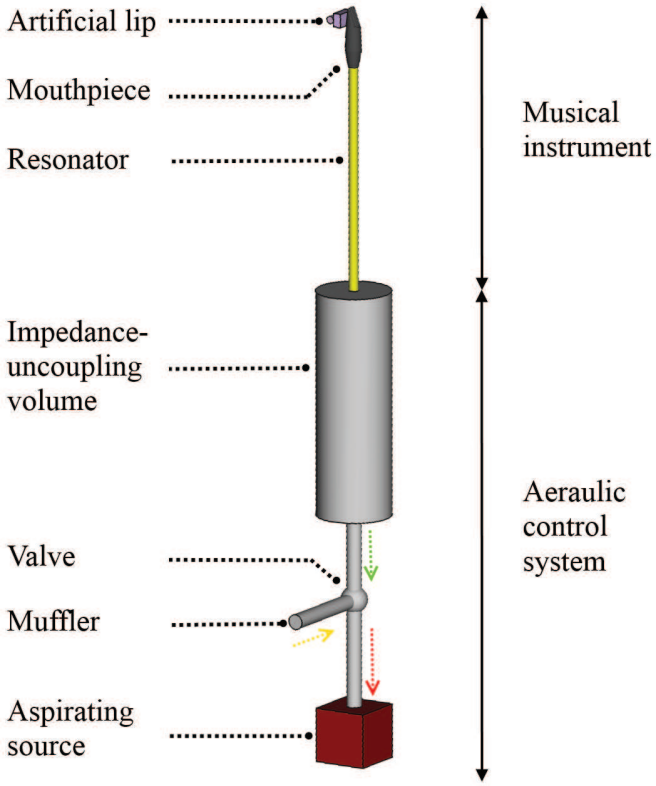

FIGURE 4.1: Schematic view of the artificial mouth.

Musical instrument: It is composed of:

- Mouthpiece: it is a tenor saxophone mouthpiece designed so that it can embed sensors for characterizing the embouchure (see §4.2.2). It has been chosen since it is bigger than a clarinet mouthpiece and allows for embedding sensors more easily. There is no neck cork, in order to obtain a clarinet-like assembly between mouthpiece and resonator, and to minimize the cross-section discontinuity.
- Artificial lip: it is made of silicone rubber (Copsil GES-30) with dimensions 1.4 cm high, 2.2 cm long and 0.9 cm thick. The artificial lip is glued on a 4 mm thick cylindrical bar, acting as the teeth and pushing the lip against the reed. The artificial lip position in the horizontal and vertical directions is controlled with two axial micrometer screws. The lip position is written (x_L, y_L), where x_L is the

distance from the lip to the tip of the mouthpiece parallel to the resonator axis, and y_L is the distance from the lip to the tip of the mouthpiece perpendicular to the resonator axis, as shown in Fig. 4.2.

- Resonator: it is a 50 cm long cylinder of 16 mm of inner diameter. The system is conceived for a resonator with no holes.

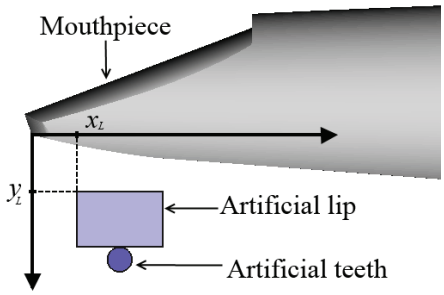

FIGURE 4.2: Schematic view of the coordinates x_L and y_L of artificial lip with respect to the mouthpiece tip.

Aeraulic-control system: The purpose of the aeraulic part is to produce self-sustained oscillations by creating a negative pressure in the mouthpiece. Moreover, the aeraulic part must not modify the acoustic properties of the resonator. It is composed of (Fig. 4.1):

- Impedance-uncoupling volume: it is installed between the resonator and the aspiration system to uncouple the acoustic impedance of the resonator from the impedance of the aspirating source, reproducing free-field conditions at the end of the resonator (see Appendix 4.6).
- Valve: a pipe connects the volume to a manual valve, which controls the ratio of air aspirated from the upstream part of the artificial mouth and from a vent to the outside.
- Muffler: an exhaust muffler is installed in the valve exit to the outside in order to minimize the air jet noise.
- Aspirating source: a duct connects the valve to a vacuum cleaner with power control and silencer system.

4.2.2 Instrumented mouthpiece

The instrumented mouthpiece allows for the measurement of the reed displacement, the pressure outside the mouthpiece (in the musician's mouth) and the pressure inside

the mouthpiece. The mouthpiece has been designed by scanning a commercial tenor saxophone mouthpiece (Vandoren V16) and modifying the geometry through Computer-Aided Design (CAD) to allow for the installation of the different sensors. The mouthpiece and the positions of the sensors are shown in Fig. 4.3. The implemented sensors are:

- two photo-interrupters (Kodenshi SG2BC), measuring the reed displacement y at 4 mm from the tip and 4 mm from the mouthpiece left and right edges (noted y_1 and y_2 respectively). For both sensors, $y = 0$ represents the closing position, and $y = H$ is the maximal opening imposed by the lip.
- two differential pressure sensors (Endevco 8507-C2), one measuring the difference between the pressure in the top of the mouthpiece and the atmospheric pressure, and another measuring the difference between the pressure inside the mouthpiece and the atmospheric pressure. The first sensor can measure the pressure in the mouth when a musician is playing or the pressure near the top of the mouthpiece (very close to the atmospheric pressure) when playing with the artificial mouth.
- two accelerometers (PCB Piezotronics 352C23), measuring the vibration of the mouthpiece and detecting the impact of the reed on the lay.

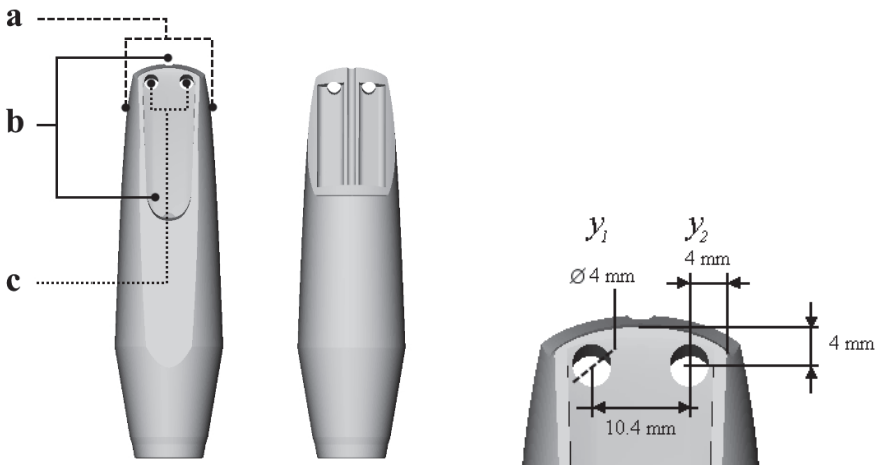

FIGURE 4.3: CAD model of the instrumented mouthpiece. The positions of the sensors are indicated as follows: a) accelerometers, b) pressure sensors, c) photo-interrupters.

Note that the instrumented mouthpiece does not measure the reed tip opening y_t that is used for describing the reed behaviour in common physical models [20, 113], but the displacement y at 4 mm from the tip. The comparison of the measured displacement and the displacement of the reed tip is shown in Fig. 4.4. In this case, y can be negative when the reed bends transversely into the mouthpiece. This means that the detection of the closing point $y = 0$ has some uncertainty, as explained below.

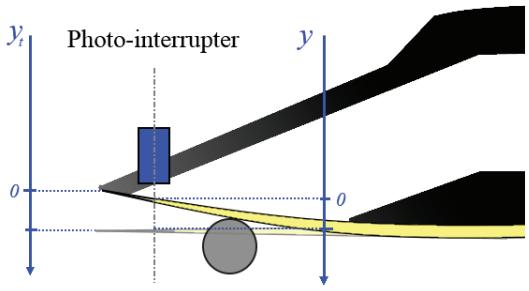

FIGURE 4.4: Schematic view of the mouthpiece-reed-lip system showing the measured reed displacement from the photo-interrupters y and the reed tip displacement y_t.

Calibration and uncertainties: The static calibration of the pressure sensors is done by comparison with hydrostatic level measurements. The dynamic relative calibration of the pressure sensors is done by using a loudspeaker in a small cavity. The bandwidth of both sensors is 0-5 kHz and they show good phase matching. The uncertainties of the pressure and acceleration measurements can be neglected.

The calibration of the photo-interrupters is done by means of a calibrator developed for this purpose (see Fig. 4.5). The calibrator uses a lever to hold the reed in closed position $y = 0$ (position a in Fig. 4.5) or in open position at an aperture $y = 0.7$ mm (b in Fig. 4.5). These two positions are in the linear range of the sensors. The output voltage measured in these two positions allows determining the sensitivity of the sensors and the voltage at the closing point of the reed for a particular measurement. This static calibration leads to uncertainties of 0.05 mm in the displacement measurement. The calibrator helps minimizing the bias in the measurement due to the accumulation of humidity on the reed or the sensors that happens while playing, and the eventual current drift in the sensors (these effects are studied in [3]).

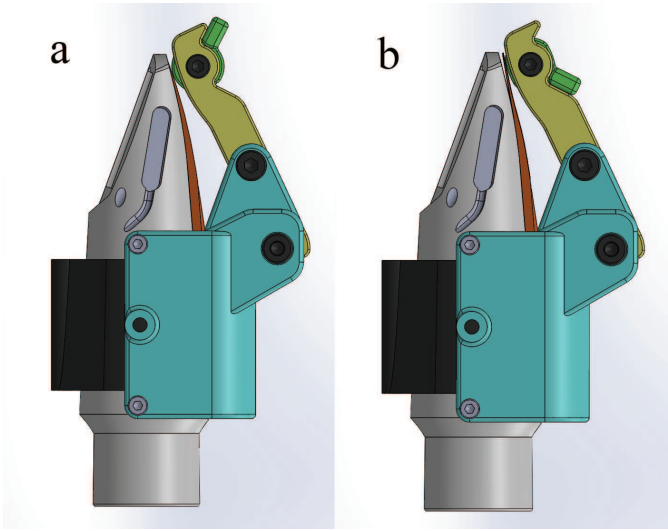

FIGURE 4.5: Schematic view of the calibrator holding the reed in closed position $y = 0$ (a) and in open position $y = 0.7$ mm (b).

In dynamic conditions, the deformation of the reed inside the mouthpiece introduces uncertainties in the displacement measurement. In particular, the calibration of the closing point of the reed is less accurate and introduces an important bias. In high-level dynamic conditions, the accelerometers provide the detection of the closing time (assumed to be $y = 0$) taking into account the deformation of the reed, allowing for the correction of this bias and decreasing the uncertainty to 0.03 mm.

4.2.3 Control of the artificial mouth

The parameters that enable the control of the artificial mouth are the lip position (x_L, y_L) and the blowing pressure P_m.

When a musician plays, the artificial lip is removed and the musician can blow in the mouthpiece. In this case, the blowing pressure P_m is the pressure in the musician's mouth (the acoustic component of $P_m(t)$ is small compared with the static component and it can be neglected). This pressure is positive and it is measured by the pressure sensor in the tip of the mouthpiece. The pressure inside the mouthpiece P is an acoustic pressure and it is measured by the pressure sensor in the mouthpiece. The pressure difference across the reed ΔP is defined as $\Delta P = P_m - P$, which is positive, and it is obtained as the difference of the pressure measured by both sensors.

In the case of the artificial mouth, the pressure inside the mouthpiece is composed of an acoustic part P and a negative static part $-P_m$. The blowing pressure P_m is the static part and is obtained as the mean pressure inside the mouthpiece with opposite sign. The pressure difference $\Delta P = P_m - P$ is the opposite of the total pressure inside the mouthpiece, directly measured by the pressure sensor inside the mouthpiece.

4.2.4 Stability and reproducibility

In order to determine the stability of the artificial mouth, the reed is installed on the mouthpiece and the system is set at a blowing pressure of $P_m = 28$ hPa. For a 1s-long measurement, the standard deviations of the frequency (obtained with a zero-crossing method) and the acoustic pressure amplitude estimated in windows of 5 periods are 0.02% and 0.67%, respectively. The artificial mouth provides very stable measurements. The reproducibility is measured in five repetitions of the installation of the reed and the setting of the artificial mouth at the same blowing pressure. For the obtained measurements, the standard deviations are 0.9%, 3.3% and 0.2% respectively for blowing pressure, acoustic pressure amplitude and frequency. These results indicate a good reproducibility of the measurements.

4.3 Working range of the artificial mouth

The working range corresponds to the values of the control parameters (blowing pressure P_m and lip position x_L and y_L) for which self-sustained oscillations occur. Within this working range, it is possible to identify the values of the control parameters for which the artificial mouth plays similarly to a musician. The playing of the musician and the artificial mouth is characterised by the playing parameters:

- the fundamental frequency f_0 of the acoustic pressure (measured in Hz),
- the peak-to-peak acoustic pressure amplitude in the mouthpiece P^{PP},
- the peak-to-peak reed displacement amplitudes at both sides of the mouthpiece y_1^{PP} and y_2^{PP}.

The optimal working range is defined by the values of the control parameters for which the playing parameters for the musician and the artificial mouth are most similar.

The working range of the artificial mouth is characterised for four different blowing pressures: 25, 30, 35 and 40 hPa. These blowing pressures are selected in order to observe reed oscillations in different dynamic levels [3, 122]. The effect of the control parameters on the playing parameters is studied for the four blowing pressures. Then, the playing of a musician is analysed, obtaining the reference playing parameters for the artificial mouth. Finally, the parameters obtained by the artificial mouth and by the musician are compared in order to identify the optimal working range.

4.3.1 Effect of the control parameters on the playing parameters

The working range of the artificial mouth is determined for four blowing pressures $P_m =$ 25 hPa, 30 hPa, 35 hPa and 40 hPa. For each pressure value, different lip positions (x_L, y_L) are explored, with increments of 1 mm for x_L and 0.1 mm for y_L.

The configurations in which auto-oscillations occur are given in Fig. 4.6, which shows the pressure amplitude as a function of the lip position for four different blowing pressure values. As can be seen in Fig. 4.6, the upper limit of each graph is almost independent of the blowing pressure and it is roughly defined by the extreme lip positions $(x_L, y_L) \approx (3.0, 1.6)$ mm and $(x_L, y_L) \approx (8.0, 0.6)$ mm. The lower limit depends on the blowing pressure, the working range being wider for higher blowing pressures. The range of values of y_L that lead to oscillations is narrower for small values of x_L (lip near the reed tip) than for large values of x_L (lip far from the reed tip). Fig. 4.6 also reveals that the

lip position x_L controls the pressure amplitude, while the lip position y_L does not affect much. For each blowing pressure, the dynamic range is around 6 dB. The total dynamic range for the studied blowing pressures is 12 dB.

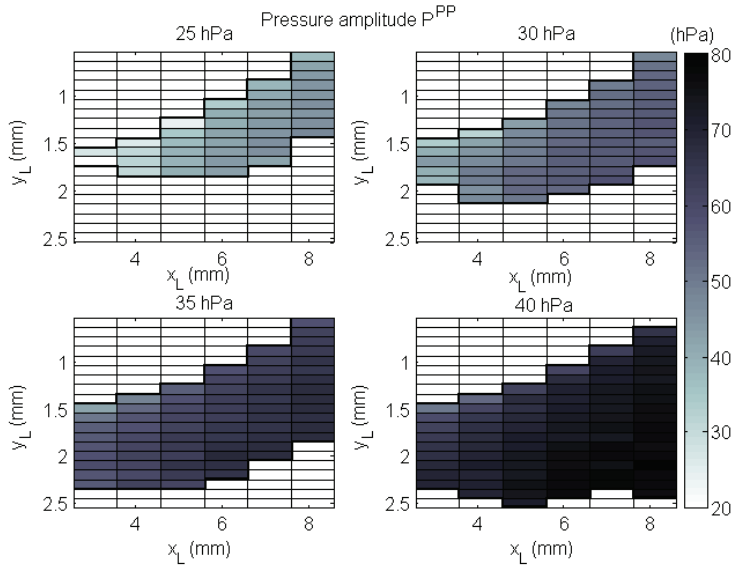

FIGURE 4.6: Working range of the artificial mouth for different blowing pressures. View of the pressure amplitude P^{PP}.

Fig. 4.7 shows the frequency of the artificial playing for the four blowing pressures and for different lip positions (x_L, y_L). In these measurements, the decrease of the frequency with the lip position y_L is observed. The frequency mostly depends on the lip position y_L and not on the blowing pressure. The frequency drop is due mainly to the increase of the reed flow, equivalent to an extra volume in the resonator [123]. The lowest frequency played by the artificial mouth at these blowing pressures is 164 Hz. The observed range of frequencies is almost 100 cents (a semitone).

Fig. 4.8 shows the displacement amplitude on the left of the mouthpiece y_2^{PP}. The reed displacement y_1, measured by the second sensor, is symmetric and provides similar results. For the upper limit of the working range, the reed displacement is very small (displacement amplitude $y_2^{PP} \simeq 0.1$ mm). This corresponds to a tight embouchure for which the lip holds the reed close to the mouthpiece. The maximal displacement amplitude (in the lower part of the working range) depends on the blowing pressure. For $P_m = 25$ hPa, the working range reaches $y_L \approx 1.7$ mm and the displacement amplitude is almost 0.5 mm. However, for $P_m = 40$ hPa, it reaches $y_L = 2.4$ mm and the displacement amplitude is 1 mm. This corresponds to a relaxed embouchure.

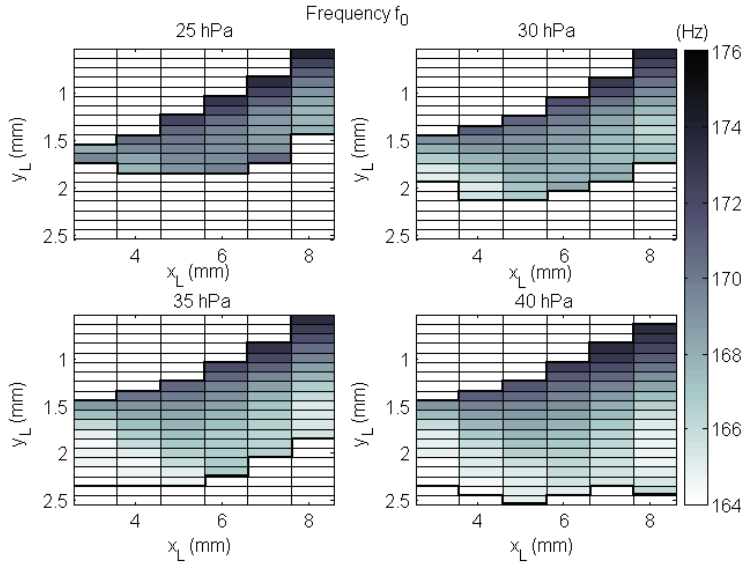

FIGURE 4.7: Working range of the artificial mouth for different blowing pressures. View of the playing frequency (in Hz).

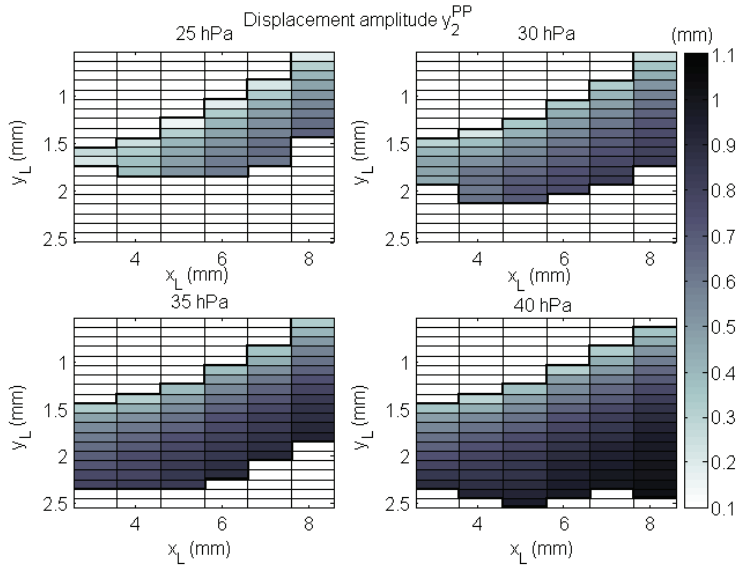

FIGURE 4.8: Working range of the artificial mouth for different blowing pressures. View of the peak-to-peak reed displacement y_2^{PP}.

4.3.2 Analysis of a musician's playing

In this section, a set of measurements obtained with a musician are analysed. The musician is asked to play at different musical nuances or blowing pressures. This permits the estimation of the playing parameters that will be used as reference values to assess the ability of the artificial mouth to reproduce the musician's playing. In a first time, the musician is asked to play freely at three different nuances *piano* (p), *mezzopiano* (mp), *mezzoforte* (mf), and with normal or relaxed embouchures; it was not possible to

play in a stable manner for the relaxed embouchure at the *p* nuance. In a second time, he is asked to play at four different blowing pressures (25, 30, 35 and 40 hPa), using a voltmeter as reference. The musician performs 5 repetitions in each situation, obtaining a total of 45 recordings.

The values of the blowing and the acoustic pressures for both sets of measurements combined are analysed using Hierarchical Cluster Analysis (HCA), applying Ward's method, in order to classify the data in four classes containing 5 to 15 samples. These classes are named according to the nuances *p*, *mp*, *mf* and *f*, because they correspond well to the musical nuances that the musician was asked to play.

The Fig. 4.9 shows the pressure amplitude as a function of the blowing pressure obtained with a musician. The error bars are the standard deviations estimated for each class.

The pressure amplitude increases with the blowing pressure as expected [17, 86], and the nuances are separated of 3 dB. The normal and relaxed embouchure follow the same distribution for the pressure amplitude and they are not distinguishable. The dynamic range of the musician is 12 dB, which is similar to the one obtained with the artificial mouth for the explored blowing pressures. For each nuance class, the standard deviation of the blowing pressure is between 6 and 12%, and for the pressure amplitude it is between 2 and 14% (corresponding to a variation of ±1.5 dB).

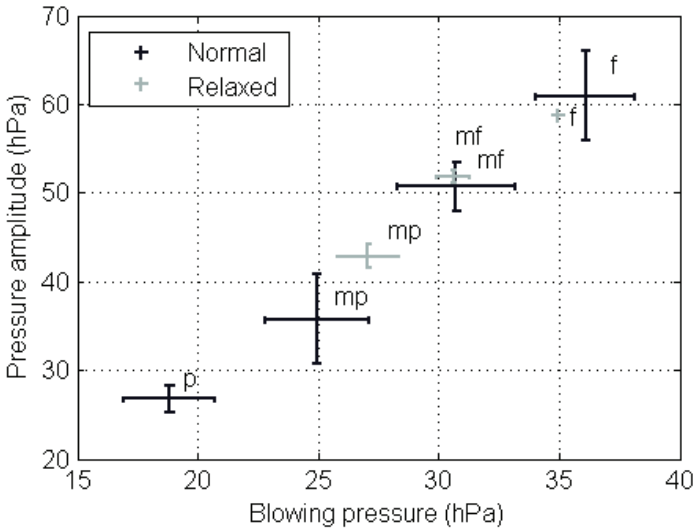

FIGURE 4.9: Peak-to-peak pressure amplitude in the mouthpiece P^{PP} as a function of the blowing pressure P_m per nuance (*p*, *mp*, *mf* and *f*) obtained with a musician (the error bars represent standard deviation $\pm\sigma$).

The Fig. 4.10 shows the fundamental frequency as a function of the blowing pressure. The different embouchures are distinguishable: the relaxed embouchures have lower playing frequencies (around 162 Hz) than the normal embouchures (whose frequencies are around 167 Hz). Moreover, the standard deviation of the playing frequency is almost

10 cents when playing at different moments without any pitch reference. The frequency shift between the normal and relaxed embouchure is around 50 cents.

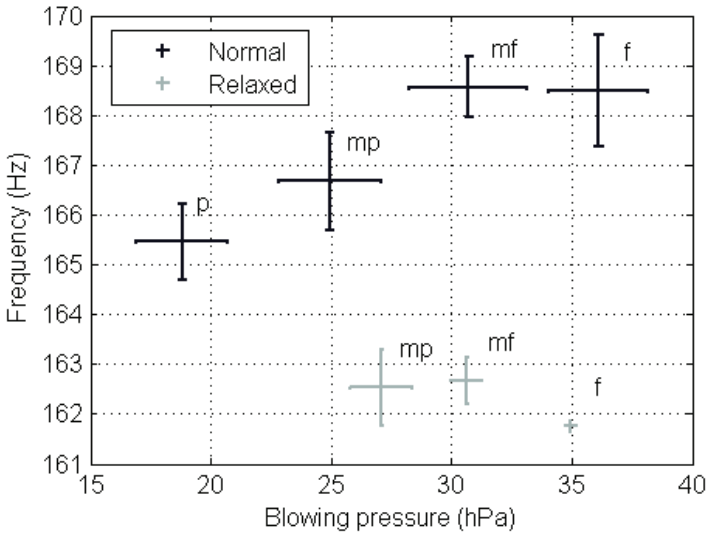

FIGURE 4.10: Fundamental frequency of the mouthpiece pressure $P(t)$ as a function of the blowing pressure P_m per nuance (p, mp, mf and f) obtained with a musician (the error bars represent standard deviation $\pm\sigma$).

The Fig. 4.11 shows the peak-to-peak reed displacement y_1^{PP} and y_2^{PP} as a function of the blowing pressure. The standard deviation within the nuance classes in the displacement measurement is quite high, between 10% and 20% for mp, mf, f, and 37% for the nuance p. This is due to the variability of the musician's embouchure. These results show clearly the effect of the relaxed embouchure, characterised by a larger reed displacement (increase of 50% in y). In this case, the results are not symmetric for both sensors, due to the musician's irregular embouchure.

4.3.3 Optimal working range

This section compares the playing parameters obtained by the musician and by the artificial mouth in the working range defined above. The reference values of the musician are interpolated from the mean values shown in Fig. 4.9, 4.10 for the four blowing pressures 25, 30, 35 and 40 hPa. Tab. 4.1 gives the reference playing parameters for the normal embouchure.

The distance between the musician and the artificial mouth is quantified by means of a similarity indicator g_m based on the Gaussian distribution, as given in Eq. 4.1. This distance is continuous, positive and it can be extrapolated to multiple dimensions using the geometric mean. Moreover, the distance contains a scale factor σ that represents

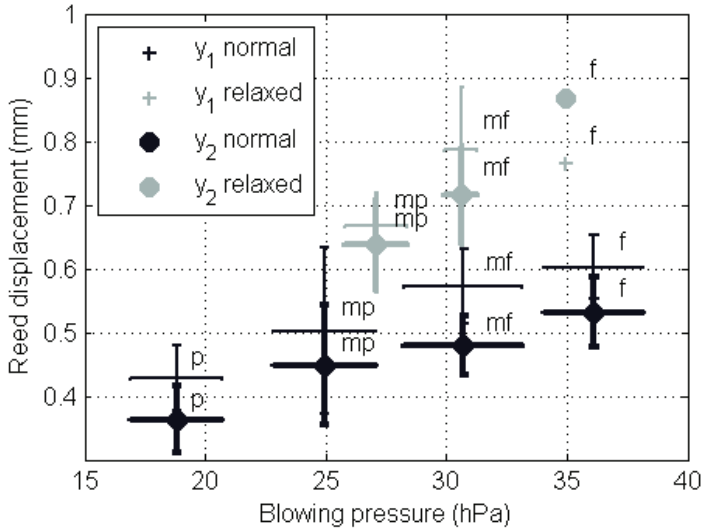

FIGURE 4.11: Peak-to-peak displacement amplitude of the reed tip $y_1(t)$ and $y_2(t)$ as a function of P_m per nuance (p, mp, mf and f) obtained with a musician (the error bars represent standard deviation $\pm\sigma$).

TABLE 4.1: Reference values for the frequency f_0, the pressure amplitude P^{PP} and the displacement y_1^{PP} and y_2^{PP} calculated from the musician's playing for the normal embouchure.

P_m (hPa)	f_0 (Hz)	P^{PP} (hPa)	y_1^{PP} (mm)	y_2^{PP} (mm)
25	166.4	36.9	0.50	0.42
30	166.7	48.1	0.57	0.49
35	168.5	59.3	0.61	0.52
40	168.5	70.5	0.61	0.52

here the uncertainty of the measurement (the error bars for the nuance classes).

$$g_m(x_L, y_L; \mu, \sigma) = \exp\left(-\frac{[m(x_L, y_L) - \mu]^2}{2\sigma^2}\right), \tag{4.1}$$

where $m(x_L, y_L)$ is the value of the considered parameter m (e.g. frequency) in the working range of the artificial mouth for a given blowing pressure, μ is the interpolated value of the same parameter obtained from the musician at the same blowing pressure (see Tab. 4.1), and σ is the average of the standard deviations obtained for each nuance (the mean of the vertical error bars in Fig. 4.9, 4.10 and 4.11). This similarity indicator g_m varies from 0 (no similarity) to 1 (identity). A threshold of 0.8 is considered as a satisfying similarity.

The Fig. 4.12 presents the similarity indicator of the frequency, for normal embouchures and for the different blowing pressures. It shows that the region in which the artificial

mouth plays at a similar frequency as the musician extends along x_L and is mainly controlled by y_L, except for the blowing pressure of 25 hPa, where the highest value of the Gaussian indicator is around 0.7. For 25 hPa, the lowest frequencies are around 167 Hz, and the reference value of the musician is lower. The lowest frequencies attained in artificial playing for the different blowing pressures are also higher than those of the relaxed embouchures for the musician (which are around 162 Hz). We can conclude that the artificial mouth cannot reproduce the studied relaxed embouchures (thus only normal embouchures will be considered hereafter).

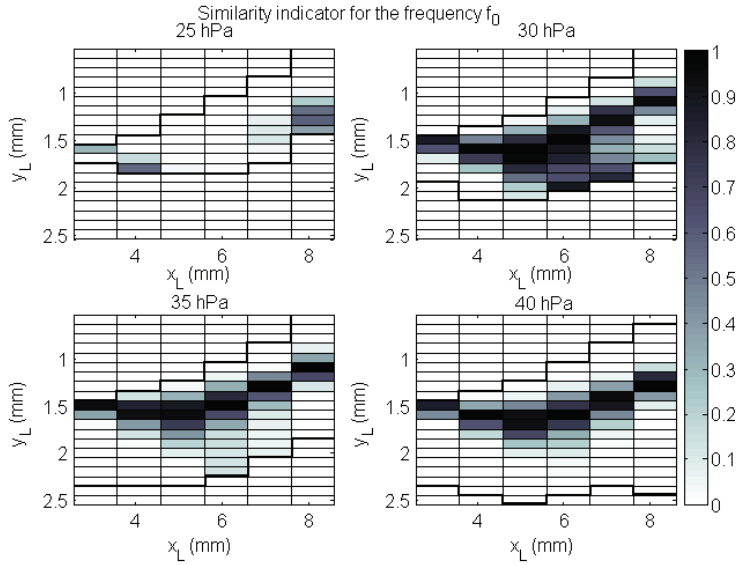

FIGURE 4.12: Similarity indicator between the artificial mouth and the musician for the frequency f_0.

The similarity indicators of the peak-to-peak pressure amplitude for the different blowing pressures are given in the Fig. 4.13. The indicators show a region of high similarity for lip positions $x_L < 6$ and a linear range adjacent to upper boundary of the working range.

The similarity indicator of the displacement amplitude for the different blowing pressures are given in the Fig. 4.14. It shows that the similarity region of the artificial mouth is a linear range separated of 0.2 mm from of the upper boundary of y_L. The results are the same for both the measured displacements y_1 and $y2$.

The intersection of the three similarity regions can be calculated as the geometric mean of the respective similarity indicators (as a multidimensional Gaussian distribution). The combined similarity indicator of the frequency, the pressure amplitude and the displacement amplitude (in Fig. 4.15) shows a region of high similarity at $x_L \approx 5$ mm, $y_L \approx 1.6$ mm, except for the blowing pressure of 25 hPa, where the frequency of the artificial mouth is too high compared to the musician (and the highest value of the Gaussian indicator is around 0.4).

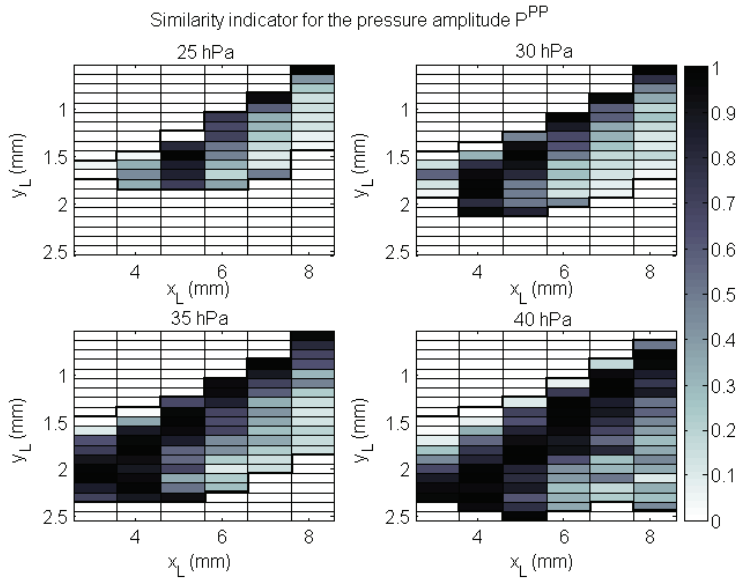

FIGURE 4.13: Similarity indicator between the artificial mouth and the musician for the pressure amplitude P^{PP}.

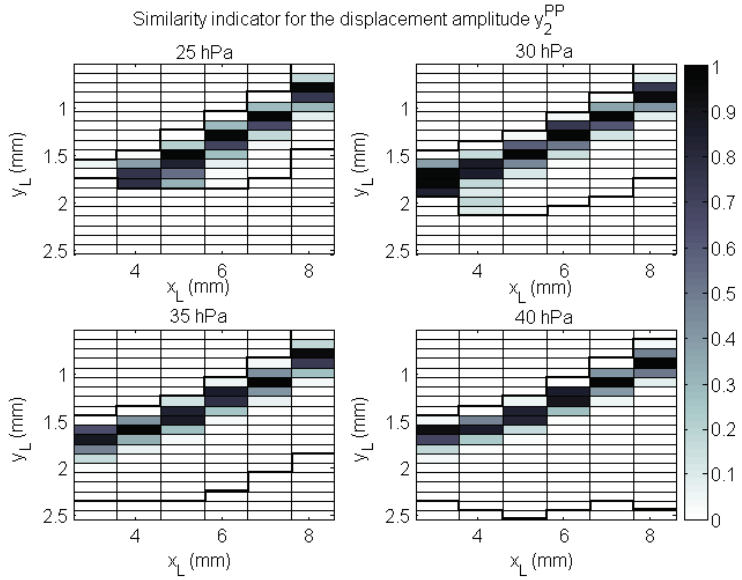

FIGURE 4.14: Similarity indicator between the artificial mouth and the musician for the displacement y_2.

The values of the playing parameters obtained for the artificial mouth in one point of the optimal working range and for the four blowing pressures 25, 30, 35 and 40 hPa are given in Tab. 4.2 for comparison. It shows that the pressure amplitudes are similar, and the main differences are a shift in frequency (the artificial mouth plays higher than the musician, specially for the lowest blowing pressures) and a shift in displacement amplitude (the maximal reed displacement is lower for the artificial mouth than for the musician).

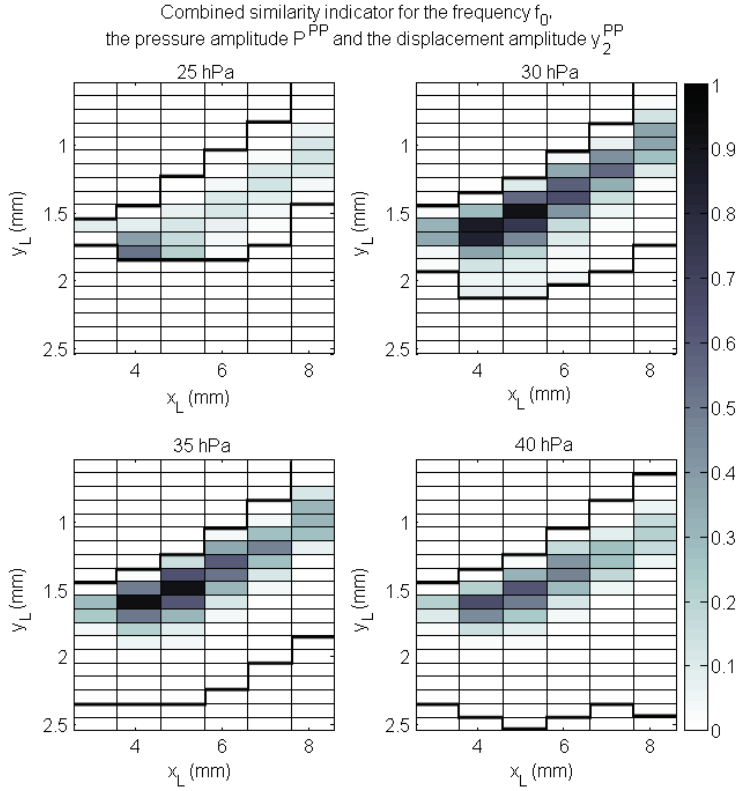

FIGURE 4.15: Combined similarity indicator between the artificial mouth and the musician for the frequency f_0, the pressure amplitude P^{PP} and the reed displacement y_2.

TABLE 4.2: Values obtained with the artificial mouth for the frequency f_0, the pressure amplitude P^{PP} and the displacement amplitude y_2^{PP} in the optimal working range for the normal embouchure.

P_m (hPa)	(x_L, y_L) (mm)	f_0 (Hz)	P^{PP} (hPa)	y_2^{PP} (mm)
25	(4.57, 1.54)	170.2	36.2	0.38
30	(4.57, 1.54)	169.2	47.5	0.49
35	(5.57, 1.44)	169.1	62.5	0.61
40	(5.57, 1.44)	169.7	69.1	0.67

4.4 Comparison of the musician and the artificial mouth

Having identified the optimal working range in which the artificial mouth plays similarly to a musician, it is possible to compare the behaviour of the reed in both situations. A graphical comparison of the pressure difference $\Delta P(t)$ and displacement $y(t)$ signals for the musician and the artificial mouth is made. Then, the error amplitude between the signals is assessed. For this, four representative measurements of the musician are chosen, with blowing pressures close to 25, 30, 35 and 40 hPa. One measurement of the artificial

mouth in the optimal working range is selected for each of the four measurements (the artificial lip positions are indicated in Tab. 4.2). The results are shown in Fig. 4.16, 4.17, 4.18 and 4.19 for 25, 30, 35 and 40 hPa, respectively. As the frequency at which the artificial mouth plays is slightly different of the desired reference, it is necessary to resample the signals in order to compare them with the musician. The comparison is done in the time scale of the musician in windows of 3 periods. Only normal embouchures are considered. Note that for $P_m = 25$ hPa, the similarity indicator is lower than for the other blowing pressures (Fig. 4.15).

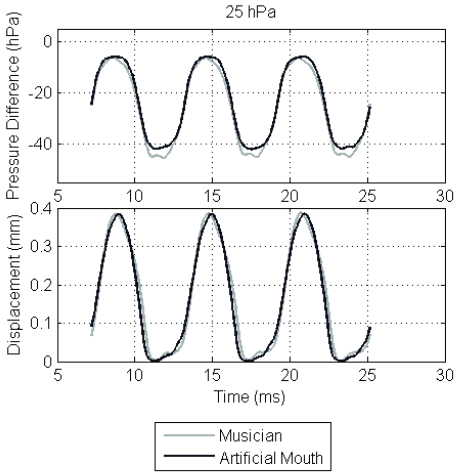

FIGURE 4.16: Pressure difference and displacement as a function of time at $P_m = 25$ hPa for the musician and the artificial mouth in $x_L = 4.57$ mm and $y_L = 1.54$ mm. The signals obtained with the artificial mouth are resampled.

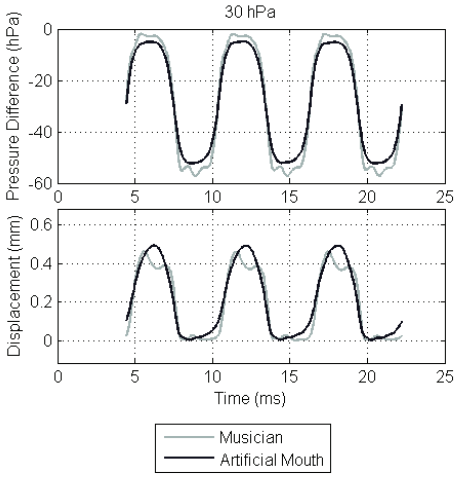

FIGURE 4.17: Pressure difference and displacement as a function of time at $P_m = 30$ hPa for the musician and the artificial mouth in $x_L = 4.57$ mm and $y_L = 1.54$ mm. The signals obtained with the artificial mouth are resampled.

When comparing the pressure and displacement signals for the musician and the artificial mouth, similarities and differences are observed. For the four blowing pressures, the

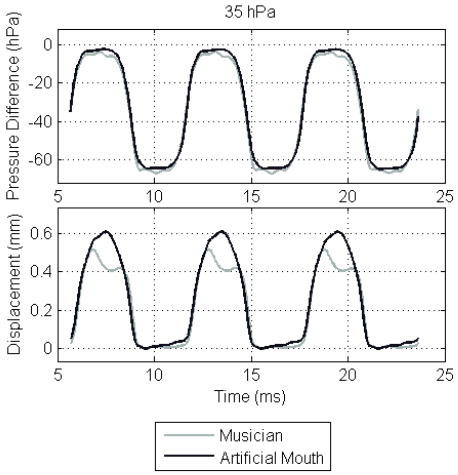

FIGURE 4.18: Pressure difference and displacement as a function of time at $P_m = 35$ hPa for the musician and the artificial mouth in $x_L = 5.57$ mm and $y_L = 1.44$ mm. The signals obtained with the artificial mouth are resampled.

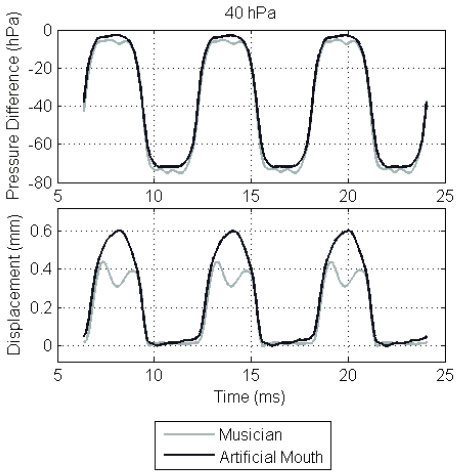

FIGURE 4.19: Pressure difference and displacement as a function of time at $P_m = 40$ hPa for the musician and the artificial mouth in $x_L = 5.57$ mm and $y_L = 1.44$ mm. The signals obtained with the artificial mouth are resampled.

signals for the musician and the artificial mouth match in the closing and the opening phases of the reed. This indicates that the equivalent stiffnesses in the closing and opening phases are the same for the musician and the artificial mouth. The main differences occur when the reed is in the closed and open positions. In the closed position, the signals for the musician show small oscillations for both the pressure difference and the displacement that are smaller for the artificial mouth. In the open position, a larger oscillation appears for the displacement and it increases with the blowing pressure (not being appreciable at 25 hPa). These oscillations come from inertial effects associated to the oscillation of the reed against the lip and the beating of the reed against the mouthpiece, and show a difference in the equivalent reed mass.

The similarity of the temporal signals between the musician and the artificial mouth is quantified using the error amplitude, calculated as the RMS amplitude of the difference between the artificial mouth and the musician. The results are presented in Tab. 4.3, expressed in % of the amplitude of the signal obtained with the musician.

TABLE 4.3: Error amplitude ϵ between the artificial mouth and the musician, for the pressure difference ΔP and the displacement y.

$\overline{P_m}$ (hPa)	$\epsilon(\Delta P)$ (%)	$\epsilon(y)$ (%)
25	7.87	15.78
30	15.91	26.88
35	5.22	31.42
40	4.37	52.56

The error amplitudes are lower for the pressure difference than for the reed displacement. For the latter, the error amplitude increases with the blowing pressure. The error for the displacement mainly comes from the difference in the oscillation of the reed against the lip.

In conclusion, the artificial mouth reproduces more accurately the closing phase, the opening phase and the closed position of the reed. In the open position, the difference between the musician's lip and the artificial one is noticeable in the displacement measurement.

4.5 Conclusion

The aspirating artificial mouth presented here allows for easy and quick reed installation. The accessibility of the reed also permits the use of a calibrator for the reed displacement measurement. Another advantage of the design is that external sensors or measuring devices can be added to the experiment without modifying the system. The design uses a section discontinuity to reproduce free-field radiation. The operation of the artificial mouth is regulated by the position of the artificial lip (adjusted with two micrometer screws) and a pressure valve, resulting in highly controllable and repeatable measurements. It can also be played as a musical instrument by a musician because of the accessibility of the mouthpiece. This allows comparing the musician's playing and the artificial excitation of the system.

The study of the working range of the artificial mouth has identified the artificial-lip positions that lead to auto-oscillations. In the explored lip positions and blowing pressures, the artificial mouth has a range of 12 dB, 1 mm of reed aperture and 100 cents in frequency.

In order to determine the control parameters of the artificial mouth for which it plays similarly to a musician, a set of 45 stationary notes played by a musician at different nuances has been analysed. This optimal working range is determined using the criteria of similar frequency, pressure amplitude and displacement amplitude for the musician and the artificial mouth. This analysis has shown that the artificial mouth plays similarly to the musician for normal embouchures, and that the main differences are in maximal reed displacement and in frequency for low blowing pressure.

The comparison of the pressure difference across the reed and the displacement signals for the musician and the artificial mouth has shown that the similarity is higher for the pressure than for the displacement. The opening and closing phases of the reed are similar (similar stiffness) but different inertial effects appear in the closed and open position (different reed equivalent mass). Resonance effects appear in the displacement for the open position in the case of the musician, but not for the artificial mouth. This shows the different behaviour of the artificial lip and the musician's.

The method developed to assess the optimal working range has been validated with one musician and a synthetic reed. It could be applied to a set of musicians or reeds to determine average optimal working ranges. The artificial mouth could also be applied to the study of the physical models describing the reed behaviour under different embouchures. Furthermore, the system will be used to characterise different cane reeds and mouthpieces with controlled geometric variations in the optimal working range.

4.6 Appendix

The aeraulic-control system is connected to the end of the resonator of the musical instrument, and it is composed by an impedance-uncoupling volume, a valve, a muffler and an aspirating source (see §4.2.1). In this appendix, the principle and design of the impedance-uncoupling system is detailed.

4.6.1 Principle

In order to avoid the acoustic coupling between the resonator and the controlled aspirating source, a volume is added between both systems. The role of this volume is to

impose a zero pressure value at the end of the resonator for the resonance frequencies of the instrument, uncoupling the impedance of the resonator and the aspirating source and reproducing free-field radiation.

In order to study this condition, a first theoretical model is done using a simple transmission-line model, where only plane-waves propagation is considered and no losses are taken into account. We consider two connected cylinders of small and large section S and S', and lengths L and L', which are respectively the resonator and the impedance-uncoupling volume (see Fig 4.20). The second cylinder (the impedance-uncoupling volume) is assumed to be closed at its end.

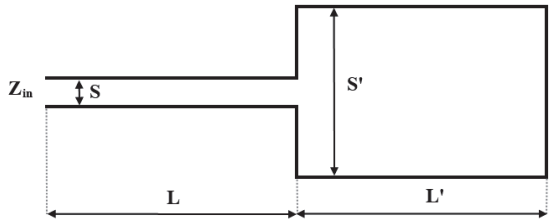

FIGURE 4.20: Schema of the two-cylinders transmission line. The respective length and section of the cylinders are S, L and S', L'.

The model allows obtaining the input impedance corresponding to the resonator connected to the volume as given in Eq. 4.2:

$$Z_{in} = Z_C \cdot \frac{-j\frac{S}{S'} \cdot cotg(kL') + j \cdot tg(kL)}{1 + \frac{S}{S'} \cdot cotg(kL') \cdot tg(kL)}, \tag{4.2}$$

where Z_C is the characteristic impedance of the cylinder of small section S, and Z'_C is the characteristic impedance of the cylinder of large section S'.

If the discontinuity of section is considerably high ($\frac{S}{S'} \longrightarrow 0$), the input impedance of the open pipe is obtained (free-field conditions). For smaller values of $\frac{S}{S'}$, the effect of the second cylinder on the input impedance of the open pipe can be minimised for $cotg(kL') = 0$, that is, when the anti-resonances of the second cylinder overlap with the resonances of the first cylinder. This condition is satisfied when the length of the second cylinder is an odd multiple or a unit fraction of the length of the first cylinder.

4.6.2 Simulation of the input impedance

A simulation of the problem using a model including losses has been done using the software *Resonans* [124]. Three cylinders are connected: a small cylinder with the role of resonator of the musical instrument, connected to a cylindrical volume (with larger section), which is connected to another cylinder of smaller section (with the role of

the pipe connecting the volume to the aspirating source of the artificial mouth). The simulation permits comparing the resonator alone and the resonator connected to the volume connected to the exiting pipe (see Fig. 4.21). In the simulation, the lengths of the resonator and the volume are 50 cm, and the diameter of the sections are 16 mm and 120 mm, which lead to a ratio $\frac{S}{S'} \simeq 1.810^{-4}$; the exiting pipe is 40 cm long and it has a section diameter of 14 mm.

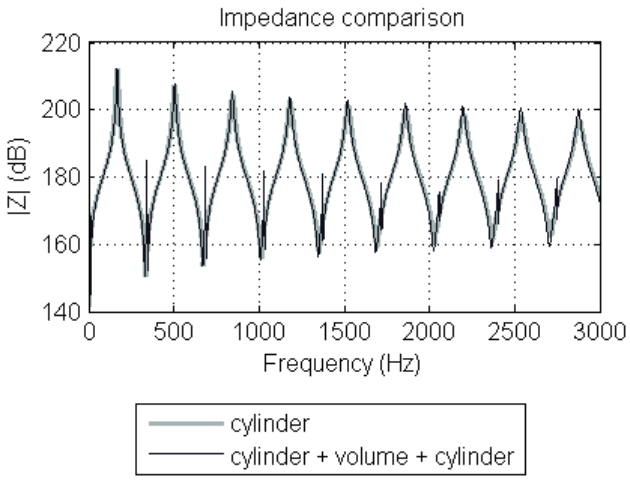

FIGURE 4.21: Simulation of the impedance done with *Resonans* for the 50 cm long resonator alone and the resonator connected to the volume connected to an exit pipe.

The impedance of the cylindrical resonator connected to the volume and the exiting pipe matches the impedance of the resonator alone, except in the anti-resonances of the resonator (and resonances of the volume), where peaks due to the resonance of the volume appear. The height of these peaks is always lower than the height of the resonance peaks of the resonator. When the section of the exiting pipe is considerably smaller than that of the volume, different lengths lead to similar impedance. In that case, the impedance of the system with the three cylinders is approximately the impedance of the first cylinder connected to the closed volume.

4.6.3 Measurements

The aeraulic-control system has been built using the principle and dimensions given above. The length of the resonator is 500 mm and its inner diameter is 16 mm. The length of the impedance-uncoupling volume is also 500 mm and its inner diameter is 120 mm.

The input impedance is measured using an acoustic impedance sensor [125] both for the resonator alone and for the resonator connected to the uncoupling system and the aspirating source. The results are given in Fig 4.22. They show that the nine first resonances of the instrument are not modified by the aeraulic-control part. Finally, the equivalent length of the mouthpiece [85] is subtracted to the length of the resonator.

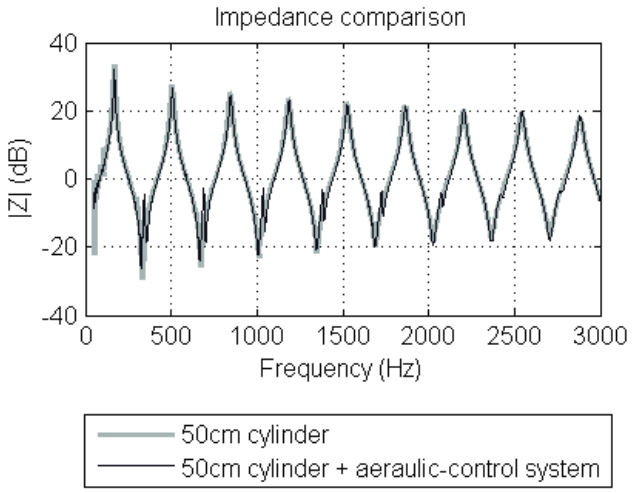

FIGURE 4.22: Comparison of the measured input impedance of the resonator alone (a 50 cm long cylinder), and the resonator connected to the aeraulic-control system.

Complement

4.7 Complement: Pressure-displacement diagrams

Having identified the optimal working range in which the artificial mouth plays similarly to a musician, it is possible to compare the behaviour of the reed when played by a musician or artificially. The reed behaviour is characterised here by the pressure-displacement diagram, which is obtained by representing the reed instantaneous displacement $y(t)$ as a function of the pressure difference across the reed $\Delta P(t)$.

4.7.1 Effect of the control parameters

The pressure-displacement diagrams obtained with the artificial mouth for different control parameters are analysed. Only the measurements for the blowing pressure value $P_m = 35$ hPa and for some lip positions are shown below. The results for the other blowing pressures are equivalent.

Effect of y_L: The pressure-displacement diagrams obtained for $x_L = 5$ mm and three different lip positions $y_L = 1.44$, $y_L = 1.84$ and $y_L = 2.34$ mm are shown in Fig. 4.23.

The peak-to-peak reed displacement increases with y_L. When the lip is close to the mouthpiece (small y_L), it is around 0.4 mm, whereas for $y_L = 2.34$ mm it reaches 0.7 mm.

For each curve, the slope of the upper part (closing phase) is almost linear, showing the absence of curling of the reed on the mouthpiece, except for $y_L = 1.44$ mm when the pressure difference exceeds a particular value ($\Delta P > 50$ hPa). When analysing the lower part of the pressure-displacement diagram (opening phase), it can be observed that it is non linear due to the curling, which varies with the lip position y_L. For the three curves an hysteresis appears, showing that the reed-lip-mouthpiece system has damping effects.

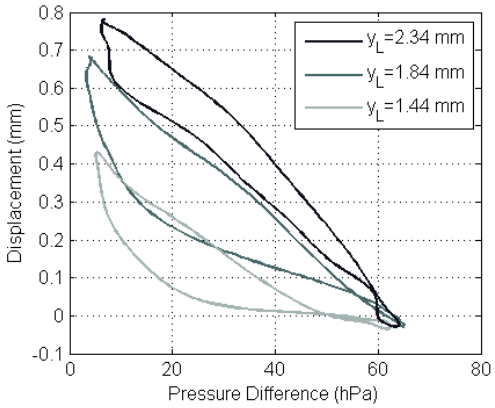

FIGURE 4.23: Pressure-displacement diagrams for $P_m = 35$ hPa, $x_L = 5$ mm, and $y_L = 1.44$, 1.84 and 2.34 mm.

Effect of x_L for constant reed opening H: In Fig. 4.24, the pressure-displacement diagram obtained with a blowing pressure value of 35 hPa, for three lip positions x_L ($x_L = 4$, 6 and 9 mm) and similar reed maximum opening ($H \approx 0.5$ mm), are shown. The corresponding lip positions y_L are 1.64, 1.34 and 0.64 mm, respectively.

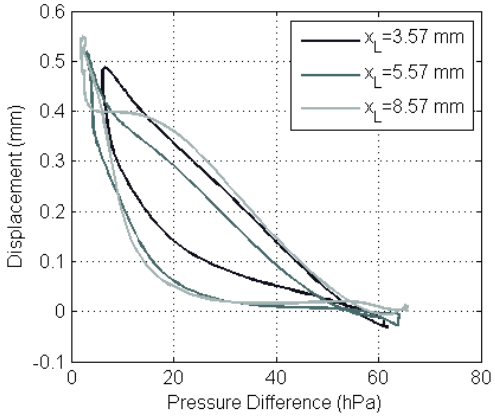

FIGURE 4.24: Pressure-displacement diagrams for $P_m = 35$ hPa, $x_L = 3.57$, 5.57 and 8.57 mm, and $y_L = 1.64$, 1.34 and 0.64 mm, respectively.

The analysis of the upper part of the curve (closing phase) shows that when the lip is near the reed tip (small x_L), the characteristic is linear, except for high pressure difference values ($\Delta P > 50$ hPa). For higher values of the lip position x_L ($x_L = 5.57$, 8.57 mm), the shape of the pressure-displacement diagram is more complex. For pressure differences higher than 50 hPa, the pressure-displacement diagram is non linear and has a small loop, suggesting that the reed beats on the mouthpiece. The slope of the upper part is the same in the region defined by $\Delta P \in [20, 50]$ hPa for the three configurations, showing that the reed stiffness is the same.

The analysis of the lower part (opening phase) of the curve shows a non-linear behaviour for the three configurations. For higher values of x_L ($x_L = 5.57$, 8.57 mm), two main

phases can be seen. The first corresponds to $\Delta P \in [25, 50]$ hPa. During this phase the reed is closed whereas the pressure difference is changing. The second phase corresponds to $\Delta P < 25$ hPa, for which the slope of the pressure-displacement diagram is greater than in the closing phase. Near the opening (pressure differences lower than 20 hPa), the shape complicates with increasing x_L and a loop appears, revealing an oscillation of the reed on the lip.

4.7.2 Comparison of the musician and the artificial mouth

In section 4.3, the measurements from the musician have been classified in nuance classes. The playing parameters have then been interpolated at the measured blowing pressures of the artificial mouth, to determine its optimal working range. Here, we compare the pressure-displacement diagrams of the musician and the artificial mouth in the optimal working range. For this, four representative measurements of the musician are chosen with blowing pressures close to 25, 30, 35 and 40 hPa. One measurement of the artificial mouth in the optimal working range is selected, comparing the pressure-displacement diagram, for each of the four measurements (the artificial lip positions are indicated in Tab. 4.2). The results are shown in Fig. 4.25, 4.26, 4.27, 4.28 for $P_m = 25$, 30, 35 and 40 hPa, respectively. Only normal embouchures are considered. Note that for $P_m = 25$ hPa, the similarity indicator is lower than for the others blowing pressures (Fig. 4.15).

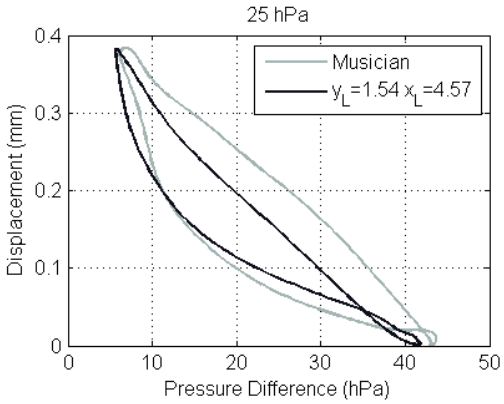

FIGURE 4.25: Pressure-displacement diagrams at $P_m = 25$ hPa for the musician and the artificial mouth in $y_L = 1.54$ mm and $x_L = 4.57$ mm.

When comparing the pressure-displacement diagrams for the musician and the artificial mouth, similarities and differences are observed. For the four blowing pressures, the trend of the closing phase of the reed (upper part of the diagrams) is linear and it is similar for the musician and the artificial mouth, indicating that the equivalent stiffness is the same. The opening phase (lower part of the diagrams) is non linear, showing the curling of the reed on the mouthpiece. This non linearity becomes more pronounced

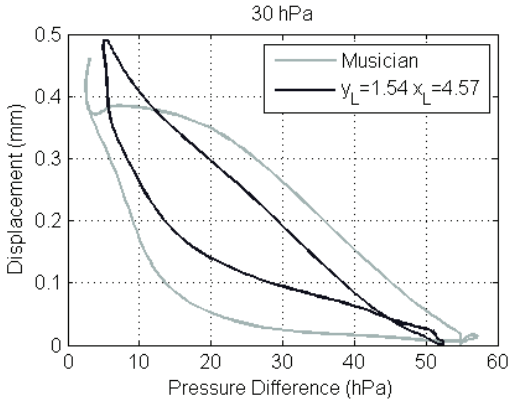

FIGURE 4.26: Pressure-displacement diagrams at $P_m = 30$ hPa for the musician and the artificial mouth in $y_L = 1.54$ mm and $x_L = 4.57$ mm.

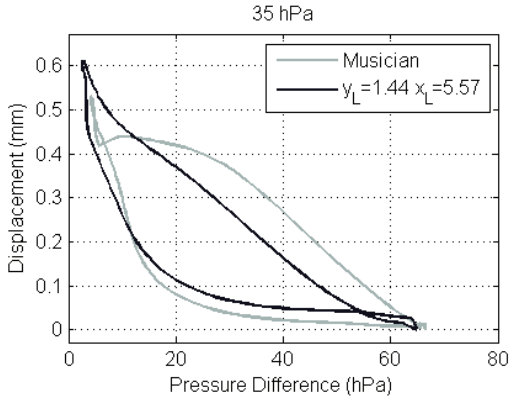

FIGURE 4.27: Pressure-displacement diagrams at $P_m = 35$ hPa for the musician and the artificial mouth in $y_L = 1.44$ mm and $x_L = 5.57$ mm.

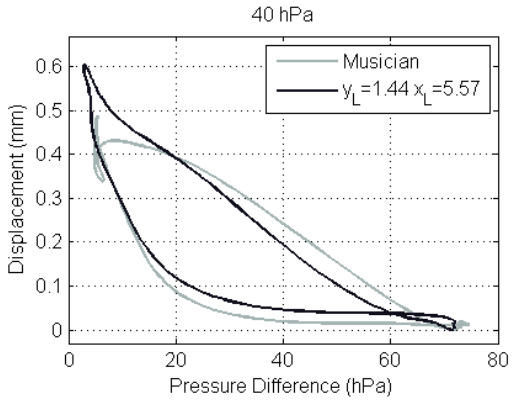

FIGURE 4.28: Pressure-displacement diagrams at $P_m = 40$ hPa for the musician and the artificial mouth in $y_L = 1.44$ mm and $x_L = 5.57$ mm.

with increasing blowing pressures. For all cases, it is similar for the musician and the artificial mouth.

All the measurements show hysteresis. The area inside the curve is associated to the reed equivalent damping. For $P_m = 25$ hPa (Fig. 4.25), $P_m = 30$ hPa (Fig. 4.26) and 35 hPa (Fig. 4.27), it is lower for the artificial mouth. The damping is mainly produced by the lip. These measurements show that the artificial lip has less damping than the musician's, and that the difference is more pronounced for the blowing pressures 25, 30 and 35 hPa.

For the four blowing pressures and for both the musician and the artificial mouth, a loop appears in the closing point of the reed. This loop comes from inertial effects associated to the beating of the reed on the mouthpiece. It is different for the musician and the artificial mouth, showing that the beating differs between the two.

For $P_m = 30$ hPa (Fig. 4.26), $P_m = 35$ hPa (Fig. 4.27) and 40 hPa (Fig. 4.28), a loop appears near the opening point of the reed for the musician, whereas it does not exist for the artificial mouth (it appears only for higher values of x_L, outside the optimal working range). This loop is caused by the oscillation of the reed against the lip and it is due to inertial effects associated to the reed equivalent mass. These results shows that the equivalent mass is higher for the artificial mouth than for the musician. For $P_m = 40$ hPa (Fig. 4.28), the pressure-displacement diagram for the artificial mouth approaches the one for the musician, except in the region near the reed opening. Stetson [37] showed that the fundamental resonance frequencies of synthetic reeds were lower than the ones of cane reeds and that they were in the first register of the instrument. Because of this, it may be possible that the differences in the inertial effects of the reed between the musician and the artificial mouth were less important for cane reeds.

4.7.3 Conclusion

The study of the effect of the lip position in the pressure-displacement diagrams has shown that the position perpendicular to the resonator y_L affects the reed aperture and non-linear curling of the reed on the mouthpiece, and the position parallel to the resonator x_L affects the presence of mass effects of the reed in the open position.

In the optimal working range, the comparison of the pressure-displacement diagrams for the musician and the artificial mouth has shown similarity in the stiffness and curling of the reed on the mouthpiece, but different hysteresis, due to the damping. Inertial effects related to the reed equivalent mass appear for the musician while not for the artificial mouth, specially in the open position. The artificial mouth reproduces more accurately

the closing than the opening of the reed, where the difference between the musician's lip and the artificial one is noticeable.

The artificial lip made of silicone has provided very repeatable measurements and precise control parameters. In order to reduce the difference between the artificial lip and the musician's, a systematic study of the influence of the lip properties on the reed behaviour could be done considering other lip thicknesses and different elasticity level of the silicone. The elastic properties of the artificial lip can be regulated by varying the proportion of the two components of the silicone rubber (Copsil GES-30). This approach was tested in the preliminary work for the study detailed here.

Future work may take advantage of the open design of the artificial mouth by including complementary sensors. The measurement of the reed displacement is delicate and could be improved by using other measurement techniques. As shown in Appendix D, the installation of an external sensor perpendicular to the reed is foreseen in the design of the artificial mouth, for example a reflectance-compensated displacement sensor [116]. The reed displacement or velocity can also be measured using a vibrometer. Both kinds of measurements enable the comparison of the reed behaviour in different points of the reed. This may help to compare the reed displacement on the lay of the mouthpiece and in front of the photo-interrupters, and to analyse the performance of the stiffness model considering transverse deformation.

The artificial mouth can also be used in alternative operating modes, such as quasi-static functioning [16, 87]. Other operating mode of the artificial mouth is obtaining the bifurcation diagram of a reed by increasing the blowing pressure from the oscillation threshold to the extinction threshold and decreasing the blowing pressure from the inverse threshold to the oscillation threshold [86]. These measurements could also contribute to the characterisation of the reed.

Chapter 5

Conclusion and perspectives

For a musician, different reeds of the same brand, cut and strength may be considered subjectively as different. A survey with almost 400 answers has shown that in a box of ten reeds, three are playable in concert and two are not playable at all. There is a clear need to better characterise reeds according to their quality.

The purpose of this work was to develop new tools for the characterisation of reeds in playing conditions, with the long-term objective to better assess reed quality. Different subjective and objective approaches have been explored. In the subjective axis, a survey and a study based on subjective tests have been conducted. In the objective axis, an instrumented mouthpiece and an artificial mouth have been developed.

The literature contains many physical models that attempt to describe the reed behaviour in playing conditions, but the experimental validation of these models is challenging. A wide variety of measurement techniques to objectively characterise reeds has been documented, but these techniques cannot be applied to playing conditions. The instrumented mouthpiece developed in this work makes it possible to perform measurements of the reed in playing conditions, and the developed parameter estimation method provides a way to assess the validity and accuracy of different physical models.

There are some precedents in the subjective characterisation of reeds, but there is no general agreement in the choice of quality descriptors. No research on the verbal attributes describing the reed quality was found. In the existing studies, the pertinence of the indicators and the performance of the evaluating panel were rarely assessed. The comparison of subjective and objective characterisations of reeds did not find strong correlations.

Measurements in playing conditions are often performed using artificial mouths. However, the working point of the artificial mouth is usually decided by a subjective criterion

of sound quality, and very few authors studied the functioning of the device in its entire working range. The capability of the artificial mouth to reproduce the musician's playing has never been studied before.

The instrumented mouthpiece that has been developed has provided the means to measure pressure difference across the reed and reed displacement in playing conditions. The displacement measurement is an important innovation, as it allows for the comparison of the measurements with physical models. A calibrator specifically developed for this purpose facilitates the calibration of the displacement for each reed and measurement. The comparison of the measurements with physical models, using a cylindrical resonator, has shown that the reed can be characterised as an equivalent stiffness for very low dynamic levels, and as a non-linear stiffness for higher dynamic levels, because of the interaction with the mouthpiece. The equivalent damping must be included in the model for medium dynamic levels, and the equivalent mass for high dynamic levels. Some limitations of the models have also been identified. The model for the mass should be asymmetric because in the opening phase the reed freely oscillates against the lip and in the closing it beats on the mouthpiece, though this problem does not appear for saxophone at the same nuance. When performing campaign measurements, the power-law model of the non-linear stiffness did not accurately describe the measurements for different musicians and reeds. The use of the instrumented mouthpiece in the campaign has shown the limits of the displacement measurement. The robustness should be improved for extensive use. Nevertheless, the current mouthpiece design has already shown interesting differences between a semiprofessional saxophonist and a beginner.

A measurement campaign using subjective and objective approaches was conducted with the participation of a panel of seven musicians and the use of twenty reeds of two different brands and cuts. The subjective tests consisted in the evaluation of the reeds in continuous scales of 'ease of playing', 'timbre' and 'quality' after free playing. The choice of the quality descriptors of the reed was based on the results of the survey performed, where the indicators 'ease of playing' and 'timbre' were identified as the preferred ones among musicians. The subjective study showed that the concordance between the musician's ratings was higher for 'ease of playing' than for 'timbre' and 'quality'. The subjective indicators 'ease of playing' and 'timbre' were found to be strongly correlated, so the subjective characterisation of the reeds was reduced to the dimension 'ease of playing'. This has proven that musicians can perceive differences of strength within the same reed class. Some brands recently divide the strength classes in subgroups, and this can help reducing the variability in 'ease of playing' for musicians. Furthermore, it would be useful to relate the strength of the reeds or static stiffness to the dynamic stiffness in playing conditions, and also to the subjective 'ease of playing'. From the objective measurements performed with the instrumented mouthpiece, it was

possible to create an accurate predictive model of the 'ease of playing' and the 'timbre' using the playing parameters obtained with the panel of musicians. This same approach could be applied to measurements with an artificial mouth, in order to classify the reeds using a dynamic measurement bench.

The aspirating artificial mouth was designed to perform reproducible measurements in playing conditions while ensuring an easy and quick reed installation. The free-field radiation of the musical instrument was imposed by using an impedance-uncoupling volume at the end of the resonator. The artificial lip is made of silicone, providing great position control and a high repeatability in the measurements. It was possible to explore the working range of the artificial mouth for the different values of the control parameters blowing pressure, parallel and perpendicular position of the lip. The comparison of the functioning of the artificial mouth in its working range with a set of measurements acquired with a musician at different dynamic levels has permitted identifying the values of the control parameters for which the playing of the artificial mouth is most similar to the musician's playing. The results have shown that the artificial mouth can reproduce normal embouchures, but not relaxed ones. The main differences observed are a shift in the playing frequency for low blowing pressures (the artificial mouth plays higher than the musician) and in the reed displacement in the open position, where strong inertial effects appear for the musician but not for the artificial mouth. Because of time constrains, the artificial mouth has not been applied to reed classification yet, though some preliminary work has been performed. It would be interesting to study the accuracy of the mechanical properties of the artificial lip, and also to study the link between the properties of the lip and the reed alone with the equivalent mechanical parameters in playing conditions.

In the future, the limitations observed in the estimation method of the equivalent reed parameters for different reeds and musicians could be explored in order to improve the physical model of the non-linear stiffness and the mass. Physical modelling could be also applied to the study of attack transients or other musical gestures. The instrumented mouthpiece could be a useful tool to link the physical measurements and different musical performances. Other parameters in the stationary part or in the transient may be introduced for the characterisation of reeds according to their perceived quality. The subjective tests performed do not contribute to reed classification beyond 'ease of playing'. Other types of subjective test, such as rating the reeds according to certain musical tasks, could be performed. This may help to link the player's technique and needs to the perceived quality.

The artificial mouth can also be used to compare mouthpieces with controlled geometrical modifications, estimating objective parameters and also comparing them with

subjective characterisations of the mouthpieces in perceptive tests. The reed displacement measurement using photo-interrupters can be substituted by other measurement techniques, for example using a vibrometer. Measuring the displacement in different points of the reed may help to improve the stiffness model. In addition, the measurements across the working range of the artificial mouth could be compared to numerical simulations of the instrument taking advantage of the precise measurement of the control parameters blowing pressure and lip position. Other operating mode of the artificial mouth is varying the blowing pressure to obtain bifurcation diagrams. Some preliminary measurements have shown the feasibility and usefulness of this kind of representation for the characterisation of the reed.

The tools and methods developed open the possibility to perform measurements of the reed in playing conditions and in repeatable manner. This work is a step forward in the search for reed quality indicators. The artificial mouth and instrumented mouthpiece may have many applications beyond those presented here. The experimental limits encountered have been discussed, proposing several improvements and guidelines for future research.

Appendix A

Computer-Aided Design of the instrumented mouthpiece and the calibrator

This appendix presents the design of a tenor saxophone mouthpiece modified to install different sensors and the design of a specific device enabling the calibration of some of these sensors.

A commercial model of mouthpiece (Vandoren V16) is scanned using tomographic techniques. The three-dimensional model is modified in order to implement different sensors without important modifications of geometry or playability. This mouthpiece designed by CAD (Computer-Aided Design) is 3D-printed in methacrylate. The design and production have been done by the Technology Transfer Center of Le Mans (*Centre de Transfer de Tecnologie du Mans*, CTTM). The mouthpiece is shown in Fig. A.1.

The sensors and the dimensions of the modifications on the mouthpiece enabling the installation of the sensors are indicated in the schema of Fig. A.2. Two photo-interrupters are installed at 4 mm of the tip of the mouthpiece, 4 mm of the sides of the mouthpiece and separated of 10.4 mm. Also, one pressure sensor is installed in the chamber of the mouthpiece (measuring the difference of pressure between the inside of the mouthpiece and the atmosphere) and another is installed on the top of the mouthpiece (measuring the difference of pressure between the inside of the musician's mouth and the atmosphere). Two accelerometers are installed next to the lay of the mouthpiece (measuring the acceleration on the mouthpiece). Lastly, two rails on the mouthpiece allow for the installation of the calibrator on the mouthpiece.

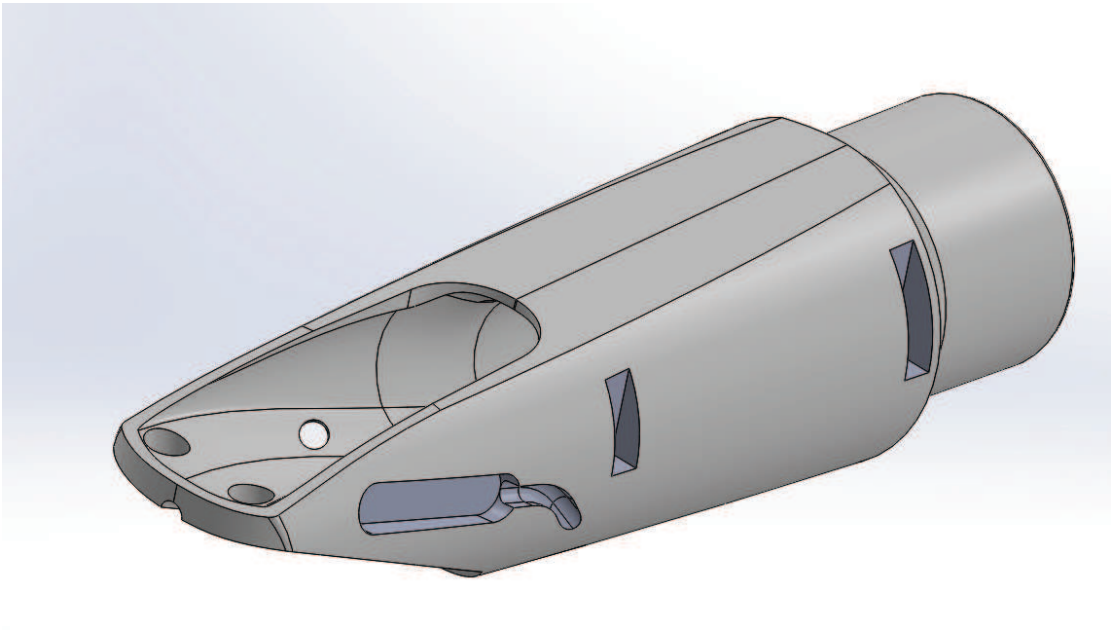

FIGURE A.1: Computer-Aided Design of the instrumented mouthpiece.

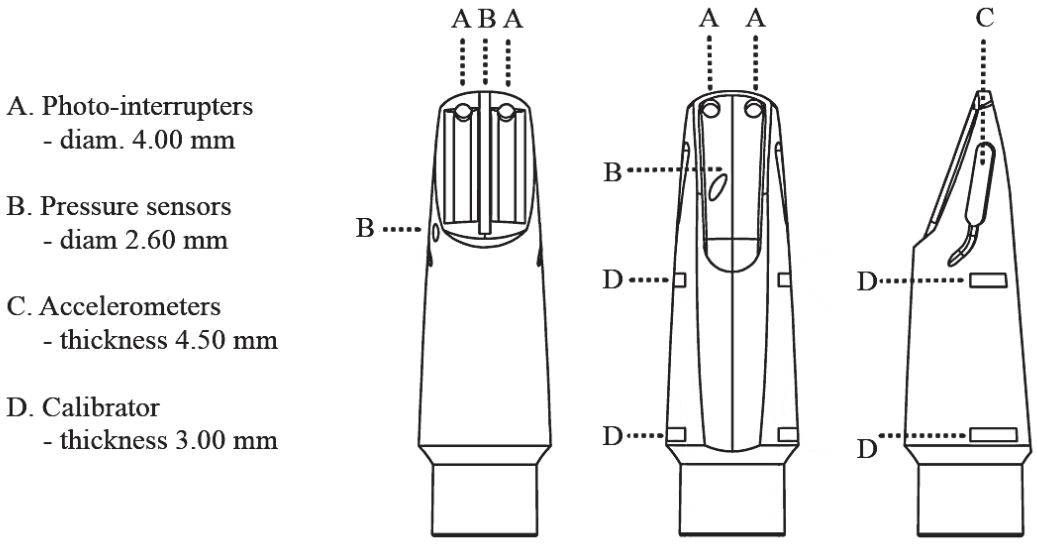

FIGURE A.2: Schema of the positions of the sensors in the instrumented mouthpiece.

A specific device has been designed and produced in order to calibrate the displacement sensors implemented in the mouthpiece. The calibrator allows positioning the reed in closed position and in an aperture of 0.7 mm in front of the sensors. The output voltage measured by the displacement sensors in these two positions allows obtaining the sensibility of the sensors for a particular measurement. The calibrator consists of a lever maintaining the reed in closed or open position (0.7 mm), an adjustable flange which controls the closing position for reeds of different cut or thickness, and a support which fits in the two rails in the mouthpiece. The principle of the calibrator is shown in

Fig. A.3.

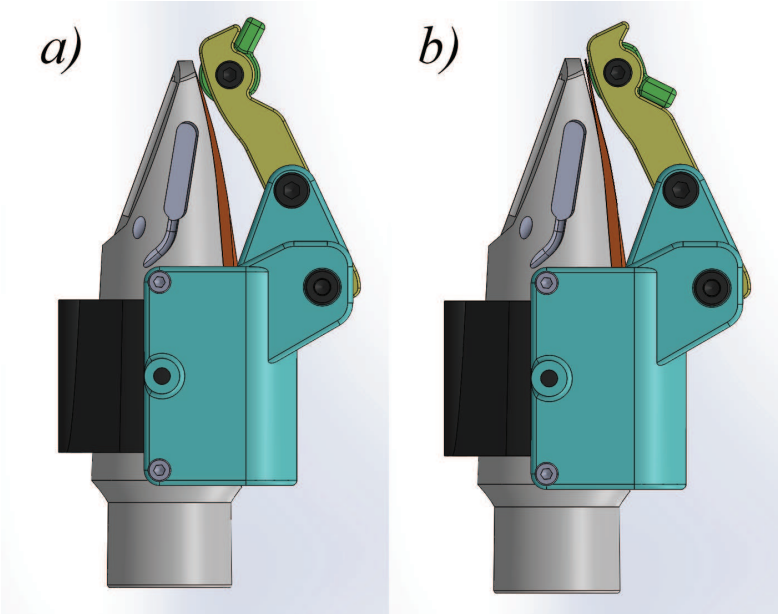

FIGURE A.3: Schematic view of the calibrator holding the reed in a) closed position and b) open position.

The technical drawings of the mouthpiece and the different parts of the calibrator are presented below as given by the manufacturer. The drawing of the mouthpiece is shown in Fig. A.4. The calibrator is composed of several pieces. The technical drawing of the assembled calibrator is shown in Fig. A.5, and the dimensioned drawings of the support, the flange and the lever are given in Figs. A.6, A.7 and A.8, respectively.

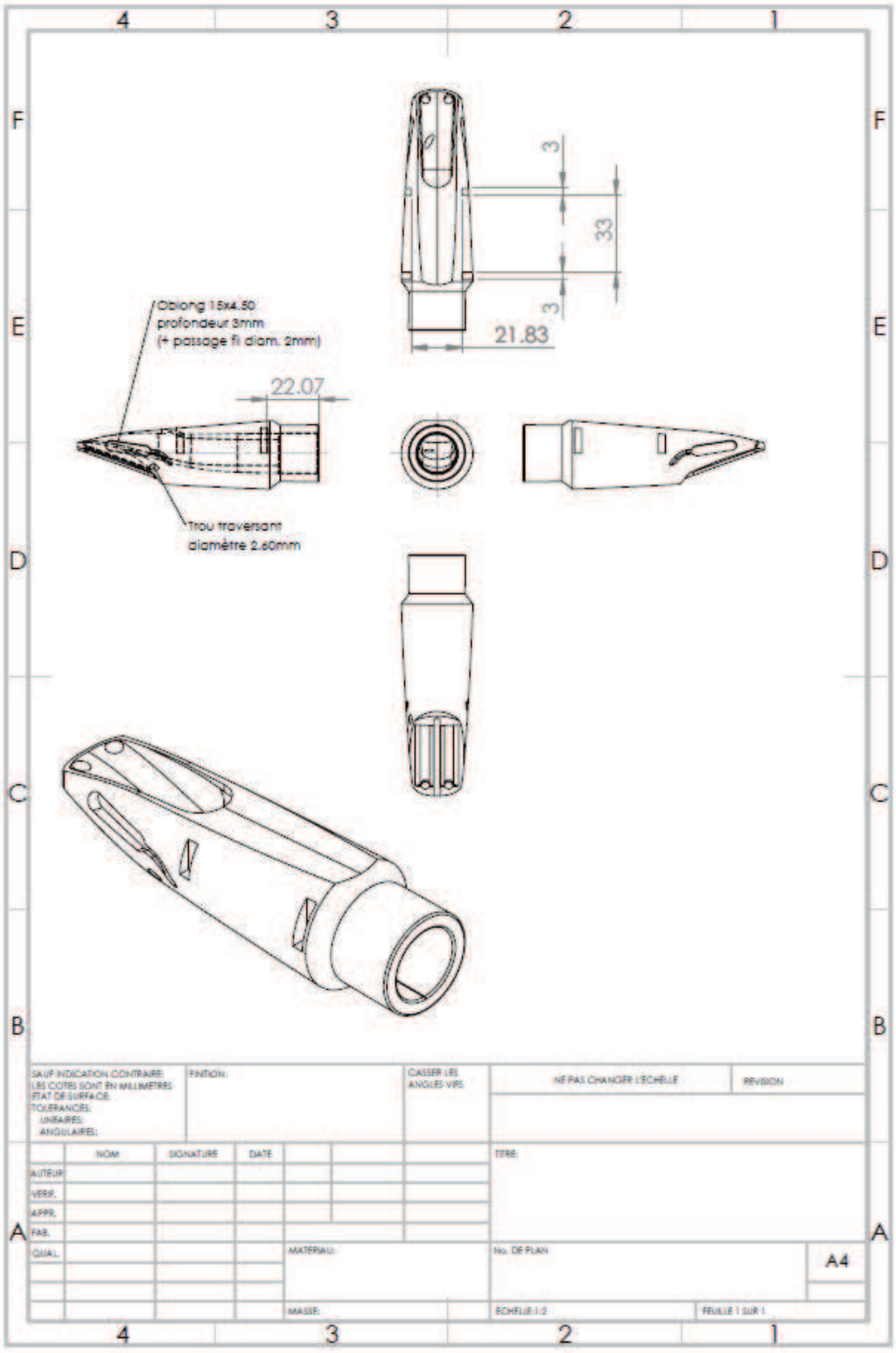

FIGURE A.4: Technical drawing of the mouthpiece. Provided by CTTM.

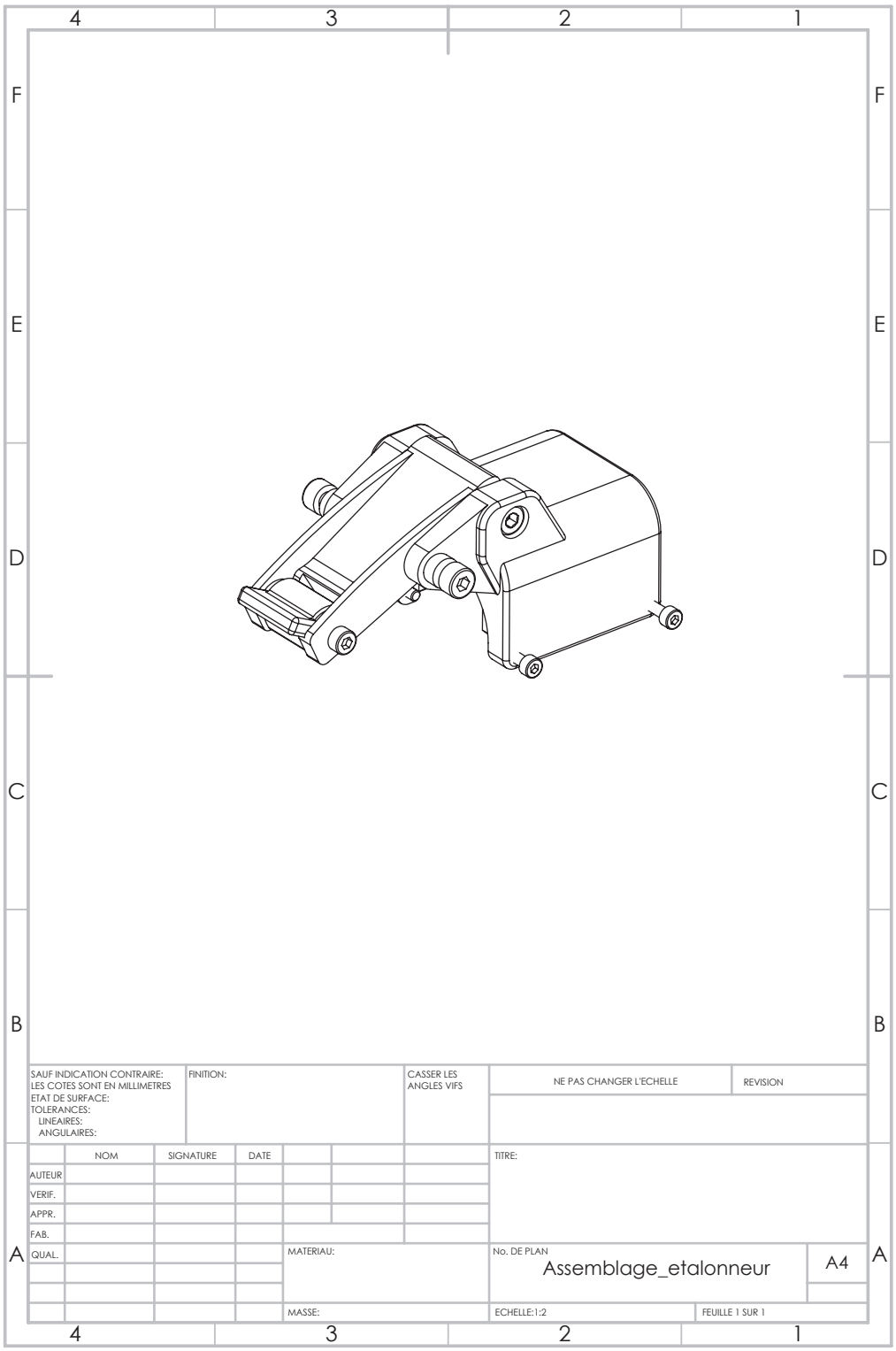

FIGURE A.5: Technical drawing of the assembled calibrator. Provided by CTTM.

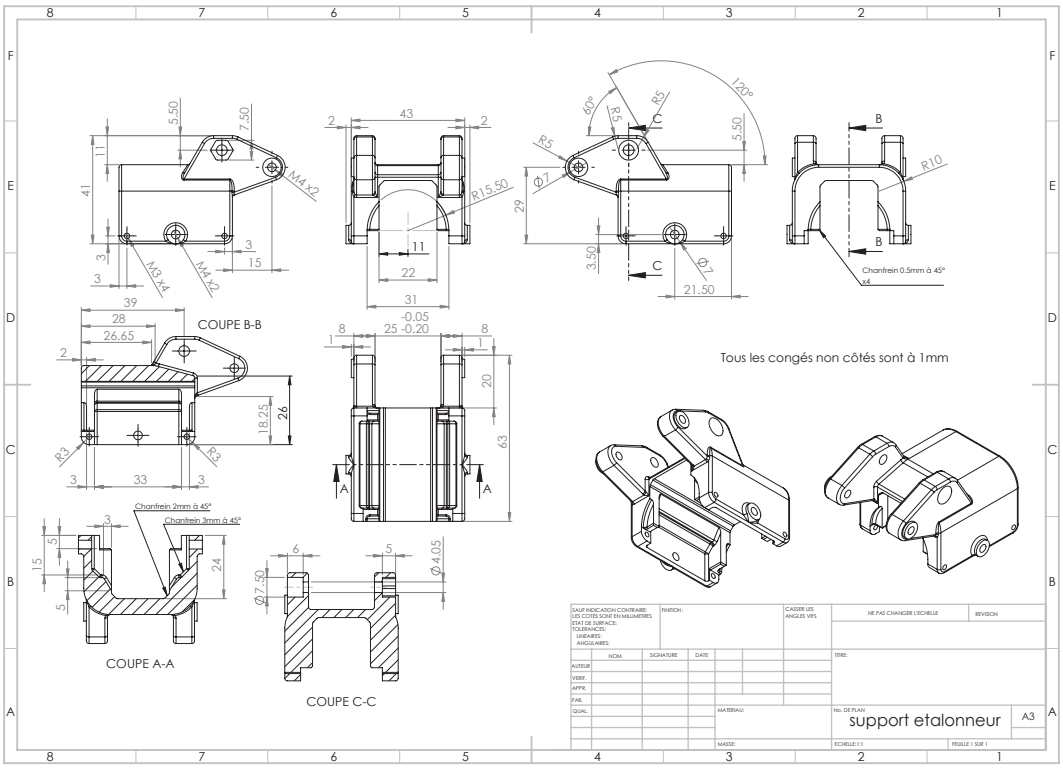

FIGURE A.6: Dimensioned drawing of the support of the calibrator. Provided by CTTM.

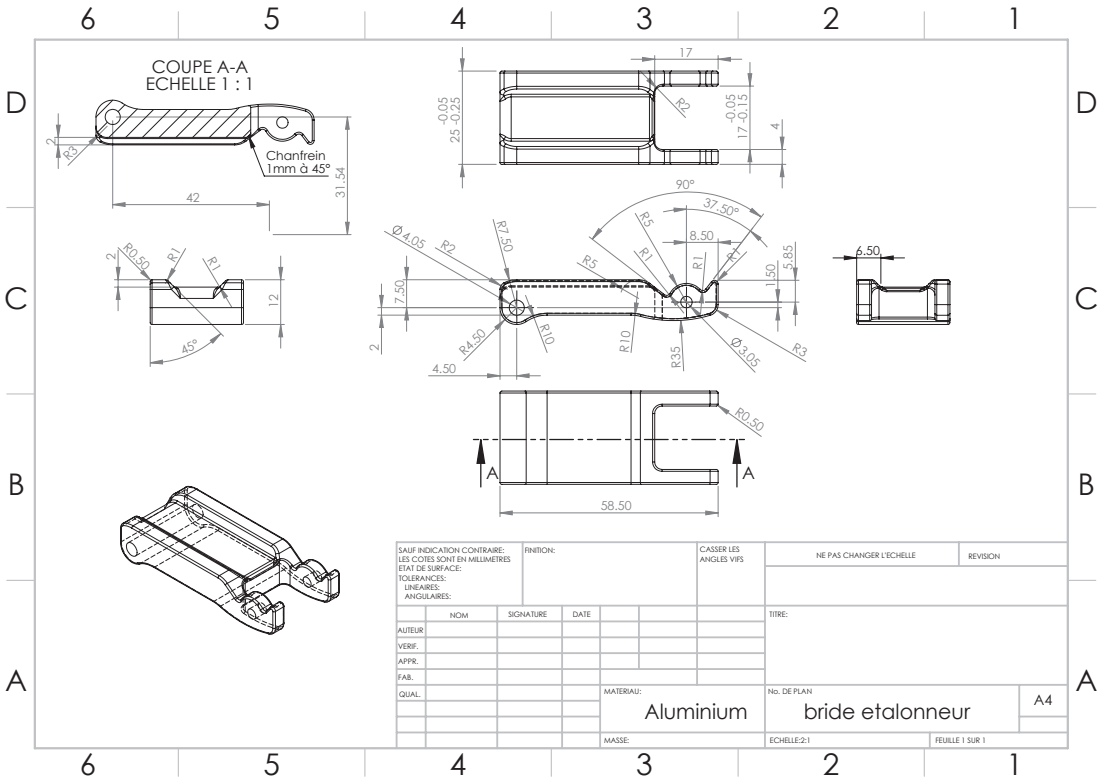

FIGURE A.7: Dimensioned drawing of the flange of the calibrator. Provided by CTTM.

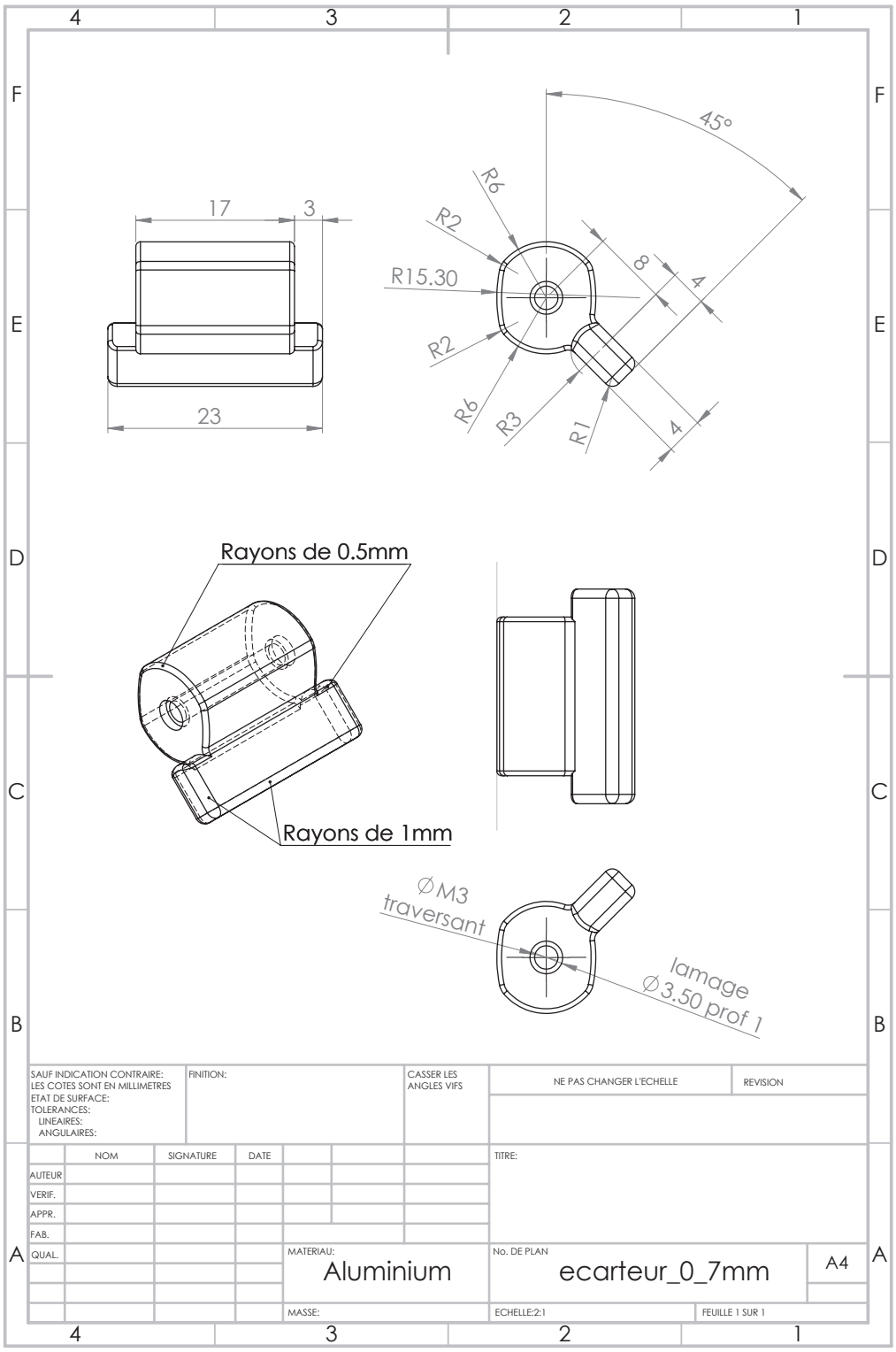

FIGURE A.8: Dimensioned drawing of the lever of the calibrator. Provided by CTTM.

Appendix B

Photointerrupters conditioning and calibration

This appendix presents detailed information about the implementation of the photointerrupters for measuring the reed displacement. The conditioning and measuring principle, and the calibration and determination of the sensor uncertainties, are detailed. The sensors are SG2BC Kodenshi (see data sheet [126] for specifications).

B.1 Conditioning of the sensors and principle of the measurement

The sensors implemented for measuring the reed displacement are reflective photointerrupters. Their geometry and dimensions are shown in Fig. B.1.

The reflective photointerrupters are essentially bipolar junction transistors in which the base behaves as a diode (composed by anode and cathode), emitting infrared light. The light is reflected in a surface facing the photointerrupter, and it is received by the collector-emitter junction. The regions of a reflective photointerrupter are cathode, anode (composing the IR-light source), emitter and collector (composing the receptive part of the photointerrupter). The regions of the photointerrupter are shown in Fig. B.1 and Fig. B.2. The conditioning circuit of a reflective photointerrupter is shown in Fig. B.2.

The characteristic response of the reflective photointerrupter SG2BC is shown in Fig. B.3.

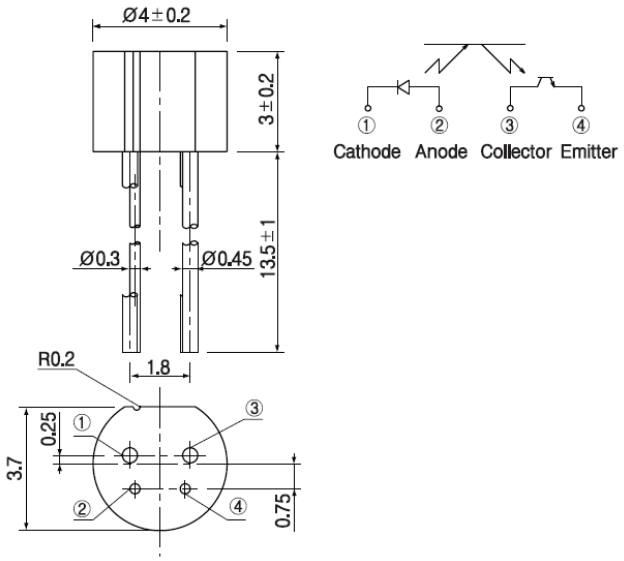

FIGURE B.1: Technical details of the sensors from the data sheet.

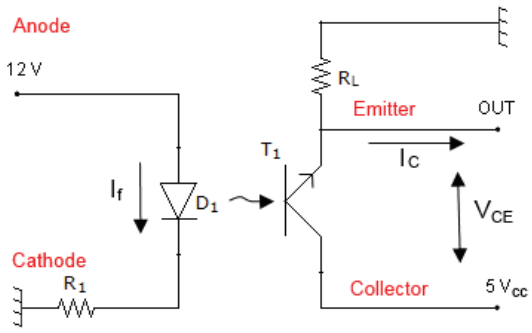

FIGURE B.2: Polarization circuit.

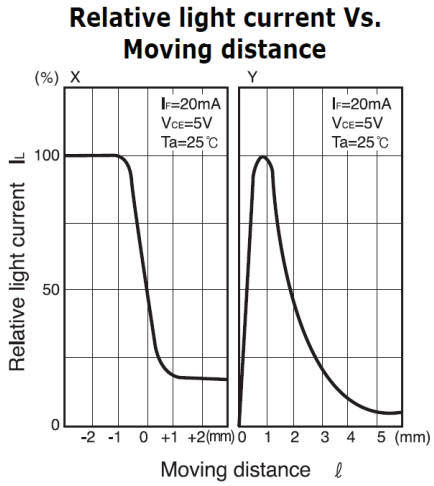

FIGURE B.3: Relative light current vs. moving distance, for reflective photointerrupter SG2BC Kodenshi (from data-sheet).

The conditioning of the photointerrupters is done in order to obtain a linear behaviour in the regime of measured displacement and a minimal heating of the sensors. For the implemented model of photointerrupters (SG2BC Kodenshi), the values of the resistors in the polarization circuit are:

$$R_1 = 780\ \Omega,$$
$$R_L = 1\ k\Omega.$$

B.1.1 Model of the measurement

Two photointerrupters are installed at 4 mm of the tip of a tenor saxophone mouthpiece (see Fig. B.4), in the right and left sides of the inner channel of the mouthpiece.

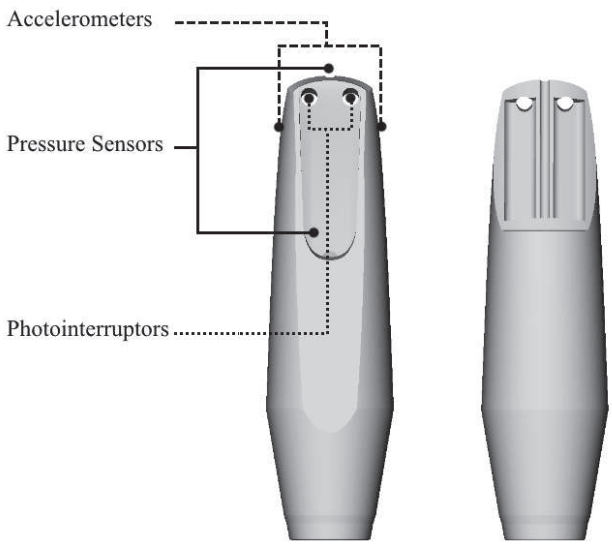

FIGURE B.4: Position of the photointerrupters in the tenor saxophone mouthpiece.

The ideal set up should provide direct measurements of the displacement of the reed tip. This theoretical displacement is equivalent to the height of the transverse section of the channel formed between the reed and the mouthpiece. On the other hand, the geometry of the mouthpiece channel must not be affected by the inclusion of the sensors. Because of physical constraints due to the dimension of the sensors, the sensors can not be installed on the tip of the mouthpiece but only at certain distance. A comparison of the ideal reed displacement y and the measured displacement $\hat{y}$ is shown in Fig. B.5. The displacement varies from the closed reed position (zero in the figure) to the maximal opening (H).

The observed distance $\hat{y}$ is the distance between the sensor and a point of the reed near the tip (see Fig. B.6). The detection of the distance from the sensor to the reed in

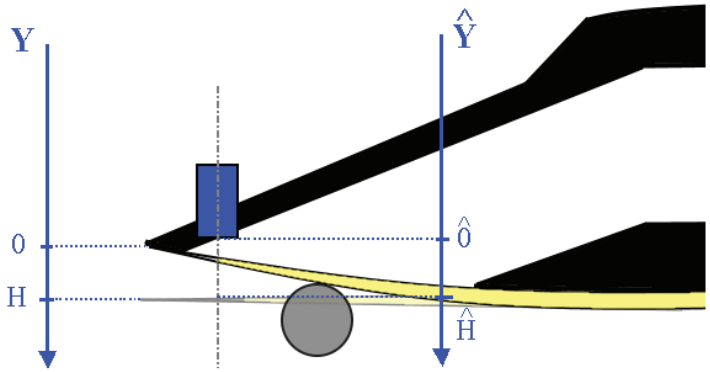

FIGURE B.5: Schema of the theoretical displacement and the measured displacement.

closed position provides the relation between the distance from the sensor to the open reed and the distance between the closed reed and the open reed $\tilde{y}$. The definition of these distances is schematized in Fig. B.6.

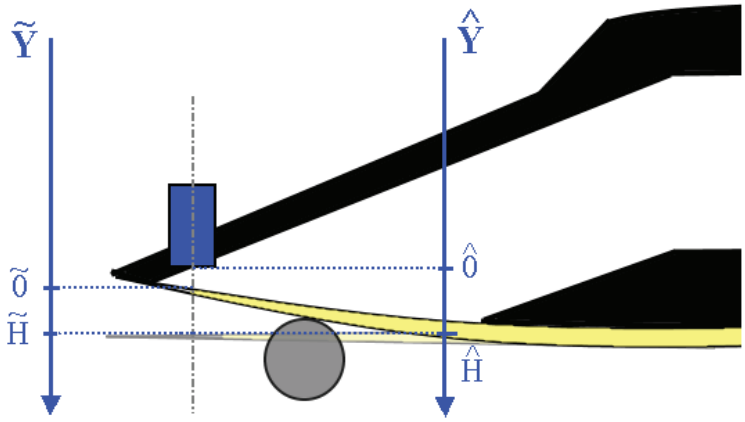

FIGURE B.6: Schema of the displacement definitions.

The relation between the measured distance $\tilde{y}$ and the distance y, referred as theoretical reed displacement, is not studied. The relation between the measured distance $\tilde{y}$ from the reed in closed position to the reed and the measured distance $\hat{y}$ from the sensor to the reed is neither studied. A difference between $\tilde{y}$ respect to y and $\hat{y}$ is that negative values of the reed displacement $\tilde{y}$ may occur when the reed transversely deforms towards the inside of the mouthpiece (when the center of the reed surpasses the lay of the mouthpiece).

The sensors' response can be approximated as linear in the range of the measured displacements (see Fig. B.7): from the closing point of the reed (CP on Fig. B.7) to the maximal aperture of the reed (MA on Fig. B.7). This range of measurements is equivalent to $\tilde{y} \in [0, 0.7]mm$. Within this range, the calibration of the sensors consists

in determining the slope a_1 of the sensors response (the sensitivity) and the voltage V_f measured at the closing point of the reed (CP).

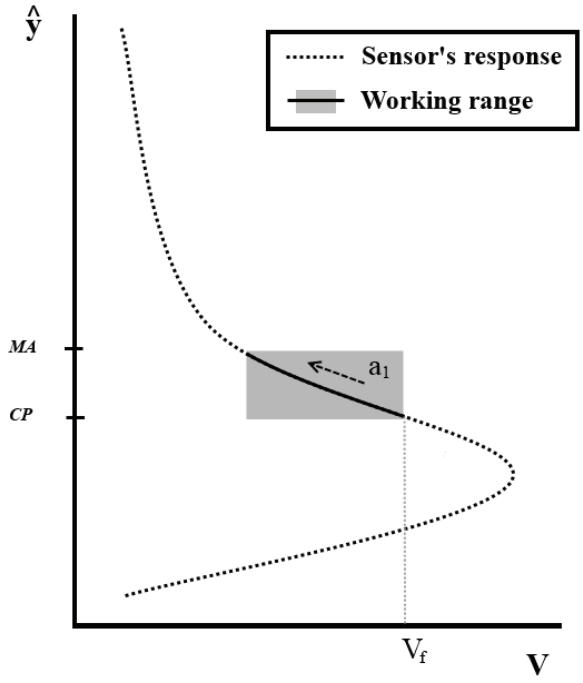

FIGURE B.7: Schema of the working range for the photointerrupters.

The measured voltage in the reference frames for $\tilde{y}$ (with closing point correction) and $\hat{y}$ (without closing point correction) is compared in Fig. B.8. These reference frames (RF) are named $\tilde{Y}$ and $\hat{Y}$ hereafter.

The notation and the definition of the variables presented in Fig. B.8 are gathered in Tab. B.1.

$\hat{y}$	distance measured in the RF $\hat{Y}$.
$\hat{0}$	origin in the RF $\hat{Y}$.
$\hat{H}$	maximal aperture of the reed in the RF $\hat{Y}$.
$\hat{y_f}$	closing point of the reed in the RF $\hat{Y}$.
$\hat{V}$	voltage referred to the RF $\hat{Y}$.
a_0	y-intercept in the RF $\hat{Y}$.
$\tilde{y}$	distance measured in the RF $\tilde{Y}$.
$\tilde{0}$	origin in the RF $\tilde{Y}$.
$\tilde{H}$	maximal aperture of the reed in the RF $\tilde{Y}$.
$\tilde{V}$	voltage referred to the RF $\tilde{Y}$.

TABLE B.1: Notation used in the model of the displacement measurement.

The closing point voltage measured in the reference frame $\hat{Y}$ is defined as:

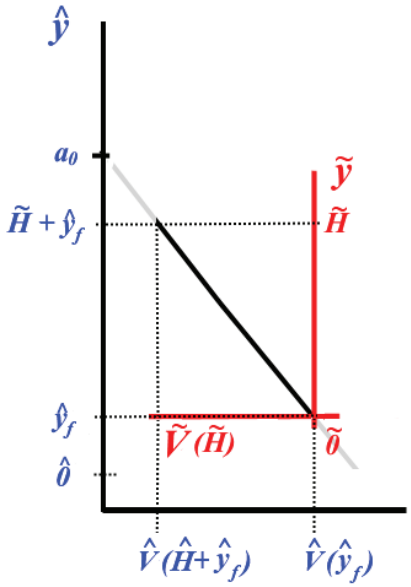

FIGURE B.8: Schema of the distances $\tilde{y}$ and $\hat{y}$, measured in the reference frames $\tilde{Y}$ and $\hat{Y}$, respectively.

$$V_f = \hat{V}\left(\hat{y_f}\right). \tag{B.1}$$

In the reference frame $\hat{Y}$, the relation between distance and voltage is written as shown in eq. B.2, where a_1 is the sensibility and a_0 the y-intercept.

$$\hat{y} = a_1 \cdot \hat{V} + a_0. \tag{B.2}$$

In the reference frame $\tilde{Y}$ the calibration relation is written

$$\tilde{y} = a_1 \cdot \tilde{V}. \tag{B.3}$$

The relation between the reference frames $\tilde{Y}$ and $\hat{Y}$ can be written as follows:

$$\tilde{y} = \hat{y} - \hat{y_f}, \tag{B.4}$$

$$\tilde{V} = \hat{V} - \hat{V}\left(\hat{y_f}\right) = \hat{V} - V_f. \tag{B.5}$$

The measured distance in the reference frame $\tilde{Y}$ can therefore be written as shown in eq. B.6.

$$\tilde{y} = a_1 \cdot \tilde{V} = a_1 \cdot \left(\hat{V} - \hat{V}\left(\hat{y_f}\right)\right) = a_1 \cdot \left(\hat{V} - V_f\right). \tag{B.6}$$

Eq. B.6 shows the relation between the displacement in the reference frame $\tilde{Y}$ and the voltage $\hat{V}$. This is the equation used for calibrating the sensors. The study of the calibration of the sensors consists in determining the coefficients of the sensitivity a_1, and the closing point voltage V_f and their uncertainties. The advantage of reference frame $\tilde{Y}$ respect to $\hat{Y}$ is that it is possible to use complementary sensors to measure V_f and to reduce the uncertainty of the closing point voltage.

B.2 Calibration and uncertainties

The calibration of the sensors consists in determining the coefficients of the sensitivity a_1 and the closing point voltage V_f. A study of the calibration and the uncertainties of the displacement measurement is developed using a calibration bench. The uncertainties associated to the calibration bench, the reflectivity variations between reeds in dry and wet situations, and the dynamic calibration of the parameter V_f are studied. A calibrator has been developed in order to calibrate the sensors for each measurement in a practical way. The uncertainties produced by this calibration are also studied.

B.2.1 Calibration principles

Two different techniques are used for calibrating the sensors: one static and one dynamic. The coefficient a_1 is obtained by means of the static calibration, which can be done by using a calibration bench or with the calibrator (see Appendix A). The bench provides a free sampling measurement of the reed displacement, and the calibrator provides a measurement of the reed position for two points. The principle of the calibration bench and the principle of the calibrator are explained in §B.2.1.1 and §B.2.1.2, respectively. The measurement of the coefficient V_f can be done statically or dynamically. The static calibration of V_f is done by using the calibration bench or the calibrator. The dynamic calibration of V_f is done using accelerometers that detect the impact of the reed on the mouthpiece and providing more accurate measurements than the static calibration. The principle of the dynamic calibration of V_f is explained in §B.2.1.3.

B.2.1.1 Principle of the calibration bench

The calibration bench consists in a table with a saxophone cork where the mouthpiece is set, and a thin rectangular plate installed on a two-axis displacement system controlled

with micrometric screws. The vertical position of the plate is adjusted to be in front of the sensors and the horizontal position controls the deformation of the reed against the mouthpiece. The system provides a measurement of the measured voltage as a function of the position of the reed (see Fig. B.9).

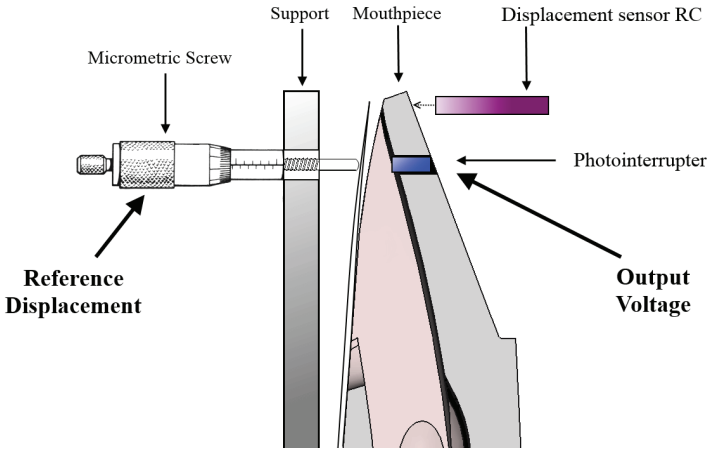

FIGURE B.9: Principle of the calibration on the calibration bench.

The closing point of the reed must be precisely determined. A detection technique is developed for this purpose. A displacement sensor (Philtec RC62 [116]) is installed in front of the upper part of the mouthpiece, in the opposite side of the face with the reed. This sensor measures the displacement of the mouthpiece on the cork when the plate pushes the reed (and the mouthpiece) once the reed is closed. The threshold detection in the voltage of this sensor allows for determining the closing point of the reed.

B.2.1.2 Principle of the calibrator

The calibration of the sensors must be done for each reed and each measurement. This process is quite slow, so a fast calibration technique is implemented.

A calibrator has been developed for this purpose (see Appendix A). The calibrator can be installed on the mouthpiece in a fixed position. It has a lever that can hold the reed in two positions: in closed position and at an aperture of 0.7 mm. The measurement of the output voltage of the photointerrupters in these positions allows for the determination of the sensitivity a_1 and the closing voltage V_f.

B.2.1.3 Principle of the dynamic calibration

The dynamic calibration provides the value of V_f when the reed is in dynamic excitation. The closing point of the reed is detected by means of two accelerometers installed on

the lay of the mouthpiece (see Fig. B.4). These accelerometers provide a measurement of the impact of the reed on the mouthpiece when it happens. More details of this calibration and some examples of measurements are given in §B.3.4.

B.3 Uncertainty measurement

In this section, the uncertainty in the determination of the calibration parameters is studied. The uncertainty is calculated as the standard deviation of the parameter in percentage, written in the form shown in eq. B.7.

$$\sigma\,(\%) = \frac{\sigma_X}{\overline{X}} \cdot 100. \tag{B.7}$$

The repeatability of the static and dynamic calibration processes and the quality of the calibration for dry reeds and wet reeds are studied.

B.3.1 Dry reeds

The repeatability of the calibration using the bench and the susceptibility of the calibration parameters to the reflectivity of dry reeds are studied in the linear response regime ($\tilde{y} \in [0, 0.7]$ mm).

B.3.1.1 Repeatability of the calibration bench

The susceptibility of the calibration parameters to consecutive installations of a same reed on the mouthpiece is studied here.

The mouthpiece is installed on the calibration bench. The setting of the reed on the mouthpiece is repeated 10 times. Results for the sensor 1 and 2 are shown in Fig. B.10, B.11 respectively.

Sensor 1 is more sensitive than sensor 2. The standard deviations of a_1 for sensors 1 and 2 are 6.61 % and 2.13 %, and the respective standard deviations of V_f are 4.11 % and 1.74 %.

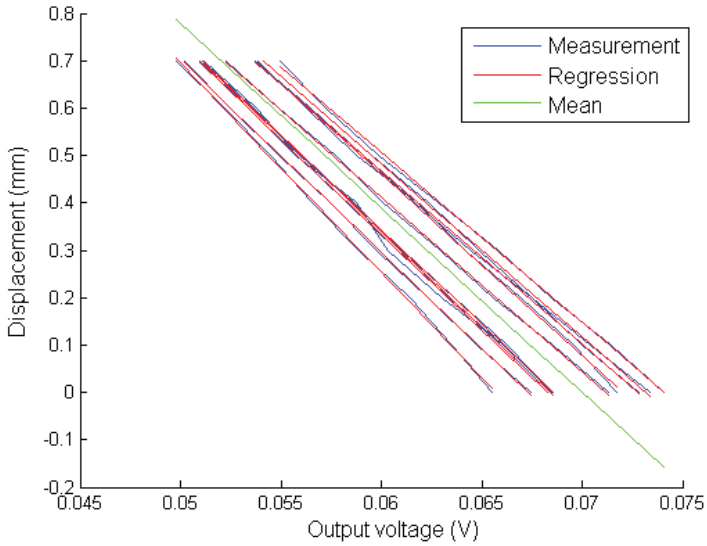

FIGURE B.10: Calibration measurement for the photointerrupter 1. Repeatability of the calibration bench.

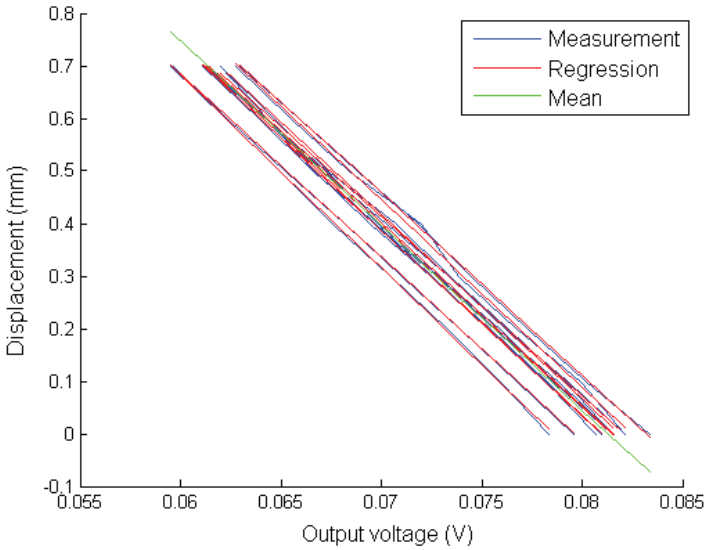

FIGURE B.11: Calibration measurement for the photointerrupter 2. Repeatability of the calibration bench.

B.3.1.2 Susceptibility to dry-reeds reflectivity

The variations of the calibration parameters due to the different reflectivity of dry-reeds is studied. The samples are 10 reeds of different force and cut. Results are shown in Fig. B.12 for sensor 1, B.13 for sensor 2.

The standard deviations for sensor 1 and 2 for a_1 are 11.7 % and 10.3 %. The standard deviations for sensor 1 and 2 for V_f are 10.0 % and 8.08 %.

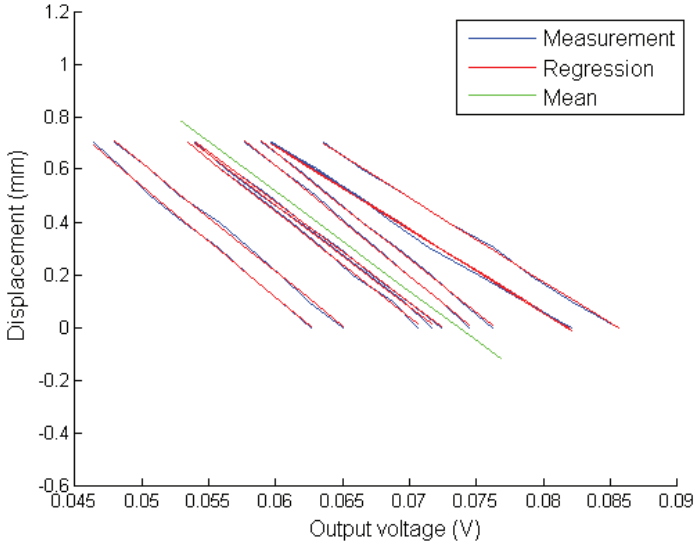

FIGURE B.12: Calibration measurement for the photointerrupter 1 for 10 reeds.

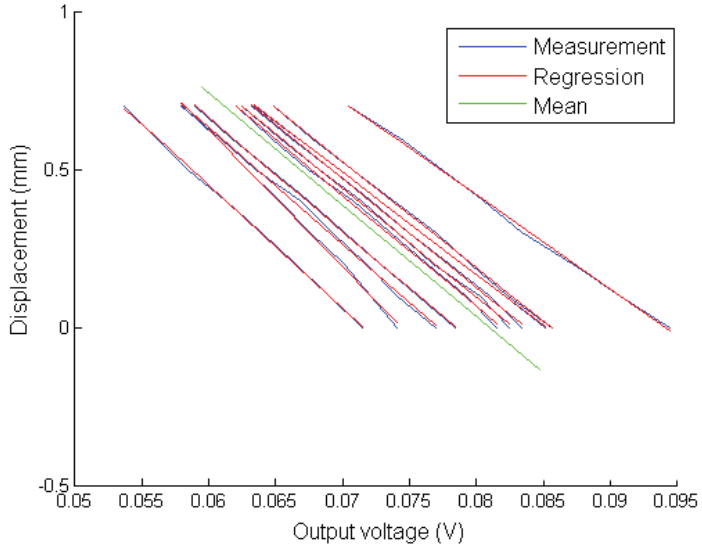

FIGURE B.13: Calibration measurement for the photointerrupter 2 for 10 reeds.

Figures B.14, B.15 show the results for sensor 1 and 2 respectively, in the RF $\tilde{Y}$. A higher sensitivity of sensor 1 to the different reflectivity of the reeds is observed.

B.3.2 Wet reeds

In the previous study, an important sensitivity of the sensors to the reeds reflectivity has been observed. As the reeds are wet when playing and this may produce variations in their reflectivity, a study of the sensitivity of the sensors to wet-reeds reflectivity is performed.

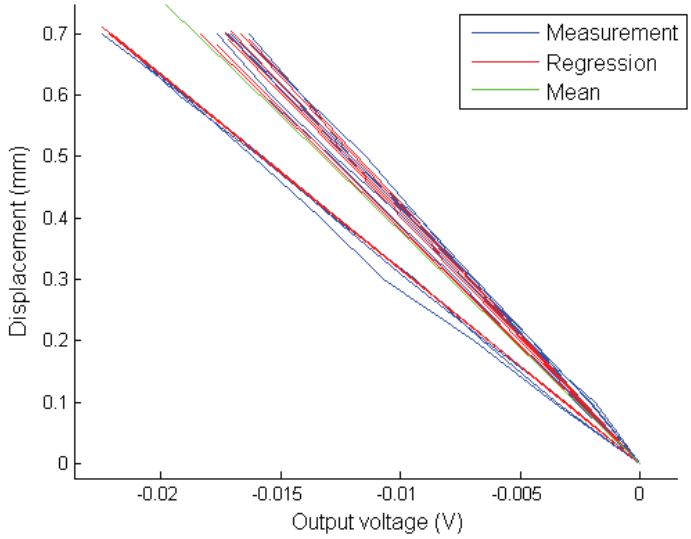

FIGURE B.14: Calibration measurement for the photointerrupter 1 for 10 reeds in the RF $\tilde{Y}$.

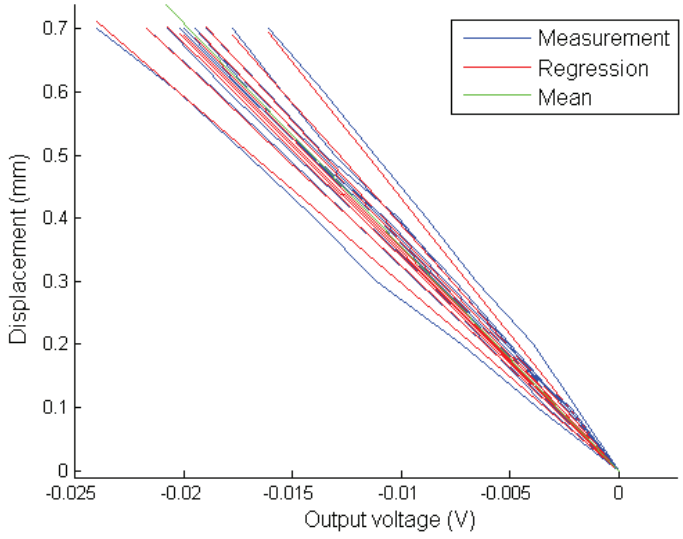

FIGURE B.15: Calibration measurement for the photointerrupter 2 for 10 reeds in the RF $\tilde{Y}$.

B.3.2.1 1 drying reed

The variation of the coefficient a_1 for one wet reed while drying is studied. The reed is put in water during 30 minutes. After 15 minutes drying in vertical position, the reed is installed on the mouthpiece and a measurement of calibration is carried out each 5 minutes. The measurements are shown in Fig. B.16, B.17 for sensor 1 and 2 respectively. In order to compare the sensitivity, it is useful to represent the voltage introducing the correction of the closing point voltage $V - V_f$.

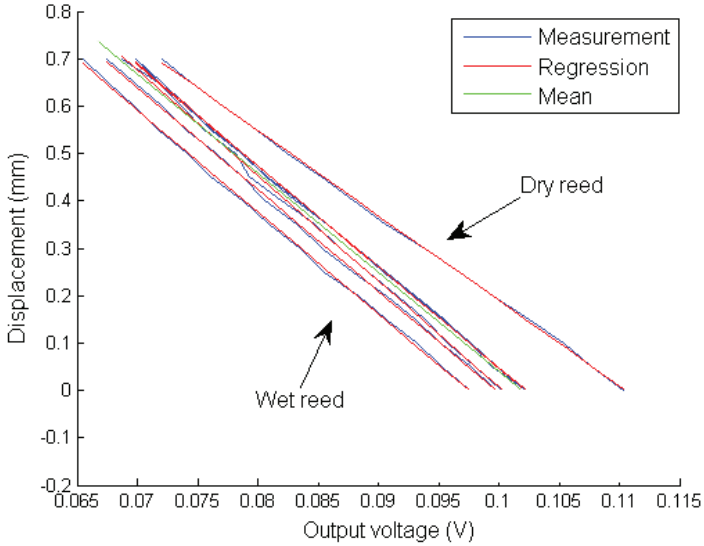

FIGURE B.16: Calibration of a drying reed for the photointerrupter 1.

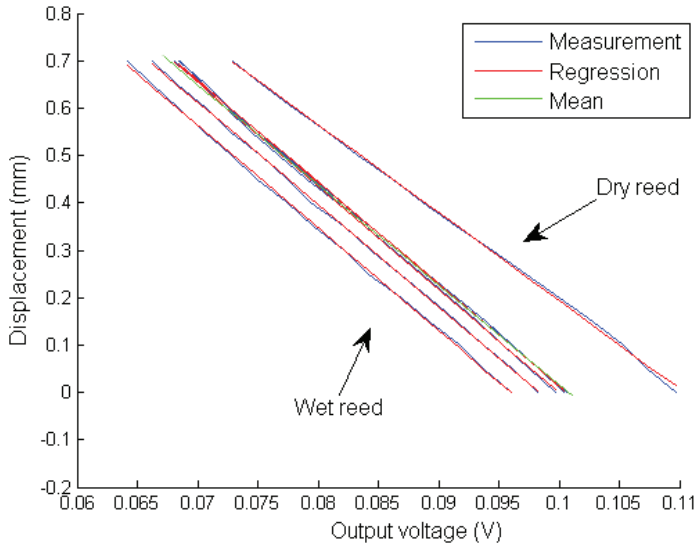

FIGURE B.17: Calibration of a drying reed for the photointerrupter 2.

The standard deviation is 7.3% for sensor 1 and 5.9% for sensor 2.

When the representation of the measurements is done in the RF $\tilde{Y}$ (Fig. B.18 and B.19), the difference between the dry and the wet states of the reed is clearly noticeable. In this strong humidity condition, the reflectivity of the reed seems rather constant and the observed relaxation time is longer than 35 minutes.

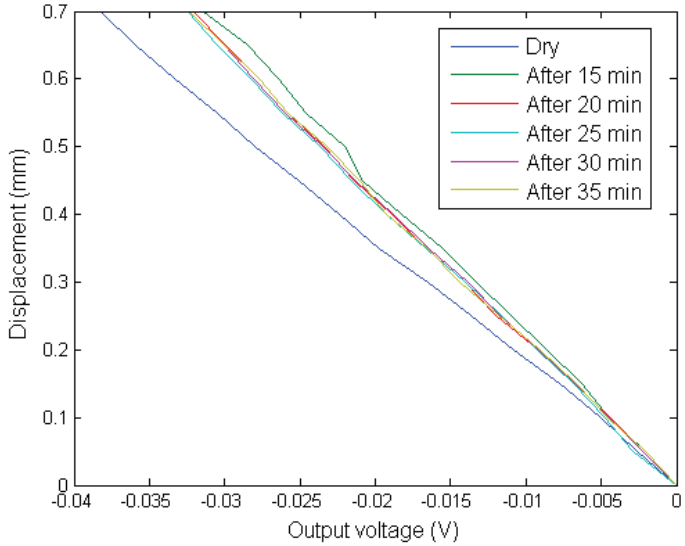

FIGURE B.18: Calibration measurement of a drying reed for the photointerrupter 1 in the RF $\tilde{Y}$.

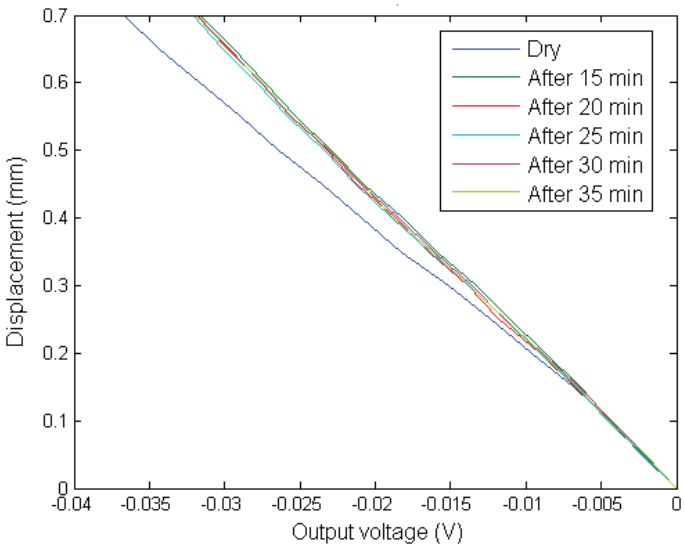

FIGURE B.19: Calibration measurement of a drying reed for the photointerrupter 2 in the RF $\tilde{Y}$.

B.3.2.2 One reed in playing conditions

The humidification of a reed while playing differs from the strong humidity conditions imposed in the previous study. To analyse this phenomenon, a calibration is conduced for a dry reed and for the same reed after playing during 10 s. The measurements are shown in Fig. B.20 for sensor 1 and in Fig. B.21 for sensor 2.

The standard deviation of a_1 for sensor 1 and 2 are 18.1% and 28.8% respectively. These

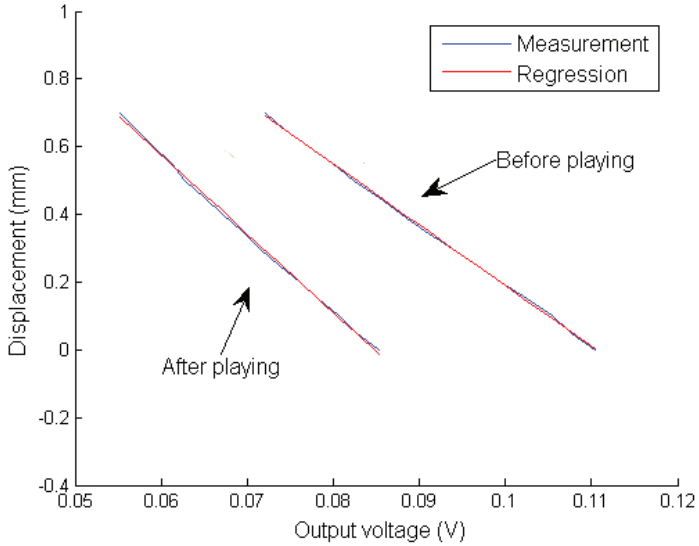

FIGURE B.20: Calibration measurement of a reed before and after playing for the photointerrupter 1.

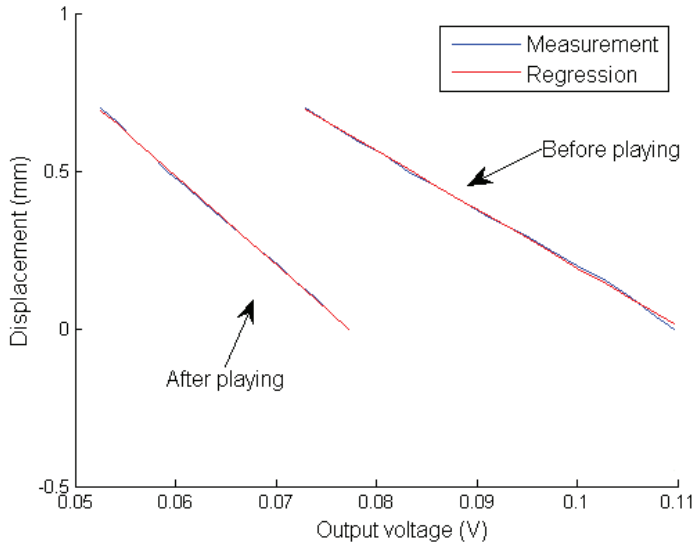

FIGURE B.21: Calibration measurement of a reed before and after playing for the photointerrupter 1.

standard deviations are very large, so accuracy can not be assured for long measurements.

B.3.2.3 Nine reeds in playing conditions

The variation of a_1 for different reeds when playing 1 s is studied in this point. A set of 9 reeds of different cut and strength is used for the study. The calibration is performed for each reed in dry conditions and after playing 1 s. The standard deviation of a_1 for

these two measurements is obtained for each reed. The mean standard deviation for sensor 1 is 2.50% and for sensor 2 is 2.43%. Also, the mean standard deviation of V_f is 4.40 % for the sensor 1 and 4.43 % for the sensor 2.

B.3.3 Current drift

A current drift has been detected when the sensors are used for more than 10 min. The heating of the emitter produces these variations in the sensors' response. The voltage drop in the resistor R_1 (see Fig. B.2) is measured for 20 minutes of continous functionning at a sampling frequency of 1 s. This experience is repeated for different values of the resistor R_1 (R_1 = 680 Ω, 780 Ω, 990 Ω, 1100 Ω, 2200 Ω).

An optimal value of R_1 where the variation is minimal ($R_1 \approx 780$ kΩ) has been identified. For this value, the standard deviation of the output is $\sigma = 1\%$.

B.3.4 Principle and uncertainty of the dynamic calibration

The static measurement of the closing point voltage V_f is delicate and needs complementary sensors in addition to the photointerrupters. The deformation of the reed in playing conditions can differ from the bending of the reed in the calibration, so that the calibrated closing point voltage is not accurate for calibrating the measurements. The static calibration of the closing point voltage is also subjected to uncertainties such as the humidification of the reed in playing conditions or the current drift in the photointerrupters. In playing conditions, the use of accelerometers can provide a dynamic calibration of the closing point voltage.

The dynamic calibration of the coefficient V_f provides an immediate measurement of the coefficient in playing conditions. The dynamic calibration use accelerometers, installed on the lay of the mouthpiece as shown in Fig. B.4, for the detection of the closing point. The static calibration of V_f is slower and provides a less accurate estimation of V_f due to the heating of the sensors (see §B.3.3) and variations of the reflectivity of the reed produced by the wetting of the reed while playing (§B.3.2). Transverse deformation of the reed produces discrepancies between the detection of the closing point in static and dynamic conditions, the dynamic calibration being more precise.

The direct detection of the closing point of the reed can be done for high dynamic levels of excitation of the reed, when impact of the reed on the mouthpiece happens (see Fig. B.22). The uncertainty of the measurement of V_f in high dynamic levels is given in §B.3.4.1. For low dynamic levels of excitation, there is no impact (see Fig. B.23), so an

indirect measurement is done by using an associated measurement in high dynamic level. The uncertainty of the measurement of V_f in low dynamic levels is given in §B.3.4.2.

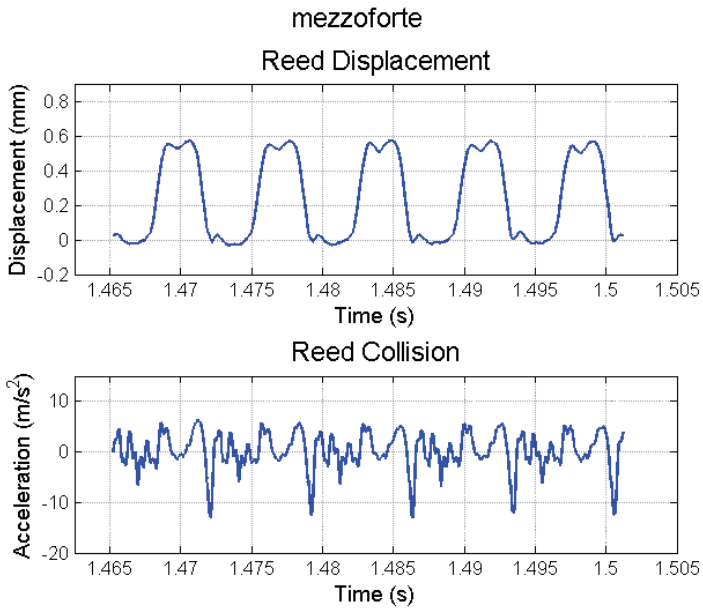

FIGURE B.22: Displacement and acceleration signals measured in high dynamic level.

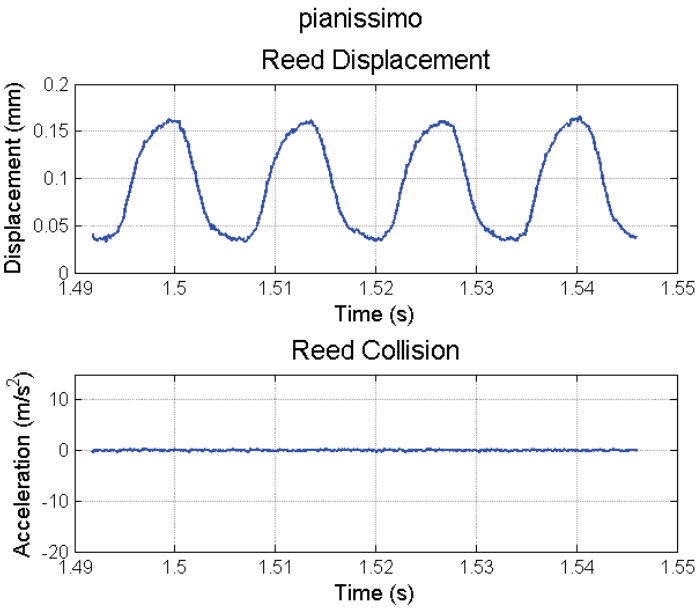

FIGURE B.23: Displacement and acceleration signals measured in low dynamic level.

B.3.4.1 High dynamic levels

The measurement of the acceleration on the lay of the mouthpiece allows for the detection of the impact of the reed on the mouthpiece. The modulations in the acceleration signals due to gravitational effects are filtered in windows of 5 periods with the Matlab function

detrend. The detection of the highest peaks in the acceleration signal, associated to the closing point of the reed, provides the direct measurement of V_f. This detection is done in 5-period windows for tracking the variations of V_f while playing.

The standard deviation of V_f is 1.9 % for sensor 1 and 0.3 % for sensor 2.

B.3.4.2 Low dynamic levels

For low dynamic levels, no impact of the reed on the mouthpiece is detected. A mean value of V_f obtained in high dynamic level is assumed. The standard deviation of V_f is 2.80 % for sensor 1 and 1.86 % for sensor 2.

B.4 Conclusion

B.4.1 Uncertainty of the sensitivity a_1

The sensitivity a_1 is measured statically. The uncertainties coming from the calibration bench and the humidity variations during playing must be considered. In order to avoid the uncertainties derived from the different reflectivity of the reeds, a calibration must be done for each reed. Also, the measurements must not exceed 1 s to avoid an increase of the uncertainty produced by the humidity. The final estimation of the uncertainty for the sensor 1 and 2 are given in eq. B.8 and B.9.

$$\left(\sigma_{a_1}^2\right)^{PT1} \longrightarrow \sigma_{Installation}^2 + \sigma_{Humidity}^2 = (6.61)^2 + (2.50)^2 \longrightarrow 7.1\% \tag{B.8}$$

$$\left(\sigma_{a_1}^2\right)^{PT2} \longrightarrow \sigma_{Installation}^2 + \sigma_{Humidity}^2 = (2.13)^2 + (2.43)^2 \longrightarrow 3.2\% \tag{B.9}$$

B.4.2 Uncertainty of the closing point voltage V_f

The estimation of the uncertainty of V_f done dynamically. The uncertainty of V_f for high and low playing dynamics are presented below.

B.4.2.1 High playing dynamics

For high playing dynamics, the uncertainty of the coefficient V_f comes exclusively from the shock detection. The results for sensor 1 and 2 are shown in eq. B.10 and B.11.

$$\left(\sigma^2_{V_f}\right)^{PT1}_{forte} \longrightarrow \sigma^2_{Accelerometers} = (1.9)^2 \longrightarrow 1.9\% \tag{B.10}$$

$$\left(\sigma^2_{V_f}\right)^{PT1}_{forte} \longrightarrow \sigma^2_{Accelerometers} = (0.3)^2 \longrightarrow 0.3\% \tag{B.11}$$

B.4.2.2 Low playing dynamics

For low playing dynamics, the uncertainty of V_f comes from the estimation of V_f from the high dynamic level reference measurement, the humidity and the current drift. Results are shown in eq. B.12 and B.13 for sensor 1 and 2.

$$\left(\sigma^2_{V_f}\right)^{PT1}_{piano} \longrightarrow \sigma^2_{Accelerometers} + \sigma^2_{Humidity} + \sigma^2_{Drift} = (2.80)^2 + (4.40)^2 + (1.0)^2 \longrightarrow 5.3\% \tag{B.12}$$

$$\left(\sigma^2_{V_f}\right)^{PT2}_{piano} \longrightarrow \sigma^2_{Accelerometers} + \sigma^2_{Humidity} + \sigma^2_{Drift} = (1.86)^2 + (4.43)^2 + (1.0)^2 \longrightarrow 4.9\% \tag{B.13}$$

Appendix C

Implementation of the reed models

This appendix contains the explicit implementation of the estimation method of the reed parameters for the different physical models used to describe the reed behaviour. Some more details about system modelling can be found in [127].

The principle for obtaining the discrete transfer functions and the explicit expressions of the filter for each model are detailed. The aim is to convert continuous-time system representations (the differential equations of the reed models) to discrete-time transfer functions.

C.1 Principle

The conversion of a discrete-time signal to a discrete filter is done by means of the Z-transform. The Z-transform is a discrete-time equivalent of the Laplace transform. The bi-linear transform (also known as Tustin's method) is a Z-transform where the parameter z is approximated as shown in eq. C.1.

$$z = e^{sT} = \frac{e^{sT/2}}{e^{-sT/2}} \approx \frac{1 + sT/2}{1 - sT/2}, \tag{C.1}$$

where T is the sampling period.

The inverse of this allows obtaining the discrete-time transfer function $G_d(z)$ from the continuous-time transfer functions $H_a(s)$. Thus, the transformation is obtained by

means of the approximation given in eq. C.2

$$s = \frac{1}{T}\ln z \approx \frac{2}{T}\frac{z-1}{z+1}, \tag{C.2}$$

resulting in

$$G_d(z) = H_a(s)|_{s=\frac{2}{T}\frac{z-1}{z+1}} = H_a\left(\frac{2}{T}\frac{z-1}{z+1}\right). \tag{C.3}$$

C.2 Models

C.2.1 K model

The equation of the low-frequency linear model is:

$$K(y(t) - H) = -\Delta P(t), \tag{C.4}$$

which can be written:

$$y(k) = -\frac{1}{K}\Delta P(k) + H. \tag{C.5}$$

In this case, the obtaining of the transfer function G(z) is trivial:

$$G(z) = \frac{1}{K}. \tag{C.6}$$

C.2.2 K_{NL} model

The equation of the non-linear stiffness model is:

$$K(y(t) - H) = \Delta P(t) + K_c \lfloor y_c - y(t) \rfloor^2. \tag{C.7}$$

The filter is the same as for the K model, but in this case the filtered signal is not $-\Delta P$ but U :

$$y(k) = \frac{U(k)}{K} + H. \tag{C.8}$$

For $y(k) \geq y_c$:

In this case, the behaviour of the oscillator is such of the linear case $y_{lin}(k)$:

$$y_{lin}(k) = \frac{-\Delta P(k)}{K} + H. \tag{C.9}$$

If $y(k) \geq y_c$:

$$U(k) = -\Delta P(k), \tag{C.10}$$

so

$$y(k) = y_{lin}(k). \tag{C.11}$$

For $y(k) < y_c$:

Then

$$U(k) = -\Delta P(k) + K_c(y_c - y(k))^2, \tag{C.12}$$

and

$$y(k) = \frac{-\Delta P(k) + K_c(y_c - y(k))^2}{K} + H, \tag{C.13}$$

so that:

$$\frac{K_c}{K}y^2(k) - (1 + 2\frac{K_c}{K}y_c)y(k) + \frac{K_c}{K}y_c^2 + y_{lin}(k) = 0. \tag{C.14}$$

This is a quadratic equation with discriminant:

$$\Delta = 1 + 4\frac{K_c}{K}(y_c - y_{lin}(k)). \tag{C.15}$$

whose solutions are:

$$\begin{cases} y_1(k) = y_c + \dfrac{K}{K_c}(1 + \sqrt{\Delta}) \\ y_2(k) = y_c + \dfrac{K}{K_c}(1 - \sqrt{\Delta}) \end{cases} \tag{C.16}$$

where $y_{lin}(k) \geq y_c$ implies $\Delta < 1$ and $y_1(k), y_2(k) > y_c$, which contradicts $y(k) < y_c$. The valid solution is $y_{lin}(k) < y_c$ and $\Delta > 1$, where only y_2 is valid. Then:

$$y(k) = y_c + \frac{K}{K_c}(1 - \sqrt{\Delta}). \tag{C.17}$$

Finally,

$$y(k) = \begin{cases} y_{lin}(k) \text{ if } y_{lin}(k) \geq y_c, \\ y_c + \dfrac{K}{K_c}(1 - \sqrt{\Delta}) \text{ if } y_{lin}(k) < y_c. \end{cases} \tag{C.18}$$

C.2.3 RK model

The equation of the model with linear stiffness and damping is:

$$R\dot{y}(t) + K(y(t) - H) = -\Delta P(t). \tag{C.19}$$

With the change of variable:

$$\mu(t) = y(t) - H \tag{C.20}$$

The equation C.19 becomes:

$$R\dot{\mu}(t) + K\mu(t) = -\Delta P(t), \tag{C.21}$$

That transforms in the Laplace domain as:

$$Rp\mu(p) + K\mu(p) = -\Delta p(p). \tag{C.22}$$

The continuous-time transfer function G(p) relating μ and $-\Delta p$ is:

$$G(p) = \frac{\mu(p)}{-\Delta p(p)} = \frac{\frac{1}{K}}{1 + \frac{R}{K}p}. \tag{C.23}$$

Discretizing this equation with the bi-linear transform we obtain:

$$G(z) = G(p)|_{p=2f_s\frac{z-1}{z+1}}, \tag{C.24}$$

with f_s the sampling frequency.

The discrete filter is written:

$$G(z) = \kappa\frac{1 + z^{-1}}{1 + a_1 z^{-1}}, \tag{C.25}$$

with

$$\begin{cases} \kappa = \dfrac{1}{K + 2f_s R}, \\ a_1 = \dfrac{K - 2f_s R}{K + 2f_s R}. \end{cases} \tag{C.26}$$

The associated equation to the filter is:

$$\mu(k) = \kappa(-\Delta p(k) - \Delta p(k-1)) - a_1\mu(k-1), \tag{C.27}$$

which written with respect to y becomes:

$$y(k) = \kappa(-\Delta p(k) - \Delta p(k-1)) - a_1 y(k-1) + \alpha, \tag{C.28}$$

with

$$\alpha = H(1 + a_1). \tag{C.29}$$

C.2.4 RK_{NL} model

The filter is the same that the RK model, but the filtered signal is U :

$$y(k) = \kappa(U(k) + U(k-1)) - a_1 y(k-1) + \alpha. \tag{C.30}$$

In this case, $y_{lin}(k)$ is:

$$y_{lin}(k) = \kappa(-\Delta P(k) + U(k-1)) - a_1 y(k-1) + \alpha. \tag{C.31}$$

For $y(k) \geq y_c$:

Then

$$U(k) = -\Delta P(k), \tag{C.32}$$

and

$$y(k) = y_{lin}(k). \tag{C.33}$$

For $y(k) < y_c$:

Then

$$U(k) = -\Delta P(k) + K_c(y_c - y(k))^2, \tag{C.34}$$

and

$$y(k) = \kappa(-\Delta P(k) + K_c(y_c - y(k))^2 + U(k-1)) - a_1 y(k-1) + \alpha, \tag{C.35}$$

that is:

$$\kappa K_c y^2(k) - (1 + 2\kappa K_c y_c) y(k) + \kappa K_c y_c^2 + y_{lin}(k) = 0. \tag{C.36}$$

That is a quadratic equation with discriminant:

$$\Delta = 1 + 4\kappa K_c(y_c - y_{lin}(k)), \tag{C.37}$$

whose solutions are:

$$\begin{cases} y_1(k) = y_c + \kappa K_c(1 + \sqrt{\Delta}) \\ y_2(k) = y_c + \kappa K_c(1 - \sqrt{\Delta}) \end{cases} \tag{C.38}$$

In order to obtain $y_{lin}(k) < y_c$ and $\Delta > 1$, only y_2 is valid. Then:

$$y(k) = y_c + \kappa K_c(1 - \sqrt{\Delta}). \tag{C.39}$$

Finally,

$$y(k) = \begin{cases} y_{lin}(k) \text{ if } y_{lin}(k) \geq y_c, \\ y_c + \kappa K_c(1 - \sqrt{\Delta}) \text{ if } y_{lin}(k) < y_c. \end{cases} \tag{C.40}$$

C.2.5 *MRK* model

The equation of the model with linear stiffness, damping and mass is:

$$M\ddot{y}(t) + R\dot{y}(t) + K(y(t) - H) = -\Delta P(t). \tag{C.41}$$

With the change of variable of eq. C.20 it becomes:

$$M\ddot{\mu}(t) + R\dot{\mu}(t) + K\mu(t) = -\Delta P(t), \tag{C.42}$$

which in the Laplace domain is:

$$Mp^2\mu(p) + Rp\mu(p) + K\mu(p) = -\Delta p(p). \tag{C.43}$$

The continuous-time transfer function G(p) is:

$$G(p) = \frac{\mu(p)}{-\Delta p(p)} = \frac{\frac{1}{K}}{1 + \frac{R}{K}p + \frac{M}{K}p^2} \tag{C.44}$$

and the dicrete-time filter, obtained with the bi-linear transform, is written:

$$G(z) = \Lambda \frac{1 + z^{-1}}{1 + b_1 z^{-1} + b_2 z^{-2}}, \tag{C.45}$$

with

$$\begin{cases} \Lambda = \dfrac{1}{K + 2f_s R + 4f_s^2 M}, \\ b_1 = \dfrac{2K - 8F_s^2 M}{K + 2f_s R + 4f_s^2 M}, \\ b_2 = \dfrac{K - 2f_s R + 4f_s^2 M}{K + 2f_s R + 4f_s^2 M}, \end{cases} \tag{C.46}$$

with f_s the sampling frequency.

The equation associated to this filter is:

$$\mu(k) = \Lambda(-\Delta p(k) - 2\Delta p(k-1) - \Delta p(k-2)) - b_1\mu(k-1) - b_2\mu(k-2), \tag{C.47}$$

or written with the variable y:

$$y(k) = \Lambda(-\Delta p(k) - 2\Delta p(k-1) - \Delta p(k-2)) - b_1 y(k-1) - b_2 y(k-2) + \beta, \quad \text{(C.48)}$$

with

$$\beta = H(1 + b_1 + b_2). \quad \text{(C.49)}$$

C.2.6 MRK_{NL} model

The equation of the model with mass, damping and non-linear stiffness is:

$$M\ddot{y}(t) + R\dot{y}(t) + K(y(t) - H) = \Delta P(t) + K_c \lfloor y_c - y(t) \rfloor^2 . \quad \text{(C.50)}$$

The filter equation is the same that such of the MRK model, but the filtered signal is U :

$$y(k) = \Lambda(U(k) + 2U(k-1) + U(k-2)) - b_1 y(k-1) - b_2 y(k-2) + \beta. \quad \text{(C.51)}$$

Here, $y_{lin}(k)$ is:

$$y_{lin}(k) = \Lambda(-\Delta P(k) + 2U(k-1) + U(k-2)) - b_1 y(k-1) - b_2 y(k-2) + \beta. \quad \text{(C.52)}$$

For $y(k) \geq y_c$:

Then

$$U(k) = -\Delta P(k), \quad \text{(C.53)}$$

and

$$y(k) = y_{lin}(k). \quad \text{(C.54)}$$

For $y(k) < y_c$:

Then

$$U(k) = -\Delta P(k) + K_c(y_c - y(k))^2, \quad \text{(C.55)}$$

and

$$y(k) = \Lambda(-\Delta P(k) + K_c(y_c - y(k))^2 + 2U(k-1) + U(k-2)) - b_1 y(k-1) - b_2 y(k-2) + \beta, \quad \text{(C.56)}$$

so that:

$$\Lambda K_c y^2(k) - (1 + 2\Lambda K_c y_c) y(k) + \Lambda K_c y_c^2 + y_{lin}(k) = 0. \tag{C.57}$$

This is a quadratic equation with discriminant:

$$\Delta = 1 + 4\Lambda K_c (y_c - y_{lin}(k)) \tag{C.58}$$

and with solutions:

$$\begin{cases} y_1(k) = y_c + \Lambda K_c (1 + \sqrt{\Delta}) \\ y_2(k) = y_c + \Lambda K_c (1 - \sqrt{\Delta}) \end{cases} \tag{C.59}$$

where only y_2 is valid. Then:

$$y(k) = y_c + \Lambda K_c (1 - \sqrt{\Delta}). \tag{C.60}$$

Finally,

$$y(k) = \begin{cases} y_{lin}(k) \text{ if } y_{lin}(k) \geq y_c, \\ y_c + \Lambda K_c (1 - \sqrt{\Delta}) \text{ if } y_{lin}(k) < y_c. \end{cases} \tag{C.61}$$

Appendix D

Technical drawings of the plate assembly of the artificial mouth

This appendix presents the components of the plate assembly of the artificial mouth containing the control system of the artificial lip position and the set-up for an external sensor. The principle and global structure of the artificial mouth are depicted in §4.2.1.

The view of the assembly is given in Fig. D.1. The parts are numbered and listed below. Other views are shown in Fig. D.2. Three elements are installed on the plate: a system holding the mouthpiece, a system controlling the position of the artificial lip, and a system allowing for the installation of an external sensor.

The system holding the mouthpiece is composed by an adapter that connects the mouthpiece to the resonator (under the plate) without inner section discontinuity, and a clamping system that holds the base of the mouthpiece and prevents the displacement of the mouthpiece produced by the force that the lip exerts against the system. These are the parts 3 to 7.

The system controlling the artificial lip position is composed of two axial linear stages and a hollow piece holding the artificial lip. This piece can be easily removed and fitted in the same position using an additional piece that provides a reference. A cylindrical bar is added to hold the artificial lip. These are the parts 8 to 15.

The plate also contains a system designed to install a complementary sensor. This sensor can be a displacement sensor [116] or a 1/4" pressure microphone. The sensor is held perpendicular to the lays in the upper part of the mouthpiece. A linear stage controls the distance between the sensor and the mouthpiece. These are the parts 16 to 21.

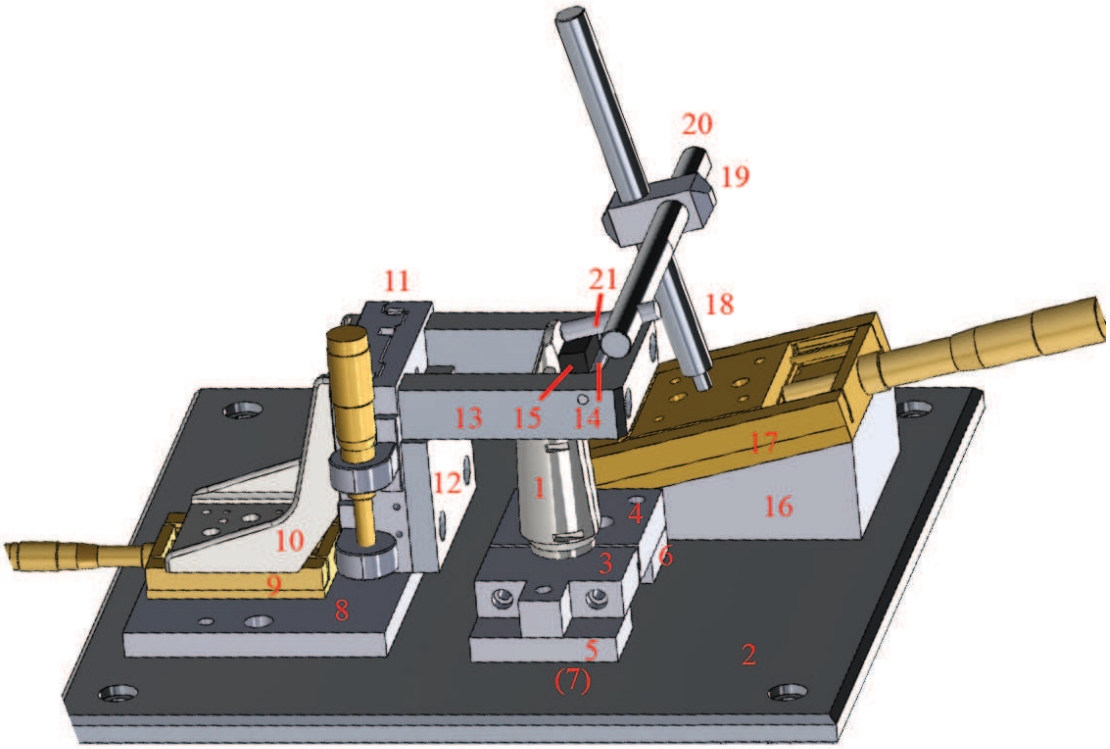

FIGURE D.1: Schematic view of the plate of the artificial mouth. The different parts are numbered. Provided by LAUM mechanical workshop.

1. Instrumented mouthpiece
2. Plate
3. Clamp for the mouthpiece base part I
4. Clamp for the mouthpiece base part II
5. Wedge I
6. Wedge II
7. Junction mouthpiece-plate-resonator
8. Support of the artificial lip system
9. Linear stage (horizontal). Double-row ball bearing linear stage, 25 mm travel, 600N load, metric, model M-UMR5.25 from Newport.
10. Mounting bracket. Outer bracket compatible with UMR5 stages, model EQ50-E from Newport.

11. Linear stage (vertical). Extended range ball bearing linear stage, 25.4 mm, M6, Model M-423 with a Vernier micrometer, 25 mm travel, 23 lb load capacity, 50.8 TPI, model SM-25 from Newport.
12. Positioning plate of the artificial lip support
13. Artificial lip support
14. Artificial teeth (cylinder with a diameter of 4 mm)
15. Artificial lip
16. Angled support
17. Linear stage. Double-row ball bearing linear stage, 51 mm, 900 N load, metric, model M-UMR8.51 from Newport.
18. Principal axis of the supplementary sensor support
19. Boss head
20. Secondary axis of the supplementary sensor support
21. Supplementary sensor

The dimensioned drawing of the plate are given in Fig. D.3. The drawings of the two clamps (parts 3 and 4) and two wedges (parts 5 and 6) are given in Fig. D.4, D.5, D.6 and D.7, respectively. For the system controlling the artificial lip position, a linear stage controls the horizontal position (part 9), and other linear stage controls the vertical position (part 11). Both stages are held with a mounting bracket (part 10). The dimensioned drawings of the junction between the mouthpiece, the plate and the resonator (part 7) are given in Fig. D.8. The drawings of the support of the artificial lip system (part 8), the positioning plate of the artificial lip support (part 12) and the artificial lip support (part 13) are in Fig. D.9, D.10 and D.11, respectively. The artificial teeth are a cylindrical bar of 4mm diameter. The artificial lip is glued to this bar in centered position using cyanoacrylate adhesive. For the system designed to install the complementary sensor, the dimensioned drawings of the angled support (part 16), the principal and secondary axes of the support (parts 18 and 20) are given in Fig. D.12, D.13 and D.14, respectively. A linear stage (part 17) controls the perpendicular distance from the sensor to the reed.

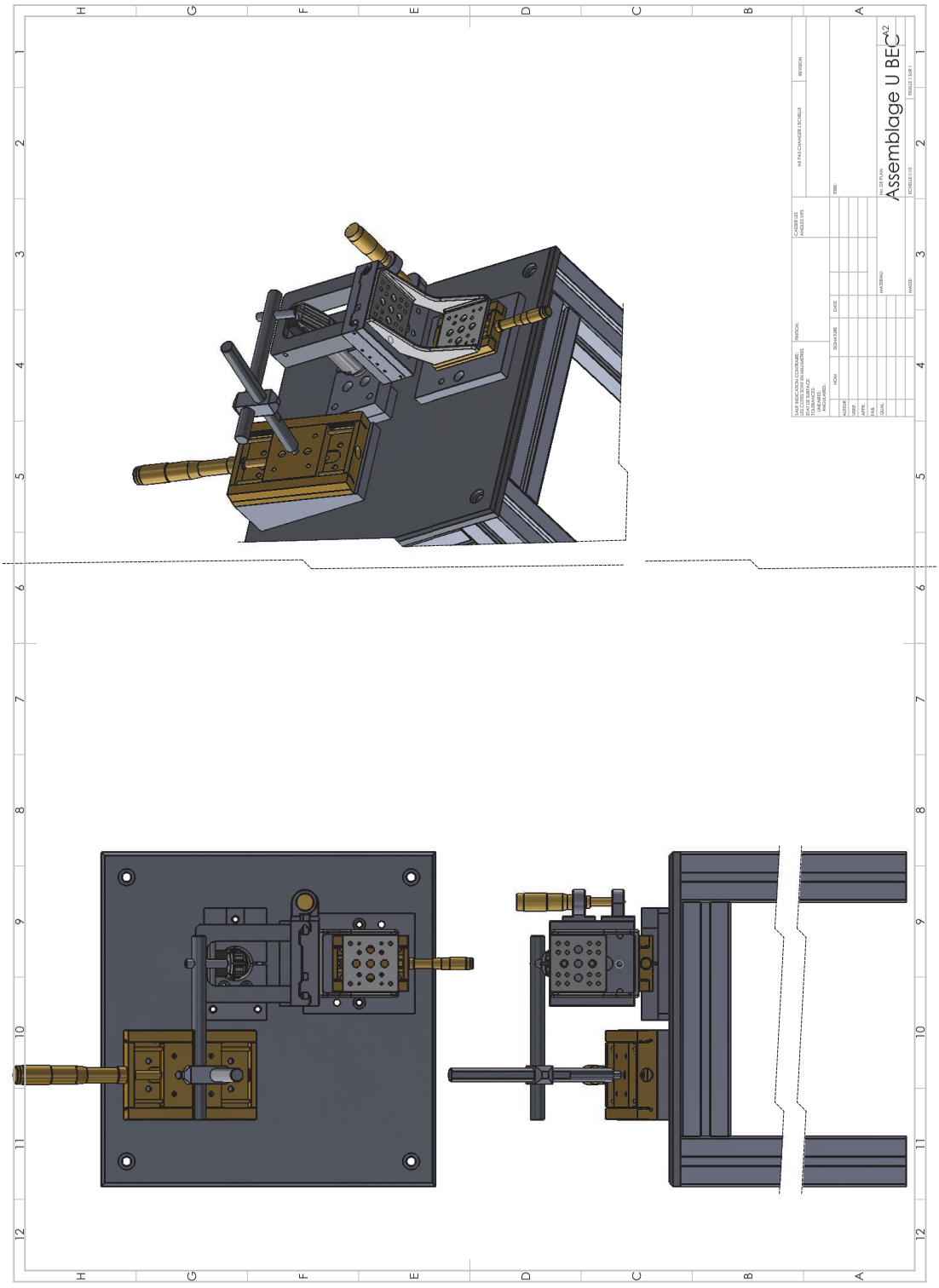

FIGURE D.2: Schematic view of the plate of the artificial mouth. Provided by LAUM mechanical workshop.

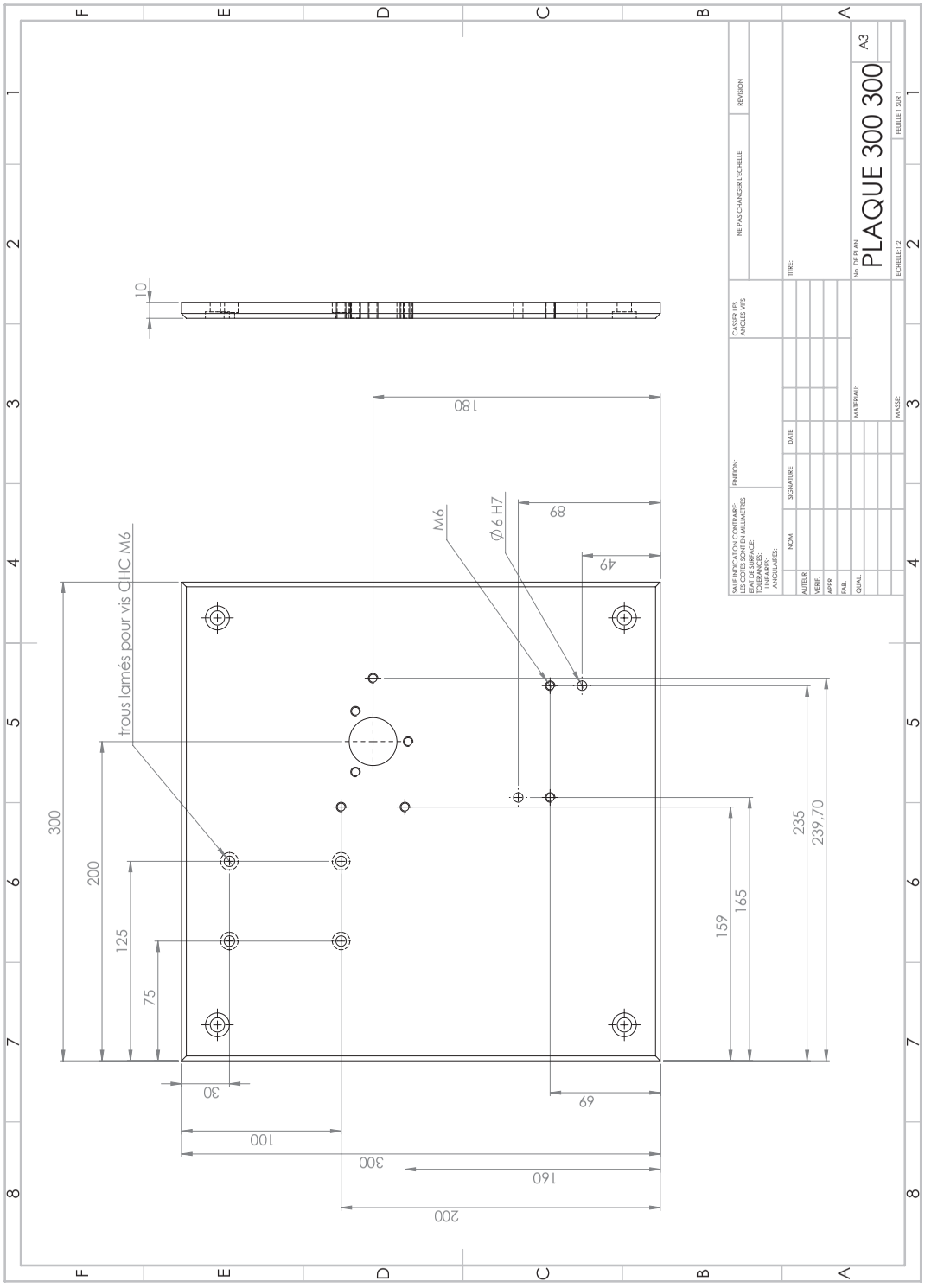

FIGURE D.3: Dimensioned drawing of the plate (2). Provided by LAUM mechanical workshop.

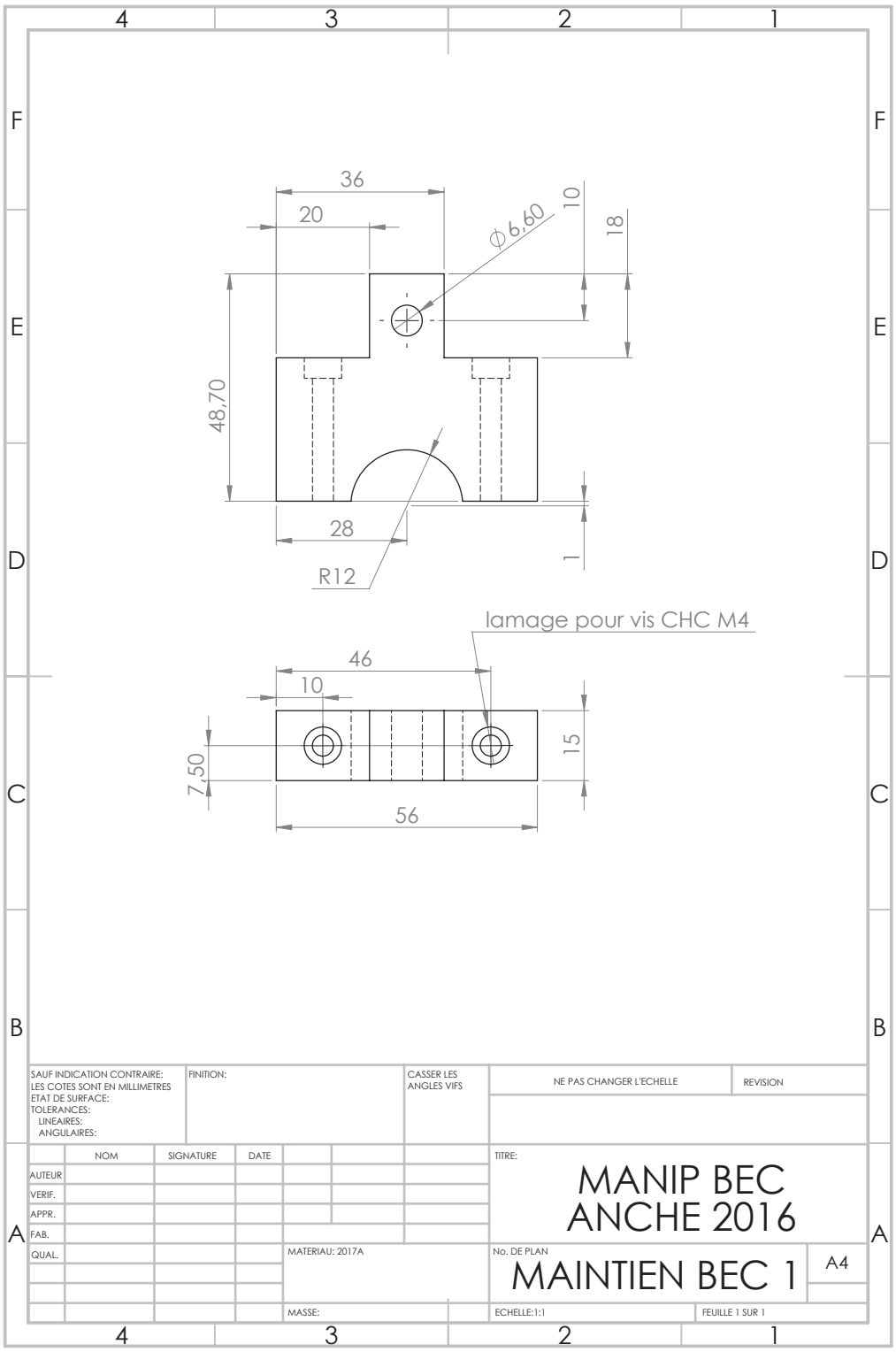

FIGURE D.4: Dimensioned drawing of the clamp of the mouthpiece I (3). Provided by LAUM mechanical workshop.

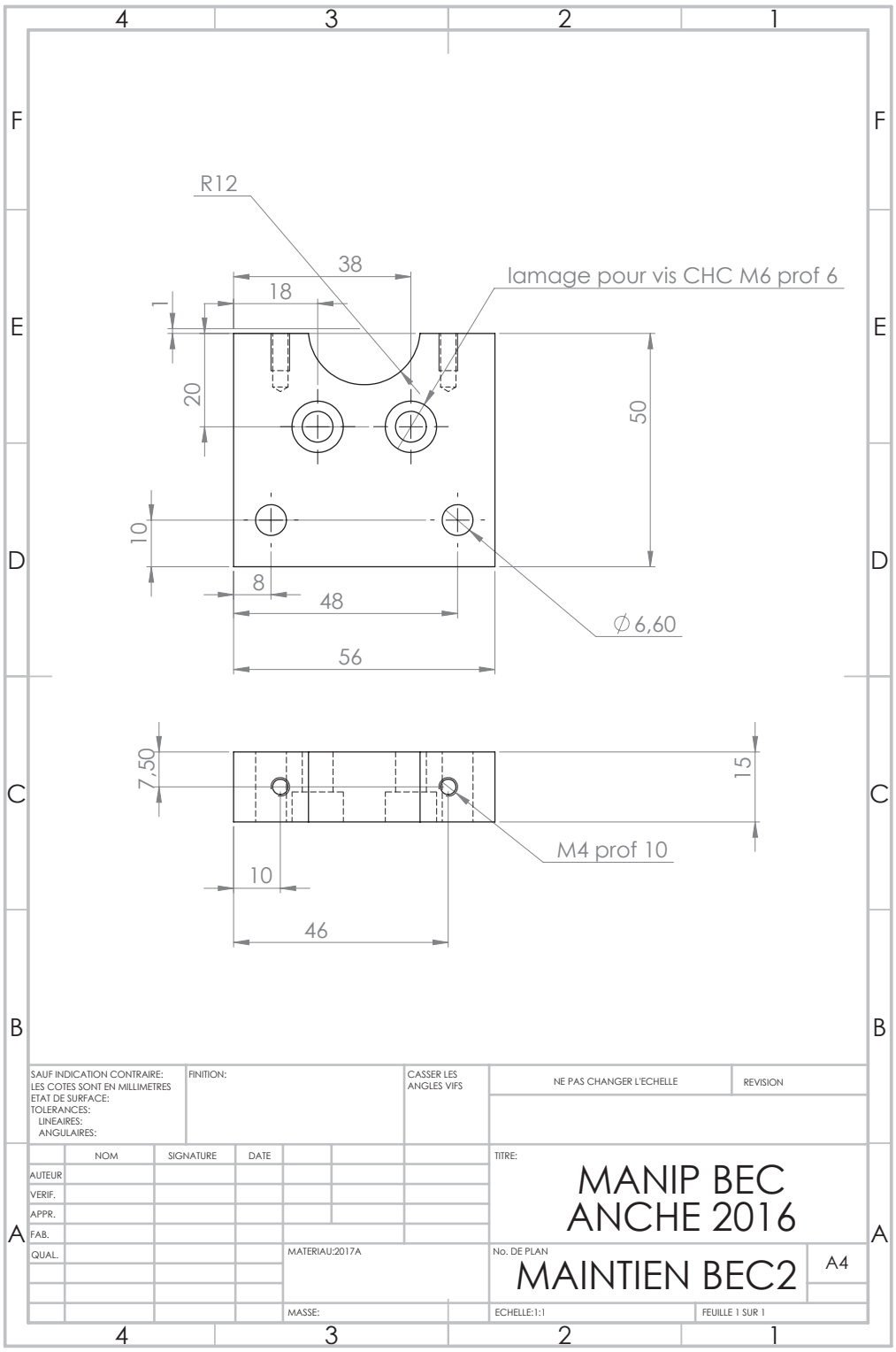

FIGURE D.5: Dimensioned drawing of the clamp of the mouthpiece II (4). Provided by LAUM mechanical workshop.

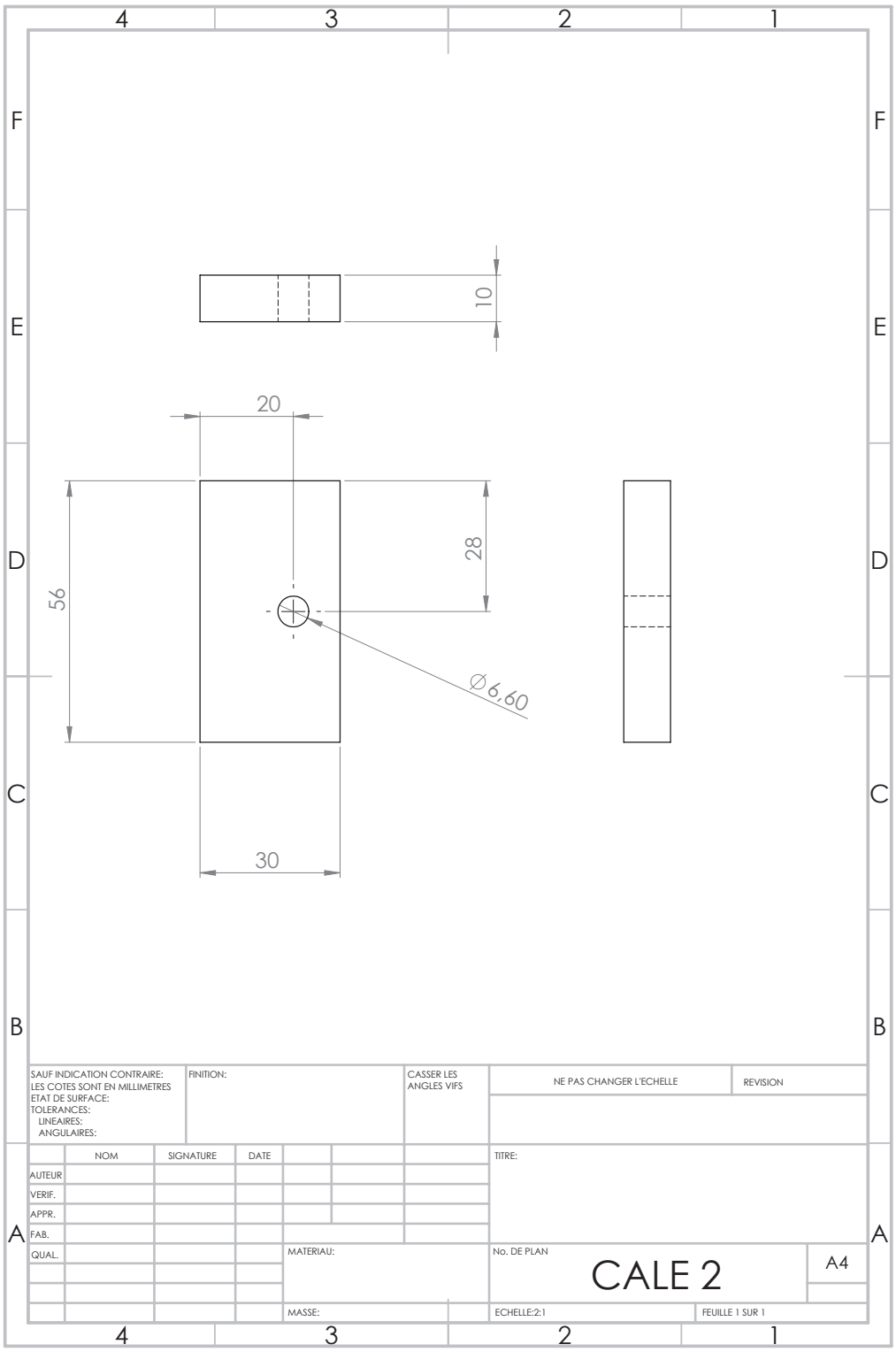

FIGURE D.6: Dimensioned drawing of the wedge I (5). Provided by LAUM mechanical workshop.

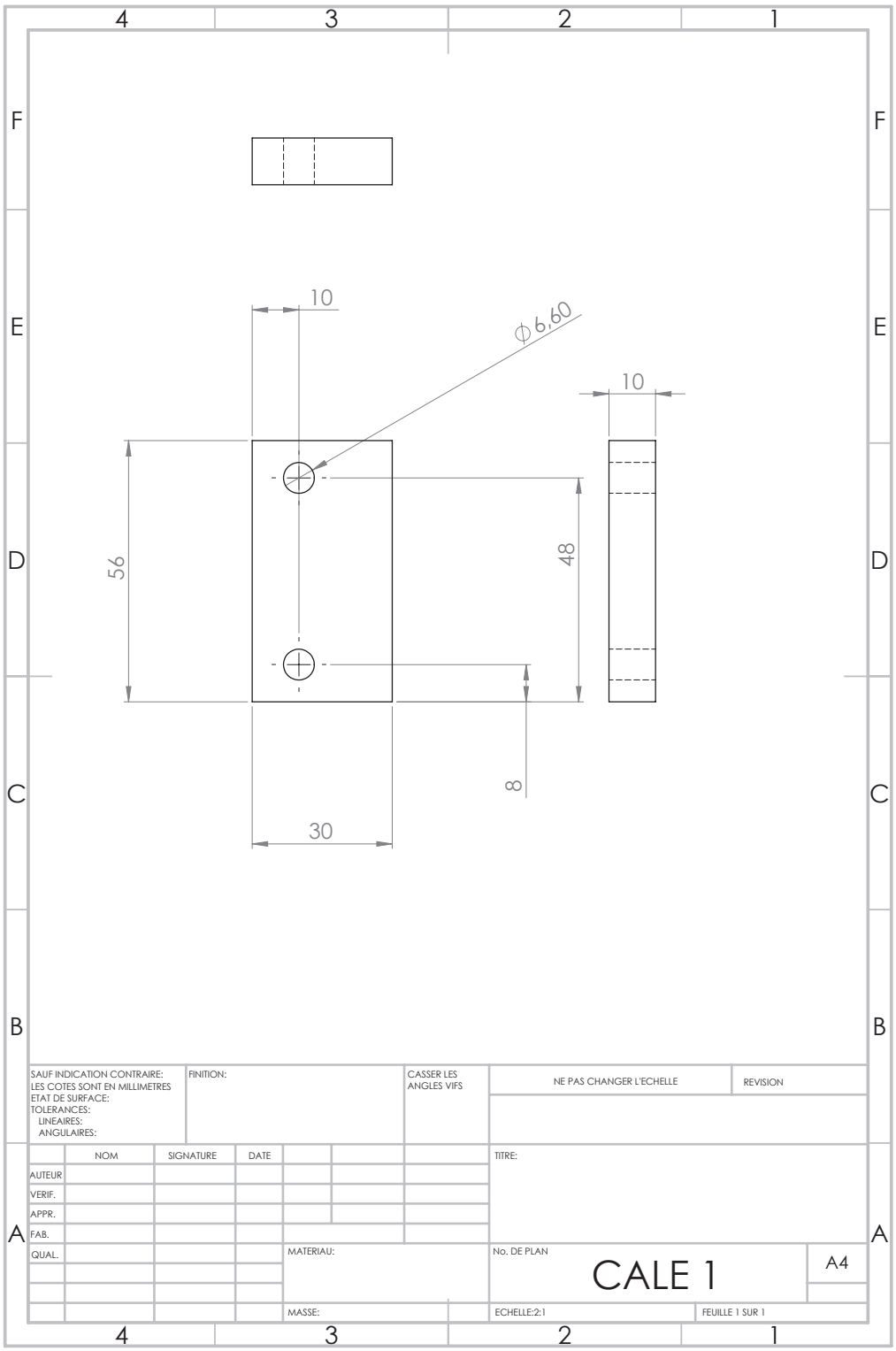

FIGURE D.7: Dimensioned drawing of the wedge II (6). Provided by LAUM mechanical workshop.

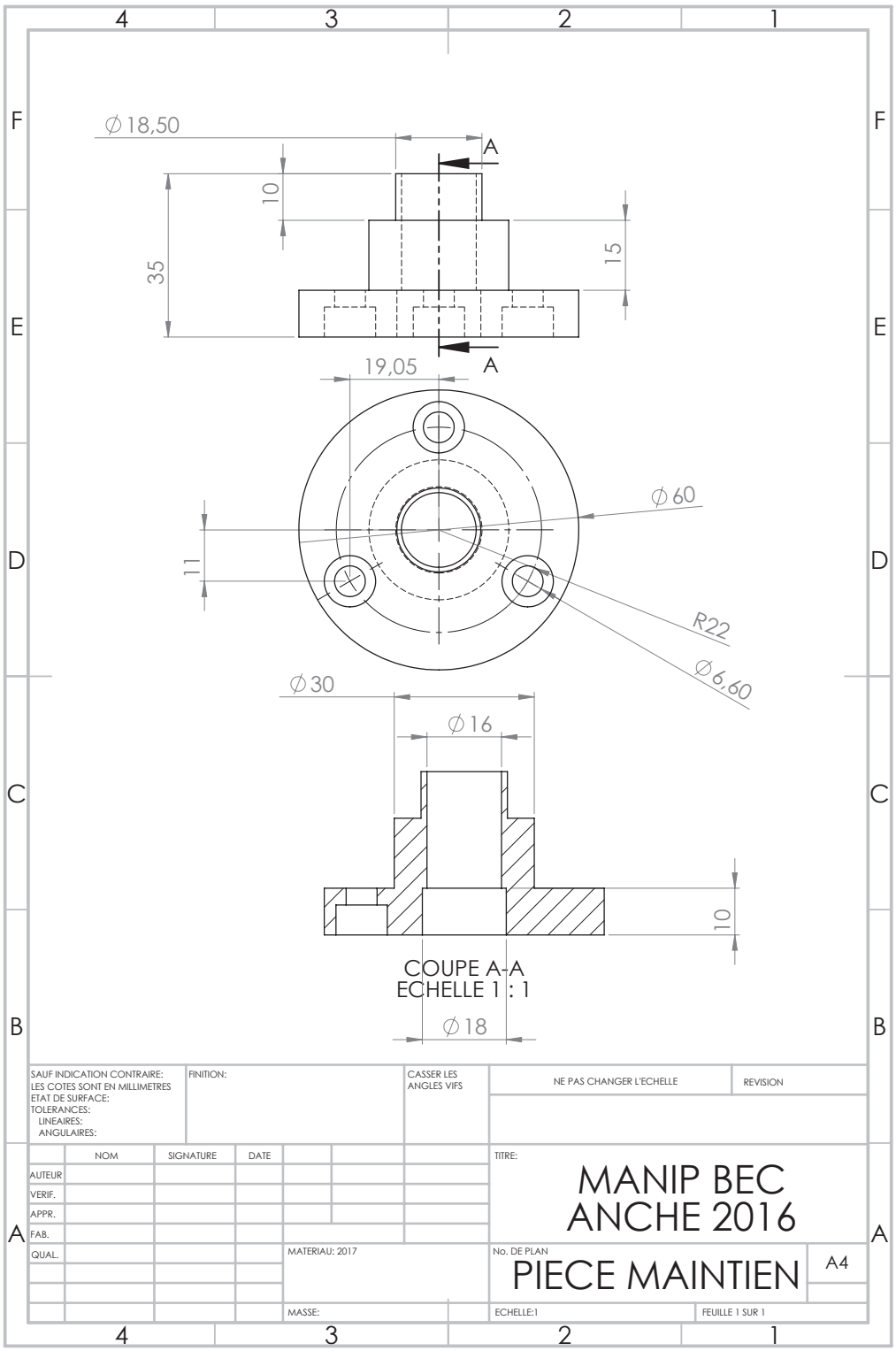

FIGURE D.8: Dimensioned drawing of the junction mouthpiece-plate-resonator (7). Provided by LAUM mechanical workshop.

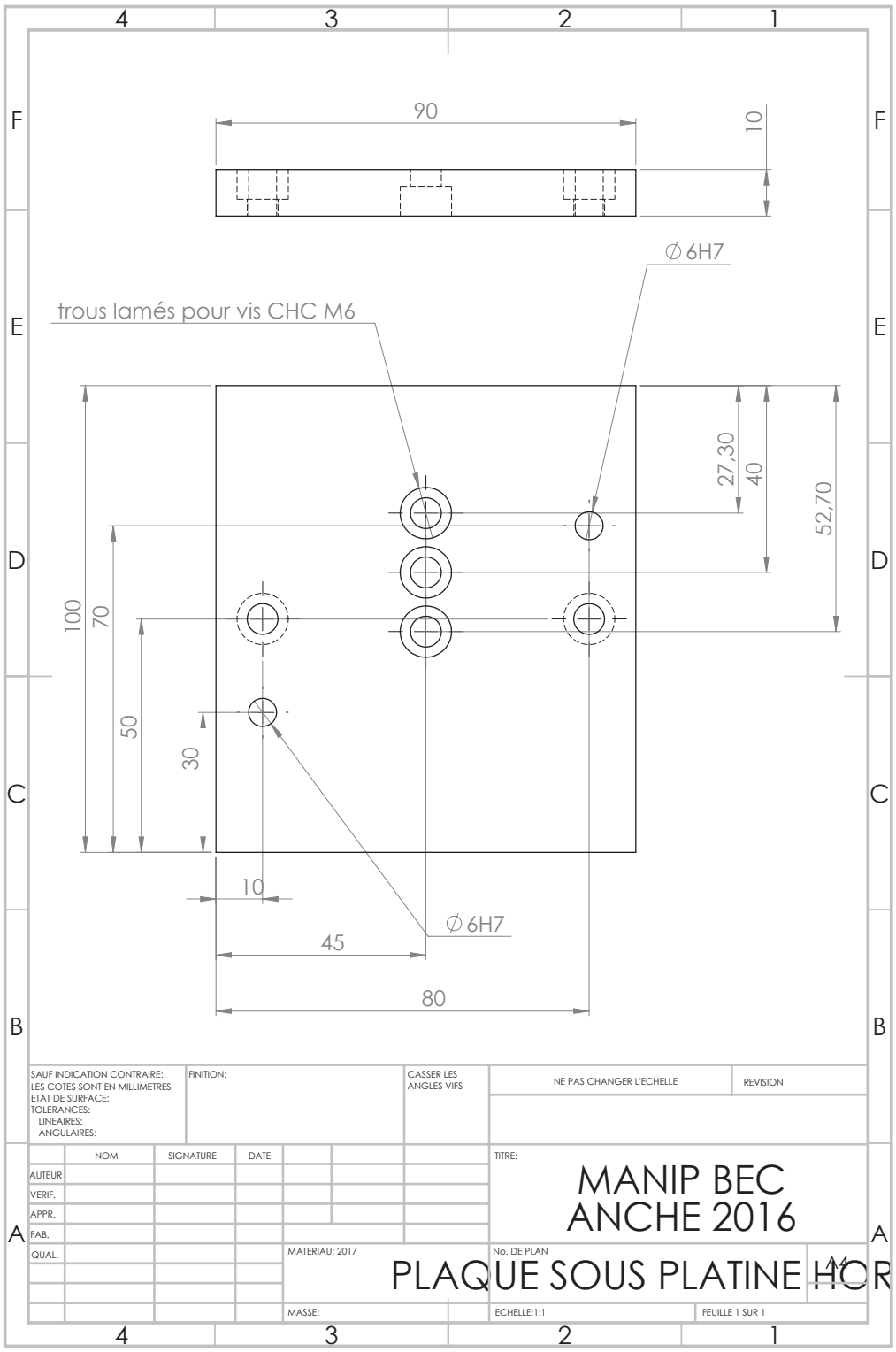

FIGURE D.9: Dimensioned drawing of the support of the artificial lip system (8). Provided by LAUM mechanical workshop.

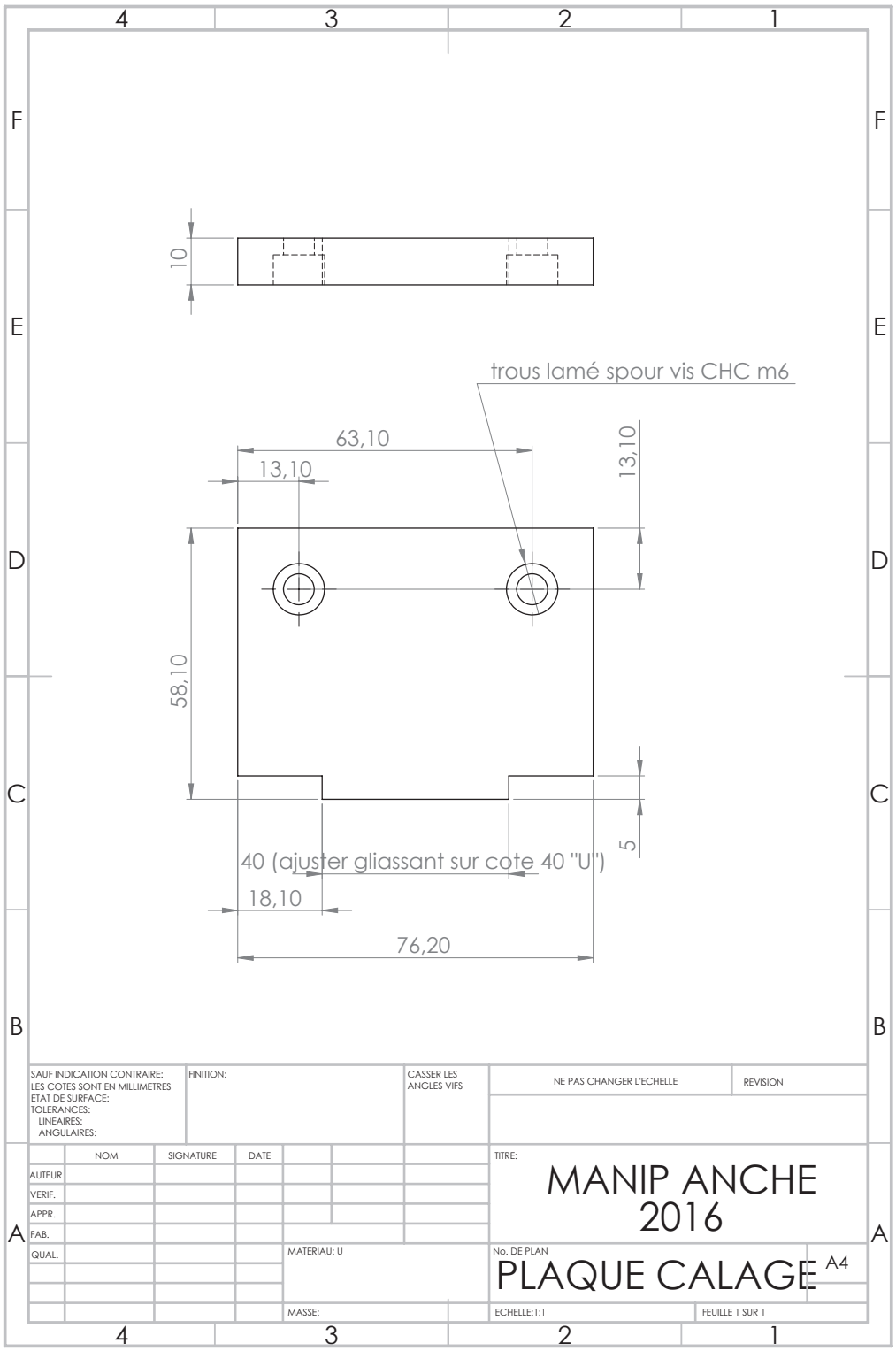

FIGURE D.10: Dimensioned drawing of the positioning plate of the artificial lip support (12). Provided by LAUM mechanical workshop.

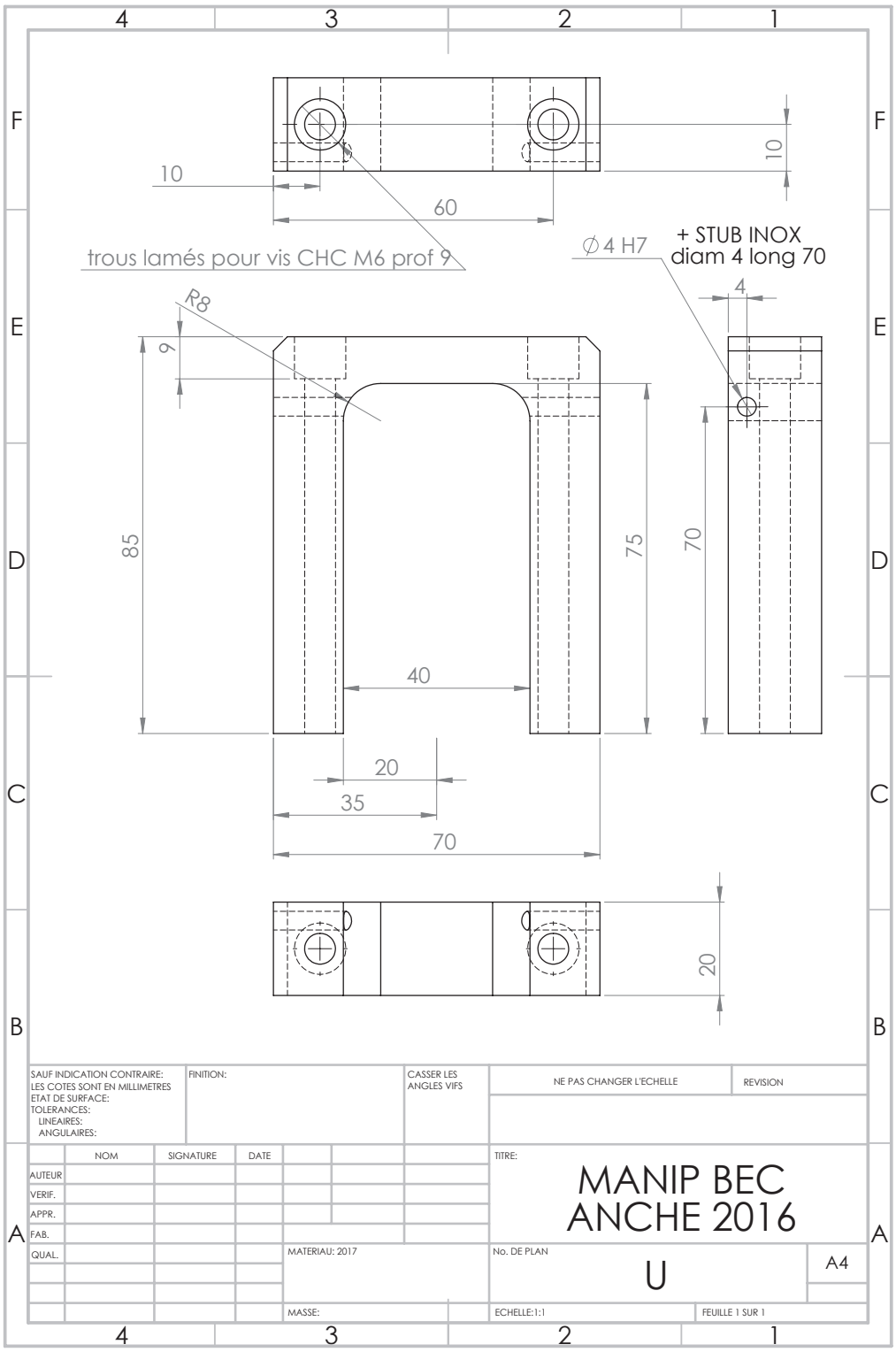

FIGURE D.11: Dimensioned drawing of the artificial lip support (13). Provided by LAUM mechanical workshop.

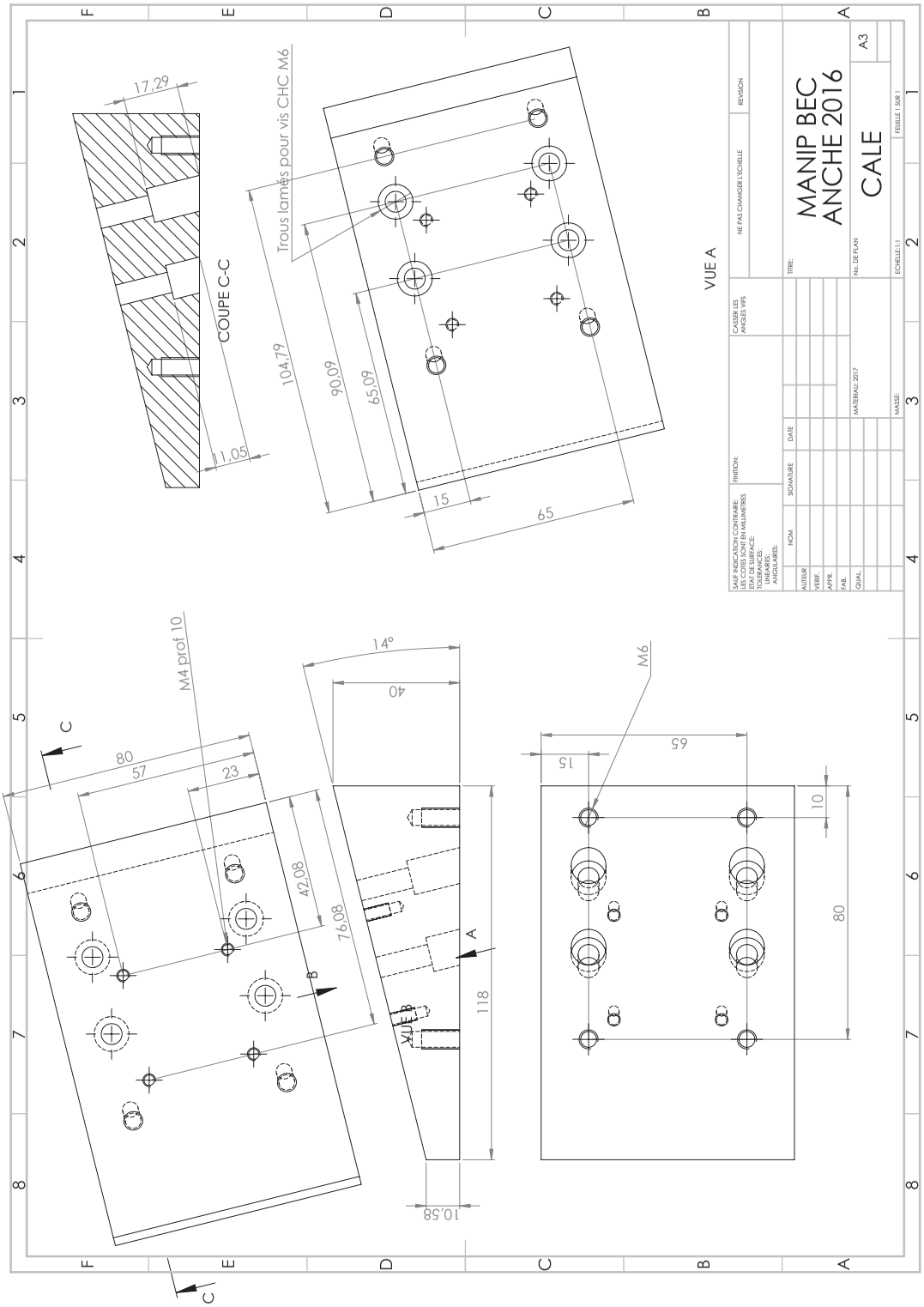

FIGURE D.12: Dimensioned drawing of the angled support (16). Provided by LAUM mechanical workshop.

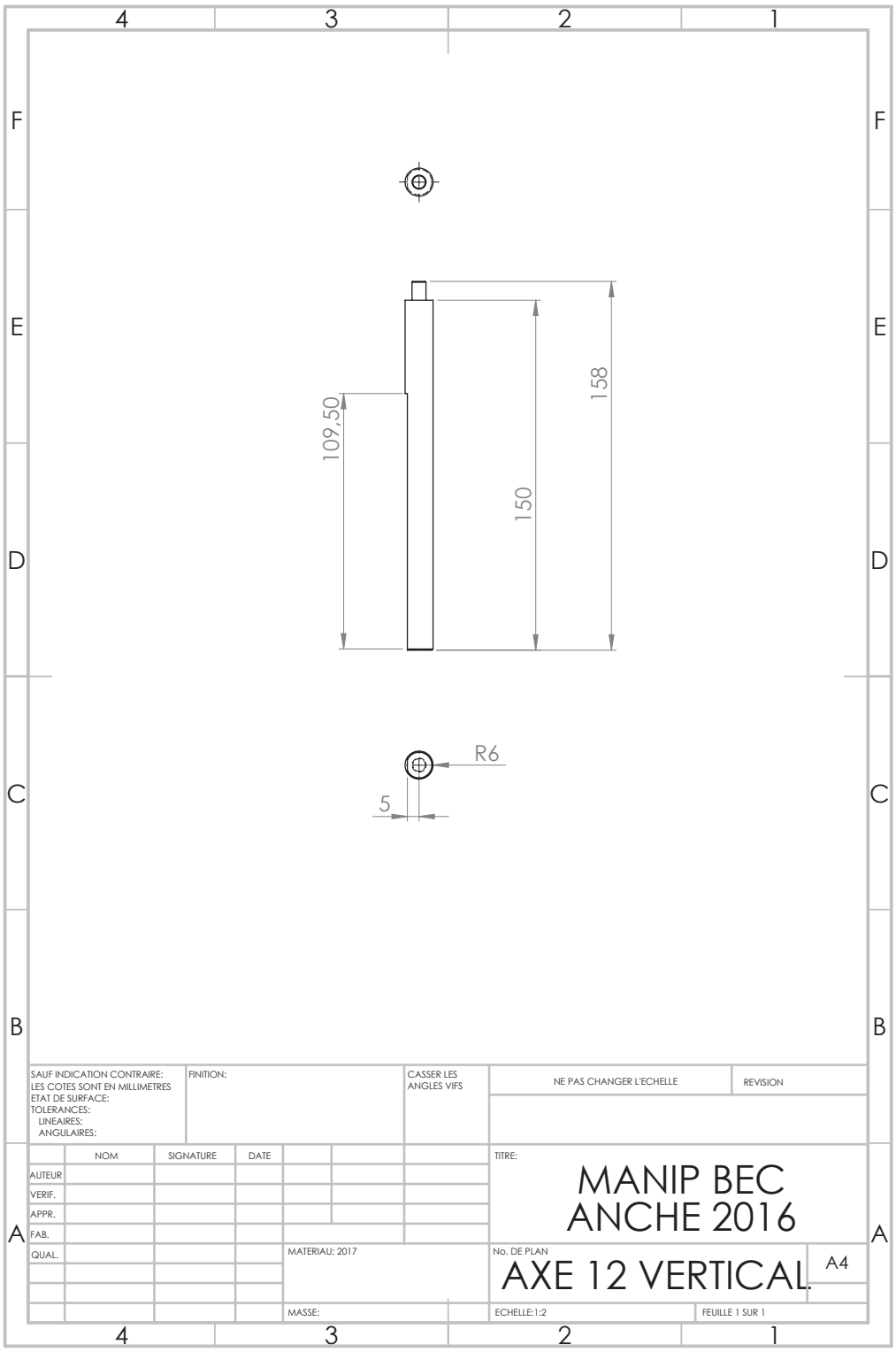

FIGURE D.13: Dimensioned drawing of the principal axis of the supplementary sensor support (18). Provided by LAUM mechanical workshop.

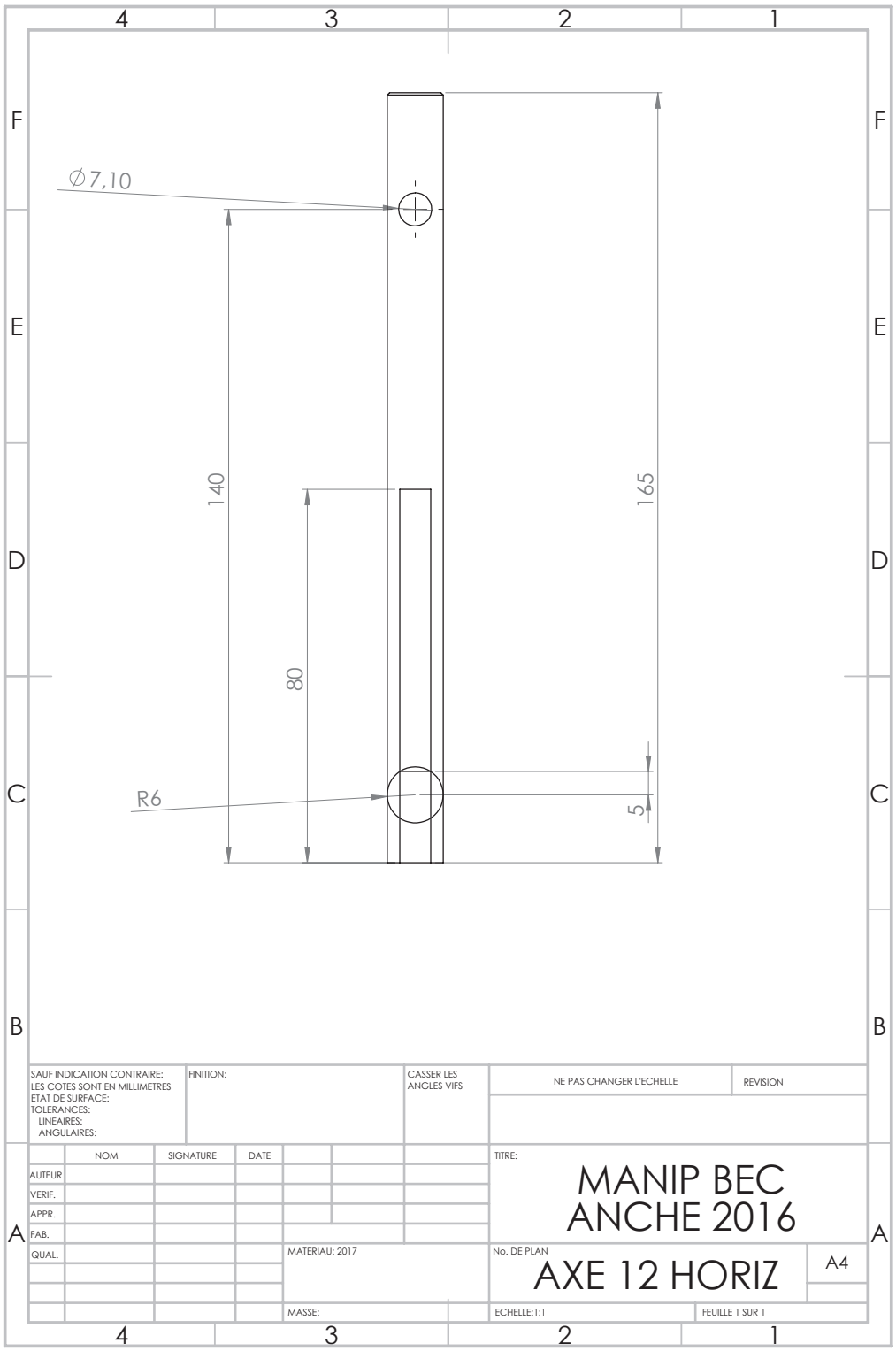

FIGURE D.14: Dimensioned drawing of the secondary axis of the supplementary sensor support (20). Provided by LAUM mechanical workshop.

Bibliography

[1] André Almeida, Christophe Vergez, and René Caussé. Quasistatic nonlinear characteristics of double-reed instruments. *The Journal of the Acoustical Society of America*, 121(1):536–546, 2007.

[2] Jean-François Petiot, Pierric Kersaudy, Gary Scavone, Stephen McAdams, and Bruno Gazengel. Modeling of the subjective quality of saxophone reeds. In *Proceedings of Meetings on Acoustics*, volume 19, page 035028. Acoustical Society of America, 2013.

[3] Alberto Muñoz Arancón, Bruno Gazengel, Jean-Pierre Dalmont, and Ewen Conan. Estimation of saxophone reed parameters during playing. *The Journal of the Acoustical Society of America*, 139(5):2754–2765, 2016. doi: http://dx.doi.org/10.1121/1.4948774. URL http://scitation.aip.org/content/asa/journal/jasa/139/5/10.1121/1.4948774.

[4] Robert E Perdue. Arundo donax, source of musical reeds and industrial cellulose. *Economic Botany*, 12(4):368–404, 1958.

[5] H-Ch Spatz, H Beismann, F Brüchert, A Emanns, and Th Speck. Biomechanics of the giant reed Arundo donax. *Philosophical Transactions of the Royal Society of London B: Biological Sciences*, 352(1349):1–10, 1997.

[6] Randall Stewart Paul. *A study and comparison of four prominent clarinet reed-making methods.* PhD thesis, University of Oklahoma, 2001.

[7] Timothy Nunnink. *A comparison of the techniques used for adjusting the single reed on the saxophone.* PhD thesis, San Diego State University, 2006.

[8] Zachary Blais. *Effects of time on the sound quality of cane oboe reeds.* PhD thesis, Worcester Polytechnic Institute, 2011.

[9] Lawrence J Intravaia and Robert S Resnick. A research study of a technique for adjusting clarinet reeds. *Journal of Research in music Education*, 16(1):45–58, 1968.

[10] Antoine Chaigne, Jean Kergomard, et al. *Acoustique des instruments de musique*. Belin, 2008.

[11] Neville H Fletcher and Thomas Rossing. *The Physics of musical instruments*. Springer Science & Business Media, 2012.

[12] SC Thompson. The effect of the reed resonance on woodwind tone production. *The Journal of the Acoustical Society of America*, 66(5):1299–1307, 1979. URL http://scitation.aip.org/content/asa/journal/jasa/66/5/10.1121/1.383448.

[13] NH Fletcher. Nonlinear theory of musical wind instruments. *Applied Acoustics*, 30(2):85–115, 1990.

[14] Sandra Carral Robles León. *Relationship between the physical parameters of musical wind instruments and the psychoacoustic attributes of the produced sound*. PhD thesis, University of Edinburgh, 2006.

[15] Avraham Hirschberg, J Gilbert, APJ Wijnands, and AJM Houtsma. Non-linear behaviour of single-reed woodwind musical instrumentx. *Journaal-Nederlands Akoestisch Genootschap*, 107:31, 1991.

[16] Jean-Pierre Dalmont, Joël Gilbert, and Sébastien Ollivier. Nonlinear characteristics of single-reed instruments: Quasistatic volume flow and reed opening measurements. *The Journal of the Acoustical Society of America*, 114(4):2253, 2003. ISSN 00014966. doi: 10.1121/1.1603235. URL http://link.aip.org/link/JASMAN/v114/i4/p2253/s1&Agg=doi.

[17] Jean-Pierre Dalmont, Joel Gilbert, Jean Kergomard, and Sebastien Ollivier. An analytical prediction of the oscillation and extinction thresholds of a clarinet. *The Journal of the Acoustical Society of America*, 118(5):3294–3305, 2005.

[18] Antoine Chaigne and Jean Kergomard. *Acoustics of musical instruments*, volume 844. Springer, 2016.

[19] A Hirschberg. *Mechanics of musical instruments; Ed. by A. Hirschberg ea*. Springer Wien, 1995.

[20] Vasileios Chatziioannou and Maarten van Walstijn. Estimation of clarinet reed parameters by inverse modelling. *Acta Acustica united with Acustica*, 98(4):629–639, 2012.

[21] Eric Ducasse. A physical model of a single–reed wind instrument, including actions of the player. *Computer Music Journal*, 27(1):59–70, 2003.

[22] Theodore A Wilson and Gordon S Beavers. Operating modes of the clarinet. *The Journal of the Acoustical Society of America*, 56(2):653–658, 1974.

[23] Vasileios Chatziioannou and Alex Hofmann. Physics-based analysis of articulatory player actions in single-reed woodwind instruments. *Acta Acustica united with Acustica*, 101(2):292–299, 2015.

[24] Lawrence E Kinsler, Austin R Frey, Alan B Coppens, and James V Sanders. *Fundamentals of Acoustics, 4th Edition, ISBN 0-471-84789-5*. Wiley-VCH, 1999.

[25] Stephen E Stewart and William J Strong. Functional model of a simplified clarinet. *The Journal of the Acoustical Society of America*, 68(1):109–120, 1980.

[26] Scott D Sommerfeldt and William J Strong. Simulation of a player–clarinet system. *The Journal of the Acoustical Society of America*, 83(5):1908–1918, 1988.

[27] Andrey Ricardo da Silva, Gary P Scavone, and Maarten van Walstijn. Numerical simulations of fluid-structure interactions in single-reed mouthpieces. *The Journal of the Acoustical Society of America*, 122(3):1798–1809, 2007.

[28] Federico Avanzini and Maarten van Walstijn. Modelling the mechanical response of the reed-mouthpiece-lip system of a clarinet. Part I: A one-dimensional distributed model. *Acta Acustica united with Acustica*, 90(3):537–547, 2004.

[29] Eric Ducasse. *Modélisation et simulation dans le domaine temporel d'instruments à vent à anche simple en situation de jeu: méthodes et modèles*. PhD thesis, Le Mans, 2001.

[30] Vasileios Chatziioannou and Maarten van Walstijn. Reed vibration modelling for woodwind instruments using a two-dimensional finite difference method approach. In *International Symposium on Musical Acoustics*, 2007.

[31] Matteo L Facchinetti, Xavier Boutillon, and Andrei Constantinescu. Numerical and experimental modal analysis of the reed and pipe of a clarinet. *The Journal of the Acoustical Society of America*, 113(5):2874–2883, 2003. ISSN 00014966. doi: 10.1121/1.1560212. URL http://scitation.aip.org/content/asa/journal/jasa/113/5/10.1121/1.1560212.

[32] T Guimezanes. *Etude expérimentale et numérique de l'anche de clarinette*. PhD thesis, Thèse de doctorat, Université du Maine, 2008.

[33] Donald Jay Casadonte. *The Clarinet Reed: an introduction to its biology, chemistry, and physics*. PhD thesis, The Ohio State University, 1995.

[34] Manuel Gangl, Alex Hofmann, and Alexander Mayer. Comparison of characterization methods for b-flat clarinet reeds. In *7th AAAA Congress on Sound and Vibration, Ljubljana, Slovenia*, 2016.

[35] Fabrice Pinard, Benoit Laine, and Holger Vach. Musical quality assessment of clarinet reeds using optical holography. *The Journal of the Acoustical Society of America*, 113:1736, 2003.

[36] Pierre-André Taillard, Franck Laloë, Michel Gross, Jean-Pierre Dalmont, and Jean Kergomard. Statistical Estimation of Mechanical Parameters of Clarinet Reeds Using Experimental and Numerical Approaches. *Acta Acustica united with Acustica*, 100(3):555–573, May 2014. ISSN 16101928. doi: 10.3813/AAA.918735. URL http://openurl.ingenta.com/content/xref?genre=article&issn=1610-1928&volume=100&issue=3&spage=555.

[37] Karl A Stetson. Study of clarinet reeds using digital holography. *Optical Engineering*, 53(11):112305–112305, 2014.

[38] Pascal Picart, Julien Leval, Francis Piquet, Jean P Boileau, Thomas Guimezanes, and Jean-Pierre Dalmont. Tracking high amplitude auto-oscillations with digital fresnel holograms. *Optics express*, 15(13):8263–8274, 2007.

[39] P Picart, J Leval, F Piquet, JP Boileau, T Guimezanes, and JP Dalmont. Study of the mechanical behaviour of a clarinet reed under forced and auto-oscillations with digital fresnel holography. *Strain*, 46(1):89–100, 2010.

[40] Subhas Chandra Mukhopadhyay, Gourab Sen Gupta, Jonathan D Woolley, and Serge N Demidenko. Saxophone reed inspection employing planar electromagnetic sensors. *Instrumentation and Measurement, IEEE Transactions on*, 56(6):2492–2503, 2007.

[41] M.S.W. Veselack. *Comparison of cell and tissue differences in good and unusable clarinet reeds*. PhD thesis, Ball State University, 1979.

[42] Peter Kolesik, Alan Mills, and Margaret Sedgley. Anatomical characteristics affecting the musical performance of clarinet reeds made from Arundo donax L.(Gramineae). *Annals of Botany*, 81(1):151–155, 1998.

[43] Stefan Glave, Jan Pallon, Chris Bornman, Lars Olof Björn, Rita Wallén, Jacob Råstam, Per Kristiansson, Mikael Elfman, and Klas Malmqvist. Quality indicators for woodwind reed material. *Nuclear Instruments and Methods in Physics Research Section B: Beam Interactions with Materials and Atoms*, 150(1):673–678, 1999.

[44] Masahiro Kawasaki, Tadashi Nobuchi, Yuta Nakafushi, Masateru Nose, Masateru Shibata, Peng Li, and Makoto Shiojiri. Structural observations and biomechanical measurements of clarinet reeds made from Arundo donax. *Microscopy Research and Technique*, 2017.

[45] Connor Kemp and Gary Scavone. Microstructure contributions to vibrational damping and identification of damage mechanisms in Arundo donax L: reed cane for woodwind instruments. *MRS Advances*, pages 1–20, 2017.

[46] Arthur E Lord Jr. Viscoelasticity of the giant reed material Arundo donax. *Wood Science and Technology*, 37(3-4):177–188, 2003.

[47] E Marandas, V Gibiat, Ch Besnainou, and N Grand. Caractérisation mécanique des anches simples d'instruments à vent. *Le Journal de Physique IV*, 4(C5):C5–633, 1994.

[48] E. Obataya and M. Norimoto. Acoustic properties of a reed (Arundo donax L.) used for the vibrating plate of a clarinet, 1999. ISSN 00014966.

[49] Hikaru Akahoshi and Eiichi Obataya. Effects of wet–dry cycling on the mechanical properties of Arundo donax l. used for the vibrating reed in woodwind instruments. *Wood Science and Technology*, 49(6):1171–1183, 2015.

[50] Bruno Gazengel, Jean Pierre Dalmont, and Jean-François Petiot. Link between objective and subjective characterizations of Bb clarinet reeds. *Applied Acoustics*, 106:155–166, 2016.

[51] Xavier Boutillon and Vincent Gibiat. Application expérimentale du bilan de puissance réactive à la mesure de l'anche de saxophone. *Le Journal de Physique IV*, 4 (C5):C5–665, 1994.

[52] Cheng-i Wang, Tamara Smyth, and Zachary C Lipton. Estimation of saxophone control parameters by convex optimization. In *CIM14, Conference on Interdisciplinary Musicology: proceedings. Conference on Interdisciplinary Musicology (9th: 2014: Berlin, Germany)*, volume 2014, page 280. NIH Public Access, 2014.

[53] Weicong Li, André Almeida, John Smith, and Joe Wolfe. How clarinettists articulate: The effect of blowing pressure and tonguing on initial and final transients. *The Journal of the Acoustical Society of America*, 139(2):825–838, 2016.

[54] Weicong Li, André Almeida, John Smith, and Joe Wolfe. The effect of blowing pressure, lip force and tonguing on transients: A study using a clarinet-playing machine. *The Journal of the Acoustical Society of America*, 140(2):1089–1100, 2016.

[55] Jer Ming Chen, John Smith, and Joe Wolfe. Experienced saxophonists learn to tune their vocal tracts. *Science*, 319(5864):776–776, 2008.

[56] Gary P Scavone, Antoine Lefebvre, and Andrey R da Silva. Measurement of vocal-tract influence during saxophone performance. *The Journal of the Acoustical Society of America*, 123(4):2391–2400, 2008.

[57] Claudia Fritz. La clarinette et le clarinettiste: Influence du conduit vocal sur la production du son. *These de Doctorat, Université Paris*, 6, 2004.

[58] Jer-Ming Chen, John Smith, and Joe Wolfe. How to play the first bar of rhapsody in blue. *J. Acoust. Soc. Am*, 123(3123.10):1121, 2008.

[59] Joe Wolfe, Maëva Garnier, and John Smith. Vocal tract resonances in speech, singing, and playing musical instruments. *HFSP journal*, 3(1):6–23, 2009.

[60] John M Grey. Multidimensional perceptual scaling of musical timbres. *The Journal of the Acoustical Society of America*, 61(5):1270–1277, 1977.

[61] RL Pratt and PE Doak. A subjective rating scale for timbre. *Journal of Sound and Vibration*, 45(3):317–328, 1976.

[62] Alastair C Disley, David M Howard, and Andy D Hunt. Timbral description of musical instruments. In *International Conference on Music Perception and Cognition*, pages 61–68, 2006.

[63] Asterios Zacharakis, Konstantinos Pastiadis, Joshua D Reiss, and George Papadelis. Analysis of musical timbre semantics through metric and non-metric data reduction techniques. In *Proceedings of the 12th International Conference on Music Perception and Cognition (ICMPC12) and the 8th Triennial Conference of the European Society for the Cognitive Sciences of Music (ESCOM 08)*, pages 1177–1182, 2012.

[64] Gottfried von Bismarck. Timbre of steady sounds: A factorial investigation of its verbal attributes. *Acta Acustica united with Acustica*, 30(3):146–159, 1974.

[65] Gottfried von Bismarck. Sharpness as an attribute of the timbre of steady sounds. *Acta Acustica united with Acustica*, 30(3):159–172, 1974.

[66] C Fritz and D Dubois. Perceptual evaluation of musical instruments: State of the art and methodology. *Acta Acustica united with Acustica*, 101(2):369–381, 2015.

[67] Jean-François Petiot, Lamya Fergani, and Marie-Françoise Lucas. Analyse signal et étude perceptive de sons de trompettes. *8ème Congrès Français d'Acoustique*, 2006.

[68] Stephen McAdams, Suzanne Winsberg, Sophie Donnadieu, Geert De Soete, and Jochen Krimphoff. Perceptual scaling of synthesized musical timbres: Common dimensions, specificities, and latent subject classes. *Psychological research*, 58(3): 177–192, 1995.

[69] Mark C Gridley. Trends in description of saxophone timbre. *Perceptual and Motor Skills*, 65(1):303–311, 1987.

[70] Roger A Kendall and Edward C Carterette. Verbal attributes of simultaneous wind instrument timbres: I. von Bismarck's adjectives. *Music Perception: An Interdisciplinary Journal*, 10(4):445–467, 1993.

[71] Arne Nykänen, Örjan Johansson, Jan Lundberg, and Jan Berg. Modelling perceptual dimensions of saxophone sounds. *Acta Acustica United with Acustica*, 95 (3):539–549, 2009.

[72] Mathieu Barthet, Philippe Guillemain, Richard Kronland-Martinet, and Sølvi Ystad. From clarinet control to timbre perception. *Acta Acustica united with Acustica*, 96(4):678–689, 2010.

[73] Mathieu Barthet, Philippe Depalle, Richard Kronland-Martinet, and Søølvi Ystad. Acoustical correlates of timbre and expressiveness in clarinet performance. *Music Perception: An Interdisciplinary Journal*, 28(2):135–154, 2010.

[74] CS McGinnis and C Gallagher. The mode of vibration of a clarinet reed. *The Journal of the Acoustical Society of America*, 12(4):529–531, 1941.

[75] John Backus. Vibrations of the reed and the air column in the clarinet. *The Journal of the Acoustical Society of America*, 93(May), 1961. URL http://scitation.aip.org/content/asa/journal/jasa/33/6/10.1121/1.1908803.

[76] Niels Bak and P Dømler. The relation between blowing pressure and blowing frequency in clarinet playing. *Acta Acustica united with Acustica*, 63(3):238–241, 1987.

[77] J Van Zon, A Hirschberg, J Gilbert, and APJ Wijnands. Flow through the reed channel of a single reed music instrument. *Le Journal de Physique Colloques*, 51 (C2):C2–821, 1990.

[78] Joël Gilbert. *Etude des instruments de musique à anche simple: extension de la méthode d'équilibrage harmonique, rôle de l'inharmonicité des résonances, mesure des grandeurs d'entrée*. PhD thesis, Université du Maine, 1991.

[79] X Meynial. *Systemes micro-intervalles pour instruments a vents a trous lateraux, oscillation d'une anche simple couplee a un resonateur de forme simple*. PhD thesis, PhD thesis, LAUM, Le Mans, 1987.

[80] Bruno Gazengel. *Caractérisation objective de la qualité de justesse, de timbre et d'émission des instruments à vent à anche simple*. PhD thesis, Université du Maine, 1994.

[81] Sébastien Ollivier. *Contribution à l'étude des oscillations des instruments à vent à anche simple*. PhD thesis, Université du Maine, 2002.

[82] Maarten Van Walstijn. *Discrete-time modelling of brass and reed woodwind instruments with application to musical sound synthesis*. PhD thesis, University of Edinburgh, 2002.

[83] Tohru Idogawa, Tokihiko Kobata, Kouji Komuro, and Masakazu Iwaki. Nonlinear vibrations in the air column of a clarinet artificially blown. *The Journal of the Acoustical Society of America*, 93(1):540–551, 1993.

[84] Tokihiko Kobata and Tohru Idogawa. Pressure in the mouthpiece, reed opening, and air-flow speed at the reed opening of a clarinet artificially blown. *Journal of the Acoustical Society of Japan (E)*, 14(6):417–428, 1993.

[85] Arthur H Benade. *Fundamentals of Musical Acoustics: Second, Revised Edition*. Courier Corporation, 2012.

[86] Jean-Pierre Dalmont and Cyrille Frappe. Oscillation and extinction thresholds of the clarinet: Comparison of analytical results and experiments. *The Journal of the Acoustical Society of America*, 122(2):1173–1179, 2007.

[87] Alberto Muñoz Arancón, Bruno Gazengel, Jean Pierre Dalmont, and Guy Plantier. Comparative study of different physical models describing the reed behaviour in artifficial playing conditions. In *ISMA 2014*, 2014.

[88] Alexander Mayer. Riam (reed instrument artificial mouth) a computer controlled excitation device for reed instruments. In *Proceedings of the Stockholm Music Acoustics Conference 2003, SMAC 03*, volume 1, pages 279–282. Royal Swedish Academy of Music, 2003.

[89] Baptiste Bergeot, André Almeida, Bruno Gazengel, Christophe Vergez, and Didier Ferrand. Response of an artificially blown clarinet to different blowing pressure profiles. *The Journal of the Acoustical Society of America*, 135(1):479–490, 2014.

[90] Didier Ferrand, Christophe Vergez, Benoit Fabre, and François Blanc. High-precision regulation of a pressure controlled artificial mouth: the case of recorder-like musical instruments. *Acta Acustica united with Acustica*, 96(4):701–712, 2010.

[91] Jean-Baptiste Doc and Christophe Vergez. Oscillation regimes produced by an alto saxophone: Influence of the control parameters and the bore inharmonicity. *The Journal of the Acoustical Society of America*, 137(4):1756–1765, 2015.

[92] Didier Ferrand, Thomas Hélie, Christophe Vergez, Baptiste Véricel, and René Caussé. Bouches artificielles asservies: étude de nouveaux outils pour l'analyse du fonctionnement des instruments à vent. In *10ème Congrès Français d'Acoustique*, 2010.

[93] Daniel Noreland, Jean Kergomard, Franck Laloë, Christophe Vergez, Philippe Guillemain, and Alexis Guilloteau. The logical clarinet: numerical optimization of the geometry of woodwind instruments. *Acta Acustica united with Acustica*, 99 (4):615–628, 2013.

[94] Jorge Solis and Kia Ng. *Musical robots and interactive multimodal systems*, volume 74. Springer, 2011.

[95] Klaus Petersen, Jorge Solis, Takeshi Ninomiya, Tetsuro Yamamoto, Masaki Takeuchi, and Atsuo Takanishi. Development of the anthropomorphic saxophonist robot WAS-1: mechanical design of the lip, tonguing, fingers and air pump mechanisms. In *Robotics and Automation, 2009. ICRA'09. IEEE International Conference on*, pages 3043–3048. IEEE, 2009.

[96] André Almeida, Julie Lemare, Mark Sheahan, John Judge, Roman Auvray, Kim Son Dang, Sebastian John, Jean Geoffroy, Jay Katupitiya, P Santus, et al. Clarinet parameter cartography: automatic mapping of the sound produced as a function of blowing pressure and reed force. In *Proc. Int. Symp. Music Acoustics*, 2010.

[97] Andre Almeida, David George, John Smith, and Joe Wolfe. The clarinet: How blowing pressure, lip force, lip position and reed hardness affect pitch, sound level, and spectrum. *The Journal of the Acoustical Society of America*, 134(3):2247–2255, 2013.

[98] Weicong Li, John Smith, Joe Wolfe, and André Almeida. Tongue, lip and breath interactions in clarinet playing: a study using a playing machine. In *Proceedings of the 21st International Congress on Sound and Vibration, ICSV21, Beijing, China*, 2014.

[99] JS Cullen, Joël Gilbert, and DM Campbell. Brass instruments: linear stability analysis and experiments with an artificial mouth. *Acta Acustica united with Acustica*, 86(4):704–724, 2000.

[100] Nicolas Ruty, Annemie Van Hirtum, Xavier Pelorson, Inés Lopez-Arteaga, and Avraham Hirschberg. A mechanical experimental setup to simulate vocal folds vibrations. preliminary results. *arXiv preprint arXiv:0710.4286*, 2007.

[101] Fabrice Silva, Nicolas Hermant, Xavier Laval, and Xavier Pelorson. Techniques expérimentales pour la caractérisation mécanique de maquettes in vitro de cordes vocales. In *12eme Congres Français d'Acoustique (CFA 2014)*, pages 1553–1559, 2014.

[102] Timo Grothe. Investigation of bassoon embouchures with an artificial mouth. In *Acoustics 2012*, 2012.

[103] Alberto Muñoz Arancón, Bruno Gazengel, and Jean Pierre Dalmont. Un bec instrumenté pour le suivi du geste instrumental des saxophonistes. In *Learning and Teaching Music in the Twenty-First Century: The Contribution of Science and Technology*, 5-6-7 November 2015.

[104] A.B. N. Musical instrument reed measuring device and method for adjusting reeds, November 11 1969. URL http://www.google.com/patents/US3477133. US Patent 3,477,133.

[105] K. Hanai. Reed testing device for single-reed instrument, March 4 2014. URL http://www.google.com/patents/US8666696. US Patent 8,666,696.

[106] B. Gazengel, J.-F. Petiot, and M. Soltes. Objective and subjective characterization of saxophone reeds. In *Proceedings of Acoustics 2012*, 23-27 April 2012.

[107] Ph. Guillemain, Ch. Vergez, D. Ferrand, and A. Farcy. An instrumented saxophone mouthpiece and its use to understand how an experienced musician plays. *Acta Acustica united with Acustica*, 96(4):622–634, July 2010. ISSN 16101928. doi: 10.3813/AAA.918317. URL http://openurl.ingenta.com/content/xref?genre=article&issn=1610-1928&volume=96&issue=4&spage=622.

[108] Alberto Muñoz Arancón, Bruno Gazengel, and Jean Pierre Dalmont. *In vivo* and *in vitro* characterization of single cane reeds. In *Stockholm Music Acoustics Conference 2013*, 2013.

[109] John Backus. Small–vibration theory of the clarinet. *The Journal of the Acoustical Society of America*, 267(1952):261–267, 1963. URL http://scitation.aip.org/content/asa/journal/jasa/35/3/10.1121/1.1918458.

[110] Cornelis Johannes Nederveen. *Acoustical aspects of woodwind instruments*. Northern Illinois University Press, 1998.

[111] Fabrice Silva, Jean Kergomard, Christophe Vergez, and Joël Gilbert. Interaction of reed and acoustic resonator in clarinet–like systems. *The Journal of the Acoustical Society of America*, 124(5):3284–95, November 2008. ISSN 1520-8524. doi: 10.1121/1.2988280. URL http://scitation.aip.org/content/asa/journal/jasa/124/5/10.1121/1.2988280.

[112] E Ducasse. Modélisation d'instruments de musique pour la synthèse sonore: application aux instruments à vent. *Le Journal de Physique Colloques*, 1990. URL http://jphyscol.journaldephysique.org/articles/jphyscol/abs/1990/02/jphyscol199051C2194/jphyscol199051C2194.html.

[113] Maarten van Walstijn and Federico Avanzini. Modelling the mechanical response of the reed-mouthpiece-lip system of a clarinet. Part II: A lumped model approximation. *Acta Acustica united with Acustica*, 93(3):435–446, 2007.

[114] Stefan Bilbao. *Numerical sound synthesis: finite difference schemes and simulation in Musical Acoustics*. Wiley Publishing, 2009.

[115] Didier Ferrand, Christophe Vergez, Fabrice Silva, et al. Seuils d'oscillation de la clarinette: validité de la représentation excitateur-résonateur. *10ème Congrès Français d'Acoustique*, 2010.

[116] *Product Data Sheet. Fiberoptic Sensor - Reflectance Compensated. Model RC62*. PHILTEC, Inc, August 2013.

[117] Jean Kergomard, Philippe Guillemain, Sami Karkar, Jean-Pierre Dalmont, and Bruno Gazengel. What we understand today on formants in saxophone sounds? In *44º Congreso Español de Acústica Encuentro Ibérico de Acústica EAA European Symposium on Environmental Acoustics and Noise Mapping (TECNIACUSTICA 2013)*, pages 1209–1216, 2013.

[118] International clarinet association. URL http://www.http://clarinet.org/.

[119] Jean C de Borda. Mémoire sur les élections au scrutin. 1781.

[120] N Tormod, Per Bruun Brockhoff, Oliver Tomic, et al. *Statistics for sensory and consumer science*. John Wiley & Sons, 2011.

[121] Garmt Dijksterhuis. Assessing panel consonance. *Food Quality and Preference*, 6 (1):7–14, 1995.

[122] Leonardo Fuks and Johan Sundberg. Blowing pressures in bassoon, clarinet, oboe and saxophone. *Acta Acustica united with Acustica*, 85(2):267–277, 1999.

[123] Whitney L Coyle, Philippe Guillemain, Jean Kergomard, and Jean-Pierre Dalmont. Predicting playing frequencies for clarinets: A comparison between numerical simulations and simplified analytical formulas. *The Journal of the Acoustical Society of America*, 138(5):2770–2781, 2015.

[124] Pauline Eveno. *L'impédance d'entrée pour l'aide à la facture des instruments de musique à vent: mesures, modèles et lien avec les fréquences de jeu*. PhD thesis, Université Pierre et Marie Curie-Paris VI, 2012.

[125] J.P. Dalmont and J.C.Le Roux. Acoustic impedance sensor designed to measure the input acoustic impedance of a waveguide, October 1 2013. URL http://www.google.com/patents/US8544327. US Patent 8,544,327.

[126] *Datasheet : Photointerrupters SG-2BC*. Kodenshi, 2016.

[127] Morten Knudsen. Experimental modelling of dynamic systems. *Lecture notes*, 2004.

UNIVERSITE BRETAGNE LOIRE

Le Mans Université

Thèse de Doctorat

Alberto MUÑOZ ARANCÓN

New techniques for the characterisation of single reeds in playing conditions

Nouvelles techniques pour la caractérisation des anches simples en situation de jeu

Résumé

Ce travail porte sur la caractérisation d'anches simples utilisées pour la clarinette ou le saxophone. Sachant que les musiciens perçoivent des différences importantes dans la qualité des anches de caractéristiques identiques (même marque, coupe et force), cette thèse propose des nouveaux outils pour la caractérisation des anches en situation de jeu.

Un bec instrumenté utilisant des capteurs embarqués est développé de façon à mesurer le déplacement de l'anche et la différence de pression de part et d'autre de l'anche. À partir de ces signaux, il est possible d'estimer des paramètres d'anche associés à différents modèles physiques. Les résultats obtenus montrent que la complexité du modèle décrivant le comportement de l'anche doit augmenter avec la nuance de jeu. Pour des nuances moyennes, le modèle physique le plus adapté pour décrire l'anche de clarinette est un oscillateur utilisant une raideur non linéaire et un terme d'amortissement. Le modèle décrivant l'anche de saxophone prend en compte un terme d'inertie supplémentaire.

Le bec instrumenté est utilisé dans une campagne de mesures comportant 7 musiciens et 20 anches, et permet de quantifier la variabilité des résultats due aux musiciens. Des tests subjectifs sont réalisés avec ces mêmes musiciens, et montrent que les différences entre les anches se réduisent à une seule dimension (facilité de jeu ou timbre). Les corrélations entre les descripteurs subjectifs et les paramètres objectifs mesurés sont étudiées afin de mieux comprendre les différences entre les anches, permettant le développement d'un modèle prédictif de la qualité des anches. Le bec est aussi mis en œuvre pour comparer le geste d'un musicien professionnel et d'un amateur et montre sa potentielle applicabilité à la pédagogie musicale.

De façon à éviter la variabilité produite par le musicien, une bouche artificielle aspirante est développée. Elle utilise le bec instrumenté et peut être jouée par un musicien ou de façon artificielle. La comparaison des mesures réalisées dans les deux situations permet d'identifier la plage de fonctionnement optimale où la bouche artificielle imite au mieux le jeu du musicien au sens de la justesse et de la nuance. Les résultats obtenus pour cette plage optimale montrent que la bouche artificielle reproduit correctement la dynamique de l'anche sauf lorsque celle-ci est en position ouverte, les propriétés mécaniques de la lèvre artificielle étant différentes de celles de la lèvre du musicien.

Les outils et les méthodes développés ouvrent la possibilité de réaliser des mesures de l'anche en situation de jeu et de façon reproductible. Les limites expérimentales rencontrées sont discutées, en proposant plusieurs améliorations et des lignes directrices pour des recherches futures.

Mots clés

Anche simple, bec instrumenté, bouche artificielle, caractérisation des anches, tests subjectifs.

Abstract

This work deals with the characterisation of single cane reeds used for clarinet or saxophone. Musicians perceive important differences of quality between reeds of the same brand, cut and strength. This thesis proposes new tools for reed characterisation in playing conditions.

An instrumented mouthpiece is developed to enable the measurement of reed displacement and pressure difference on both sides of the reed using embedded sensors. From these signals, it is possible to estimate reed parameters of different physical models. Results reveal that the complexity of the physical model describing the reed behaviour must increase with the dynamic level. For medium level dynamics, the most relevant physical model for clarinet assumes that the reed is an oscillator with non-linear stiffness and damping. For saxophone reeds, the model includes an equivalent mass.

The instrumented mouthpiece is used in a measurement campaign involving 7 players and 20 reeds, quantifying the variability of the results due the musicians. Subjective tests conducted with these musicians show that reeds can be mainly described by one dimension (ease of playing or timbre). The correlations between the subjective descriptors and the measured objective parameters are studied to better understand the perceived differences between reeds, developing a predictive model of reed quality. The mouthpiece is also applied to the comparison between an experienced player and a beginner, showing its potential applicability to music pedagogy.

In order to avoid the variability of the musician, an aspirating artificial mouth is developed. It uses the instrumented mouthpiece and it can be played by a musician or artificially. The comparison of the measurements made in both cases allows for the identification of the optimal working range in which the artificial mouth best reproduces the musician's playing according to intonation and playing level. Results obtained for this optimal working range show that the artificial mouth reproduces accurately the reed dynamics except in the open position, the mechanical properties of the artificial lip being different from those of the musician's lip.

The tools and methods developed open the possibility to perform measurements of the reed in playing conditions and in reproducible manner. The experimental limits encountered are discussed, proposing several improvements and guidelines for future research.

Key Words

Single reed, instrumented mouthpiece, artificial mouth, reed characterisation, subjective tests.